UNIVERSITÉ DE LIÈGE

Compartment Fire Models for Structural Engineering

Jean-François CADORIN

FACULTE DES SCIENCES APPLIQUEES

Thèse de doctorat **2003**

UNIVERSITE DE LIEGE

FACULTE DES SCIENCES APPLIQUEES

Compartment Fire Models for Structural Engineering

par

Jean-François CADORIN

Docteur en Sciences appliquées
de l'Université de Liège
Ingénieur civil des Constructions

Thèse de doctorat

2003

Collection des Publications de la Faculté des Sciences appliquées n° **234**
Secrétariat de la FSA, Institut de mécanique et génie civil, Sart-Tilman,
chemin des chevreuils, 1 (Bât. B52) - 4000 LIEGE 1, BELGIQUE

Thèse défendue, avec succès, le 17 juin 2003, pour l'obtention du grade de Docteur en Sciences appliquées de l'Université de Liège.

Jury : J.-C. DOTREPPE, Professeur à l'Université de Liège, Président
J.-M. FRANSSEN, Professeur adjoint à l'Université de Liège, Promoteur
M. HOGGE, Professeur à l'Université de Liège
J.-B. SCHLEICH, Chargé de cours à l'Université de Liège
D. DRYSDALE, Professor at the University of Edinburgh
M. KOKKALA, Research Professor, VTT, Technical Research Centre of Finland, Espoo
P. SPEHL, Ingénieur principal au Bureau SECO à Bruxelles, Maître de conférences à l'ULB et à l'Ecole Nationale des Ponts et Chaussées de Paris

Liège (Belgique) – Novembre 2003

Dépôt légal : D/2003/0480/43

ISSN 0075-9333

Acknowledgements

Professor Jean-Marc Franssen is gratefully acknowledged for having initiated and supervised this work.

I also thank Professors J-C. Dotreppe, M. Hogge and J-B. Schleich, from University of Liège.

Professor D. Drysdale, University of Edinburgh, U.K., Professor M. Kokkala, VTT, Finland, Professor P. Spehl, SECO, Belgium, as external members of the jury of this thesis, are particularly acknowledge for their careful reading of this dissertation and helpful comments.

I am particularly grateful to M. L.G. Cajot and M. Haller from profilARBED, Arcelor, to Dr D. Pintea from "Politehnica" University of Timisoara and to C. Pérez-Jimenez from University of Liège.

Contents

Notation

Abbreviations

1ZM	one-zone model
2ZM	two-zone model
RHR	rate of heat release

Greek symbols

ε^*	[]	Relative emissivity of steel profile-gas interface
ε_p	[]	Relative emissivity of partition-gas interface
γ	[]	partial safety factor
γ	[]	the ratio of specific heat
$\gamma_{q,1}$	[]	partial safety factor associated with the floor area of the compartment
$\gamma_{q,2}$	[]	partial safety factor associated with the danger of fire activation
$\gamma_{n,i}$	[]	i= 1 to 10; partial safety factor associated with the active measures
θ_1	[]	factor related to the burning rate stoichiometry; (Babrauskas method)
θ_2	[]	factor related to the partition steady state losses; (Babrauskas method)
θ_3	[]	factor related to the partition transient losses; (Babrauskas method)
θ_4	[]	factor related to the opening height effect; (Babrauskas method)
θ_5	[]	factor related to the combustion efficiency (Babrauskas method).
λ	[W/mK]	conductivity of the material of the partition
ρ	[kg/m^3]	density of the material of partition
ρ_∞	[kg/m^3]	density of ambient air
ρ_a	[kg/m^3]	density of ambient air
ρ_j	[kg/m^3]	density of the material of the finite element j
ρ_g	[kg/m^3]	gas density (1ZM)
ρ_U & ρ_L	[kg/m^3]	gas densities of, respectively, the upper (U) and lower (L) layer (2ZM)
σ	[]	constant of Stefan-Boltzman (5.67 10^{-8})
ξ_{ox}	[]	concentration of oxygen in the gas inside the compartment

Alphabetic symbols

a_1	[]	fraction of the height of the compartment
a_2	[]	fraction of the floor area of the compartment
$A_{i,VV,cl}$	[m^2]	Area of the closed opening
A_f	[m^2]	floor area of a compartment
A_{fi}	[m^2]	horizontal burning area of fuel

$A_{fi,max}$	[m^2]	maximum horizontal burning area of fuel
A_p	[m^2]	total area of partitions of the compartment (excluding openings)
A_{pu}	[m^2]	area of the ceiling and of the walls, excluding the floor and openings
$A_{p,j,i}$	[m^2]	total area of partitions n°j connected to the zone i
A_t	[m^2]	total area of partitions of the compartment (including openings)
A_w	[m^2]	total area of vertical opening
$A_{v,j,i}$	[m^2]	area of vertical opening n°j connected to the zone i
b	[$J/m^2s^{1/2}K$] = $\sqrt{(\rho c \lambda)}$	
b_w	[m]	width of vertical vent
b_i	[m]	width of vertical vent n°i
c	[J/kgK]	specific heat of the material of the partition
$\mathbf{C}$	[J/Km^2]	capacity matrix of partition
$\mathbf{C_{el,j}}$	[J/Km^2]	capacity matrix of finite element j
C_d	[]	discharge coefficient
c_j	[J/kgK]	specific heat of the material of the finite element j
$c_v(T)$	[J/kgK]	specific heat of the gas in the compartment at constant volume
$c_p(T)$	[J/kgK]	specific heat of the gas in the compartment at constant pressure
D	[m]	fire diameter
D_c	[m]	compartment depth
e_i	[m]	thickness of the insulation on a protected steel profile
e_p	[m]	thickness of the partition
$E_{1ZM}(t_s)$	[J]	total energy in the two-zone model system (E_g+energy in partitions)
$E_{2ZM}(t_s)$	[J]	total energy in the two-zone model system (E_U+E_L+energy in partitions)
E_g	[J]	internal energy (1ZM)
E_U & E_L	[J]	internal energies of, respectively, the upper and lower layer (2ZM)
F_c	[$m^{1/2}$]	compartment factor
g	[m/s^2]	gravitational acceleration constant
$\mathbf{g}$	[W/m^2]	vector of thermal loads
$\mathbf{g_{el,j}}$	[W/m^2]	vector of thermal loads of finite element j
h	[W/m^2K]	convective heat transfer coefficient
h_w	[m]	height of a vertical vent
H	[m]	height of the compartment
$H_{c,eff}$	[J/kg]	effective combustion heat of fuel
$H_{c,net}$	[J/kg]	complete combustion heat of fuel
$H_{c,net,i}$	[J/kg]	complete combustion heat of fuel of type i
H_F	[m]	vertical distance between the burner and the ceiling
H_q	[m]	height of fuel
k_j	[W/Km]	conductivity of the material of the finite element j
k_p	[W/Km]	conductivity of the material of the partition
$\mathbf{K}$	[W/Km^2]	conductivity matrix of partition
$\mathbf{K_{el,j}}$	[W/Km^2]	conductivity matrix of finite element j
L_c	[m]	compartment length
L_j	[m]	length of finite element j
L_H	[m]	horizontal flame length
m	[]	combustion efficiency factor
$\dot{m}_e$	[kg/s]	rate of mass entrainment in the fire plume
m_{fi}	[kg]	total mass of fuel
$\dot{m}_{fi}$	[kg/s]	pyrolysis rate
$\dot{m}_{i,\alpha,\beta}$	[kg/s]	rate of mass of gas exchange through vent. i = *U* or *L* or *g*. β = *in* or *out*. α = *VV* or *HV* or *FV*.
M_i	[kg]	mass of fuel of type i
$\dot{m}_{fi,data}$	[kg/s]	pyrolysis rate defined in the data
$M_{fi,c}$	[kg]	total mass of fuel in the compartment

m_g	[kg]	mass of the gas in the compartment (1ZM)
m_{ox}	[kg]	mass of oxygen in the compartment
$m_{ox,ini}$	[kg]	mass of oxygen in the compartment at initial time
$m_{ox,in}$	[kg]	mass of oxygen coming in the compartment through vents
$m_{ox,out}$	[kg]	mass of oxygen going out of the compartment through vents
m_U & m_L	[kg]	mass of the gas of, respectively, the upper and lower layer (2ZM)
$\dot{m}_{VV}$	[kg/s]	rate of mass of gas exchange through vertical vent.
$N_{eq,ce}$	[]	number of equations for the ceiling
$N_{eq,f}$	[]	number of equations for the floor
$N_{eq,j}$	[]	number of equations for the wall n°j
$N_{eq,p}$	[]	number of equations for all the partitions
N_{TC}	[]	number of thermocouples
O	[$m^{-1/2}$]	opening factor, equal to Awhw1/2/At
p	[Pa]	absolute pressure in the compartment considered as a whole.
p_f	[]	probability of structural failure due to a fire during the whole life of a structure
p_{fi}	[]	probability of getting of fully developed fire
$p_{f,fi}$	[]	probability of structural failure in case of fire
p_t	[]	target probability
q''	[W/m^2]	heat flux to the boundaries of a steel element
q_i	[J]	energy content of the zone i, $i = U$ or L or g.
q_f	[J/m^2]	fire load density (per unit floor area of compartment)
$q_{f,d}$	[J/m^2]	design fire load density
$q_{f,k}$	[J/m^2]	characteristic fire load density
$q_{f,k,eff}$	[J/m^2]	effective characteristic fire load density
$q_{f,k,net}$	[J/m^2]	net characteristic fire load density
$q_{f,net}$	[J/m^2]	net fire load density
$\dot{q}_{fi,p}$	[W/m^2]	energy radiated from the fire per unit area of lower layer partition
$\dot{q}_{i,\alpha,\beta}$	[W]	energy exchange through vent. $i = U$ or L or g. $\beta = in$ or out. $\alpha = VV$ or HV or FV.
$\dot{q}_g$	[W]	energy used to heat the gas in the compartment
$\dot{q}_{i,p}$	[W/m^2]	energy exchange between partitions and zone i ($i = U$ or L or g)
q_{net}	[W/m^2]	net heat flux at the boundaries of a steel profile
$\dot{q}_p$	[W]	energy loss to the partitions by conduction through it,
$\dot{q}_{v,c}$	[W]	energy loss by convection through the openings,
$\dot{q}_{v,r}$	[W]	energy loss by radiation through the openings,
Q^*	[]	Froude number
Q_H	[]	Froude number
r	[m]	horizontal distance between the burner and steel element
R	[]	the universal gas constant
RHR	[W]	rate of heat release
RHR_c	[W]	convective part of the heat release rate
$RHR_{fi,eff}$	[W/m^2]	effective rate of heat release per unit floor area of compartment
RHR_{data}	[W]	rate of heat release defined in the data
RHR_{fi}	[W/m²]	rate of heat release per unit floor area of compartment
RHR_r	[W]	radiative part of the heat release rate
t	[s]	time
t_c	[s]	time constant of the compartment
t_{fl}	[s]	time of flashover
t_s	[s]	time of switch from the 2ZM to the 1ZM
t_α	[s]	time at which RHR equal 1MW (defining the growing phase of a fire)
T	[K]	temperature
$\mathbf{T_{el,j}}$	[K]	vector of node temperature of finite element j

T_{fl}	[K]	temperature at which flashover occurs
T_g	[K]	temperature of the gas (1ZM)
T_{ign}	[K]	ignition temperature of fuel
T_{loc}	[K]	fictive temperature for localised effect of fire
T_{out}	[K]	temperature of the gas outside the compartment
$\mathbf{T_p}$	[K]	vector of node temperature of partition
$T_{p,j}$	[K]	temperature of node j
T_{post}	[K]	temperature of the gas during the post-flashover phase
T_{pre}	[K]	temperature of the gas during the pre-flashover phase
T_s	[K]	temperature of the section
T_U & T_L	[K]	temperatures of the gas of, respectively, the upper and lower layer (2ZM)
T_Z	[K]	temperature of a zone
T_∞	[K]	steady state temperatures
V	[m³]	volume of the compartment (constant)
V_f	[$m^{5/2}$]	ventilation factor
$\dot{V}_{FV}$	[m³]	rate of volume of gas through a forced vent
V_U & V_L	[m³]	volumes of, respectively, the upper and lower layer (2ZM)
y	[]	non dimensional ratio between the distance from the virtual source and the total length of the flame
z'	[m]	position of the virtual source
Z_{FV}	[m]	height of a forced vent
Z_p	[m]	height of neutral plane
Z_q	[m]	fuel height
Z_s	[m]	altitude of zones interface
Z_{sill}	[m]	height of the sill of a vertical vent
Z_{soffit}	[m]	height of the soffit of a vertical vent

Subscripts

c	variable related to convetive heat transfer
data	variable set in the data of OZone or, in general, use as input of a method
e	variable related to the entrainment into the fire plume
ce	variable related to the ceiling
f	variable related to the floor area
fi	variable related to the fire source
FV	variable related to the forced vent
g	variable related to the single zone of 1ZM
HV	variable related to the horizontal vent
i	equal to *U* for variable related to upper layer, to *L* for variable related to lower layer and to *g* for variable related to the single zone of 1ZM
in	variable related to a quantity added to a compartment zone
L	variable related to the lower layer
max	maximum value of variable
out	variable related to a quantity subtracted from a compartment zone
p	variable related to partitions
pj	variable related to partitions n°j
r	variable related to radiative heat transfer
U	variable related to the upper layer
VV	variable related to the vertical vent
w	variable related to the window

1

Introduction

1.1 Context

The work presented in this thesis is a contribution aiming at a more scientific approach of fire engineering and fire safety of buildings. The topic is of direct relevance to public safety which is a major research axis of the beginning of this new century. Fire claims the live of around 10-20 people per million of the population each year. The total cost of fire, including losses and protections, to the developed nations of the world is about 1% of gross domestic product each year (Cox 1999). The benefit of fire research has been shown statistically. For example, a recent study in the USA (Shaenman 1991) has suggested that total annual savings of $5-9 billion could be traced to the National Institute of Standards and Technology's fire research programme, costing less than $9 million per year.

Fire safety can have a major impact on the overall conception of buildings, i.e. on architectural conception, on the design, on the cost, etc. The strong tendency of doing unconventional buildings leads to unavoidable situations for which prescriptive fire design, i.e. a design which fulfils some predetermined protective measures, is inappropriate. The solution then requires the determination of the fire development in the compartment, of the temperatures in the structural elements and, finally, of their mechanical behaviour. It thus becomes a necessity for engineers to improve their knowledge in performance fire design and also to have tools which allow them to perform this design.

Fire safety is a multidisciplinary field of the engineering science. To perform a fire safety analysis of a building, a wide variety of knowledge has to be used: physics, chemistry, fluid dynamics, material sciences, structural behaviour, psychology, toxicology etc.

Although fire safety engineering has various aspects, i.e. human behaviour, evacuation, toxicity, fire detection, fire suppression, etc., this work deals mainly with the structural safety in case of fire, and, in a minor extent, to the safety of people and firemen in general.

1.2 Structural fire safety engineering

The calculations performed to assess the structural fire safety are:

- Evaluation of the thermal action of the fire on the structure;
- Calculation of the temperature field in the structure;
- Calculation of the mechanical behaviour of the structure exposed to fire.

In a prescriptive design, the standard fire resistance is calculated, i.e. the ability of a structure to fulfil required functions, for the exposure to heating according to the standard temperature-time curve for a specified load combination and for a stated period of time (Eurocode 1-EN 1991-1-2). The two important points of a prescriptive fire design are the facts that the required period of time is based on the expertise of fire safety regulators and that the fire heating is represented by a standard temperature-time curve also called nominal fire curve.

In a performance-based analysis, the first step of the process (SFPE 2000) is to establish the fire safety goals, objectives, and performance criteria. Risk to life and property is usually used as a performance basis. Once the performance criteria are established, different calculations can be performed to determine whether the specified performance criteria will be achieved by a proposed design.

In the performance-based approach, the evaluation of the thermal action on the structure exposed to fire requires the evaluation of the dynamics of fires, which is a major advance compared to the use of nominal fire curves in prescriptive design.

The work presented here is focused on an important branch of the fire safety engineering discipline, i.e. the study and the modelling of fires in compartments in order to estimate the action of fires on the structures.

1.3 Compartment fire models

Models that can be used for evaluating the dynamics of compartment fires can be classified in three categories, from the simplest to the most complex:

- Analytical models;
- Zone models;
- Field models (CFD).

These tools, that will be called in this study "compartment fire models", enable the calculation of one or more aspects of compartment fires, i.e. temperatures development, smoke propagation, etc.

Analytical models are usually based on simple theoretical developments or correlations obtained from experimental results. They have the form of simple equations and are suitable for hand calculations. They can be classified as follows: nominal; equivalent time; parametric temperature-time curves.

Zone model is the generic name given to a fire model which is based on the assumption that the compartment in which the fire takes place can be divided in zone(s) in which the temperature

can reasonably be considered to be uniform. In zone models, the energy and, usually, mass balances in zones of the fire compartment are solved numerically, some of the fire phenomena being modelled on the basis of fundamental principles and others being modelled by analytical models or correlations. Zone models are implemented in numerical software that solve the equations.

The field models are largely based on fundamental principles but up to now, still use some correlations and approximations. They are implemented in very complex software.

Depending on the type of model that is used, some evaluations may involve only few simple calculations, while others, such as CFD analyses, may require a huge number (even billions) of calculations and thus extensive computing time. Such complex analyses are costly, not only in computing time but also in engineer occupation due to the difficulty to define the data and to analyse and use the results produced by the tool.

The research efforts presented here are in fact devoted to analytical fire models and zone models.

1.4 State of the art regarding analytical fire models and zone models

Early developments

Although in the thirties Ingberg already pointed out the influence of the fire load, i.e. the total amount of combustible material that can burn in a compartment, on the severity of a fire on structures, in Japan, Kawagoe and colleagues (1958, 1963) first proposed in the fifties that one might be able to estimate the outcome of a fire scenario.

Kawagoe (1958) found that the rate of mass loss and the rate of heat released by the fire was proportional to the ventilation factor of the compartment vertical opening, being defined as the area of the opening multiplied by the square root of its height, leading to the so-called Kawagoe's correlation.

Kawagoe and Sekine (1963) have computed temperature-time curves by integrating the energy balance of compartment fires with the time. This method was limited to ventilation controlled fire with a constant rate of heat release.

In Sweden, Magnusson and Thelandersson (1970) have extended the method of Kawagoe to the complete fire process. The rate of heat released by the fire was time dependent but limited to a maximum value obtained by Kawagoe's correlation. This method is described extensively in (Peterson et al. 1976). These authors have provided series of temperature-time curves for various fire loads, ventilation conditions and thermal properties of the boundaries of the compartment.

These two groups of researchers have thus set the bases of what is now called "zone models". In the methods above, the temperature is assumed to be uniform within the whole compartment, leading to a one-zone.

Parametric temperature-time curves

Due to the lengthy computation needed at that time for the Kawagoe method and to the many assumptions, Lie (1974, 1996) has proposed a parametrical expression fitted on Kawagoe's computed temperature-time curves. The parametric method is easier to apply (as it has no iterative process) and is expected to lead to an equivalent quality of the results.

Parametric temperature-time curves have also been fitted on the results of the calculation made by Magnusson and Thelandersson. To the knowledge of the author, the procedure used has not been published, but the parametric curves are proposed in the Eurocode 1 (ENV 1991-1-2) published in 1993 dealing with the action on structures exposed to fire. In the late nineties, work undertaken in a ECSC research have conducted Franssen (2000, NFSC1 1999) to propose several improvements to this parametric model of the Eurocode. Improvements concerned the way to take into account multiple layers in partitions and were also aimed at extending the method to the fuel controlled regime. Although the improvements on partitions are mainly theoretical, the one on the burning regime is strongly empirical.

Two other methods for obtaining parametric temperature-time curves were proposed in the last years (Ma and Mäkeläinen 2000, Barnett 2002). The main interest of these methods is the shape of the curves which are shown to be closer to the temperature-time curve measured during full-scale fire tests. These methods are largely empirical.

Zone models

As said above, the first zone models were developed in the sixties and were numerical one-zone models aimed at modelling the post-flashover fire phase.

Very few numerical one-zone models were developed since that time. In a recent review of fire models (Olenick and Carpenter, 2003) only three one-zone models, aimed at modelling the post-flashover fire phase, are mentioned being still supported or developed: COMPF (Babrauskas and Williamson, 1978), NAT (Curtat and Fromy, 1992) and OZone (Cadorin and Franssen, 1999).

On the other side, in the early eighties, Cooper (1982b, 1983) has developed a mathematical model for estimating available safe egress time in fires. This model is based on the observation that in the early stage of a fire there is an accumulation of combustion products in a layer beneath the ceiling, with a more or less horizontal interface between this upper hot layer and the lower layer where the temperature of the gases remains much cooler, leading to a two zone phenomenon. Cooper (1985) then developed one of the first numerical two zone models, ASET. This model has been recently updated by Janssen (2000) and proposed as a didactical support to his book "An Introduction to Mathematical Fire Modeling".

In the review of Olenick and Carpenter (2003), fifteen fire models based on the two-zone assumption are reported to be still supported or developed. They have been made for a wide variety of purposes, but mainly related to smoke propagation or time for evacuation. As these codes are mainly focused on the modelling of the pre-flashover fire phase, none of them deals with structural safety.

1.5 Objectives of this work

The main goals of this work are to:

(1) Establish clearly the basis of the most widely used compartment fire models. A particular attention is given to the Eurocodes 1 methods as no background document has ever been formally published.

(2) Better understand their validity and application field by comparing the models between them and with full scale fire tests.

(3) Develop a new zone model that is:

- based on well defined hypotheses;
- well documented;
- extensively compared to full scale fire tests,
- based on original developments such as the combination of the two- and one-zone models, the implicit formulation of partition model...;
- aimed at the analysis of structures exposed to fire.

(4) Develop a new parametric fire model valid in pre- and post-flashover fire phase and based on the solution of energy balance of a compartment fire with some calibrations of certain parameters on numerical results. The method is suitable for hand calculation of the most common simple situation. Except MacCaffrey's method (1981) that is limited to the pre-flashover fire phase, other methods presented up to now have been obtained either by correlation with experiments or by curve fitting on numerical results.

A careful attention has been drawn throughout this work on the applicability of these new developments by the scientific and technical community. In particular, a practical design tool, OZone V2, has been developed to realise a performance based analysis of the behaviour of simple steel elements in a compartment fire situation. It includes three modules which enable successively to, (1) estimate the temperature evolution in a compartment fire, (2) calculate the temperature in protected or unprotected steel elements submitted to that compartment fire, taking into account if necessary the localised effect of the fire, (3) estimate the fire resistance of this element.

It should finally be mentioned that, in the recent edition of Eurocode 1 (November 2002) EN1991-1-2 “Actions on Structures exposed to fires”, it is explicitly allowed to perform fire design of structures on the basis of the calculation of temperature developments during a fire. The subject of this dissertation is thus in complete agreement with this possibility.

1.6 Contents

In chapter 2, a description of compartment fire physics is given. The development of fires in enclosures is explained and the main physical phenomena are described (rate of heat release, fire plume, vent flow, heat transfer to partitions...). The analytical models and correlations most widely used to model these phenomena are given.

The first part of chapter 3 is a review of the existing compartment fire models, from the well-known nominal fire curves to the most sophisticated computational fluid dynamic fire models. Analyses of some of these models are made and the needs for improvements are pointed out in the second part of chapter 3.

The description of the zone model developed in this work is given in chapters 4, focused on the formulation of the model.

In chapter 5, the different fire scenarios in relation with the model are presented as well as their impact on the design of structural steel elements.

Comparisons of the compartment fire model included in OZone with full scale fire tests are presented in chapter 6. These comparisons enable to assess the code and to define some limits beyond which the code is not able to predict reasonably the fire course.

Finally in chapter 7, the new parametric fire curves developed by the author are presented.

2

Fundamentals of fires in compartments

2.1 Introduction

The course of a fire in a compartment can evolve in different ways and its evolution is conditioned by various parameters. For example a fire in an ashtray in an empty room will not propagate due to the absence of material which is able to burn, and will thus self extinguish after a few minutes. The consequence of such fire will be limited to a small amount of smoke and will not be of concern for life or structural safety. The same burning ashtray, set in a hall full of empty plastic bottles, may spread firstly to the bottles in its neighbourhood and, in a short time, the fire may fully engulf the hall. The environment in the hall will then be untenable for people and the fire impact on the structure be very strong. These two examples show that, before modelling a fire, it is important to understand the different possible development, or scenarios, of fires in a compartment and to point out the parameters that influence the fire behaviour (section 2.2).

A fire in a compartment may be divided into distinct interrelated phenomena (section 2.3). These phenomena, such as the fire source, the vent flow..., have been studied experimentally or theoretically by numerous researchers who have produce models, usually applicable in a predetermined domain. In this chapter, a review of these models that describe particular phenomena is presented.

The parameters that have to be considered in a compartment fire design are also described, i.e. fire load, rate of heat release, etc.

The analytical expressions presented here may be used for hand calculations of the development of compartment fires. For this purpose, readers are invited to refer to the recent book "Enclosure Fire Dynamics" (Karlsson and Quintiere, 2000) that covers this subject extensively.

The models representing the compartment fire in its entirety, called compartment fire models, are presented in chapter 3. These models are aimed at the evaluation of the evolution of one or several characteristics (temperature of gas, smoke...) of the environment in compartment and may use the models for particular fire described here.

2.2 Development of fire in enclosures

The aim of this section is to give an overview of the possible developments of a fire in an enclosure and to define, in the context of fire science, some basic vocabulary (in bold).

Fire is a chemical, exothermic reaction that may occur when three elements are brought together: fuel, oxygen and a heat source. These three elements are frequently referred to as "fire triangle". To exist and to sustain, a fire needs:

- Enough oxygen for the combustion;
- Enough heat to raise the material to its ignition temperature;
- Some sort of fuel or combustible material.

If one of these three elements is missing, there will not have a fire or the fire will extinguish.

Concerning its development in time, a fire can be divided in several **phases**, see Figure 2.1 and Figure 2.3.

1. The first one is the **ignition** of the fire, usually at a point source (Figure 2.1b).
2. Then comes the **propagation** phase or **rising** phase, during which the fire spreads. Some combustion gases are rising toward the ceiling, a fire plume is forming above the fire source. Some air is entrained in the fire plume and a hot smoke layer is forming in the upper part of the compartment (Figure 2.1c) leaving a clear layer in the lower part. The temperatures rise in the compartment and, from here, the situation can evolve towards one of the 2 following possibilities:
    - Either the temperature of the gases become so elevated that, after a certain period of time, it causes the sudden ignition of every object in the compartment. This phenomenon is called the **flashover**. After flashover time, there is a **fully developed fire** (Figure 2.1d and Figure 2.2b.).
    - Either there is no spread of the fire to the whole compartment, because the propagation is so slow that the temperature rise is not sufficient to cause the flashover, or because the fire can find no combustible material in its close vicinity. The fire remains **localised** (Figure 2.1c and Figure 2.2a).

3. In the next period, the fire is **fully developed**, i.e. the fire keeps on burning at a rather constant rate, leading to small variations of the temperatures. (Figure 2.1d and Figure 2.2b)
4. The last phase is the **cooling** phase or **decreasing** phase. During this phase the mean temperature may remain rather high during a certain time and the influence on the structure can be important.

The ignition and the propagation phases of the fire depend mainly on the fuel characteristics because oxygen is usually widely available during these phases.

The period up to flashover is often called pre-flashover fire phase during which the fire is usually localised. After flashover, the fire phase is called post-flashover. A post-flashover fire is a fully developed fire if combustible material is present on the main part of the floor.

On the other hand, the amount of ventilation has a big influence during the fully developed phase of the fire. Two situations are possible:

- The ventilation is large enough to have no influence on the fire source development. There is suficient oxygen available for combustion. The fire is said to be **fuel controlled** because the heat released in the compartment depends mainly on the characteristics of the material that is burning.
- The ventilation is small, considering the size of the fire, and there is not enough oxygen to combust all the pyrolysed fuel. The fire is said **ventilation controlled** because the rate of heat release in the compartment depends mainly on the amount of available oxygen and therefore on the ventilation conditions.

In most cases, localised/pre-flashover fires are fuel controlled and fully developed/post-flashover fires are ventilation controlled. Nevertheless, even if these situations are scarce, a pre-flashover fire might be ventilation controlled in a compartment with few openings and a post-flashover fire might be fuel controlled in a compartment with very large openings.

2.3 Elements of compartment fire

Based on observations and measurements during real and laboratory compartment fires, it is possible to subdivide the complex and interrelated phenomena occurring during a compartment fire into a number of discrete elements that will be discussed in the next sections in which associated models will be presented.

As illustrated in Figure 2.4 (Mowrer, 2002), the main phenomena in a pre-flashover fire include:

(1) The fire source (sections 2.4.1 to 2.4.4);
(2) Partitions heat transfer (section 2.5);
(3) Vent flows and mechanical ventilation (section 2.7);
(4) The smoke layer, also called upper layer (section 2.2);
(5) Fuel heating (section 2.4.2.2 and 0);
(6) The lower layer (section 2.2);
(7) The fire plume (section 2.6);
(8) The ceiling jet (section 2.8).

In case of post-flashover fires, items (6) to (8) does not exist anymore because all the fuel is burning and the whole compartment is engulfed in flames.

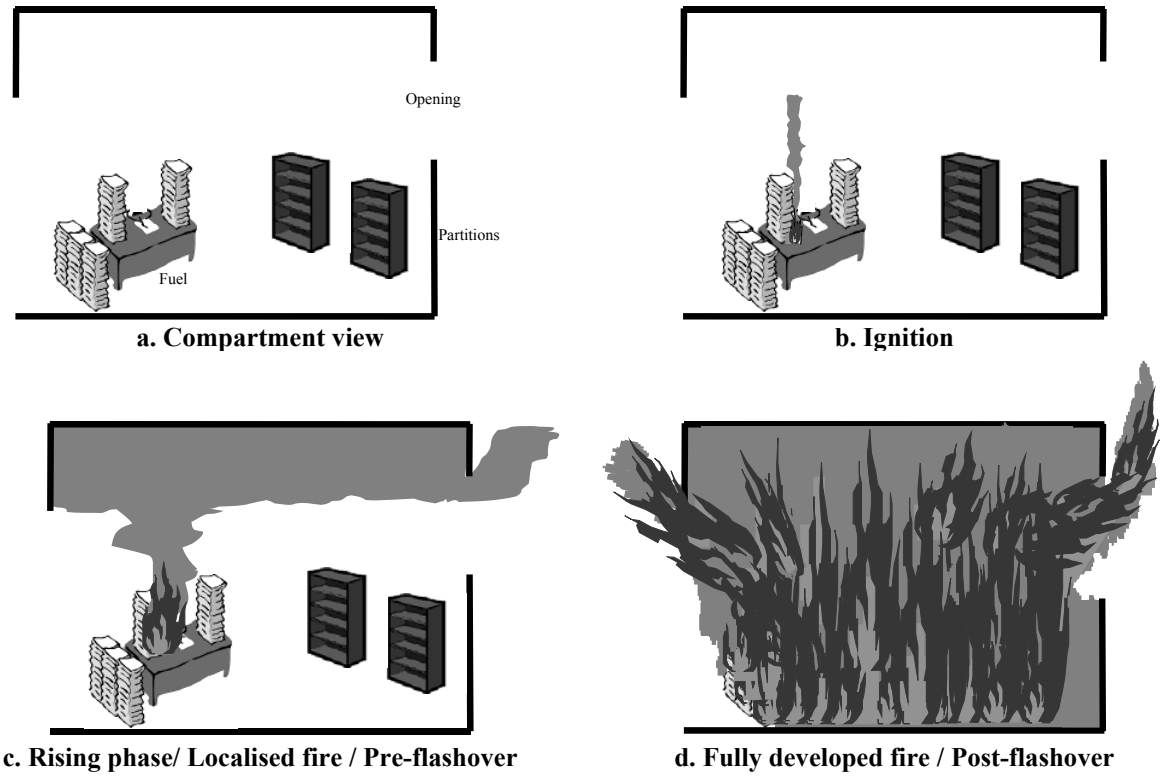

a. Compartment view **b. Ignition**

c. Rising phase/ Localised fire / Pre-flashover **d. Fully developed fire / Post-flashover**

Figure 2.1 Phases of a compartment fire

a.  b. 

Figure 2.2 Localised (a.) and fully-developed (b.) fire tests (NFSC2)

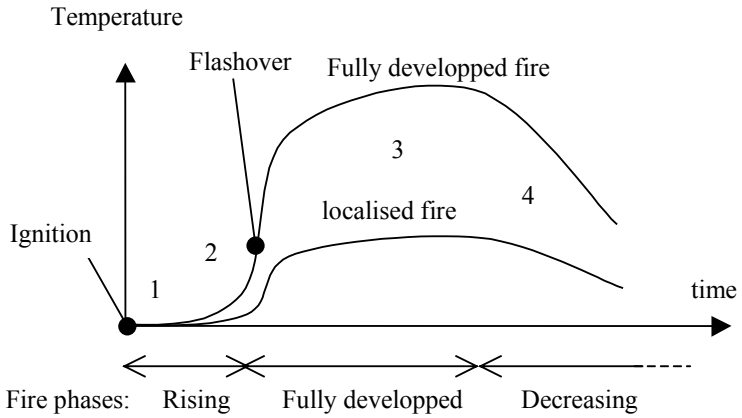

Figure 2.3 Evolution of the gas temperatures during a compartment fire

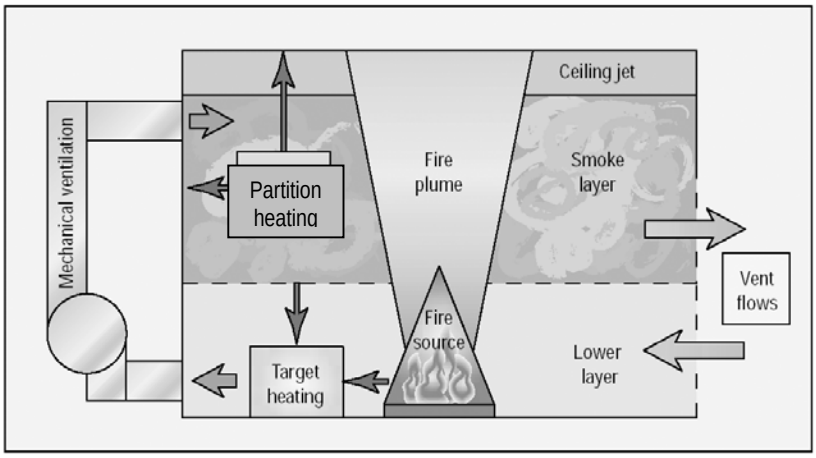

Figure 2.4 Schematic view of the main phenomena of a compartment fire (Mowrer, 2002)

2.4 Fire source

Fuel heating

2.4.1 Physics and chemistry of fires

A fire is a highly complex combustion system which can be divided in a number of distinct but interdependent processes, Figure 2.5. Heat transfer from the flame and from the environment back to the fuel induces decomposition and/or evaporation of solid fuel producing a stream of gaseous fuel; this phenomenon is the pyrolysis. The gaseous fuel reacts then with oxygen producing combustion products and heat. The heat produced leads to sustain the process (Simmons, 1995). This situation is the diffusion flame that is characterised by the fact that the fuel and the oxygen are initially separated and burn in the region where they mix (Drysdale, 1999). Diffusion flames are involved in solid burning and thus in compartment fires. Premixed flames are flames in which the fuel and the oxygen are intimately mixed when they burn, cited here for information.

The number of chemical reactions involved in this process can be very high (i.e. hundreds) but it is very convenient to look at the overall chemical reaction of wood combustion.

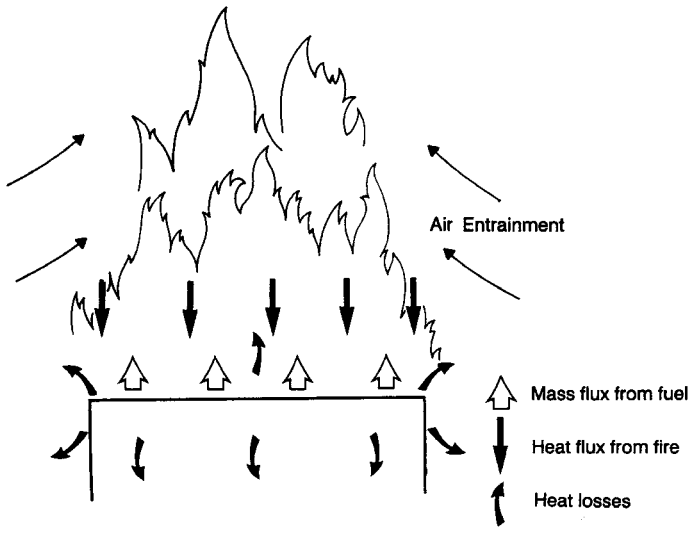

Figure 2.5 Schematic representation of a burning surface (Drysdale, 1999)

As an example, the combustion chemistry a cellulosic material can be simplified to a single chemical reaction, Eq. (2.1). If the material is represented by $\boldsymbol{C_4H_6O_3}$ then,

$$C_4H_6O_3 + 4O_2 \Rightarrow 4CO_2 + 3H_2O \tag{2.1}$$

Considering the mass of each molecule, the mass balance of Eq. (2.2) can be written.

$$102 + 128 \Rightarrow 176 + 54 \tag{2.2}$$

The burning of wood can be simplified into Eq. (2.3) stating that, in a fire, 1kg of wood plus 1.3kg of oxygen gives 2.3 kg of combustion products and releases an energy of H_c Joules.

$$1 \text{ kg of fuel} + 1.3 \text{ kg of } 0_2 = 2.3 \text{ kg of combustion products} + H_c \text{ J} \tag{2.3}$$

This equation can be generalised to other fuel by introducing the stoichiometric ratio r of the oxygen requirement of the fuel, Eq. (2.4).

$$1 \text{ kg of fuel} + r \text{ kg of } 0_2 = (1+r) \text{ kg of combustion products} + H_c \text{ J} \tag{2.4}$$

For wood, see Eq. (2.3), the oxygen/fuel stoichiometric ratio is 1.3. As the oxygen fraction in air is about 23%, the air/fuel stoichiometric ratio for wood is 5.6. In Table 2.1 some example of fuel properties are given. Other values can be found in various publications (Drysdale, 1999; Karlsson and Quintiere, 2000; SFPE, 1995...).

Such a simple approach is in most cases appropriate to assess various aspects of fire safety, for example structural response or smoke propagation. A more precise approach may be needed for other applications, for example, to evaluate the concentration of toxic gases in the fire compartment.

Table 2.1 Example of fuel properties (Karlsson and Quintiere 2000)

Fuel	***1/r* []**	**$H_{f,net}$ [MJ]**
Ethanol	0.480	26.8
Heptane	0.284	44.6
Polyvinilchloride (PVC)	0.710	16.4
Polymethylmethacrylate	0.521	25.2

Combustion Heat of Fuel - H_c

The energy released by the combustion of one unit of mass of fuel in an oxygen bomb calorimeter under high pressure and in pure oxygen is $H_{c,net}$, the complete (or net) combustion heat of the fuel. Under these conditions, all the fuel is burnt, leaving no residue and releasing all its potential energy. In real fires, the energy that the same unity of mass is able to release is lower than $H_{c,net}$. Usually about 80% of the complete combustion heat is released. A part of the combustible is not pyrolysed leaving some soot and not all of the volatiles produced by pyrolysis are completely oxidised. The effective combustion heat of fuel is defined as the ratio between the heat release rate during a real fire and the rate of mass of fuel loss during this real fire, Eq. (2.5).

$$H_{c,eff}(t) = \frac{RHR(t)}{\dot{m}_{fi}(t)} \tag{2.5}$$

The efficiency of the combustion is represented by the combustion efficiency factor m, ratio

between the effective and the complete combustion heat of the fuel, Eq. (2.6).

$$m(t) = \frac{H_{c,eff}(t)}{H_{c,net}} \tag{2.6}$$

The values of the effective combustion heat and therefore of the combustion efficiency factor depend on many parameters, the temperature in the compartment, the way of storage of fuel… and are actually varying with time t. Nevertheless, in most cases the combustion efficiency factor is assumed to be constant for simplicity.

2.4.2 Fire load

The fire load in a compartment is defined as the total energy that could theoretically be released in the compartment in case of fire. It consists of the different elements present in the compartment (furniture, etc.), of construction elements, of partition linings… and, in general, of all the combustible content. The fire load is usually expressed in Joules and is the sum of the product of the mass M_i of each items present in a compartment by its heat of combustion $H_{c,i}$, Eq. (2.7). It is also very common to use the equivalent wood mass, i.e. the mass of wood which would release the same amount of energy as the fire load (the fire load in J divided by the combustion heat of wood in J/kg).

$$m_{fi} = \sum_i H_{c,i} M_i \tag{2.7}$$

2.4.2.1 Fire Load Density - q_f

The fire load density $q_{f,k}$ is the fire load per unit area related to the floor area. It is obtained by survey in real compartments. Data are available for different types of occupancies of compartments (Robertson, 1970; Culver, 1976; Thomas, 1995; Kumar, 1995 & 1997; Korpela, 2000; EN1991-1-2, 2002). In order to obtain these data, the mass of all types of combustible present in compartments is measured or estimated. This mass is then multiplied by the combustion heat of the materials that constitute the fire load. This quantity is then divided by the floor area of the compartment, according to Eq. (2.8).

$$q_{f,net} = \frac{1}{A_f} \sum_i H_{c,i} M_i \tag{2.8}$$

The combustion heat used in Eq. (2.8) is either the net or the effective combustion heat, depending on the author. The fire load density may also be defined as the fire load per unit area related to the surface area of the total enclosure, including openings. In this case, the fire load density is noted q_t.

2.4.2.2 Net versus effective fire load

When giving value for the combustion heat, fire load or rate of heat release, it is important to know whether the combustion efficiency is taken into account in the value or not. We will thus considered that a net value of a parameter is related to the estimation of the parameter with the net combustion heat (evaluated in bomb calorimeter conditions) while an effective value is related to the estimation of the parameter with the effective combustion heat (expected to occur in real fire conditions). For example, $q_{f,k,net}$, the net characteristic fire load density is linked to $q_{f,k,eff}$, the effective characteristic fire load density, by Eq. (2.9), m is the combustion efficiency factor that is also called m factor.

$$q_{f,k,eff} = m \quad q_{f,k,net} \tag{2.9}$$

2.4.3 Ignition of fuel

As it is the first step of any compartment fire, ignition is probably the most important phenomenon: without ignition, there is no fire. Many studies have been conducted on this subject, leading to a wide variety of test methodologies to evaluate the potential of being ignited that a material has. Materials are classified in function of this criteria, called "reaction to fire", evaluated by laboratory tests. Nevertheless as the present work is focused on the evaluation of the temperatures in compartments when there is a fire, the reaction to fire will not be treated in detail, readers are invited to refer to specific publications.

Babrauskas (2001) reports that ignition temperature of wood exposed to the minimum heat flux possible for ignition is around 250°C. The surface temperature of fuel is usually considered to be the best empirical parameter to describe the ignition of fuel, nevertheless the temperature of the environment in which the fuel is present is usually prefered. It is particularly convenient to use the latter parameter in compartment fire modelling because the environment temperature is the main results of such models.

The ignition of a fire happens generally in a single location in the compartment. Well known exceptions are arson fires that are often ignited in many places. This can lead to much faster rising phase and very short pre-flashover phase, increasing the murderous character of fires.

2.4.4 Rate of heat release (RHR)

The rate of heat release is the most important parameter during the course of a fire. In the early stage of a fire, it may even be the single variable to consider. It controls to a considerable extent all phenomena that occur during the first stages of a fire: the plume flow, the hot layer temperature... In subsequent fire stages, other parameters become very important: ventilation conditions, thermal properties of partitions... but the rate of heat release remains of primary importance.

The rate of heat release is the quantity of energy that is released by the fire per second. The RHR depends on the type and quantity of fuel present in the compartment, on the ventilation conditions, on the phase of the fire (rising, stationary, decreasing)… This quantity is time dependent.

The pyrolysis rate $\dot{m}_{fi}$ is the quantity of mass of solid fuel that is transformed into combustible gases per second. It is indeed the mass loss rate of fuel. The rate of heat release is related to the pyrolysis rate by Eq. (2.10). The effective combustion heat has been defined in section 2.4.2.

$$RHR(t) = H_{c,eff}(t)\,\dot{m}_{fi}(t) \tag{2.10}$$

Eq. (2.10) is only valid for free burning fires i.e. when the oxygen does not limit the amount of heat release by the fire. It is very common to use the expression “burning rate” as a synonym of pyrolysis rate. It is inappropriate because mass loss and burning might be not proportional in under-ventilated conditions. Thus in this text, pyrolysis rate or mass loss rate is preferred to burning rate.

Models for the estimation of the rate of heat release exist for different types of burning item (Babrauskas, 1995 & 2000): Wood cribs; Pool fires; Various furniture types (sofa, mattress…); Christmas trees; Television set; etc.

In the following sections, after having explained how rate of heat release can be estimated, a wood model and some furniture models are briefly presented. The effect of the compartment is then pointed out and in particular the effect of the ventilation condition is presented.

2.4.4.1 Estimation of rate of heat release

There are two main ways to estimate RHR by measurements: by measurement of the mass of the fuel or by measurement of the oxygen depletion in the combustion products. With the first method, the fuel is placed on a load cell (Figure 2.6) and the total mass of the fuel is measured during the fire tests (Figure 2.7a). The mass loss rate (Figure 2.7b) is then deduced from the mass measurement by derivation and the rate of heat release is estimated by multiplying the mass loss rate by the combustion heat of the fuel. For example the measured fuel mass and rate of calculated rate of mass loss for the test made at the laboratory of CTICM, France, referred as test NFSC19 in the NFSC database (see section 3.6) are presented on Figure 2.7.

The oxygen depletion method consists of the measurement of the oxygen concentration in the combustion gases produced by the fire. From that measurements, the oxygen mass rate that has burnt is deduced and then the heat release rate is obtained by multiplying the oxygen mass rate by the combustion heat of oxygen. A typical test configuration used for this type of measurement is shown on Figure 2.8.

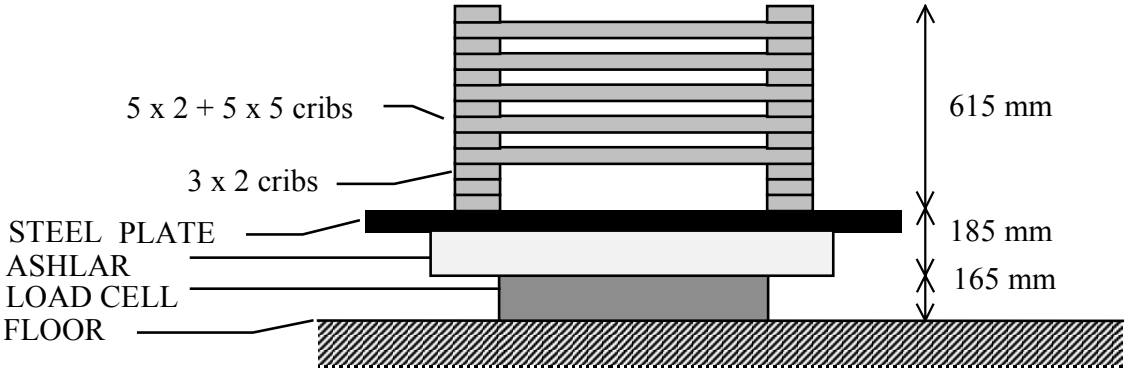

Figure 2.6 Example of apparatus used to measure mass loss rates (Hostikka et al., 2001)

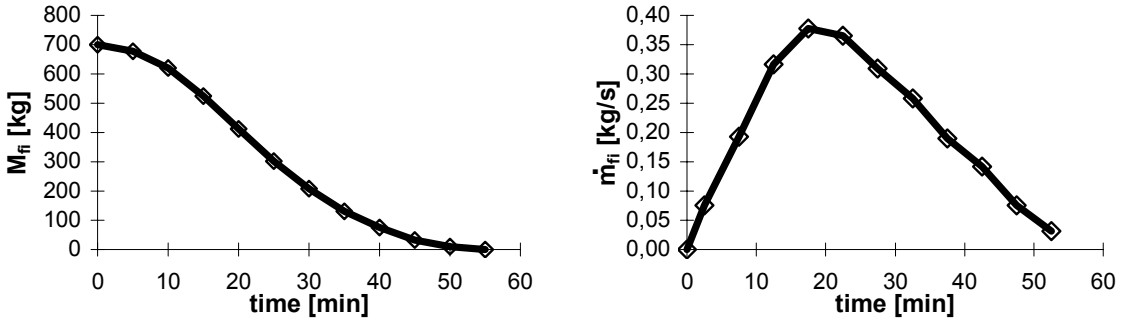

a. Mass of fuel (measured) b. Rate of mass loss (calculated)

Figure 2.7 Mass loss of fuel measurement

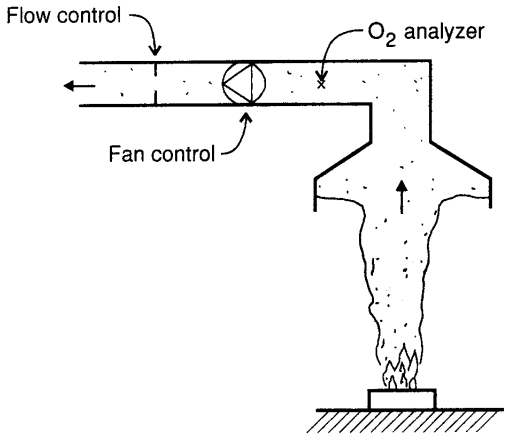

Figure 2.8 Schematic view of oxygen consumption calorimeter (Karlsson and Quintiere, 2000)

2.4.4.2 Free burning measurements

A model for free burning wood pallet is presented on Figure 2.9 (Babrauskas, 1995). It shows that the peak RHR of wood pallet is proportional (linear) to the stack height of the pallets.

Other free burning models (liquid pool fires, wood crib), are also available in Babrauskas (1995)

Some databases of burning item measurements have been gathered. They consist in the collection of fire tests of typical items. On Figure 2.10, a fire test of a sofa is presented. It is interesting to note that the RHR at this stage is already 0.8 MW. On Figure 2.11 test results are presented. They concern fire tests of various upholstered furniture (sofa, mattress etc.). Four typical fire behaviour are shown: Quickly developing, high peak of RHR; Delayed fire development, moderate peak RHR; Slow fire development, low peak RHR; Very limited burning.

The tests of Figure 2.10 and Figure 2.11 are from the database that has been made in the CBUF project (Sundström, 1995; Van Hees, undated). In this project four models have been developed for estimating the heat release rate of burning items. They are shown to work very well for the CBUF database (Sundström, 1997).

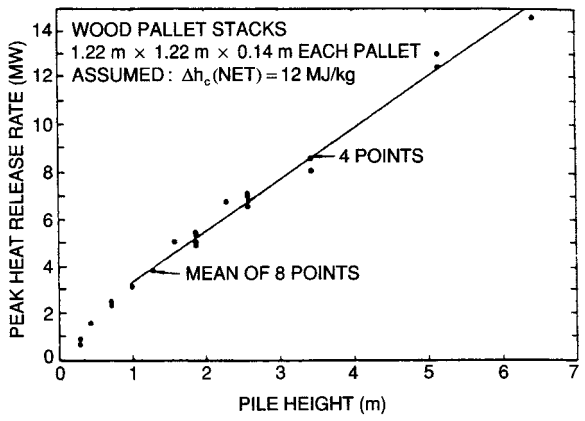

Figure 2.9 free burning of wood pallet (Babrauskas, 1995)

Figure 2.10 Sofa fire. The RHR at this point is about 800kW. (Sundström, 1997)

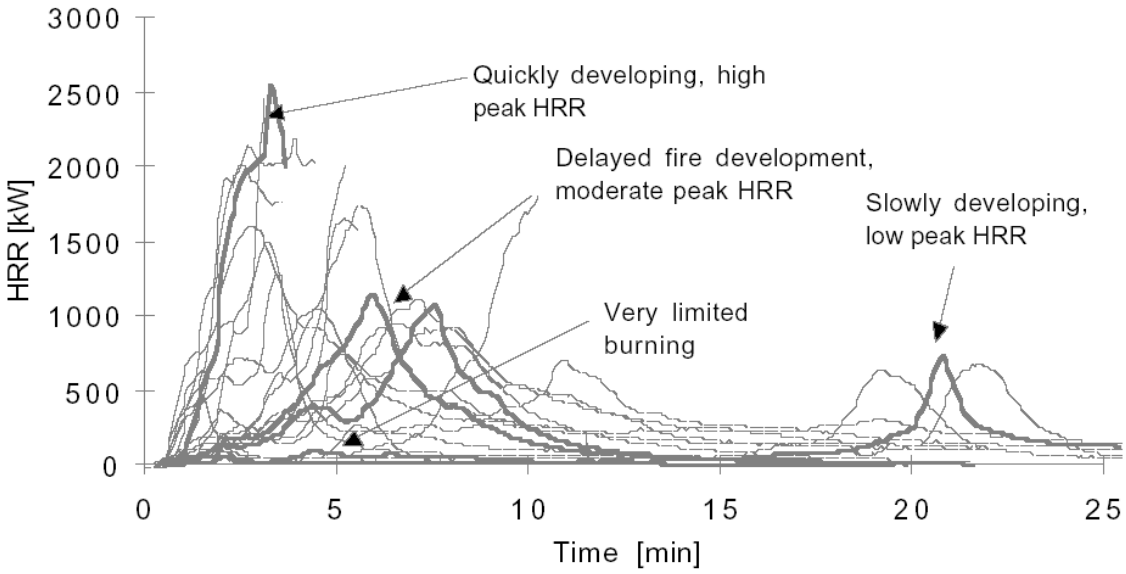

Figure 2.11 RHR as a function of time measured in the Furniture Calorimeter for a selection of European upholstered furniture and mattresses (27 items). Four typical RHR curves (type curves) are shown in bold. (Sundström, 1997)

The collection of test methods, models, and correlations formulae can be viewed as a tool-kit. The user can select different components of this tool-kit according to his preferences.

However, it is noted that modelling, and especially the correlations, rely on the basic test data. Therefore care should be taken if the models are considered for use of products very different in design from those covered by the CBUF database and modelling principles.

Another database has been published by Saquevist (1993). It contains RHR measurements for various item such as mattresses, plaster board... or various room occupancies such as bedrooms or offices containing typical furniture. This database is available on the internet web site of SP, Sweden.

2.4.4.3 Influence of the compartment

The models presented in the previous sections are free burning measurements i.e. the burning is not influenced by the surrounding environment and happens as if it was outside. In

compartments, the burning is influenced by the conditions in the compartment: the gas temperatures, the partition temperatures, the oxygen available…

In general, a given fire load burns faster and at a higher rate in a compartment than in free burning conditions. In a compartment, the heating of the fuel is not only driven by the flames as it is in free burning condition, but also by the smoke layer and the partitions.

Kawagoe's studies (1958) showed that the ventilation condition might reduce the burning in comparison to the one that would occur in free burning conditions. Kawagoe has measured the rate of burning of wood cribs contained within full scale and reduced scale compartments with different sizes of ventilation opening, Figure 2.12. The pyrolysis rate $\dot{m}_{fi}$ [kg/s] was found to correlate very well with the ventilation factor $V_f = A_w\, h_w^{1/2}$ [$m^{5/2}$] as expressed by the so-called Kawagoe correlation, Eq. (2.11).

$$\dot{m}_{fi} = 0.09 A_w \sqrt{h_w} = 0.09 V_f \tag{2.11}$$

For very large opening, Thomas in 1967 (Drysdale, 1999) found that the Kawagoe correlation was not applicable anymore, Figure 2.13. This represent the transition between ventilation and fuel controlled fires. Burning rates during fuel controlled fires are driven by the fuel characteristics. On Figure 2.13, the influence of the fire load density is clearly demonstrated.

The Kawagoe correlation states that the rate of mass loss is coupled to the air inflow in the compartment. This is difficult to understand as it is known that in confined situation the rate of mass loss is increased by the surrounding heat feedback. The Kawagoe correlation should thus only apply to wood crib in which the burning surface is largely shielded from the influence of the compartment. Considering that, Harmathy has proposed the following correlation, Eq. (2.12) , to distinguish between ventilation and fuel controlled fires, the transition being ill-defined (Harmathy, 1972; Thomas, 1975; Drysdale, 1999).

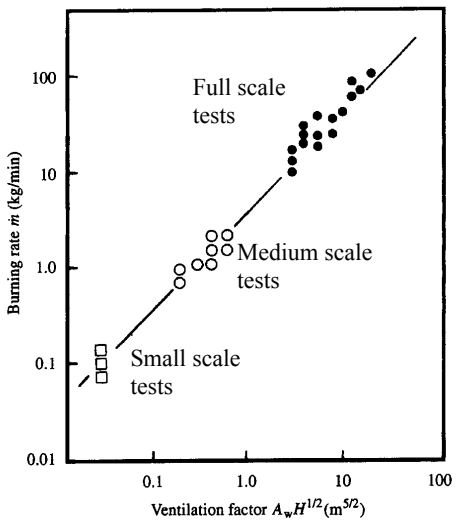

Figure 2.12 Kawagoe correlation (line) and tests in under-ventilated conditions (Kawagoe, 1958)

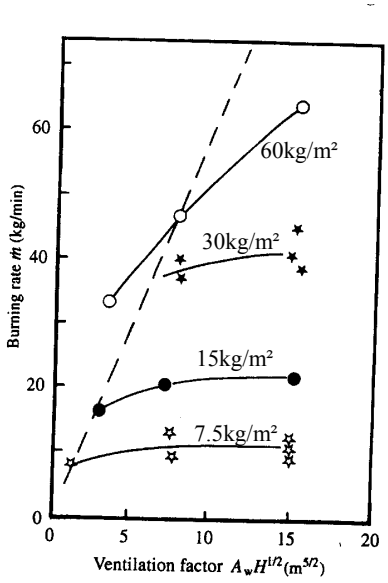

Figure 2.13 Fire tests with fire load densities between 7.5 and 60 kg/m² and large openings and Kawagoe correlation (dotted line) (Thomas, 1967)

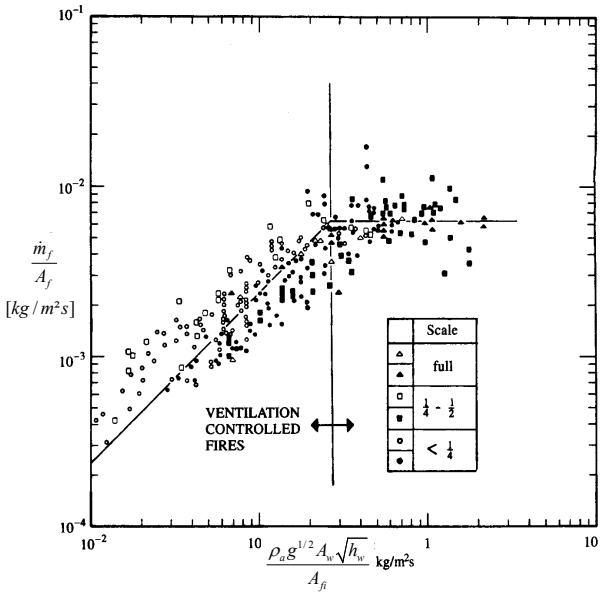

Figure 14 Identification of the transition between ventilation- and fuel-controlled burning for wood cribs (Harmathy, 1972)

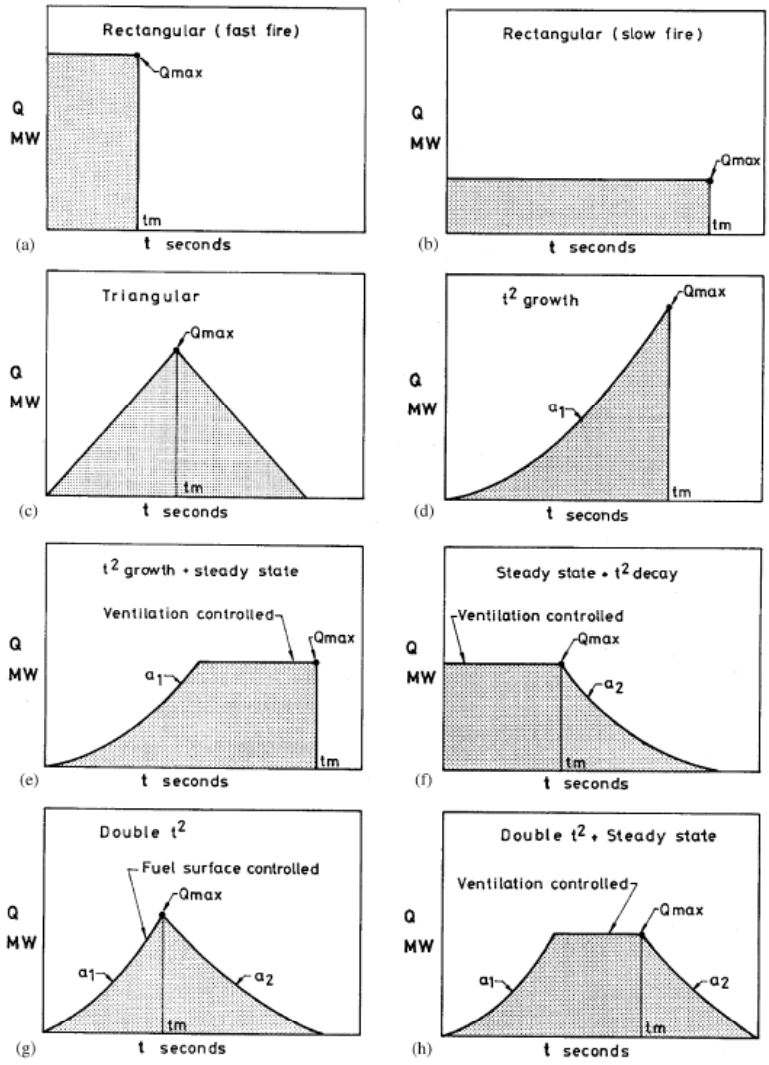

Figure 2.15 Various design fire curves (Barnett, 2002)

$$\text{Ventilation control:} \quad \frac{\rho_a g^{1/2} A_w \sqrt{h_w}}{A_{fi}} < 0.235$$
$$\text{Fuel control:} \quad \frac{\rho_a g^{1/2} A_w \sqrt{h_w}}{A_{fi}} > 0.290 \qquad (2.12)$$

2.4.4.4 Design fires

It is obvious that a structural engineer can not design a beam for all possible load combinations which can be applied to this beam during its life. A limited number of design loads must be defined, provided this will lead to a safe design.

Similarly, for fire safety, the aim of a design is not to simulate all the possible fires which could occur in a compartment. The purpose of a design is to assess with a reasonable accuracy the risk due to a fire.

For fire modelling, design fires are usually defined in terms of rate of heat release. A wide variety of heat release rate profiles can be found in the literature (Figure 2.15). Unfortunately, very little guidance can be found to decide which shape is appropriate to which situation.

In the last edition of Eurocode 1 on actions on structures exposed to fire (EN1991-1-2) a design fire curve is defined in Annex E. This design fire curve has been proposed in the "Natural Fire Safety Concept" research project (NFSC1, 1999) and implemented in the code OZone. A description can be found in chapter 5 of this manuscript.

2.4.5 Flashover

Many definitions of flashover are given in the literature, the most common of which are (Drysdale, 1999):

(1) the transition from a localised fire to the general conflagration within the compartment when all fuel surfaces are burning;
(2) the transition from a fuel controlled to a ventilation controlled fire; and
(3) the sudden propagation of flame through the unburnt gases and vapour collected under the ceiling.

Martin and Wiersma (1979) point out that (2) is the results of (1) and is not a fundamental definition. (3) is improper to define flashover but is probably an important phenomenon which drives flashover.

The first definition is being used in this work, although Thomas (1974) has pointed out that it may not be applied to long and deep compartments in which it may be impossible for all the fuel to burn at the same time.

Flashover is a very important phenomenon which can occur during compartment fires. It is the ultimate tenability limit within a room. It is very unlikely for occupants to survive within a room after flashover as flames are present everywhere fuel is available and as temperatures are high. The fire impact on structures is also usually considerably higher after flashover than in the growing phase.

Table 2 Temperatures and heat flux leading to flashover for various experiments (Peacock *et al.*, 1999)

Source	Temperature [°C]	Heat flux [kW/m²]
Häggland	600	No data
Fang	450-650	17-33
Bundick & Klein	673-771	15
	634-734	
Lee & Breese	650	17-30
Babrauskas	600	20
Fang & Breese	706 ± 92	20
Quientiere & McCaffrey	600	17.7-25
Thomas	520	22
Parker & Lee	No data	20

It is thus very useful to well understand this phenomenon and to be able to predict it. Many full scale experimental studies of flashover have been made. Some parameters which influence it and some empirical formulae have been deduced from these experiments.

A lot of variables influence the transition from a localised to a fully developed fire. The main parameter is recognised to be the convective and radiative heat fluxes received by the non ignited fuel. This flux is linked to the surrounding temperatures (i.e. partitions, fire source…) and therefore to the upper layer temperature which is often chosen to characterise flashover. This is because it is probably one of the most important variables but also because it is an important parameter in pre-flashover fire and thus is the main result of many fire models.

In a recent overview (Peacock *et al.*, 1999) of flashover studies, the upper layer temperature and the heat flux received by the fuel leading to flashover obtained in different experimental studies have been collected and are summarised in Table 2.

The temperature values are included between 450 and 800°C with most values between 600 and 700°C. The heat flux values are between 15 and 33kW/m². This table shows the high level of uncertainty on the flashover phenomenon. If the definition has to be unique, the most common admitted value to characterise flashover is 600°C or 20kW.

2.5 Heat transfer to partition

In this dissertation, the term "partition" represents all the solid surfaces that enclose the compartment, namely the walls (vertical), floor and ceiling (horizontal). It used as a synonym of boundary.

The simplest way to estimate the heat transfer to partition is to assume that the partition is a semi-infinite solid and that the partition surface temperature is equal to the gas temperature. The solution of the general heat conduction equation of this particular situation is given by Eq. (2.13) (Karlsson and Quintiere, 2000).

$$\dot{q}_p = \sqrt{\frac{c\rho_p k_p}{\pi t}} A_p \left(T_g - T_{out} \right) \tag{2.13}$$

This equation enables to introduce the b factor equal to the square root of $c\rho_p\lambda_p$ that is often use to characterise the thermal behaviour of partitions.

For very thin solids, or for conduction through solid that goes for a long time, the process of conduction becomes stationary, and the rate of heat flowing through the solid is given by Eq. (2.14).

$$\dot{q}_p = \frac{k_p}{e_p} A_p \left(T_g - T_{out} \right) \tag{2.14}$$

The thermal penetration time t_p, given by Eq. (2.15), can be defined to be the limit between the transient (governed by Eq. (2.13)) and the stationary (governed by Eq. (2.14)) regimes of heat transfer through partitions. Here α is the thermal diffusivity in m^2/s and given by $k_p/c\rho_p$.

$$t_p = \frac{e_p^2}{4\alpha} = \frac{e_p^2 c\rho_p}{4k_p} \tag{2.15}$$

More general methods can also be used to solve the general heat conduction equation, i.e. finite difference, finite element...

2.6 Fire plumes

When a mass of hot gases is surrounded by colder gases, the hotter and less dense, mass will rise upward due to the density difference, or buoyancy. This phenomenon happens above a burning fuel source. The buoyant flow is referred to as a fire plume. Cold air is entrained by the rising hot gases, causing a layer of hot gases to be formed below the ceiling.

Different analytical expressions of the properties of fire plume have been proposed by several authors. Four of them (Heskestad, 1995; Karlsson and Quintiere, 2000) are given here:

- Heskestad plume model;
- Zukoski plume model;
- McCaffrey plume model;
- Thomas plume model.

It should be mentioned that some of these empirical formulas have been obtained by fit on the total energy release rate RHR and others on the convective part of it RHR_c.

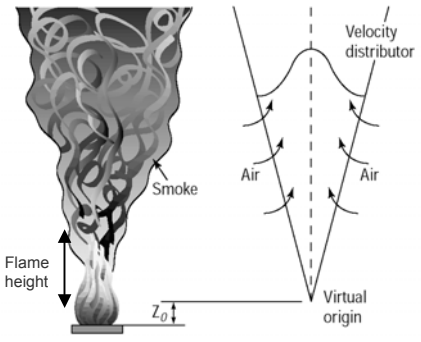

Figure 2.16 Fire plume and associated schematic model

2.6.1 Heskestad

The Heskestad plume correlation is given by Eqs. (2.16) to (2.19).

The virtual origin of the plume is at the altitude z_0 :

$$z_0 = 0.083\, RHR^{2/5} - 1.02D \tag{2.16}$$

The flame height L_{fl} is given by :

$$L_{fl} = 0.235\, RHR^{2/5} - 1.02D \tag{2.17}$$

The plume mass flow rate above the flame height ($z > L_{fl}$,) is given by :

$$m_p = 0.071 RHR_c^{1/3}\ (z - z_0)^{5/3} + 1.92\ 10^{-3}\, RHR_c \tag{2.18}$$

The plume mass flow rate below or at the flame height ($z < L_{fl}$,) is given by :

$$m_p = 0.0056\, RHR_c \frac{z}{L_{fl}} \tag{2.19}$$

Heskestad plume correlation is the most widely used model. It has been shown in the research project "Development of design rules for steel structures subjected to natural fires in Closed Car Parks" (CCP 1997) that it is the model which best fit to CFD plume simulations.

2.6.2 Zukoski

The Zukoski plume correlation is given by Eq. (2.20).

$$m_p = 0.21 \left(\frac{\rho_\infty^2 g}{c_p T_\infty} \right)^{1/3} RHR_c^{1/3}\ z^{5/3} \tag{2.20}$$

2.6.3 McCaffrey

The McCaffrey plume correlation is given by Eqs. (2.21) to (2.23).

$$m_p = 0.011\, RHR \left(\frac{z}{RHR^{0.4}} \right)^{0.566} \quad for\ \ 0 < \frac{z}{RHR^{0.4}} < 0.08 \tag{2.21}$$

$$m_p = 0.026\, RHR \left(\frac{z}{RHR^{0.4}} \right)^{0.909} \quad for\ \ 0.08 < \frac{z}{RHR^{0.4}} < 0.20 \tag{2.22}$$

$$m_p = 0.124\, RHR \left(\frac{z}{RHR^{0.4}} \right)^{1.895} \quad for\ \ 0.20 < \frac{z}{RHR^{0.4}} \tag{2.23}$$

2.6.4 Thomas

The Thomas plume model, Eq. (2.24), is intended for entrainment in the near field or flame region, when the mean flame height is considerably smaller than the fire diameter. In this region, the entrained air is less influenced by the heat release rate then by the fire perimeter, and therefore the fire diameter.

$$m_p = 0.59\, D\, z^{3/2} \tag{2.24}$$

2.7 Vent flow

On Figure 2.17 and on Figure 2.18 typical pressure profiles and gas flow velocities in vertical opening are presented in case of respectively a pre-flashover fire and post-flashover fire.

For a rectangular opening, the mass flow through a vertical vent, m_{VV}, can be estimated by integrating the Bernoulli law on the opening height, Eq. (2.25).

$$\dot{m}_{VV} = C_d \, b_w \int_{Z'}^{Z''} \frac{p_A(z)}{R\,T_A} \sqrt{2\,R\,T_A \left(1 - \frac{p_B(z)}{p_A(z)}\right)}\, dz \tag{2.25}$$

With A : variable at origin of the flux
B : variable at destination of the flux
Z' & Z'': bounds of integration on height Z
b_w : width of the opening
C_d : discharge coefficient

Z_S is the height of the interface between the hot gases toward the ceiling and the cold gases toward the floor. Z_p is the height of the neutral plane, i.e. the height at which the pressures inside and outside the compartment are equals.

In pre-flashover conditions the mass flow through opening leaving the compartment can be estimated by the simple relationship given by Eq. (2.26) (Rocket, 1976).

$$\dot{m}_{VV,out} = \frac{2}{3} C_d \, A_w h_w^{1/2} \rho_a \left(2g \frac{T_a}{T}\left(1 - \frac{T_a}{T}\right)\right)^{1/2} \left(1 - \frac{Z_p}{h_w}\right)^{3/2} \tag{2.26}$$

With A_w : area of the opening
h_w : height of the opening

Eq. (2.26) can be reduced to the following proportionality (Drysdale, 1999), Eq. (2.27).

$$\dot{m}_{VV,out} \propto g^{1/2} \rho_a A_w h_w^{1/2} = g^{1/2} \rho_a V_f \tag{2.27}$$

Eq. (2.27) enables to introduce the ventilation factor $V_f = A_w h_w^{1/2}$ that is of major importance in the compartment fire dynamic and that will be very often used in this dissertation.

It is also interesting to note that in post-flashover condition the neutral plane is usually at about one third of the height of the opening.

$$\frac{Z_p - Z_{sill}}{Z_{sof} - Z_{sill}} \approx \frac{1}{3} \tag{2.28}$$

The heat transfer by convection through the opening is then given by Eq. (2.29).

$$\dot{q}_{VV} = \dot{m}_{VV} \, c_p \, T_g - \dot{m}_{VV} \, c_p T_{out} \approx 0.5 \, V_f c_p \left(T_g - T_{out}\right) \tag{2.29}$$

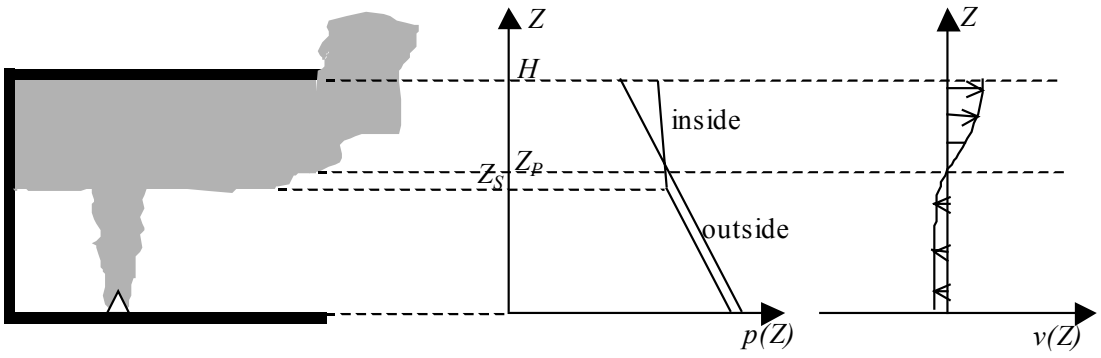

Figure 2.17 Pressure profile and gas velocity in opening during a pre-flashover compartment fire

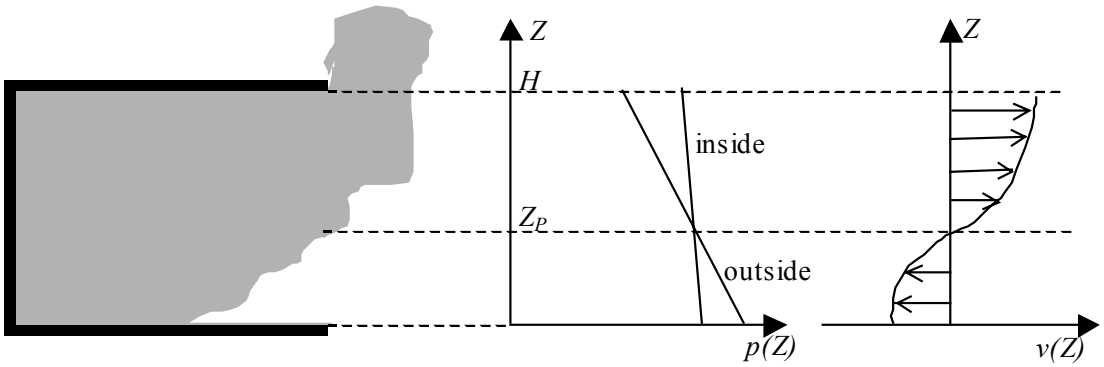

Figure 2.18 Pressure profile and gas velocity in opening during a post-flashover compartment fire

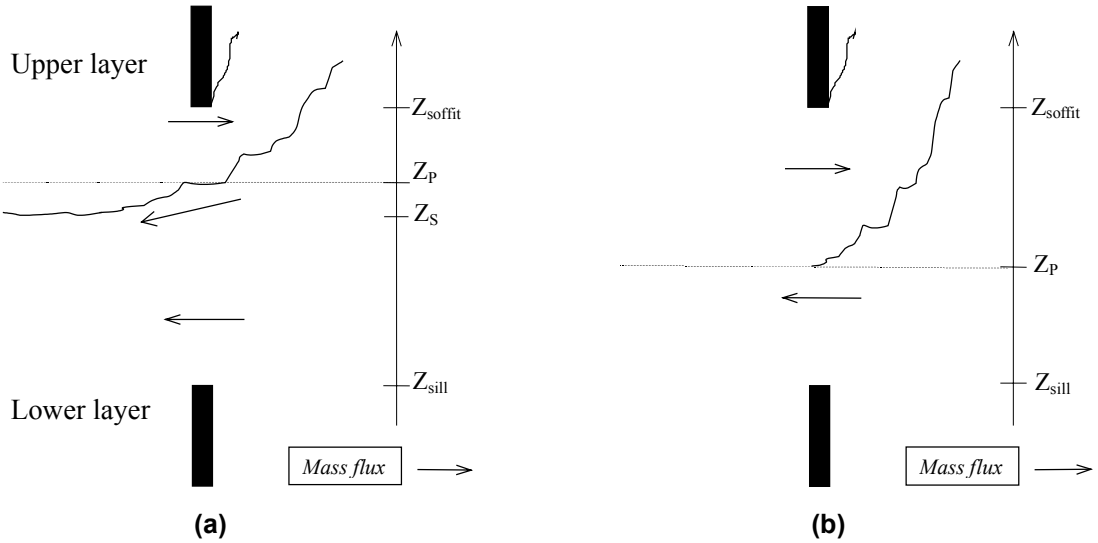

Figure 2.19 vent flow in pre- (a) and post-flashover (b) compartment fires

2.8 Ceiling jet

The ceiling jet is the flow of hot gases that spread out radially when the fire plumes impinges on the ceiling of a compartment (see Figure 2.4). Various correlations exists to determine the temperature and velocity flow in the ceiling jet, for example (Alpert, 1972). They usually are used to design fire detection and fire suppression (sprinkler) devices, matters which are not directly treated in this work.

2.9 Energy balance

The energy balance of a compartment fire can be written as stated in Eq. (2.30). This equation express the fact that, at each instant, the energy released by the fire (*RHR*) is equal to the energy loss to the partitions by conduction through it ($\dot{q}_p$), plus the energy loss by convection ($\dot{q}_{v,c}$) and radiation ($\dot{q}_{v,r}$) through the vents, plus the energy used to heat the gas in the compartment ($\dot{q}_g$). The controlled volume is the upper layer for the pre-flashover phase and the whole compartment for the post-flashover phase.

$$RHR - \left(\dot{q}_p + \dot{q}_{v,c} + \dot{q}_{v,r} + \dot{q}_g \right) = 0 \tag{2.30}$$

The energy used to heat the gas in the compartment is very small compare to the other terms and is thus often neglected. As it is usually quite small, the term taking into account the radiation through the vents is also often neglected, leading to the simplified energy balance of Eq. (2.31).

$$RHR - \left(\dot{q}_p + \dot{q}_{v,c} \right) = 0 \tag{2.31}$$

3

Overview and analysis of existing compartment fire models

Note:

This chapter is divided into two parts. In the first part, a review of existing models of compartment fire is presented, sections 3.1 to 3.4. In the second part, analyses of some of these models is presented, sections 3.5 to 3.10.

PART 1 : EXISTING MODELS

3.1 Introduction to the overview

Compartment fire models are aimed at estimating the evolution of the characteristics of the environment within a compartment during a fire. As this work is concerned with structural behaviour, it will focus on the temperature evolution within the compartment.

Compartment fire models may or may not include explicitly some of the sub-models described in chapter 2. In fact, the degree of development of these sub-model distinguish to a large extent one compartment fire model from another. In the most simple models, the user must specify some or all the particular elements, while in more complex compartment fire models, the model evaluates the same phenomena based on fundamental principles. For example, zone models generally use the Bernoulli equation, that is a particular solution of the fluid dynamics equations, to estimate the vent flow, see section 2.7, while CFD codes calculate this flow directly based on the fundamental dynamics of the fluid flow. Nevertheless most models require at least a few empirical correlations. For example only a few attempt to calculate fire growth based on fundamental principles have been done for the specification of the fire source.

There are several possibilities to model the fire within a building compartment. Some of the most widely used models are:

- pre-flashover analytical fire models;
- post-flashover analytical fire models:
  - nominal fire curves;
  - equivalent time methods;
  - parametric temperature-time curves;
- numerical models:
  - one-zone models;
  - two-zone models;
  - computational fluid dynamic models.

The objective of this chapter is not to explain all the models (hypothesis, developments, field of application) in an exhaustive way. The main aim is to give an overview of what exists and to give the basis on which the work made in this thesis has been established. Even if all these methods constitute important engineering tools, only the one on which the research efforts of this work are focused will be further discussed, i.e.:

- equivalent time methods;
- parametric curves;
- zone modelling.

3.2 Pre-flashover fire

3.2.1 McCaffrey, Quintiere and Harkleroad (1981)

McCaffrey *et al.* (1981) have proposed a method for predicting the upper layer gas temperatures of a pre-flashover compartment and the likelyhood of the occurence of flahsover. They have based their work on a simplified energy balance. Using some simple assumptions described in chapter 2 of this work to estimate the loss of energy to the partitions and through the vents, they deduce a simple relationship fot the temperature rise given by Eq. (3.1).

$$\frac{\Delta T}{T_a} = C X_1^{\ N} X_2^{\ M} \tag{3.1}$$

with $X_1 = \dfrac{RHR}{\sqrt{g}\rho_a T_a c_p A_w \sqrt{h_w}}$ and $X_2 = \dfrac{h_k A_t}{\sqrt{g}\rho_a c_p A_w \sqrt{h_w}}$

where $h_k = \sqrt{\dfrac{c\rho_p k_p}{t}}$ *if* $t < t_p$

$h_k = \dfrac{k_p}{e_p}$ *if* $t > t_p$

X_1 and X_2 are dimensionless parameters. The first parameter represent the ratio of the energy released by the fire to the energy convected through the windows; the second parameter represent the ratio of the energy lost to the boundary to the energy convected through the windows. The different variables of these equations have been defined in chapter 2. The value of the coefficients C, N and M (1.63, 2/3 and –1/3) have been set to best fit with experimental fire tests (see Figure 3.1).

MaCaffrey et al. take the temperature rise to be the parameter that indicate the onset of flashover condition in a compartment. Assuming that ΔT = 500°C is a conservative criterion, from Eq. (3.1) it is thus easy to determine the values for the physical parameters controlling the fire wich correspond to this temperature rise of 500°C.

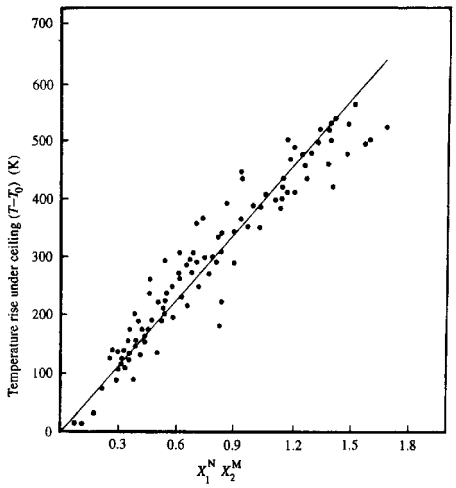

Figure 3.1 Correlation of upper-layer temperatures and the product $X_1^N X_2^M$

3.2.2 Foote, Pagni and Alvares

Foot et al. have proposed some analytical formulation to take into account the effect of forced ventilation on compartment fires. This method is based on the model of McCaffrey et al. (see section 3.2.1) and its formulation can be found in Walton (1995).

3.3 Post-flashover fire

The simplest way to represent a fire is by a relation giving the evolution of the temperature of the gases as a function of time. Such functions are called *nominal fire curves* and are presented first.

Parametric fires provide a simple mean to take into account the most important physical phenomenon which may influence the development of a fire in a particular building. Like nominal fires, they consist of time temperature relationships, but these relationships contain some parameters deemed to represent particular aspects of the reality. In almost every parametric fire which can be found in the literature, three parameters are taken into account, in one way or another, namely

- the fire load present in the compartment,
- the compartment geometry and the openings present in the partitions and
- the type and nature of the different walls of the compartment.

Parametric fires are based on the hypothesis that the temperature is uniform in the compartment, which limits their field of application to post-flashover fires in compartments of moderate dimensions. They nevertheless form a significant step forward toward the consideration of the real nature of a particular fire when compared to nominal fires, while still having the simplicity of some analytical expressions, i.e. no sophisticated computer tool is required for their application. The three mentioned parameters are the data that the user has to determine in each particular case.

As they are the basis of the Eurocode method, the Swedish method are first described. Eurocode 1 curves are then presented. They have been improved several times. The last version is given in annex A of EN 1991-1-2 (2002).

Other methods are due to Babrauskas (1979, 1981), Law (Walton 1995), Lie (1974, 1995), Ma and Mäkeläinen (2000) and Barnett (2002). They are not analysed in detail in this work, only basic information is given.

The main interest of these curves of Ma and Mäkeläinen (2000) and Barnett (2002) is that they have a shape closer to the shape of temperature-time curves measured during full scale fire tests. The main parameter of the model is the maximum temperature in the compartment during the fire. These authors propose to estimate the maximum temperature by empirical formulae coming from literature.

3.3.1 Nominal Fire Curves

Historically, nominal fire curves were developed for the purpose of experimental testing of elements with the aim of classification of these elements, because it was highly desirable that different elements tested in different laboratories would be submitted to the same thermal action.

When it comes to representing a fire in a building, these curves are a very poor representation of reality. The main characteristic of the nominal fire curves is that they are completely independent of conditions that will govern a real fire that would attack the structure of a building. For example, the same curve is used in a large industrial hall or in a small room of an office building.

Yet, for historical reasons, because of the so many years during which they have been used, they continue to be, by far, the most often used representation of a fire in practical structural design applications. This is why the nominal fire curves are mentioned here, although they are far from any performance-based concept.

Some of the most widely used curves are represented on Figure 3.2, namely the ISO curve, the ASTM curve, the hydrocarbon fire curve and the external fire curve. It can be noticed that no cooling down phase is present in any of these curves. Another important feature is that there is only one temperature for the compartment, which means that the temperature is supposed to be uniform in the compartment.

There are only two ways by which some kind of fire performance based design can be exercised with nominal fire curves:

- By the choice of the nominal curve; usually the hydrocarbon curve when liquid fuel is supposed to burn, the ISO or the ASTM curve for a fire in a building, and the external curve for a structural element located outside the envelope.
- By the choice of the time during which the fire has to be considered, 30, 60 or 90 minutes for example, depending on different conditions regarding the building and on the consequences of a failure.

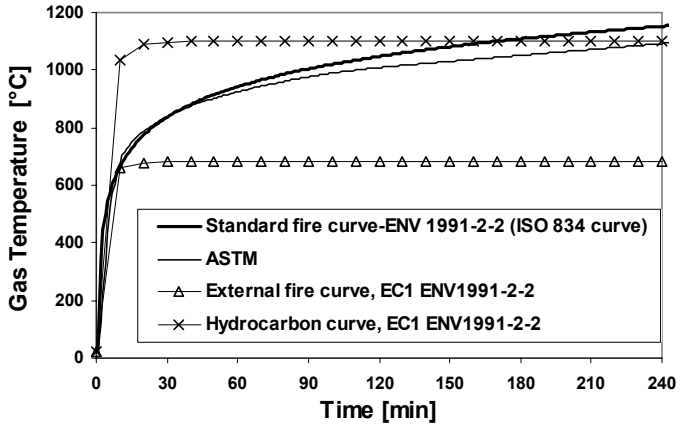

Figure 3.2 Nominal fire curves

3.3.2 Equivalent time methods

3.3.2.1 Principle and review of equivalent time methods

Standard fire curves are far from any real fire. Nevertheless a lot of fire tests on structural elements submitted to standard fire curves have been performed and thus, it is interesting to relate real fires to the standard tests. The concept of equivalent fire severity was thus introduced, stating that the effect of a real fire on a structure is equivalent to the effect of a certain duration, the equivalent time, of a standard fire on the same structure.

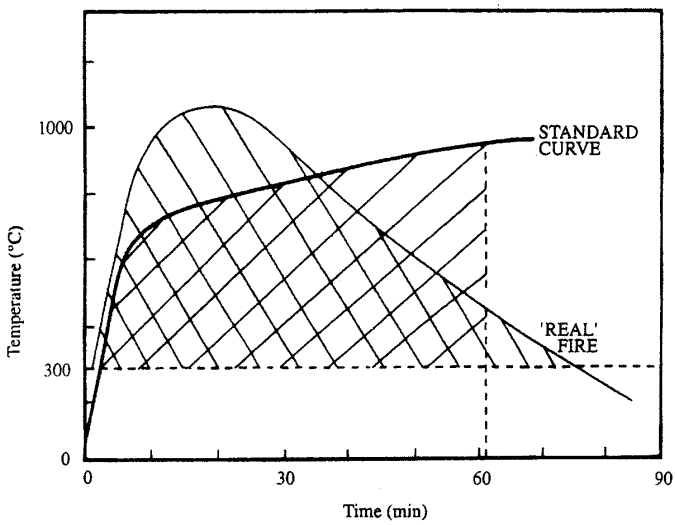

Figure 3.3 Equivalent fire severity according to Ingberg

In 1928, Ingberg has shown that the fire severity, i.e. the effect of a fire on a structure, was correlated to the fire load present in the fire compartment. Ingberg postulates that if the areas above a base line of 300°C and below temperature time curves of two fires are equal, the severities are identical, see Figure 3.3. If one of these fires is a standard fire curve of a given duration, the equivalent time of fire exposure is that standard fire duration.

Although the method proposed by Ingberg was given in a tabulated form, Eq. (3.2) represents it, expressing that the equivalent time is proportional to the fire load.

$$t_e \propto q_f \tag{3.2}$$

The work of Kawagoe (1963, 1964) leads to Eq. (3.3) which first includes the effect of the ventilation.

$$t_e = k_2\, q_f \left(\frac{A_t}{A_w \sqrt{h_w}} \right)^{0.23} = k_2\, q_f\, O^{-0.23} \tag{3.3}$$

Pettersson (1976) has then included the effect of the thermal inertia of partitions through the coefficient k_3 of Eq. (3.4)

$$t_e = k_3\, q_f \frac{A_f}{\left(A_w \sqrt{h_w}\, A_t \right)^{1/2}} \tag{3.4}$$

A wide variety of equivalent time formulas exists. Two recent reviews have been done by Law (1997) and in the NFSC1 (1999) research. The formulae given above have been selected in order to point out the main evolutions of the time equivalent concept.

As the Eurocode 1 methods are further analysed in this work, they will be described more in details in the next paragraphs. The main difference between Eurocode methods and others is the way the ventilation is taken into account in the formulation.

So, equivalent time can be defined to be the time during which a structural element has to be submitted to a standard fire curve in order to obtain the same decisive effect as a fire, in a given compartment and for a given fire load, would have produced on the structural element.

3.3.2.2 ENV version (1993)

Annex E of Eurocode 1 offers a simple equation (3.5) to determine the required fire resistance time $t_{e,d}$ for a compartment, equivalent to the same duration of an ISO curve fire.

$$t_{e,d} = q_{f,d} k_b w_f \tag{3.5}$$

Before starting the calculation, it is necessary to determine the floor area of the compartment A_f as well as the total fire load $Q_{fi,k}$,mainly depending on the combustibility of the component parts and of the stored material. Annex D of EC1 1993 can be applied for this purpose. The design fire load density $q_{f,d}$ can be obtained from the multiplication of the characteristic fire load $q_{f,k}$ by the safety factors γ_n and γ_q for the accepted failure risk in the case of fire and the influence of active fire measures, equation (3.6).

$$q_{f,d} = \gamma_q \gamma_n q_{f,k} = \gamma_q \gamma_n \frac{Q_{fi,k}}{A_f} \tag{3.6}$$

The conversion factor k_b in equation (3.5) accounts for the heat transfer in the neighbouring component parts of the compartment. It depends on the thermal properties of the walls and ceilings of the enclosure. Where no detailed assessment of the thermal properties of the enclosure is made, the conversion factor k_b may be taken as:

$k_b = 0{,}07$ [min · m^2/MJ] when q_d is given in [MJ/m^2]

Otherwise k_b may be related to the thermal property $b = \sqrt{(\rho c \lambda)}$ of the enclosure according to Table 3.1.

The ventilation factor w_f can be calculated by Eq. (3.7)

$$w_f = \left(\frac{6}{H}\right)^{0.3} \left(0.62 + 90 \frac{(0.4 - \alpha_v)^4}{(1 + b_v \alpha_h)} \right) \geq 0.5 \tag{3.7}$$

This equation depends on the height of the compartment H and on the ratios of the vertical (α_v) and horizontal (α_h) opening areas to the floor area A_f. The dimensionless factor b_v is determined by Eq. (3.8).

$$b_v = 12.5\left(1 + 10\alpha_v - \alpha_v^2\right) \geq 10 \tag{3.8}$$

For small fire compartments [$A_f < 100$ m^2] without openings in the roof, the factor w_f may also be calculated as:

$$w_f = O^{-1/2} A_f / A_t \tag{3.9}$$

Table 3.1 Conversion factor k_b depending on the thermal properties of the enclosure

$b=(\rho c \lambda)^{1/2}$	k_b
[J/m^{2}s$^{1/2}$K]	[min m^2/MJ]
$b > 2\,500$	0,04
$720 \leq b \leq 2\,500$	0,055
$b < 720$	0,07

3.3.2.3 EN version (2002)

Only few modifications of the ENV method are proposed in the EN1991-1-2. It is mentioned that this approach may be used where the design of members is based on tabulated data or other simplified rules, related to the standard fire exposure.

It is also noted that the method is material dependent and that it is not applicable to composite steel and concrete or timber constructions. It is thus applicable to reinforced concrete, protected steel and to unprotected steel.

The equivalent time of ISO-fire exposure is defined now by :

$$t_{e,d} = \left(q_{f,d}\ k_b\ w_f\right) k_c \quad \text{[min]} \tag{3.10}$$

where $q_{f,d}$ is the design fire load density

The k_b and w_f have undergone no modification since the ENV1991-1-2. A new factor k_c is introduced into the formula, it is a correction factor function of the material composing structural cross-sections. k_c is equal to one for reinforced concrete and protected steel and equal to 13.7 O for unprotected steel.

3.3.3 Swedish fire curves (Magnusson, Thelanderson, 1970)

Parametric fire curves were presented by Magnusson and Thelanderson (1970) and Petterson *et al.* (1976). They are based on the application of one of the first numerical one-zone model (Petterson *et al.* 1976) (see section 3.4.1.1) and on comparison with experimental tests. These curves are often referred to as the Swedish Method.

The maximum heat release rate considered for calculating the Swedish fire curves is based on the evaluation of the mass loss rate by the Kawagoe relationship (see section 2.7) considering an effective combustion heat of 10.8 MJ/kg. The shape of the rate of heat release curves, based on experimental measurements, is shown on Figure 3.4.

No equations are available for these parametric fire curves, they are provided on tabulated and graphical form (Figure 3.5) for different fire loads and opening factors, $O = A_w h_w^{1/2}/A_t$. This latter parameter has in fact been introduce by the authors of the method described here.

The graphs of Figure 3.5 are for a compartment with partitions made of lightweight concrete, with a b factor (square root of the thermal inertia, $b = \sqrt{c\rho\lambda}$) of 1160 J/m^{2}s$^{1/2}$K. To take into account other thermal properties of the partitions the opening factor and the fire load should be multiplied by a factor which depends on the nature of the partitions.

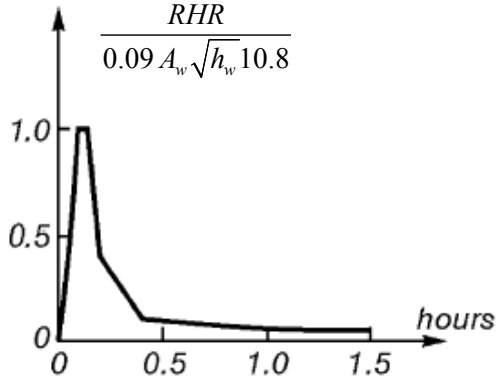

Figure 3.4 Heat release rate curves considered for calculating the Swedish fire curves.

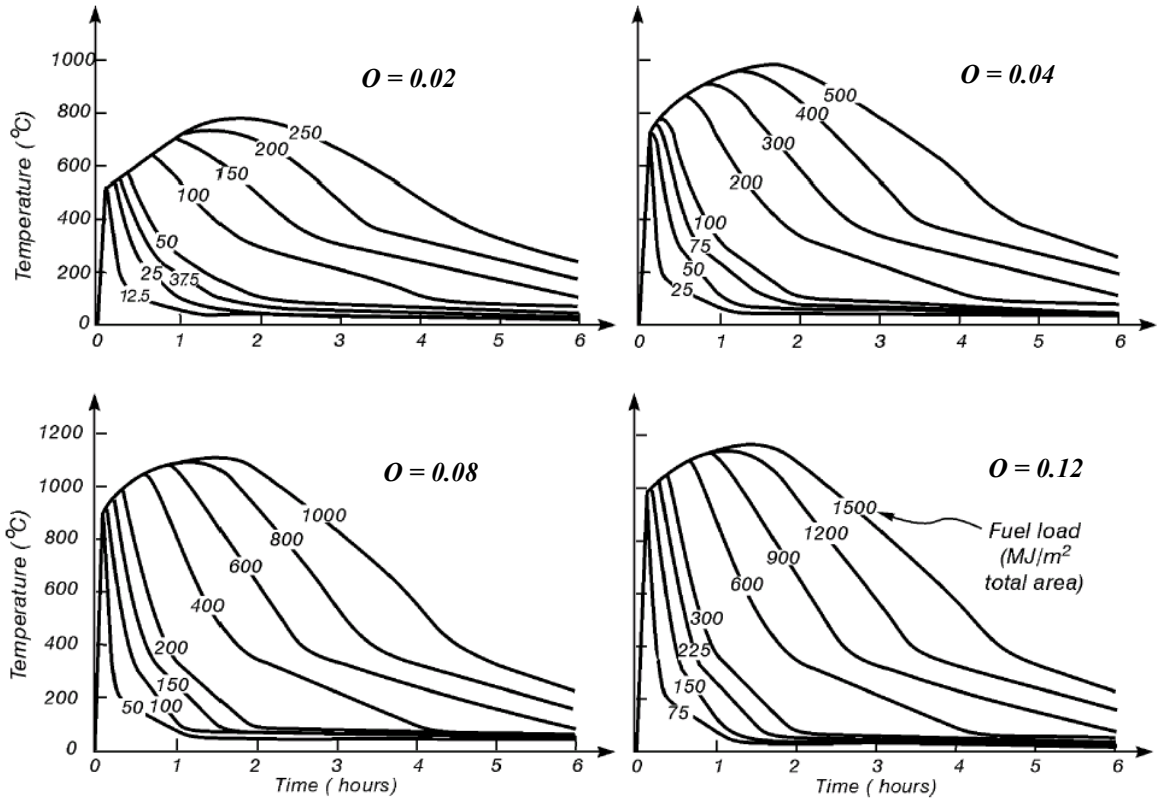

Figure 3.5 Swedish fire curves (Peterson 1976)

3.3.4 Parametric model of Eurocode 1

Eurocode 1 gives an equation for parametric fires, allowing a time–temperature relationship to be produced for combinations of fuel load, ventilation opening and partition material. According to Feasey and Buchanan (2002), the Eurocode ENV1991-1-2 (1993) parametric fire curves, described in section 3.3.4.1, were derived to give a good approximation to the burning period of the Swedish curves shown in Figure 3.5. Unfortunately the background of these parametric fire curves has not been published formally.

In the EN 1991-1-2 published in 2002, the basic equations of the ENV version have been kept but some improvements have been proposed. Improvements are mainly related to the burning regime, the effect of the partition material and the decreasing phase. The basis of these improvements (Franssen 2000, NFSC1 1999, ARBED 2001) are described and the formulation is explained, section 3.3.4.2.

Feasey and Buchanan (2002) have analysed the ENV1991-1-2 (1993) and proposed some improvements which will be described briefly in section 3.3.4.3.

3.3.4.1 ENV version (1993)

The evolution of the gas temperature in the compartment is given by :

$$\Theta_g = 1325\left(1 - 0.324e^{-0.2\,t^*} - 0.204e^{-1.7\,t^*} - 0.472e^{-19\,t^*}\right) \tag{3.11}$$

with $t^* = \Gamma\ t$ (3.12)

$$\Gamma = \frac{\left(O/0.04\right)^2}{\left(b/1160\right)^2} \tag{3.13}$$

$$O = \frac{A_v\sqrt{h_v}}{A_t} \tag{3.14}$$

$$b = \sqrt{c\rho\lambda} \tag{3.15}$$

and t time, in hour; A_v area of vertical openings, in m², h height of vertical openings, in m, A_t total area of enclosure (walls, ceiling and floor, including openings), in m²; and c, ρ, λ thermal properties of boundary of enclosure (b in J/m²s$^{1/2}$K).

Eq. (3.11) describes the evolution of the temperature during the heating phase, the duration of which is determined by the fire load and the opening factor according to equation (3.16).

$$t_d^* = 0.13 \times 10^{-3} \quad q_{t,d} \quad \Gamma/O \tag{3.16}$$

with $q_{t,d}$ design value of the fire load density related to A_t, in MJ/m².

The temperature-time curve in the cooling phase is given by:

$$\Theta_g = \Theta_{\max} - 625\left(t^* - t_d^*\right) \qquad \text{for } t_d^* \le 0.5 \tag{3.17}$$

$$\Theta_g = \Theta_{\max} - 250\left(3 - t_d^*\right)\left(t^* - t_d^*\right) \qquad \text{for } 0.5 \le t_d^* \le 2.0 \tag{3.18}$$

$$\Theta_g = \Theta_{\max} - 250\left(t^* - t_d^*\right) \qquad \text{for } 2.0 \ge t_d^* \tag{3.19}$$

with $\Theta_{\max}$ maximum temperature in the heating phase, for $t^* = t_d^*$.

For a two layer partitions, Eq. (3.20) is proposed to evaluate an equivalent b factor.

$$b_{eq} = \sqrt{\frac{s_1 \; c_1 \; \lambda_1 \; + \; s_2 \; c_2 \; \lambda_2}{\dfrac{s_1 \; c_1 \; \lambda_1}{b_1^2} \; + \; \dfrac{s_2 \; c_2 \; \lambda_2}{b_2^2}}} \quad \text{with } s_i \text{ the thickness of layer } i \tag{3.20}$$

This parametric fire is valid for compartments up to 100 m² of floor area, without openings in the roof and for a maximum compartment height of 4 m. b must be in the range of 1000 to 2000 J/m^{2}s$^{1/2}$K, and O must be lie between 0.02 and 0.20 m$^{1/2}$.

Figure 3.6 shows the shape of the temperature-time curve given by equations (3.11) to (3.19) for an opening factor O equal to 0.04 and the b factor (square root of $\lambda c\rho$) equal to 1160 J/m^{2}s$^{1/2}$K and thus for a Γ factor, Eq. (3.13), equal to 1 for which t^* is equal to t, Eq. (3.12). When t^* equal t, Eq. (3.11) is the standard fire curve given by the Swedish Building Regulations. For the heating phase, the method consists thus to make a time scale modification (Wickström 1985), function of the opening factor and of the b factor, of the Swedish standard fire curve. For this case, the heating curve is also very similar to the ISO curve, see Figure 3.6.

Increasing the opening factor would lead to a shorter but more severe fire. Increasing the thermal effusivity would lead less severe fire without modification of the fire duration. In the example above, the fire load is 150 MJ/m², leading to a fire duration of 30 minutes. Modifying the fire load has an influence on the duration of the heating phase. It is interesting to note that the maximum temperature for this particular case is about 800°C after 30 minutes and that the total fire duration is about 110 minutes.

It is also interesting to note that the parametric curve on Figure 3.6 corresponds quite well to the Swedish fire curve which would be obtained with the same opening factor and same fire load; see Figure 3.5, upper right graph, a curve between 100 and 200 MJ/m^2 curves.

When there is more than one opening, Figure 3.7, the following procedure, Eqs. (3.21) to (3.23) is proposed to calculate the equivalent opening factor.

$$A_{w,t} = A_{w1} + A_{w1} + ... + A_{wn} \tag{3.21}$$

$$h_{w,t} = \frac{A_{w1}A_{w1} + A_{w2}h_{w2} + ... + A_{wn}h_{wn}}{A_{wt}} \tag{3.22}$$

$$O = \frac{A_{wt}\sqrt{h_{vt}}}{A_t} \tag{3.23}$$

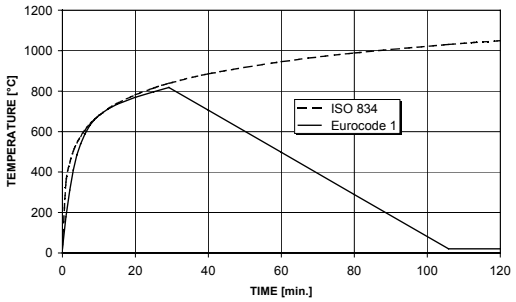

Figure 3.6 parametric fire and ISO curve

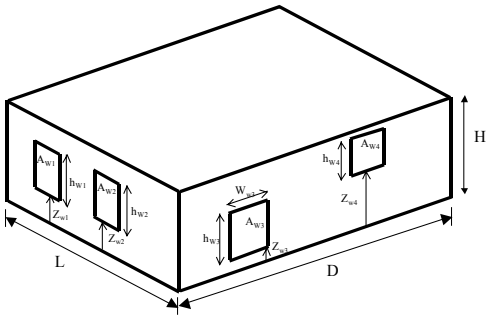

Figure 3.7 Compartment with multiple openings

3.3.4.2 EN version (2002)

The curves proposed in the 2002 edition of EC1 are based on the EC1 1993 curves. Eqs. (3.11) to (3.15) remain identical. Nevertheless several improvements have been introduced. They are based on work by Franssen (2000) in the NFSC1 (1999) research with additional improvements made by ARBED (2001). The improvements have been made on the basis of theoretical developments and to comparison with full scale fire tests.

The improvements mainly concern three aspects :

- the way to take into account partitions with layers of materials having different thermal properties;
- the introduction of a fuel controlled fire by setting a minimum fire duration
- some modifications in the decay phase.

Basis of improvements

a) Fire regime

One of the main hypotheses on which the parametric fire of EC1 1993 is based is that the fire is ventilation controlled and thus that energy release during the fire is directly related to the ventilation conditions. Indeed, considering that the heat content of the fuel is 16 MJ/kg and that 2/3 of the fuel load has been burnt at the end of the heating phase (Figure 3.8), Eq. (3.16) can easily be transformed into the following one :

$$\dot{m}_{fi} = 337 A_w \sqrt{h_w} \tag{3.24}$$

where $\dot{m}_{fi}$ is the burning rate in kg/h.

Eq. (3.24) is Kawagoe's correlation for the burning rate of wood cribs in an air controlled fire. It is thus obvious that the ENV1991-1-2 method is only valid for ventilation controlled fires that involve cellulosic fire load and it is proposed to extend the application of the method to fuel controlled fires.

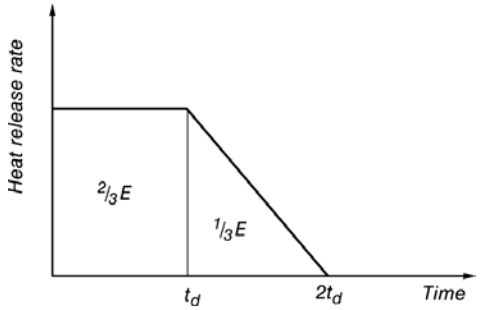

Figure 3.8 Shape of rate of heat release behind EC1 parametric fire curves

b) Boundary conditions

There are two major problems with equation (3.20) which was proposed in the EC1 1993.

The first one is that this equation is symmetric in 1 and 2. In other words, a wall made of a heavy material insulated from the fire by a lightweight material has the same b_{eq} as a wall with a core made of the lightweight material covered by a layer of the heavy material. It is clear that, in reality, the energy transferred from the hot air to the wall will be mainly influenced by the material which is in direct contact with the air.

The second one is that the thickness of each layer plays the same role. Due to this, a wall made of a reasonable thickness of a material 1 covering a very thick material 2 will have an equivalent effusivity almost equal to b_2 whereas, in reality, this material 2 will play a secondary role.

Formulation

a) Fuel controlled fires

The new method allows determining if the fire is ventilation controlled or fuel controlled. The procedure is to first calculate the fire duration of the heating phase in case of ventilation controlled fire and to check if this duration is higher than a minimum duration, t_{lim}. The minimum fire duration is the one of the fire if it is fuel controlled. This duration of fuel controlled fire is thus assumed to be known.

The duration of the ventilation controlled fire is evaluated with the hypothesis of Kawagoe, i.e. the rate of burning is proportional to the ventilation factor. This hypothesis was already adopted in the EC1 1993, nevertheless the coefficient of 0.13 in Eq. (3.16) is now set to 0.2, see Eq. (3.26). For a given ventilation factor, a slower rate of burning is thus considered.

The duration of the fire in case of fuel controlled fire $t_{\lim}$ is supposed to be dependent of the rate of growth of the fire (see chapter 5 section 5.4.2 for the definition of the fire growth rate). In case of slow fire growth rate, $t_{\lim}$ is fixed to 25 minutes; in case of medium fire growth rate, $t_{\lim}$ is fixed to 20 minutes and in case of fast fire growth rate, $t_{\lim}$ is fixed to 15 minutes.

The maximum temperature $\Theta_{\max}$ in the heating phase happens for $t^* = t_d^*$

$$t_d^* = t_{\max} \cdot \Gamma \quad \text{[h]} \tag{3.25}$$

$$\text{with } t_{\max} = \max\left[(0{,}2 \cdot 10^{-3} \cdot q_{t,d} / O)\ ;\ t_{\lim}\right] \text{[h]} \tag{3.26}$$

where

$q_{t,d}$ is the design value of the fire load density related to the total surface area A_t of the enclosure whereby $q_{t,d} = q_{f,d} \cdot A_f / A_t$ [MJ/m^2]. The following limits should be observed: $50 \le q_{t,d} \le 1\,000$ [MJ/m^2].

$q_{f,d}$ is the design value of the fire load density related to the surface area A_f of the floor [MJ/m^2] taken from Annex E of EC1 2002.

The time t_{max} corresponding to the maximum temperature is given by t_{lim} in case the fire is fuel controlled. If t_{max} is given by $(0{,}2 \cdot 10^{-3}\ q_{t,d} / O)$, the fire is ventilation controlled.

When $t_{max} = t_{lim}$, t^* used in equation (3.11) is replaced by

$$t^* = t \cdot \Gamma_{lim} \quad [h] \tag{3.27}$$

$$\text{with } \Gamma_{lim} = [O_{lim}/b]^2 / (0{,}04/1\,160)^2 \tag{3.28}$$

$$\text{where } O_{lim} = 0{,}1 \cdot 10^{-3} \cdot q_{t,d} / t_{lim} \tag{3.29}$$

If ($O > 0{,}04$ and $q_{t,d} < 75$ and $b < 1\,160$), Γ_{lim} given by Eq. (3.28) has to be multiplied by k given by:

$$k = 1 + \left(\frac{O - 0.04}{0.04}\right)\left(\frac{q_{t,d} - 75}{75}\right)\left(\frac{1160 - b}{1160}\right) \tag{3.30}$$

According to Franssen (2000), in case of fuel controlled fires, this formulation is based on the following theoretical remarks: The limit opening factor that has been introduced in the above paragraph allows the fire to slow down in case of large openings that lead to get a fuel controlled fire. In this sutuation, not all the air entering through the openings is used for combustion but convective losses, that slow down the temperatures, remains linked to the total mass of gas exchanged. This modification slows down the fire and reduces the temperature level. There is yet an influence of the openings which is still present when the fire is fuel controlled; the amount of gas passing through the openings is higher than what the fictitious opening factor O_{lim} tends to indicate. A more important part of the energy produced by the fire is therefore extracted of the compartment by mass transfer, and this also tends to limit the elevation of the temperature in the compartment.

The coefficient 0.1 10^{-3} in Eq. (3.29) and the formulation of Eq. (3.30) have been chosen to get a good correlation with the fire tests.

b) Boundary conditions

1. The limits of the b factor have been extended to $100 \le b \le 2200$ J/m²s$^{1/2}$K.

2. To account for an enclosure surface with different layers of material, $b = \sqrt{(\rho c \lambda)}$ should be introduced as (Franssen 2000):

   If the index 1 represents the layer directly exposed to the fire, the index 2 the next layer, etc.

   If $b_1 < b_2$, $b = b_1$ (3.31)

   If $b_1 > b_2$, a limit thickness s_{lim} is calculated for the exposed material according to

   $$s_{lim} = \sqrt{\frac{3 \;\; 600 \;\; t_{max} \;\; \lambda_1}{c_1 \;\; \rho_1}} \quad [m], \text{ with } t_{max} \text{ given by Eq. (3.26)} \tag{3.32}$$

   If $s_1 > s_{lim}$ then $b = b_1$ (3.33)

If $s_1 < s_{lim}$ then $b = \frac{s_1}{s_{\lim}} b_1 + \left(1 - \frac{s_1}{s_{\lim}}\right) b_2$ (3.34)

s_i is the thickness of layer i

$b_i = \sqrt{(\rho_i c_i \lambda_i)}$

ρ_i is the density of the layer i

c_i is the specific heat of the layer i

λ_i is the thermal conductivity of the layer i

This formulation is based on the thermal penetration concept. The method has been compared to finite element simulation with a reasonable agreement.

3. To account for different b factors in walls, ceiling and floor, b should be introduced as:

$$b = (\Sigma(b_j A_j)) / (A_t - A_v) \quad (3.35)$$

where

A_j is the area of enclosure surface j, openings not included

b_j is the thermal property of enclosure surface j according to Eqs (3.15) and

c) Decreasing phase

The temperature-time curves in the cooling phase are given by :

$$\Theta_g = \Theta_{max} - 625\left(t^* - t^*_{max} x\right) \quad \text{for } t^*_{max} \le 0.5 \quad (3.36)$$

$$\Theta_g = \Theta_{max} - 250\ \left(3 - t^*_{max}\right)\left(t^* - t^*_{max} x\right) \quad \text{for } 0.5 \le t^*_{max} \le 2.0 \quad (3.37)$$

$$\Theta_g = \Theta_{max} - 250\left(t^* - t^*_{max} x\right) \quad \text{for } 2.0 \ge t^*_{max} \quad (3.38)$$

where t^* is given by Eq. (3.12);

$t^*_{max} = (0{,}2 \cdot 10^{-3} \cdot q_{t,d} / O) \cdot \Gamma$;

if $t_{max} > t_{lim}$, $x = 1{,}0$ or if $t_{max} = t_{lim}$, $x = t_{lim} \cdot \Gamma / t^*_{max}$.

These modifications, through the x factor and modified t^*_{max}, have been done to improve the correlation with fire tests (ARBED 2001).

3.3.4.3 Feasey & Buchanan (2002) proposals for improving ENV

Independently of the work made for the EN1991-1-2 (2002), Feasey and Buchanan have analysed the ENV 1991-1-2 (1993) fire curve and propose some improvements to give a better estimation of temperatures in post-flashover compartment fires. These improvement proposals are based on design fires calculated using the COMPF2 program (Babrauskas and Williamson 1979). They have first calibrated COMPF2 using results from a large number of full scale fire tests made in by Arnault et al. in 1973 and 1974 at CTICM, France. These tests have also been used in this work and are described in Chapter 6.

The recommended changes to the EC1 1993 parametric fire are to:

1. change the reference value of b from 1160 to 1900 W $s^{0.5}/m^2$ K in Eq. (3.13). The justification of this is that the COMPF2 calculation of the fire temperatures in a room of dense concrete (b=1900) is closer to the standard curve;
2. remove the lower limit of b =1000 $Ws^{0.5}/m^2K$, and use the actual value calculated for the construction materials;
3. calculate the rate of temperature decay, $\Gamma_{dec} = \Gamma = \frac{(O/0.04)^2}{(b/1160)^2}$ in Eq. (3.16) using a new fictitious time which is based on square root rather than squared terms, $\Gamma_{dec} = \sqrt{\frac{O/0.04}{b/1900}}$.

These rules have been found by trial and error, to get better fit between EC1 1993 formula and COMPF2 calculations.

They support the urgent need for further research into post-flashover fire behaviour and point out that deep compartment (as the one of the tests made by Kirby et al., 1994, see chapter 6 of this work) still need to be fully understood.

The rule 2 has also been adopted in the EC1 2002 while the rules 1 and 3 are not used.

3.3.5 Other parametric models

3.3.5.1 Babrauskas (1981, 1979)

Babrauskas (1981, 1979) has proposed a method for estimating the evolution of the gas temperature T_g during a compartment fire. This method has the form of Eq. (3.39) and the complete formulation can be found in SFPE handbook (Walton 1995).

$$T_g = T_a + (T^* - T_a) \cdot \theta_1 \cdot \theta_2 \cdot \theta_3 \cdot \theta_4 \cdot \theta_5 \tag{3.39}$$

where T_a is the ambient temperature; T^* is an empirical constant equal to 1725K; θ_1 is a factor related to the burning rate stoichiometry; θ_2 is a factor related to the steady state losses through the partitions; θ_3 is a factor related to the transient losses through the partitions; θ_4 is a factor related to the opening height effect; θ_5 is a factor related to the combustion efficiency.

The time dependency of the gas temperature is reflected through the coefficient θ_3 related to the partition transient losses.

3.3.5.2 Law

Law has proposed a method for the estimation of maximum gas temperature during a compartment fire. The method is empirical and is derived from experimental fires conducted by various laboratories. The complete formulation can be found in SFPE handbook (Walton 1995).

3.3.5.3 Lie (1974, 1995)

On the basis of temperature time computed by Kawagoe and Sekine (1963) with a zone model, Lie (1974, 1995) has proposed a relation to estimate the evolution of the gas temperature during a compartment fire, Eq. (3.40).

$$T_g = 250\left(\frac{10}{O}\right)^{0.1O^{0.3}} e^{-\frac{t}{O^2}}\left(3\left(1-e^{-0.6t}\right)-\left(1-e^{-3t}\right)+4\left(1-e^{-12t}\right)\right)+C\left(600\,O\right)^{0.5} \tag{3.40}$$

The fire duration τ is estimated on the basis of the Kawagoe relationship, Eq. (3.41).

$$\tau = \frac{Q}{330 V_f} \tag{3.41}$$

where Q is the total fire load and $V_f = A_w h_w^{1/2}$ is the ventilation factor.

For time larger then τ, the temperature is given by Eq. (3.42).

$$T_g = -600\left(\frac{t}{\tau} - 1\right) + T_{\max} \tag{3.42}$$

3.3.5.4 Ma & Mäkeläien (2000)

25 complete gas temperature-time curves collected from different laboratories have been non-dimensionalised by the maximum gas temperature and the time to reach the maximum temperature, are illustrated in Figure 3.9.

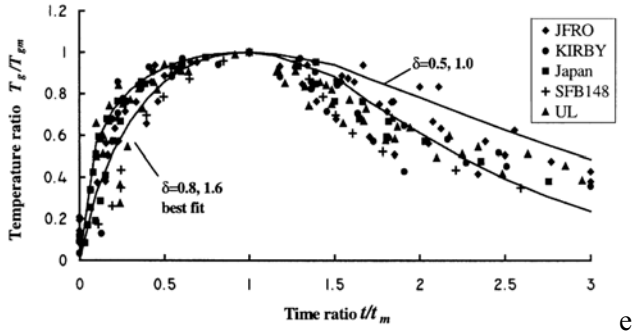

e

Figure 3.9 Non-dimensional temperature-time curves (Ma and Mäkeläien 2000)

It can be seen that these temperature-time curves are of similar shape. A non-dimensional expression based on curve-fitting procedure can be given by the Eq. (3.43).

$$\frac{T_g - T_0}{T_{gm} - T_0} = \left(\frac{t}{t_m}\exp\left(1 - \frac{t}{t_m}\right)\right)^{\delta} \tag{3.43}$$

where T_g is the gas temperature (°C), T_{gm} the maximum gas temperature (°C), T_0 the room temperature (20°C), t the time (min), t_m the time corresponding to the maximum gas temperature (min), and δ the shape constant of curve. For the ascending phase and the decaying phase, δ has different values. The constant for the descending phase is approximately twice that for the ascending phase.

T_{gm} is estimated with a new correlation proposed by the authors. t_m is estimated under the hypothesis of a ventilation controlled fire.

3.3.5.5 BFD Curves (Barnett 2002)

The basic equation that produces a ‘‘BFD Curve’’ is

$$T_g = T_0 + T_{gm}\, e^{-z} \quad with \quad z = \frac{\left(\log t - \log t_m\right)^2}{S_c} \tag{3.44}$$

where T_g is the temperature at any time t (°C), T_0 the ambient temperature (°C), T_{gm} the maximum temperature generated above T_0 (°C), log is natural logarithm (dimensionless

numbers), t the time from ignition of fire (min), t_m the time at which T_{gm} occurs (min), and S_c the shape constant for the temperature–time curve (dimensionless numbers).

T_{gm} is estimated with method coming from the literature, for example Law or Babrauskas methods (Walton, 1995). t_m is estimated according to design fire curves (see chapter 2, figure 2.14) which has to be defined by the user. A formula is proposed to estimate S_c which depend on the ventilation condition.

3.4 Numerical fire models

3.4.1 Zone Models

Zone models are numerical tools commonly used to evaluate the development of the temperature of the gases within a compartment during the course of a fire. Based on a limited number of hypotheses, they are easy to use and provide a good evaluation of the situation provided they are used within their real field of application. Different developments of numerical fire modelling have appeared since the first zone models were proposed (Kawagoe and Sekine, 1963; Pettersson et al., 1976; Babrauskas and Williamson, 1978), including multi-compartment and computational field dynamics models. Although single compartment zone models are the least sophisticated among numerical fire models, they have their own field of application and are essential tools in fire safety engineering practical applications.

The main hypothesis in zone models is that the compartment is divided into zones where each zone has a uniform temperature distribution at any time. In single zone models, the temperature is considered to be uniform in the whole compartment. This type of model is thus usually used in the case of fully developed fires. In two-zone models, there is a hot gas layer which is close to the ceiling and a cold gas layer which is close to the floor. Two-zone models are thus normally used in case of localised fires or during the pre-flashover phase.

For zone models, the data have to be supplied with a higher degree of detail than for the parametric curves and equivalent time methods. For example,

- every dimension of the compartment and of the openings must be given here, instead of a single opening factor,
- each wall can be described exactly with the presence of different materials if necessary, instead of a single thermal effusivity,
- not only the quantity of combustible material has to be given, but also the rate in time at which this energy is released.

3.4.1.1 One-zone models

One-zone models is the name given to numerical programs which calculate the development of the temperature of the gases as a function of time, integrating the ordinary differential equations which express the conservation of mass and the conservation of energy in the compartment. These models are based on the fundamental hypothesis that the situation, i.e. the temperature, is uniform in the whole compartment.

Solving the energy balance between the gas in the compartment, the walls, the openings and the energy released by the fire, and solving also the mass balance between the incoming and outgoing air through the openings as well as the combustion products released by the fire, a one-zone model gives not only the evolution of the temperature of the gases in the compartment, but

also additional information such as the temperatures in the walls or the velocity of the gases through the openings.

Figure 3.10 shows how a compartment is modelled, with different terms of the energy and mass balance represented.

Examples of one-zone models are COMPF2 (Babrauskas and Williamson 1979), NAT (Curtat 1992), OZone (Cadorin 2003a & b).

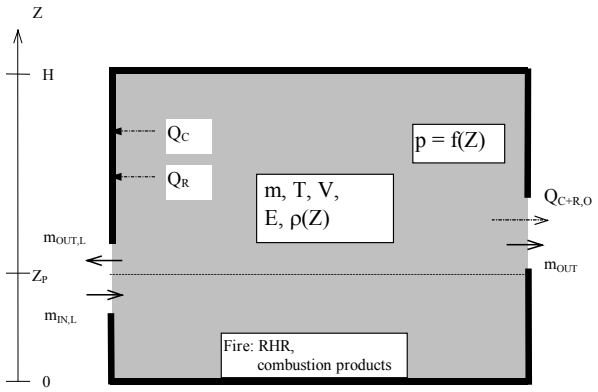

Figure 3.10 a one-zone model

3.4.1.2 Two-zone models

When the size of the fire is small compared to the size of the compartment in which it develops, the hypothesis of uniform temperature is not valid. Another hypothesis is based on the observation that in such a case there is an accumulation of combustion products in a layer beneath the ceiling (upper layer), with a more or less horizontal interface between this upper hot layer and the lower layer where the temperature of the gases remains much cooler. The main hypothesis of a two-zone model is that the situation, i.e. the temperature, is uniform in each layer, but different from one layer to another.

The equations expressing the equilibrium of mass and of energy are written for each of the two layers and exchange between the two layers has to be considered.

The data to be supplied are the same as those supplied for one-zone models. They concern the description of the geometry of the compartment, the definition of the walls, the openings and the combustible material.

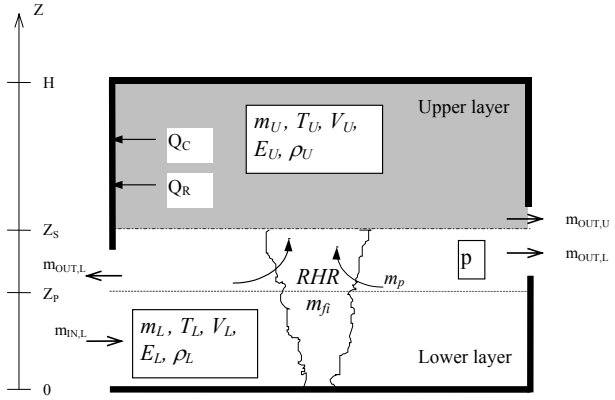

Figure 3.11 a two-zone model

As a result of the simulation, a gas temperature is given in each of the two layers, as well as information on walls temperatures and flux through the openings. An important result is the evolution as a function of time of the thickness of each layer. The thickness of the lower layer, which remains at rather cold temperature and contains no combustion product, is very important to judge the tenability of the compartment for the occupants.

It has to be judged by the user whether the results are still consistent with the hypothesis of the two-zone stratification. This is for example not the case if the thickness of the upper layer increases so much that it actually fills the whole compartment. Another case is when the temperature in the upper layer is so high that it leads to the flashover in the whole compartment, destroying the layer stratification and producing a situation which is closer to the hypothesis of a one-zone model.

Figure 3.11 shows how a compartment is modelled by a two-zone model, with different terms of the energy and mass balance represented.

Figure 3.11 is typical of a simple situation where the compartment exchanges mass and energy only with the outside environment. These kinds of models have yet the capability to analyse more complex buildings where the compartment of origin exchanges mass and energy with the outside environment but also with other compartments in the building. This is of particular interest to analyse the propagation of smoke from the compartment of origin towards other adjacent compartments where it can also be a thread for life. Such a situation, analysed by *multi-compartment two-zone models*, is depicted on Figure 3.12.

The main field of application of two-zone models is: Pre-flashover fire phase/localised fires; Simple geometry; Smoke propagation in multi compartment. Examples of two-zone models are ASET (Cooper 1983), CCFM (Forney 1987), CFAST (Jones 2000), OZone (Cadorin 2003a & b) etc.

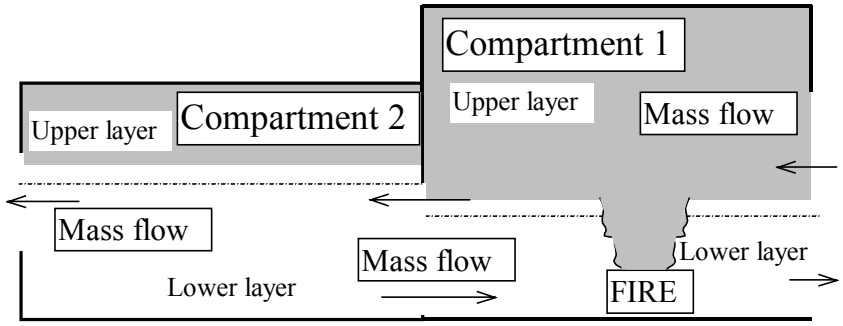

Figure 3.12 a multi-compartment two-zone model

3.4.2 Computational Fluid Dynamic Models

Computational Fluid Dynamic models (CFD models), also called Field models, are the most sophisticated models used to simulate compartment fires.

This type of model is used in many engineering disciplines and is based on a time dependent and three dimensional solution of the fundamental conservation laws. The partial differential equations of the thermodynamic and aerodynamic variables (Navier-Stokes equations) are solved in a very large number of points in the compartment. These equations are usually solved by finite volume method.

With the Direct Numerical Simulations (DNS) technique, the basic equations are solved in their whole complexity. Such codes need very short time steps and very refined spatial grids in order to simulate all time and spatial scales coming from the turbulent and the chemical scales. DNS needs extremely long computational time and are used only for academic cases or very simple applications.

The most widely used alternative to DNS is to implement a turbulence submodel in the CFD. The basic equations are pre-averaged on the time scale, which makes high frequency vibrations disappear, and a turbulent model takes into account the short spatial scales. This submodel enables to make a coarser mesh and to increase the computational time.

The turbulent k-ε model is often used. k-ε model is based on two additional equations. One for the turbulent kinetic energy k and one for the rate of dissipation of turbulent kinetic energy ε. It is important to know that there are several k-ε models and that they are all based on empirical coefficients, determined from experimental results. Moreover most of the flows induced by fire do not have characteristics of fully turbulent flow. So the use of k-ε model is often controversial.

Another common turbulence model is called Large Eddy Simulation (LES). The flow equations are solved not only for the mean flow but also for the largest eddies. The LES technique has been mainly used to simulate large outdoor fires. Compartment fire simulations are still scarce and limited to research work but this technique is probably the alternative of the k-ε turbulence model [Karlsson 2000].

The results are given with a much greater degree of details than the one of zone models because the variables, such as temperature, velocity and chemical species concentration, are given in all the points of the grid defining the compartment. Due to the big amount of results, post processors are of primary importance for CFD codes.

Figure 3.13 illustrates a compartment fire modelled by a field model (Sinai 2003). Figure 3.13a prensents an isometric view of the surface mesh on the symmetry plane and floor and Figure 3.13b shows the temperature on the symetry plane calculated by the code.

The main field of application of CFD is: Pre-flashover fire phase/localised; Complex geometry; Smoke movement in multi compartment.

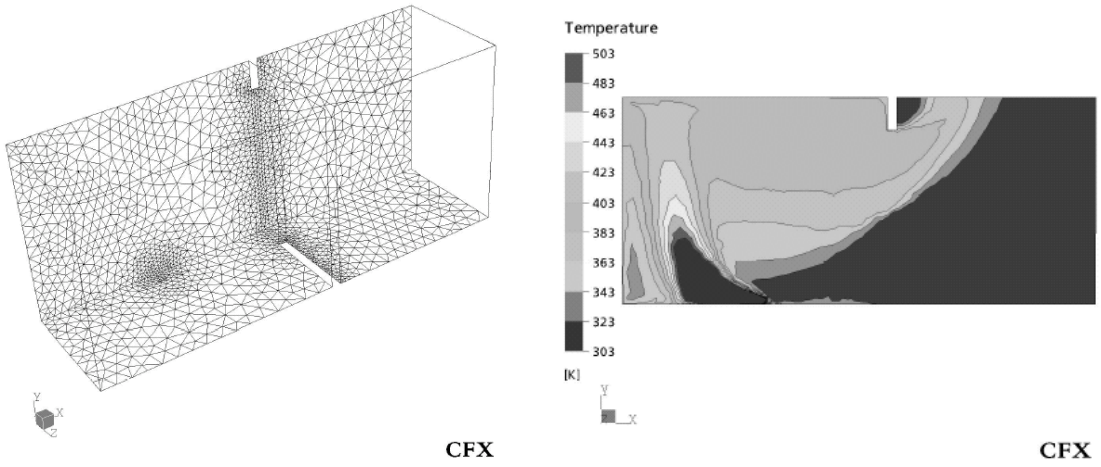

a. **b.**

Figure 3.13 CFD modelling of a compartment fire a. Isometric view of the surface mesh on the symmetry plane and floor. b. temperature on the symetry plane (Sinai 2003)

Examples of CFD fire models are CFX (CFX-5, 2000), SOFIE (developed at Cranfield University), SMARTFire (developed at Universty of Greenwich), FDS (developed at NIST), etc.

3.4.3 Fire model surveys (Friedman 1992; Olenick and Carpenter 2003)

Numerical fire models are quite numerous nowadays. It is often difficult to compare them because many of them have been made for different purposes.

Two fire model surveys have been made during the last decade. Such work is very useful for fire engineers because it helps to understand the purposes and the capabilities of each model.

A first fire model survey has been made by Friedman and published in 1992 (Friedman 1992). In the process Friedman identified 74 computer models which address fire and smoke.

A new survey has been made and recently published (Olenick and Carpenter 2003). A short summary of the models gathered in this survey is given on a website (http://www.firemodelsurvey.com/).

They are sorted out by type and purpose: Zone, Field, Detector Response, Egress or Fire Endurance models. A total of 170 models are reported in this second survey. 54 zone models and 20 field models have been identified.

The information given on the models are: Model Name; Version; Classification; Very Short Description; Modeler(s); Organization(s); User's Guide; Technical References; Validation References; Availability; Price; Necessary Hardware; Computer Language; Size; Contact Information; Detailed Description.

This information is not available for all the referred models. Some of these models are not developed anymore and some modellers did not reply to the author of the survey.

PART 2 : ANALYSES OF MOST IMPORTANT MODELS

3.5 Introduction to the analyses

Analyses of different models presented in the first part of this chapter are presented here. Considering the huge number of models, it is obvious that not all the models have been analysed in detail. A particular attention has been given to the models proposed in Eurocode 1.

Various studies made on the ENV version of Eurocode 1 are presented even if this version is now superseded by the EN version because they enable to better understand the models, their evolution and their limits. These studies include contributions of the author and have been used for improving the methods for the EN version.

The fire tests have been collected in a database during the NFSC 1 research (1999). They are briefly described in section 3.6. A more detailed description of most of these tests is given in chapter 6 which mainly concerns the comparison of the new numerical fire model OZone with full scale fire tests.

Comparisons have been performed between:

- Parametric fires of ENV and full scale fire tests (NFSC1 1999), section 3.7.
- Parametric fires of EN and full scale fire tests (ARBED 2001), section 3.7.
- Parametric fire and equivalent time method of ENV (Franssen *et al.* 1996) section 3.8.
- Equivalent time methods between each other (Law 1997, NFSC1 1999) section 3.9.1.
- Equivalent time method of ENV and full scale fire tests (Cadorin *et al.* 1999) section 3.9.2.

A original study of the influence of the section and of the insulation on calculated equivalent time is then made, section 3.9.3.

Finally, some zone models are then compared on an academic example, section 3.10.

3.6 NFSC database of full scale fire tests

The database contains 87 tests made in Australia, France, and UK which can be summarised by Table 3.2.

These have been performed in the CTICM fire laboratory of Maizières-les-Metz in France and in the BRE fire laboratory of Cardington in UK.

The dimensions of the fire compartment are: maximum volume of 35 m^3; maximum surface A_t of 128 m^2; maximum height of 3,13 m.

The openings are always in only one wall. There is no horizontal opening in any test.

The fire load in the tests consists of wood cribs, real furniture, paper and a car. The fire load density per unit floor area was equal to 30 kg of wood/m^2 in more than half of the tests. One test was performed with a fire load of 90 kg of wood/m^2. The fire load density distribution for all the tests of the database is given on the Figure 3.14.

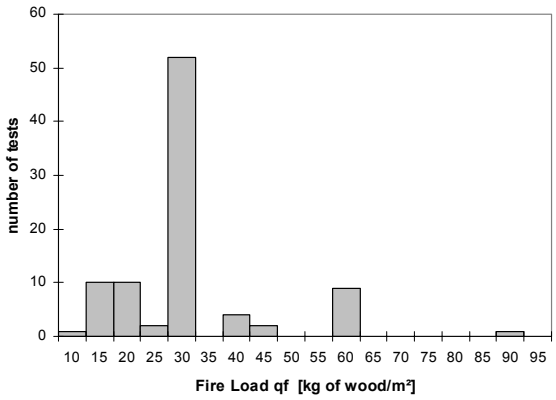

Figure 3.14 Overview of the fire load of the tests of the NFSC1 database

Table 3.2 Summary of the tests of the NFSC1 fire tests database

Input number	Number of Tests	Country	Date	RHR or mass loss measurement	Description available in section
1 to 6	6	Australia (BHP Research Melbourne Laboratories	1992	No	
7 to 15	9 [1]	UK (BRE-Cardington)	1994	No	7.5.5
16 to 53	38 [1, 2]	France (CTICM)	1973	Yes	7.5.1
54 to 63	10 [1]	France (CTICM)	1974	Yes	7.5.2
64 to 66	3 [1]	France (CTICM)	1993	Yes	
67	1 [1]	France (CTICM)	1994	No	7.5.4
68	1	France (CTICM)	1995	Yes	
69 to 71	3 [1]	France (CTICM)	1996	Yes	7.5.3
72	1 [2]	France (CTICM)	1997	Yes	
73	1 [2]	France (CTICM)	1994	Yes	
74	1 [2]	France (CTICM)	1994	Yes	
75	1 [2]	France (CTICM)	1994	Yes	
76 to 83 (B1 to B8)	8 [2]	UK (BRE-Cardington)	2000	Yes	

[1] OZone has been compared to these tests. A more detail description is thus given in chapter 6.
[2] Tests considered when applying parametric temperature-time curves according to Annex A of EN1991-1-2.

3.7 Comparison of parametric fires of ENV and of EN with full scale fire tests

The tests of the database (section 3.6) have been used for comparison with the methods of ENV (NFSC1 1999) and EN (ARBED 2001).

On Figure 3.15 and Figure 3.16, each test is represented by one point obtained from the maximum temperature in the air calculated by the Eurocode proposal (vertical axis) and measured in the test (horizontal axis). For the tests, the temperature is the average value of several measurement made by different thermocouples located in the compartment. The full line on this figure represents the place where all the points should be located if the prediction was perfect. The dotted line represents a linear regression of the points.

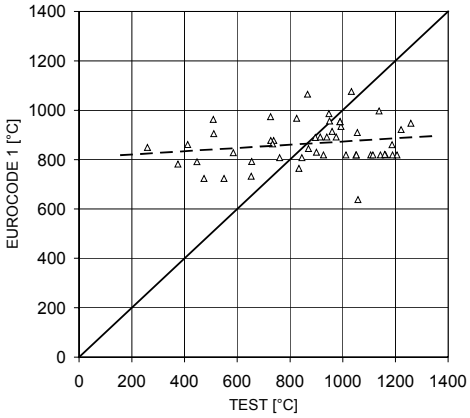

Figure 3.15 ENV 1991-1-2 (1993)

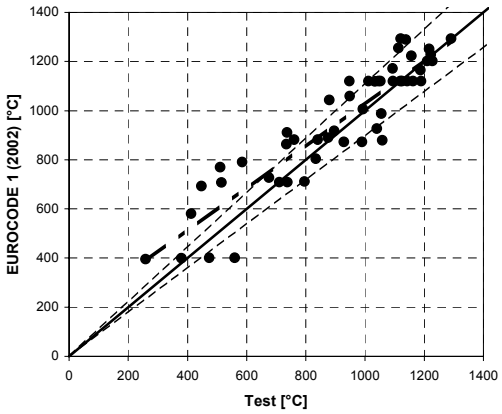

Figure 3.16 EN 1991-1-2 (2002)

It appears that, with the test series considered here, there is virtually no correlation between the measured maximum temperature and the maximum temperature predicted by the parametric fire of ENV1991-1-2 (Figure 3.15). The coefficient of correlation between the experimental results and the calculated results is only 0,19.

The improvements proposed for the EN 1991-1-2 (2002) lead to a much better correlation between the method and the tests (Figure 3.16).

3.8 Comparison between equivalent time and parametric fire curves of ENV

A comparison between the parametric fire curves and the equivalent time methods from, respectively, Annex B and Annex E of ENV1991-1-2 is presented.

3.8.1 Principle of the calculation of the equivalent time of fire curve to the ISO fire curve

In order to make this comparison, we have to transform the temperature curve measured during tests into some equivalent times. This is done by calculations of temperatures in a structural element submitted to the mean temperature and observation of the maximum temperature reached by this structure. Three structures have been chosen here;

- *Unprotected steel section*. In this case, the calculation of the uniform temperature is made by the method described in § 4.2.5.1. of Eurocode 3 : Part 1-2 (ENV1993-1-2, 1993). A section factor of 211 m^{-1} was chosen corresponding, for example, to a HE 200 A section.
- *Protected steel section*. The same section factor is taken as for the unprotected section. The lightweight insulating material has the following properties: c_P = 850 J/(kgK); λ_P = 0.15 W/(m²K); ρ_P = 300 kg/m^3 ; e_P = 20 mm. Those characteristics are similar to, say, vermiculite. The calculation of the uniform temperature is made with the method described in § 4.2.5.2. of Eurocode 3 : Part 1-2 (ENV1993-1-2, 1993).
- *Concrete structure*. The temperature is calculated in a semi-infinite concrete volume, at a penetration depth of 3 cm. The calculations are made with the non linear finite element code SAFIR of the University of Liège (Franssen, 2003).

For the thermal calculations, steel thermal properties are taken from Eurocode 3 : part 1-2 (1993) and concrete thermal properties are taken from Eurocode 4 : part 1-2 (ENV1994-1-2, 1994).

The temperature in the structures submitted to the ISO curve is first calculated as a function of time. The same calculation is made for the same structures submitted to the natural fire curves measured during the tests. In each case, the maximum temperature obtained in a structure submitted to a parametric temperature-time curve (400°C on the example given on Figure 3.17) is reported on the corresponding curve obtained by the first calculation when the structure was submitted to the ISO curve. The moment when this temperature is obtained is defined as the equivalent time (7.5 min on the example on Figure 3.17).

In other words, the equivalent time is here defined to be the time during which a structural element has to be submitted to the ISO standard fire curve in order to obtain the same effect (i.e. maximum structural element temperature) as the natural fire curve would have produced.

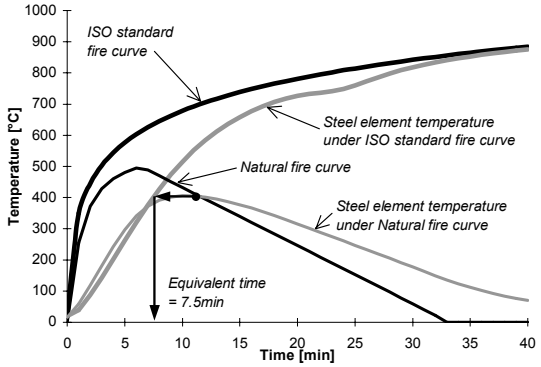

Figure 3.17 Principle of equivalent time calculation from a natural fire curve

3.8.2 First look on the equations of the 2 methods

It is interesting to notice that t_d* from the parametric fire curve of ENV1991-1-2, given by Eq. (3.16), is in fact the equivalent time of a very light steel element (with a very high section factor, see EC3 Part 1.2). In other words, an element the temperature of which is very close to the gas temperature. In the parametric fire curve, t_d* is proportional to the opening factor O while in the equivalent time method of the same document, $t_{e,d}$ is proportional to $O^{-1/2}$. It will be verified by the parametric study whether this apparent contradiction has practical effects.

3.8.3 Parametric study

A parametric study has been made with the two methods. Six parameters are taken into account:

- the floor area of the compartment, A_f in m² 16, **25**, 36, 64, 100, 144, 256, 324, 400
- the design fire load density, q_d in MJ/m² 250, 500, **750**, 1000, 1250, 1500, 1750, 2000
- the opening height, h_w in m 0.2, 0.5, 1.0, **1.5**, 2.0, 2.5
- the position of the sill of the opening, h_s in m 0.0, **0.5**, 1.0
- the width of the opening, w in m 0.5, 1.0, 2.0, 3.0, **4.0**, 5.0
- the characteristics of the walls, b in J/m²s$^{0.5}$K 500, 1000, **1300**, 1600, 2000

The bold values are those of the reference case (vertical lines on Figure 3.18). The variation is made separately on the parameters. While one of them is allowed to vary from the reference case, the values of the other parameters remain fixed to the values of the reference case. This

leads to 38 different cases. For the reference case we have the 7 bold values of the parameters and for the 37 other cases we have 6 bold values and one non bold value.

The results of this study are in case of annex B a set of temperature-time curves and in case of annex E a set of equivalent time. Figure 3.18 shows the results obtained by the 2 methods for the variation of the parameters.

3.8.4 Results

The position of the sill of the opening has no influence on the results, for the annex B method as well as for the annex E method. The five other results of the parametric study are shown on Figure 3.18. The equivalent time is given in minutes as a function of the different parameters. Dotted lines are segments linking at least one point which is out of the field of application of the method used to obtained this point.

In some cases, the variation of the equivalent time calculated from the results of the Annex B with a parameter is different for the unprotected steel element than for the two protected elements. This is due to the fact that the maximum temperature calculated in the unprotected steel is mainly influenced by the maximum temperature in the air, whereas the maximum temperature in the protected elements is also influenced by the duration of the fire. Going from a severe but short fire to a less severe but longer one is generally favourable for a pure steel section, but it can be more critical for a protected element.

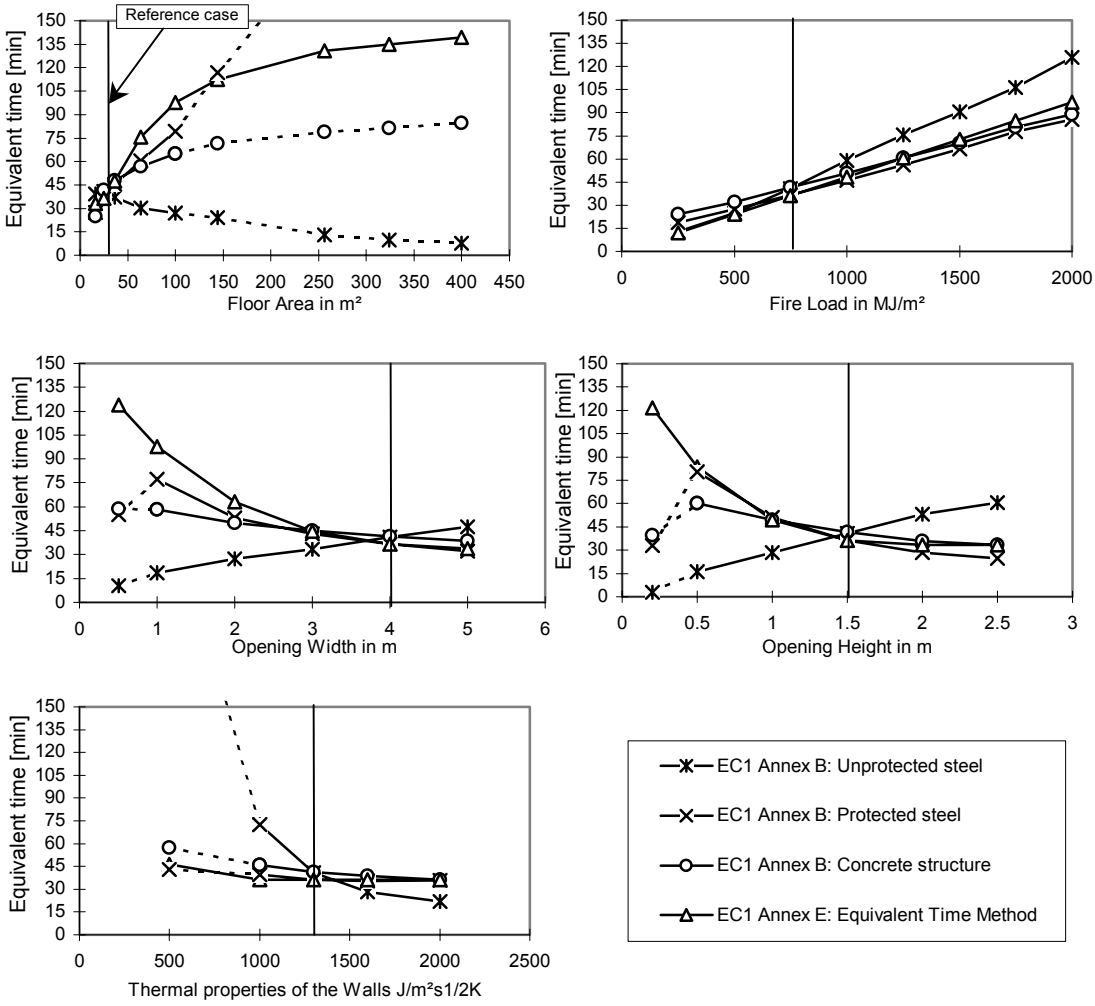

Figure 3.18 Results obtained by the 2 methods

The same effect also explains why the apparent contradiction between Annex B and Annex E mentioned in section 3.8.2 disappears when temperatures are calculated in protected elements, but not in unprotected elements.

3.8.5 Conclusions

This study shows that, despite apparent contradiction in the equations, the methods proposed in Annex B and in Annex E are coherent for protected steel elements and concrete elements.

When considering an unprotected steel element, these two methods have lead in some cases to very different results. Neither of two methods is systematically safer than the other.

If it is considered that Annex B provides a good approximation of the air temperature-time curve in the compartment, based on more refined models, thus allowing the calculation of the temperature in each structure type, whereas Annex E is an attempt to simplify the solution even further and to propose equivalent time irrespective of the structure, then this study tends to indicate that the approximation is valid in case of protected elements, but may not be valid in case of unprotected steel elements.

3.9 Equivalent time

3.9.1 Comparisons of equivalent time methods

Law (1997) has compared some equivalent time methods to a set of fire tests in a small compartment (no reference is given on these tests) and to the deep compartment tests made by Kirby (1993). She concludes that for small compartment fires, the correlation by Law, Petterson and Harmathy gave promising results but that the other methods, including EC1 method, gave poor estimations of tests results. She points out that the best methods take into account the thermal properties of the partitions of the enclosure. She also found that none of these formulas were able to predict the deep compartment fire behaviour.

A parametric study made in NFSC1 research (1999) showed that different equivalent time methods considered gave very different results (up to 300% of difference).

Considering the formula taking into account the fire load, the ventilation condition and the partition properties, there are two families of main methods. The first family is a set of formula (all but two methods) for which the influence of the different parameters is very similar, the other one is composed of two methods, DIN (1998) and Eurocode 1 (1993), which are in fact fully identical.

Figure 3.19 presents the results of this study for the variation of the width of the opening. This figure shows that the influence of a width variation is similar on all methods excepted the Eurocode method for which the ventilation condition is taken into account by a factor which is mainly proportional to the height of the compartment. This formulation is based on the work by Schneider who ran a multi-room zone model, MRFC, (Thomas *et al.*, 1997) to calculate temperature in compartment and used a reinforced concrete slab as structural element for comparison with nominal fire curve.

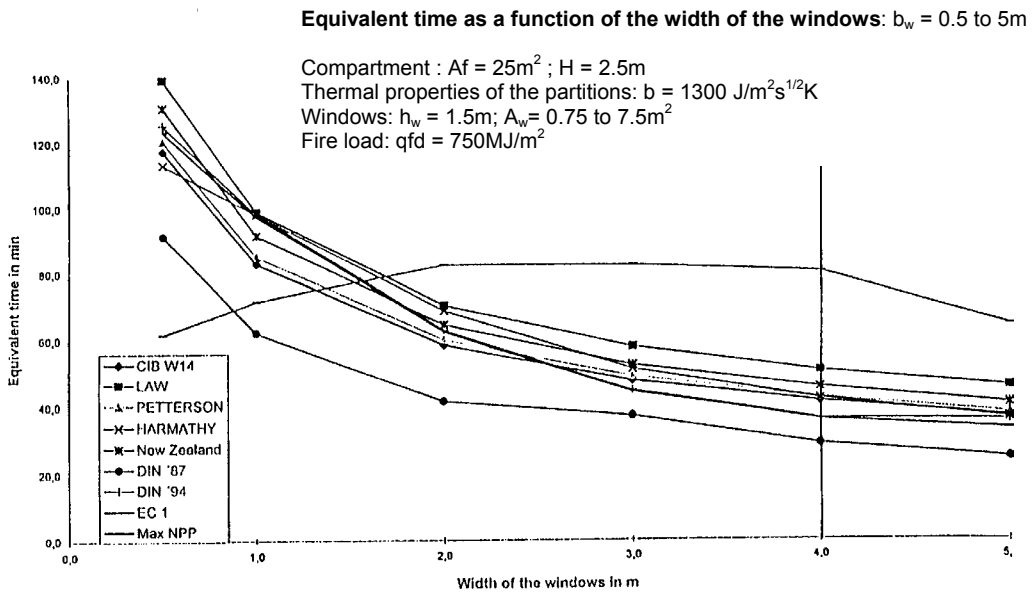

Figure 3.19 Comparison of equivalent time formula for varying opening width of a compartment (NFSC1 1999)

3.9.2 Comparisons of ENV method and full scale fire tests

The point of this work is to compare the method of equivalent time described in the ENV and the fire tests which were collected in the database presented in section 3.6. In order to do this a "real equivalent time" has been calculated for each test using as data the temperature time curve measured during the test, according to section 3.8.1, taking the measured temperature-time curve place of natural fire curve. Also for each test the Eurocode method has been applied using the real conditions applied to the test (fire load, geometry of the compartment, wall characteristics).

The calculations have been done for an unprotected steel profile HEB200 and for the same profile protected by a lightweight insulating material with the following properties: c_P = 850 J/(kgK); λ_P = 0.15 W/(m²K); ρ_P = 300 kg/m^3 ; e_P = 20 mm.

These conclusions written below are of course limited to the fire condition covered by the database and to the steel section and insulation chosen for the comparison. These latter parameters are investigated in the next section.

Unprotected steel profile

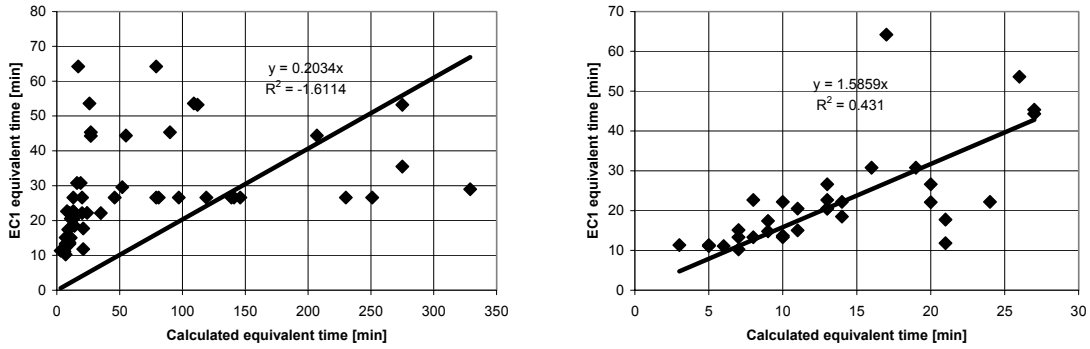

a. all tests **b. tests with calculated equivalent time < 30min**

Figure 3.20 Equivalent time of ENV versus fire experiments - unprotected steel section

There is no correlation when all the results are taken into account, Figure 3.20a. However for equivalent times obtained from test included between 0 min and 30 min, the correlation is better, Figure 3.20b.

The wide distribution of the equivalent times that are beyond 30 min has no consequence on the structural safety because after 30 min of ISO fire, the temperature of an unprotected steel section is so high that the resistance of this profile becomes negligible. For unprotected sections, there is thus nearly no difference in the ultimate load bearing capacity between equivalent times of 30 min and of 60 min. Moreover for these tests the equivalent time obtained with the annex E of EC1 part 2.2 is at least equal to about 30 min.

The wide distribution is also due to the fact that after 30 min of ISO fire, the slope of the temperature time curve in an unprotected steel section is very low. For a small difference of maximum steel temperature in the section submitted to the natural fire curve there is a wide difference in the calculated equivalent time.

Figure 3.20b shows the comparison with the test equivalent time lower than 30 min. A rather good correlation is obtained and except in 3 cases the equivalent time method is safe.

Protected steel profile

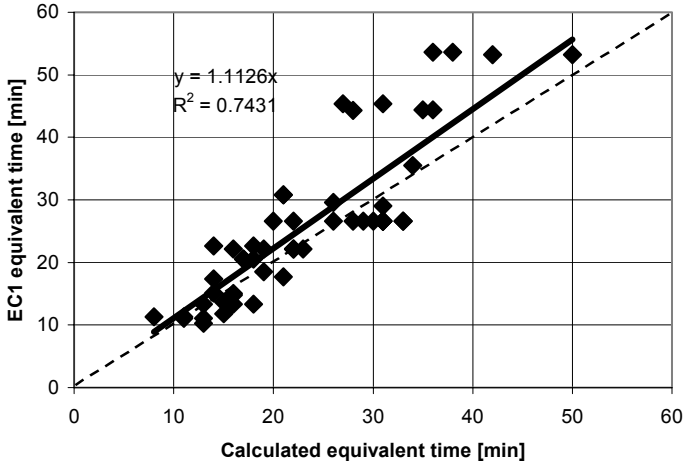

Figure 3.21 Equivalent time of ENV1991-1-2 versus fire experiments - protected steel section

In case of a protected steel profile (Figure 3.21) the correlation between the "real" equivalent time and the equivalent time calculated with the ENV method is very good.

3.9.3 Influence of the section factor and of the thermal insulation

The main hypothesis of the equivalent time methods is that equivalent times are supposed to be independent of the structure. ENV 1991 1-2 (1993) does not give information on the type of structure for which it is valid. Thus according to this document, this method can be used for any structural elements. In EN 1991 1-2 (2002), it is stated that the method is suitable for protected and unprotected steel members and for concrete structures. Anyway no information is given on the effect of the section dimension and of the insulation material thermal properties.

The aim of the work presented in this section is to investigate the influence of the structure itself on a calculated equivalent time.

This study is limited to steel members and to six different compartment fires with short, medium or long duration and low or high maximum temperature.

Therefore a parametric study is made to see the influence of:

- The effect of the section factor of the steel member;
- The effect of the thermal resistance (e_i/λ) of the insulation material.

The six fires (Figure 3.22) are:

- A short fire (20min) reaching a gas temperature of 1150°C
- A medium fire (60min) reaching a gas temperature of 1000°C
- A long fire (120min) reaching a gas temperature of 1000°C
- A short fire (20min) reaching a gas temperature of 575°C
- A medium fire (60min) reaching a gas temperature of 500°C
- A long fire (120min) reaching a gas temperature of 500°C

The parameters are the section factor of the steel section that is between 20 to 500 m^{-1} covering the main part of the hot rolled steel profile production, and, if the section is protected, the thermal resistance of the insulation e/λ that is between 0.033 and 0.267 m^2K/W.

Figure 4.23 shows the results of the study in case of unprotected steel member. For each of the six fires, it is obvious that the influence of the section factor Ap/V is very important.

Figure 3.24 presents the results of the study for the protected steel profiles. Even if the results for compartment fire with the high maximum temperature (about 1000°C) are satisfactory, they are extremely bad for low maximum temperature (about 500°C), considering that the equivalent time is supposed to be independent of these two parameters.

It seems thus that these two parameters should be included in equivalent time methods or, at least, the domain on which this influence can be neglected should be further studied.

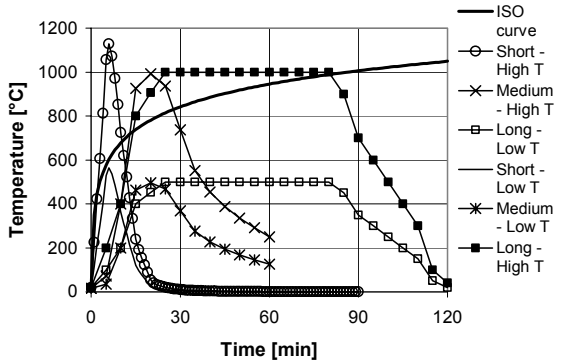

Figure 3.22 ISO curve & fire curves of different fire durations and different maximum temperatures used in the parametric study

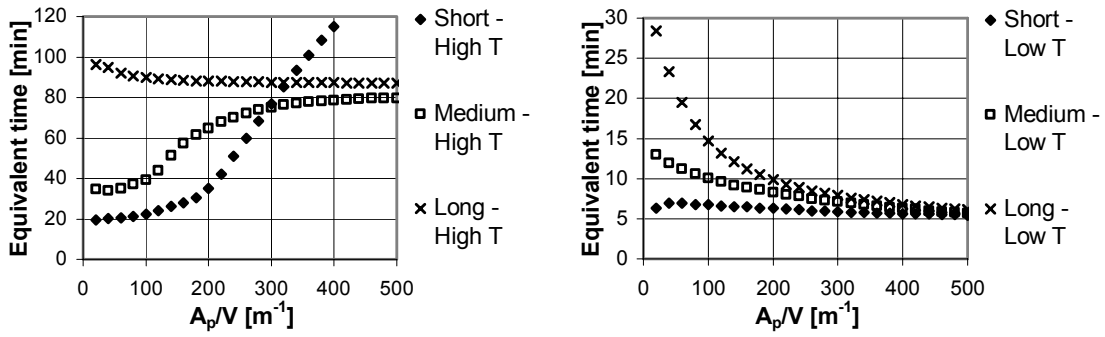

(a) High Maximum Temperature **(b) Low Maximum Temperature**

Figure 4.23 Unprotected steel – effect of the section factor

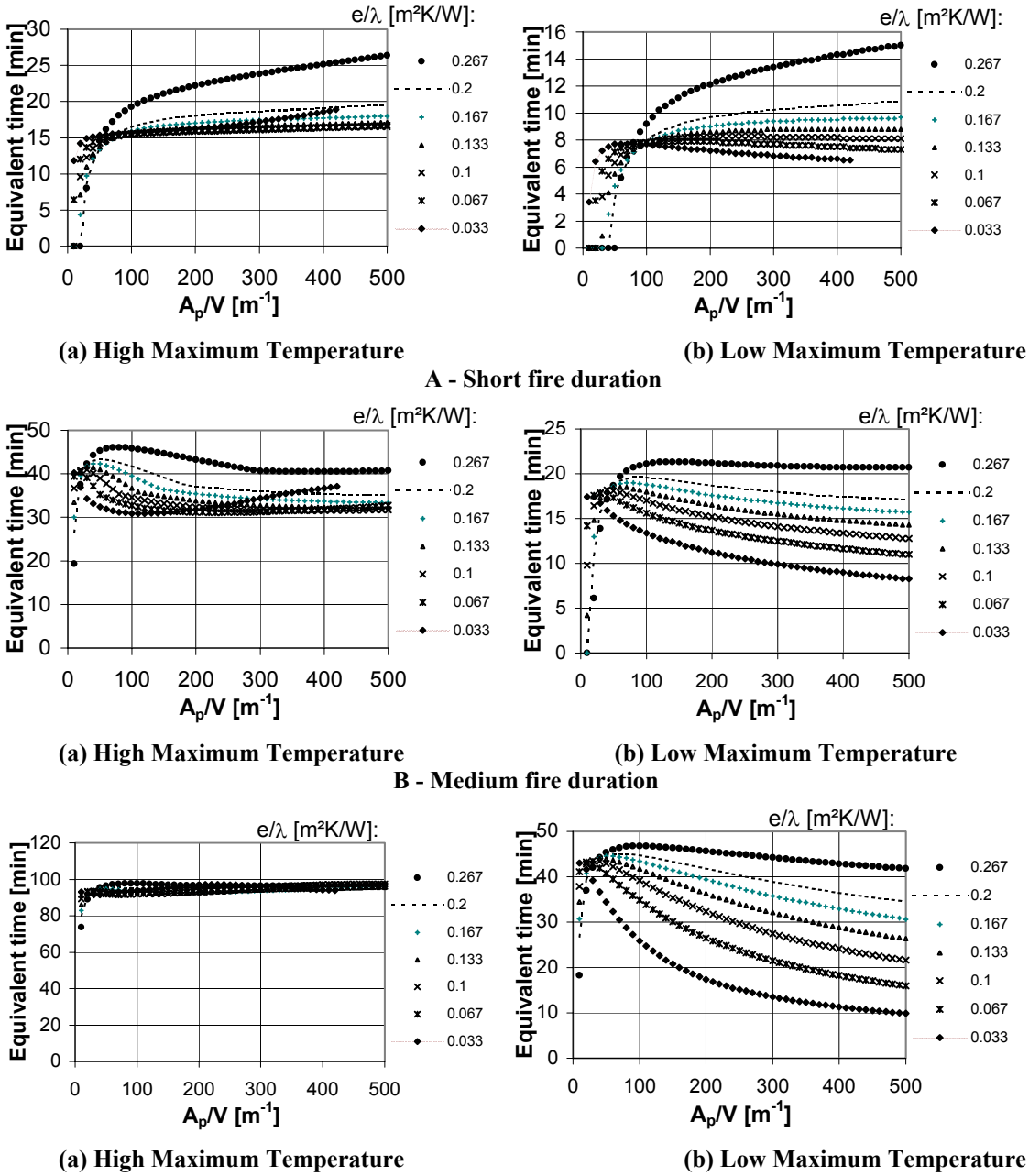

(a) High Maximum Temperature (b) Low Maximum Temperature

A - Short fire duration

(a) High Maximum Temperature (b) Low Maximum Temperature

B - Medium fire duration

(a) High Maximum Temperature (b) Low Maximum Temperature

C - Long fire duration

Figure 3.24 Influence of the section factor on equivalent time for different thermal resistances of insulation

3.10 Comparison of some zone models

A comparison of 7 zone models (either two or one zone models) has been made by various researchers (including the author) of the NFSC1 research (1999) on an academic example. The compartment is quite large (floor area 20 m by 20m; height of 3m) with small openings (total of 8m²) and the fire has a maximum rate of heat release of 2.5MW.

Partitions heat transfer are not modelled in CCFM. A fraction of the heat release rate that is lost to the boundaries has to be set in the data. The default value of 70% of the RHR has been used in the simulation presented here.

The scatter obtained in this comparison is very high, Figure 3.25a. The lowest temperature is about 55°C, the highest is about 300°C. CCFM gives very high temperature due to the fact that partitions are not modelled in this code. The shape of the temperature-time curve obtained with ARGOS is strange, the high temperatures up to 280°C occurring between 5 and 10 min are not explained.

Other models, Figure 3.25b, give results with a lower but nevertheless very high dispersion (the lowest temperature is about 55°C, the highest is about 110°C.). Even the shapes of the curves are quite different.

While the differences between some codes were identified, such as various specific heat of gas considered, other causes of bias were not clear, even with a deep analysis of the technical reference of each codes.

This comparison shows that, even for a well defined academic example, the results given by different zone models might be very different and the causes of these differences are difficult to identify.

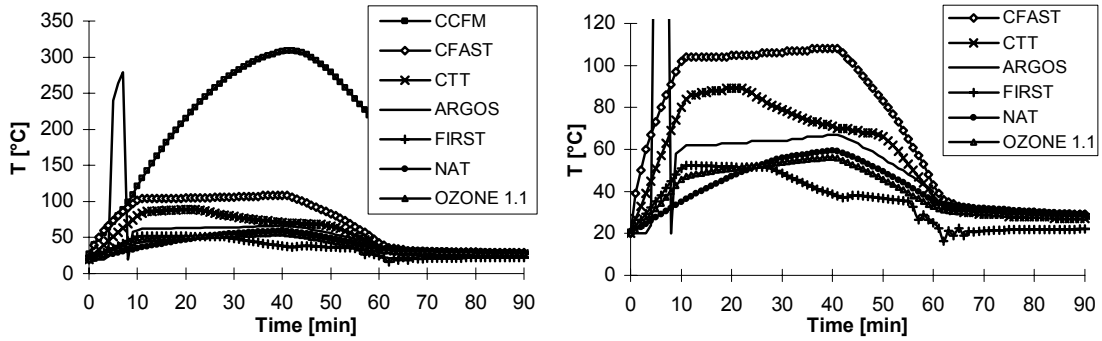

a. All models **b. Except CCFM**

Figure 3.25 Comparison of different numerical fire models – Upper Layer Temperature

3.11 Conclusions

3.11.1 Equivalent time methods

It has been shown by Law (1997) and in the NFSC1 research (1999) that the different methods of equivalent time could give results with difference up to 300% from one method to an other. Moreover, the Eurocode and DIN 1998 method are based on a ventilation factor completely different than other methods and thus the influence of a variation of some parameters on the Eurocode and Din equivalent time may be the opposite than its influence on other methods.

The equivalent time method of annex E ENV1991-1-2 (1993) has been compared to the parametric fire curves given in annex A of the same document. It has been found that these two methods give results which are coherent while evaluating the temperature in a protected steel element or in a concrete element. When considering an unprotected steel element, these two methods have lead in some cases to very different results.

The method of annex E of ENV1991-1-2 (1993) has also been compared to a database of full scale fire tests, giving very good results in case of protected steel structures. For unprotected steel structure the comparison is not so good but seems to give reasonable results.

The conclusions of these two study are of course limited to the conditions covered by the parametric study and to the particular steel sections and concrete element used in the comparisons.

Additional work on the influence of the steel section and the protection characteristics on the equivalent time has shown that in fact, such good correlations were probably fortuitous and only applicable to the particular elements chosen for the studies.

In the EN version of the Eurocode (2002), an additional term is set in the equivalent time formula. This term is equal to 1 for protected steel section and for concrete structure and equal to 13.7 O for unprotected steel and has been proposed by Schleich (1996) to improve the coherence between the results of the parametric fire and equivalent time models of the ENV for unprotected steel elements. This proposal has not been analysed in this work.

The background of the Eurocode 1 method has not been published in the open literature. The ventilation factor that is mainly proportional to the compartment height is particularly dubious and its basis is unclear.

There is an urgent need for more research to include the influence of the section and of the insulation on the equivalent time or at least to better define its application field. Nevertheless, in view of the enhancement of other more advanced methods, including analytical models, and of the generalisation of computer aided calculations, a reasonable decision should be to give up the use of the too simple concept of equivalent time and prefer model that better describe the dynamics of compartment fires.

3.11.2 Parametric fire models

A comparison (NFSC1, 1999) of the Eurocode 1 ENV1991-1-2 (1993) parametric fire model and a database of full scale fire tests showed a very bad correlation between the model and the tests.

The improvements brought to the ENV model and included in the EN1991-1-2 (2002) parametric fire model lead to have a much better agreement between the method and the full scale fire tests of the database. The improvements concern the way to take into account partitions with layers made of different materials and the introduction of the fuel controlled regime in the model.

Nevertheless, some remarks can be raised on this parametric fire model of the EN:

- The ENV model has been improved by using some tests and this improved model (EN) is compared to the same test for validation.
- The duration of the decreasing phase is not equal to the heating phase duration. This is inconsistent with the fact that the decreasing phase begins when 2/3 of the total fire load is burned (see Figure 3.8) which would lead to have identical duration for the heating and the decreasing phase.
- In fact, as the Eurocode method is based on the Swedish curves, the rate of heat release which is behind the Eurocode curves for the estimation of the fire duration should have the shape given on Figure 3.4 and not the one given on Figure 3.8.
- The way to consider a fuel controlled fire is unsatisfactory. For a fuel controlled fire, no link exists anymore between the heat release rate and the compartment temperatures or the fire duration. Moreover, the opening factor O is not relevant in fuel controlled fires.

- Also for fuel controlled fire, the duration of the heating phase, t_{lim}, is linked to the fire growth rate. This is surprising as the fire growth rate is a characteristic of pre-flashover fire and the parametric fire of Eurocode is a post-flashover method.
- It is obvious that Θ_g given by Eq. (3.11) tend to 1350°C when t tend to infinity. This means that the temperature in any compartment with a very high fire load tend to 1350°C. This value should depend on the RHR and on the geometry and the partition material of the compartment.
- As they are based on calculation made for a fire load made of cellulosic material, these curves should only be valid for this type of fire load.
- The opening factor O is related to A_t , the total boundary area of the compartment (including opening area). The physics behind this hypothesis is not obvious or at least confusing.
- The method proposed to calculate V_f for multiple openings is not likely to give good results when the openings are at very different height, for example one on the lower part and an other one on the upper part of the compartment.
- No pre-flashover phase is considered.

Two others parametric fire curves have recently been proposed. The main interest of these curves is that the shape of the fire curves are closer to temperature time curves measured during compartment fire experiments. In the BFD method, it is proposed to consider a design fire curves but its use is limited to the estimation of the fire duration. The way to estimate the different parameters, including the maximum temperature during the fire course, of these methods is unfortunately fully empirical or based on simple existing methods (Law, Babrauskas...).

3.11.3 Motivations for building a new numerical fire model

As explained in the previous sections, a lot of compartment fire models exists. Thus it is not obvious that it is well-founded to add a new model to the already long list of models.

The mean reasons which lead the author to build a new compartment fire model are listed hereafter:

- The high dispersion obtained in the comparison of existing codes on simple, well defined examples.
- The field of application of these codes was not well defined.
- The existing models were either pre-flashover or post-flashover. None of them were well designed to be able to model both pre- and post-flashover phase of a fire.
- None of these models were specifically built to evaluate the action of compartment fires on structures.

It has thus been decided to write a new fire model, based on the zone model approach, with the main aim of evaluating the fire resistance of structural elements submitted to compartment fires. This fire model is called OZone and is described in chapter 4 and 5.

The choice of a zone model is based on the fact that, even if CFD fire models are much more sophisticated and provide a more detailed evaluation of the situation during a fire, they are of complex use and have a long computing time. Up to now there are few applications of field models in simulation of fire resistance, especially in case of fully developed fire.

It is true that computational fluid dynamic models will probably enter more and more in the daily life of fire safety engineers and thus are one of the major axis of the fire safety research. Nevertheless other methods will remain essential and still need development.

These comments show that the development of zone models is not yet stopped, and their applications will be numerous during many years.

4

A new numerical model of pre- and post-flashover compartment fires

4.1 Introduction

The aim of this chapter is to present the basic hypothesis and the formulation the new compartment fire model called “OZone”. This zone model has been developed under the scope of the ECSC research projects “Natural Fire Safety Concept” (NFSC1, 1999) and "Natural Fire Safety Concept - Full Scale Tests, Implementation in the Eurocodes and Development of an User Friendly design tool" (NFSC2, 2000).

As said in chapter 3, a wide variety of zone models already exist. The reasons which lead to build a new model have been explained in section 3.11.3. The first main reason is that a high dispersion exists in the comparison of existing codes on simple, well defined examples. It was thus thought that the only way to fully understand this type of code was to build a new one. The other main reason was that none of the existing models was specifically built with the aim of

evaluating the fire resistance of structural elements.

This code includes a two-zone and a one-zone model with the ability to switch automatically from the two-zone to the one-zone model if some criteria are encountered. It thus deals with localised as well as fully developed fires. The wall model is based on the finite element method and is fully coupled to the zone equations. Different combustion models have been developed to cover different utilisation of the code, i.e. test simulations or design situations.

Considerations as how this model is used for the design of steel elements are presented in chapter 5 of this thesis.

Comparisons between OZone simulations and full scale fire tests (localised and fully developed) performed by various laboratories are presented in chapter 6.

4.2 Overview of the compartment model and of its basic assumptions

The aim of this section is to give an overview of the main assumptions on which the different models and sub-models included in OZone are based and to explain the heat and mass transfer in the compartment model. The formulations of the main model and of the submodels are given in the next sections.

OZone is composed of one main model which includes:

- a two-zone model (compartment and partitions);
- a one-zone model (compartment and partitions);
- a model to switch from the two-zone to the one-zone model.

Some sub-models are connected to the main model. Submodels enable the evaluation of:

- the heat and mass transfer between the inside of the compartment and the ambient external environment through vertical, horizontal and forced vents (vent model).
- the heat and mass produced by the fire (combustion model);
- the mass transfer from the lower to the upper layer by the fire plume (air entrainment model);

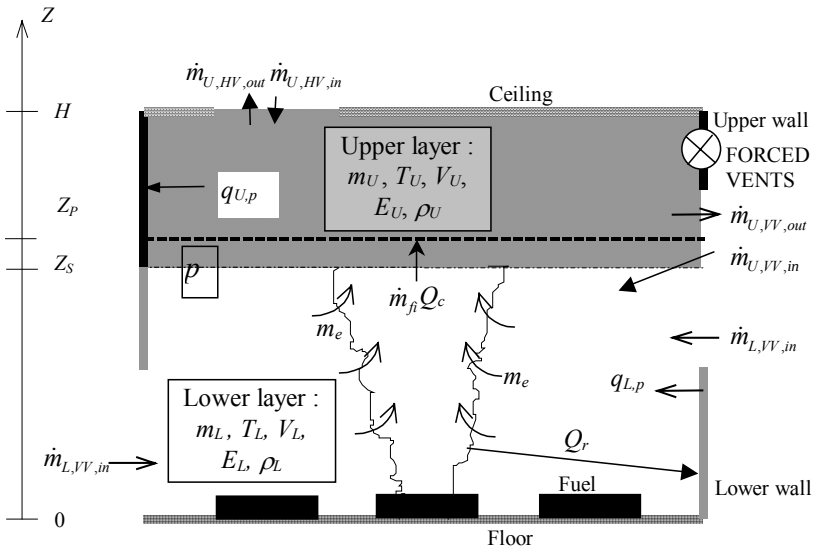

Figure 4.1 Schematic view of two-zone model and associated submodels

Figure 4.1 shows a schematic view of the two-zone model and its submodels for heat and mass transfer. In the two-zone model, the compartment is divided in an upper and a lower layer. In each layer the gas properties (temperature, density…) are assumed to be uniform. The pressure is assumed to be constant throughout the whole compartment volume (except when evaluated mass exchange through vents).

The layers are separated by an adiabatic horizontal plane (at height Z_s). They are only connected by an air entrainment model. An air entrainment model is an empirical model which enables the estimation of the rate of mass entrained from the lower to the upper layer by buoyancy in the fire plume. The plume volume is not considered (no mass or heat balance is calculated here). It is thus included in the lower layer volume.

The upper zone is supposed to be opaque and upper layer partitions (wall and ceiling) are connected to this zone by radiative and convective heat transfers. The lower layer is clear and lower layer partitions are connected to this zone by convective heat transfer only. Vertical partitions are thus divided in 2 parts, one in the lower layer and one in the upper layer. The height of the two parts is equal to the heights of the zones. These heights are varying with time.

The fire is defined by its rate of mass loss, its rate of heat release (*RHR*) and its area. Q_c is the convective part of the *RHR* and Q_r is the radiative part of the *RHR*. Q_c is often in the range of 0.6 to 0.8 *RHR* (Karlsson 2000) and has been fixed in the code to 0.7 *RHR*. The radiative part is thus fixed to 0.3 *RHR*. In this model Q_c is transmitted to the upper layer and Q_r to the lower layer partitions (through a source term in the lower layer partition formulation). In the lower layer, the heat is thus transferred by radiation from the fire to the lower layer partitions and then transferred by convection from the partitions to the lower layer and by conduction within the partitions.

Even if the lower layer is clear, the radiation between partitions is not evaluated because, on one hand, temperatures of the different partitions are often quite low and similar, leading to low radiative heat flux between partitions, and, on the other hand, the radiative heat flux from the fire to the partitions should often be preponderant as the flame temperature is relatively high.

Heat and mass transfered through horizontal, vertical and forced vents are exchanged with the layer at the same height, with some exceptions for incoming air through vertical vent which is always added to the lower layer , see Figure 4.1, and for forced vent close to the zone interface.

Some switch criteria are defined so that they represent a limit beyond which one-zone model assumptions becomes closer to the physics of the fire situation than the two-zone model ones. If, during a two-zone model simulation, a switch criterion is met (time t_s), the two-zone model is abandoned and replaced by a one-zone model. The switch is made in such a way that the total energy and mass present in the 2ZM system at time of switch are fully conserved in the 1ZM system, Figure 4.2.

Figure 4.3 shows a schematic view of the one-zone model and its submodels for heat and mass transfer. In the one-zone model, the compartment is represented by a single zone. In this zone the temperature and density are assumed to be uniform. The pressure is assumed to be constant on the whole compartment volume (except while evaluating mass exchange through vents). The gas in the zone is supposed to be opaque and partitions are connected to the zone by radiative and convective heat transfers.

The fire is defined by its rate of mass loss, its rate of heat release and its area. All mass and energy coming from the fire are added to the single zone.
Heat and mass transfer through horizontal, vertical and forced vents are exchanged with the single zone.

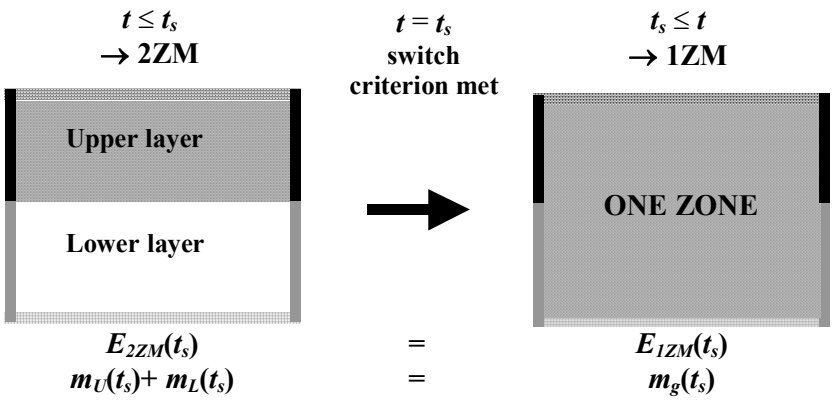

Figure 4.2 Transition from 2ZM to 1ZM

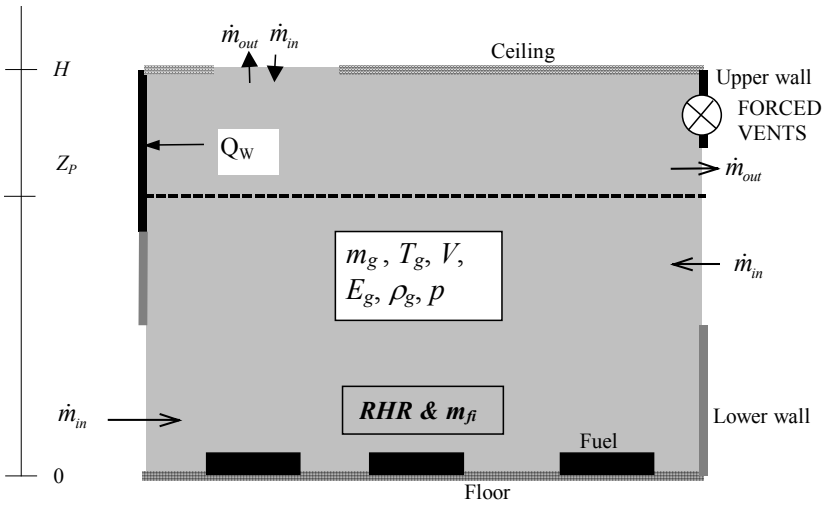

Figure 4.3 Schematic view of one-zone model and associated submodels

The three curves defining the heat release rate, the rate of mass loss and the fire area function of time have to be defined by the user. The input curves correspond to fuel controlled fire, i.e. to the fire which would occur without any influence of the compartment. These curves may be modified by the software if the ventilation is limited (combustion models) or if gas temperature is sufficiently high to lead to flashover.

4.3 Formulation of the main model

The procedure usually presented in the literature sets the limits of the compartment on the inside surface of the wall and adds a partition sub-model on top of it. In this work; the proposed procedure amounts in fact to set the limit of the main model on the outside boundary of the compartment. The main model thus includes the zone(s) and the partitions. The equations describing the situation inside the compartment and in the partitions are solved simultaneously with an implicit procedure; the energy balance between the gas and the partition is totally respected. The finite element method is used to represent the partition and coupled it to the zone equations.

The flux at partition boundaries are dependent of the surface temperature of the partition. When using the finite difference method, the temperature is calculated in the middle of each element. A simple way to evaluate the surface temperature is to assume that it is equal to the temperature at the centre of the first element (Drysdale 1999). This latter assumption is only valid if

elements are small. When using the finite element method, temperatures are evaluated at each node; the surface temperature is thus directly evaluated. This comment shows that the finite element method enables to discretise a partition with less (and thus bigger) elements than the finite difference method.

With an explicit and uncoupled time integration procedure, the zone temperature calculated at time t is used to evaluate the partition temperatures at time $t+\Delta t$, and zone temperature at $t+\Delta t$ are then evaluated on the base of these partition temperatures. For one time step Δt used to evaluate zone temperature, five time steps may be needed to evaluate the partition temperatures. Some assumptions have to be made on the evolution of zone temperatures (constant, linear…) during the calculation of the temperatures in the partition. Time steps with an explicit procedure have to be short enough to make this assumption valid (Drysdale 1999). On the other hand it is well known that an implicit procedure enables the use of bigger time steps.

Partitions can be modelled by one dimensional finite elements in the case of a single zone model; on the other hand, partitions of the two-zone model should theoretically be modelled by two dimensional finite elements. One dimensional finite elements used in case of 2ZM, lead to neglect the vertical fluxes in walls and to artificially create or remove some energy. This is because the thickness of both zones varies with time, thus changing the boundary conditions of a part of the wall. For instance, a part of wall that is initially connected to the lower layer may later become connected to the upper layer if the upper layer thickness increases.

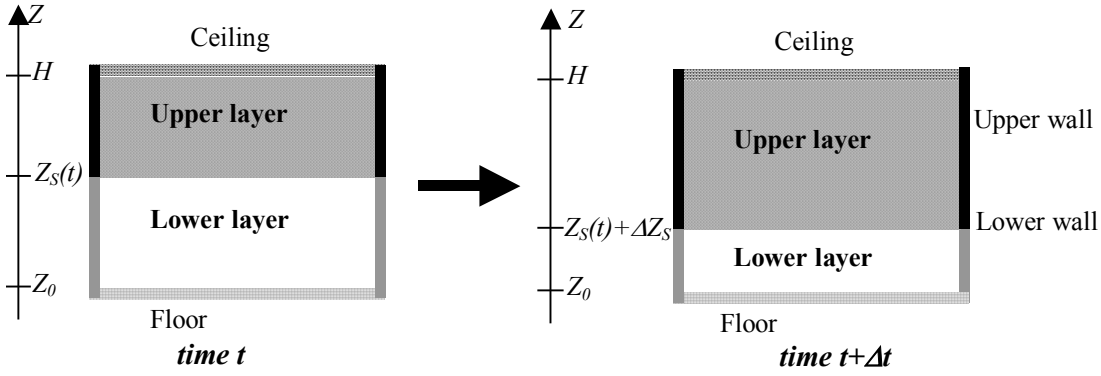

Figure 4.4 2ZM & partition model at times t and $t + \Delta t$

Considering an increasing upper layer thickness during the time interval Δt (Figure 4.4), a wall section of height ΔZ_S is transformed from lower wall to upper wall. As the temperatures in the lower wall are generally lower then those in the upper wall, some energy is thus artificially created here in the model. On the contrary if the upper layer thickness is decreasing, some energy is lost. The only way to be absolutely rigorous when modelling walls in 2ZM would be to make a single two dimensional partition model which would take into account vertical fluxes and the variation of Z_S in the boundary condition of the two dimensional elements.

A one dimension partition model is nevertheless considered in OZone, for the two-zone as well as for the one-zone model. Preliminary work on a two-zone model with a two dimensional partition model (Capus, 1998) has indeed shown that the partition model based on one dimension finite elements is a sufficiently good approximation of the reallity; the difference on the gas temperature calculated with 1D or 2D partition model being of a few degrees only. In most cases, the two dimensional character of the heat transfer can be neglected. The increase in computing time and the significant difficulties encountered in defining the compartment are quite important if the walls are represented by 2D elements whereas it has a marginal effects on

the results of principal interest, the zone temperatures and the zone thickness. Moreover, even in high compartment with small floor area for which the 2D effect may become more important, the error in neglecting it should be much smaller than one due to the assumption of uniform temperature in zones.

4.3.1 Two-zone model

Numerical two-zone models are normally based on eleven physical variables. These variables are linked by seven constraints and four differential equations describing the mass and energy balances in each zone. The time integration of these differential equations gives the evolution of the variables describing the gas in each zone. The mass balance equation expresses the fact that, at any moment, the variation of the mass of the gas in a zone is equal to the sum of the mass of combustion products created by the fire plus the mass coming into the compartment through the vents and the mass going out of the compartment through the vents. The energy balance equation expresses the fact that, at any moment, there is a balance between the energy which is produced in the compartment by the combustion and the way in which this energy is consumed: by the heating of the gases in the compartment, by the mass loss of hot air through the openings (including a negative term accounting for the energy of incoming air), by the radiation loss through the openings and, finally, by the heating of the partitions. The term "partition" represents all the solid surfaces that enclose the compartment, namely the walls (vertical), floor and ceiling (horizontal).

The eleven variables which are considered to describe the gas in the compartment are: the mass of the gas of respectively the upper and lower layer, m_U and m_L; the temperatures of the gas, T_U and T_L,; the volumes, V_U and V_L; the internal energies, E_U and E_L; the gas densities ρ_U and ρ_L, of respectively the upper (U) and lower (L) layer and finally the absolute pressure in the compartment considered as a whole, p.

The seven constraints are, Eqs. (4.1):

$$\begin{aligned} &\rho_i = \frac{m_i}{V_i} \\ &E_i = c_V(T_i) m_i T_i \qquad\qquad i = U,\ \ L \\ &p = \rho_i R T_i \\ &V = V_U + V_L \end{aligned} \tag{4.1}$$

The specific heat of the gas at constant volume, $c_v(T_i)$, and at constant pressure, $c_p(T_i)$, the universal gas constant, R, and the ratio of specific heat, $\gamma(T_i)$, are related by Eqs. (4.2):

$$\begin{aligned} &R = c_p(T_i) - c_v(T_i) \\ &\gamma(T_i) = \frac{c_p(T_i)}{c_v(T_i)} \end{aligned} \tag{4.2}$$

The variation of the specific heat of the gas with the temperature is taken into account by the following relation obtained by a linear regression on the tabulated data for air (combustion products are thus ignored) given in the SFPE Handbook of Fire Protection Engineering (1995):

$$c_P(T) = 0.187\,T + 952 \tag{4.3}$$

The mass balance equations have the general form of Eqs. (4.4) and (4.5). A dotted variable $\dot{x}$ means the derivative of x with respect to time.

$$\dot{m}_U = \dot{m}_{fi} + \dot{m}_{U,VV,out} + \dot{m}_{U,HV,in} + \dot{m}_{U,HV,out} + \dot{m}_{U,FV,in} + \dot{m}_{U,FV,out} + \dot{m}_e \tag{4.4}$$

$$\dot{m}_L = \dot{m}_{U,VV,in} + \dot{m}_{L,VV,in} + \dot{m}_{L,VV,out} + \dot{m}_{L,FV,in} + \dot{m}_{L,FV,out} - \dot{m}_e \tag{4.5}$$

The energy balance equations have the general form of Eqs. (4.6) and (4.7).

$$\dot{q}_U = Q_c + \dot{q}_{U,p} + \dot{q}_{U,VV,out} + \dot{q}_{U,VV,r} + \dot{q}_{U,HV,in} + \dot{q}_{U,HV,out} + \dot{q}_{U,FV,in} + \dot{q}_{U,FV,out} + \dot{q}_e \tag{4.6}$$

$$\dot{q}_L = \dot{q}_{L,p} + \dot{q}_{U,VV,in} + \dot{q}_{L,VV,in} + \dot{q}_{L,VV,out} + \dot{q}_{L,VV,r} + \dot{q}_{L,FV,in} + \dot{q}_{L,FV,out} - \dot{q}_e \tag{4.7}$$

Four basic variables have to be chosen to solve the system. Provided that the zone temperatures, T_U and T_L, the height of separation of zones, Z_S and the difference of pressure from the initial time, Δp are selected, Eqs. (4.4) to (4.7) can be transformed (Forney, 1994) in the system of ordinary differential equations (ODE) formed by Eqs. (4.8) to (4.11).

$$\dot{\Delta p} = \frac{(\gamma - 1)(\dot{q}_U + \dot{q}_L)}{V} \tag{4.8}$$

$$\dot{T}_U = \frac{1}{c_p(T_U)\rho_U V_U}\left(\dot{q}_U - c_p(T_U)\dot{m}_U T_U + V_U \dot{\Delta p}\right) \tag{4.9}$$

$$\dot{T}_L = \frac{1}{c_p(T_L)\rho_L V_L}\left(\dot{q}_L - c_p(T_L)\dot{m}_L T_L + V_L \dot{\Delta p}\right) \tag{4.10}$$

$$\dot{Z}_S = \frac{1}{\gamma(T_L)PA_f}\left((\gamma(T_L) - 1)(\dot{q}_U + \dot{q}_L) - V_L \dot{\Delta p}\right) \tag{4.11}$$

4.3.2 One-zone model

In the case of a one-zone model, the number of variables which describe the gas in the compartment as a whole is reduced to six; i.e. the mass of the gas, m_g; the temperature of the gas, T_g; the volume of the compartment (constant), V; the internal energy, E_g; the pressure in the compartment, p; the gas density, ρ_g.

The number of constraints is reduced to 4:

$$\begin{aligned} \rho_g &= \frac{m_g}{V} \\ E_g &= c_V(T_g) m_g T_g \\ p &= \rho_g R T_g \\ V &= \text{constant} \end{aligned} \tag{4.12}$$

Eq. (4.13) expresses the mass balance.

$$\dot{m}_g = \dot{m}_{fi} + \dot{m}_{g,VV,in} + \dot{m}_{g,VV,out} + \dot{m}_{g,HV,in} + \dot{m}_{g,HV,out} + \dot{m}_{g,FV,in} + \dot{m}_{g,FV,out} \tag{4.13}$$

Eq (4.14) expresses the energy balance.

$$\dot{q}_g = RHR + \dot{q}_{g,p} + \dot{q}_{g,VV,in} + \dot{q}_{g,VV,out} + \dot{q}_{g,VV,r} + \dot{q}_{g,HV,in} + \dot{q}_{g,HV,out} + \dot{q}_{g,FV,in} + \dot{q}_{g,FV,out} \tag{4.14}$$

Two basic variables have to be chosen to solve the system. Provided that the zone temperature, T, and the difference of pressure from the initial time, Δp, are chosen, Eqs. (4.13) and (4.14)

can be transformed in the system of ordinary differential equations (ODE) formed by Eqs. (4.15) and (4.16).

$$\dot{\Delta p} = \frac{(\gamma - 1)\dot{q}_g}{V} \tag{4.15}$$

$$\dot{T}_g = \frac{1}{c_p(T_g)\ \ \rho_g\ \ V}(\dot{q}_g - c_p(T_g)\ \dot{m}_g\ \ T_g + V\ \dot{\Delta p}) \tag{4.16}$$

4.3.3 Partition model

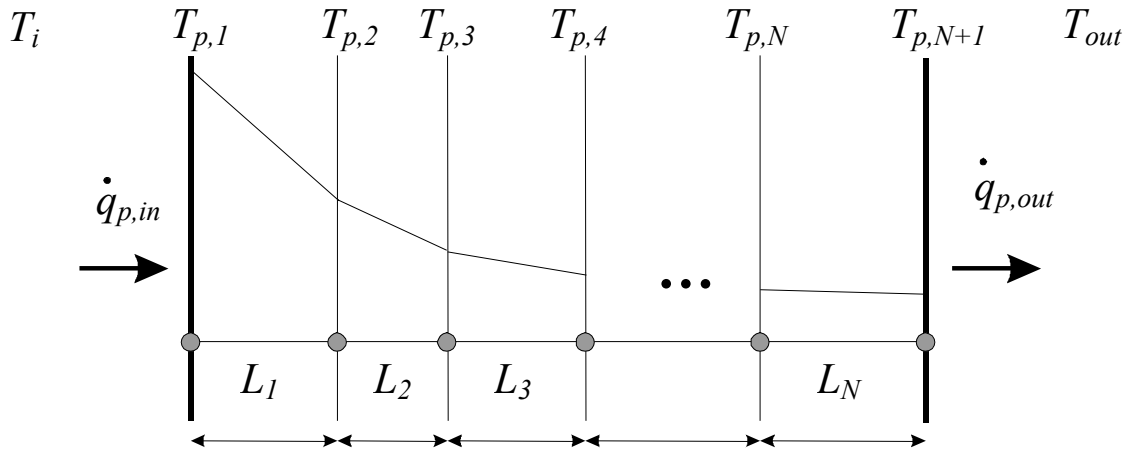

Figure 4.5 one dimensional finite elements discretisation of partitions

A partition is discretised by a one dimension finite element model as depicted in Figure 4.5. With this discretisation, the temperature is computed at the interface between the different layers, or elements, and a linear temperature variation on the thickness of each element is assumed.

The equilibrium of each finite element *j* is described by the following equation:

$$\mathbf{K}_{el,j}\ \ \mathbf{T}_{el,j}\ +\ \mathbf{C}_{el,j}\ \ \dot{\mathbf{T}}_{el,j}\ = \mathbf{g}_{el,j} \tag{4.17}$$

with $$\mathbf{T}_{el,j} = \begin{Bmatrix} T_{p,j} \\ T_{p,j+1} \end{Bmatrix} \tag{4.18}$$

$$\mathbf{K}_{el,j} = \frac{k_j}{L_j}\begin{bmatrix} 1 & -1 \\ -1 & 1 \end{bmatrix} \tag{4.19}$$

$$\mathbf{C}_{el,j} = c_j\ \ \rho_j\ \ L_j \begin{bmatrix} 0.5 & 0 \\ 0 & 0.5 \end{bmatrix} \tag{4.20}$$

and $$\mathbf{g}_{el,1} = \begin{Bmatrix} \dot{q}_{p,in} \\ 0 \end{Bmatrix};\ \mathbf{g}_{el,2}\ \ to\ \ \mathbf{g}_{el,n-1} = \begin{Bmatrix} 0 \\ 0 \end{Bmatrix};\ \mathbf{g}_{el,n} = \begin{Bmatrix} 0 \\ \dot{q}_{p,out} \end{Bmatrix} \tag{4.21}$$

Eqs. (4.19) and (4.20) are in fact simplified expressions because the material properties have been considered as constant in each element, thus taking them as constant multipliers of the

matrix; the temperature dependency in the element could also be taken into account by Gauss integration techniques but it has not been done in this model. Eq. (4.20) is furthermore the diagonalised version of the true matrix. An advantage of the diagonal form is that it smoothes the spatial oscillations which could arise in the solution if too thick elements are used in the discretisation. Another advantage is related to the computing strategy, as will be explained in the formulation of equation (4.24).

The assembly of the n partition equations of type (4.17) that can be written for each of the N finite elements making the partition produce the system of Eqs. (4.22) in which the size of the vectors and the matrices are N+1 and (N+1) x (N+1), respectively.

$$\mathbf{K}\ \mathbf{T}_p\ +\ \mathbf{C}\ \dot{\mathbf{T}}_p = \mathbf{g} \tag{4.22}$$

$$\text{where } \mathbf{g} = \begin{Bmatrix} \dot{q}_{p,in} \\ 0 \\ \\ 0 \\ \dot{q}_{p,out} \end{Bmatrix} \tag{4.23}$$

The energy transmitted at the partition interface results from heat transfer by convection and radiation between the zone and the partition and between the fire and the partition. The energy transmitted at the interface between the outside world and the partition is due to heat transfer by convection and radiation.

From the system of Eqs. (4.22), it is easy to derive analytically the system of Eqs. (4.24).

$$\dot{\mathbf{T}}_p = \mathbf{C}^{-1}\ \left(\mathbf{g}\ -\ \mathbf{K}\ \ \mathbf{T}_p\right) \tag{4.24}$$

This system of equations is a set of N differential equations for the N temperatures of the partition. The temperature of the compartment is only present in the first term of the load vector, see Eqs. (4.21), (4.23) and (4.26) to (4.29). The system has a similar form as the system of Eqs. (4.8) to (4.11) (2ZM) and of Eqs. (4.15) and (4.16) (1ZM) established for the variables of the gas zones.

4.3.4 Connection of the zones and the partitions equations

Partitions can be divided into three types: the ceiling; the floor and the walls. The basic finite element formulation is the same for the three types of partitions but the boundary conditions are different.

4.3.4.1 Two-zone model

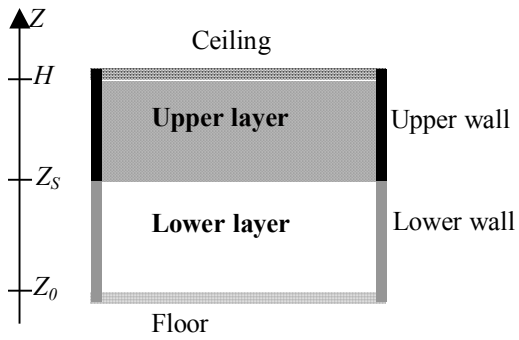

Figure 4.6 2ZM & partition model

In the 2ZM, the ceiling is always connected to the upper layer and the floor to the fire and to the lower layer. Vertical partitions are divided in two parts, an upper section, connected to the upper layer and a lower section connected to the fire and to the lower layer (Figure 4.6). The area of each part is calculated by multiplying the length of the wall by its height. The height varies with time and is function of the height of separation of the zones, Z_S. The area of the openings included in each partition is subtracted.

The finite element discretisation of the two parts are identical, only the boundary conditions are different.

The system of Eqs. (4.24) has to be constructed once for the ceiling, once for the floor and 2M times if the enclosure has M different types of walls. $N_{eq,ce}$ and $N_{eq,f}$ are the number of nodes of the ceiling and of the floor, and $N_{eq,i}$ is the number of nodes of the wall n°j. The partitions thus leads to $N_{eq,p}$ differential equations according to Eq. (4.25).

$$N_{eq,p} = N_{eq,f} + N_{eq,ce} + 2\sum_{j=1}^{M} N_{eq,j} \tag{4.25}$$

For all types of partition, the energy transmitted at the interface between the external environment and the partition is due to heat transfer by convection and radiation, given by Eq. (4.26).

$$\dot{q}_{p,out} = h\left(T_{out} - T_{w,N+1}\right) + \varepsilon_r \sigma \left(T_{out}{}^4 - T_{w,N+1}{}^4\right) \tag{4.26}$$

The upper layer is composed of a mixture of combustion products and fresh air entrained by the plume from the lower layer. It is considered to be opaque and radiation between partitions connected to it are neglected. The energy transmitted between the inside surfaces of upper partition and the upper layer results from heat transfer by convection and radiation according to Eq. (4.27).

$$\begin{aligned} \dot{q}_{pj,in} &= h\left(T_U - T_{w,1}\right) + \varepsilon_r \sigma \left(T_U{}^4 - T_{w,1}{}^4\right) \\ \dot{q}_{U,p} &= \sum_j A_{p,j,U} \dot{q}_{pj,in} \end{aligned} \tag{4.27}$$

The lower layer is essentially filled of fresh air and very little combustion products. It is thus considered as transparent. The energy exchanged between the inside surfaces of lower partitions and the lower layer results only from heat transfer by convection according to Eq. (4.28). Moreover the partition exchange heat with the fire by radiation, this term is represented by $q_{fi,p}$. The total heat exchange with partition is thus given by Eq. (4.29).

$$\dot{q}_{L,pj} = h\left(T_L - T_{w,1}\right)$$
$$\dot{q}_{L,p} = \sum_j A_{p,j,L}\dot{q}_{pj,in} \tag{4.28}$$

$$\dot{q}_{p,in} = \dot{q}_{L,pj} + \dot{q}_{fi,p} \tag{4.29}$$

$q_{fi,p}$ is obtained by dividing the radiative part of the rate of heat release Q_r by the total area of lower partitions, including the opening area and including the floor according to Eq. (4.30).

$$\dot{q}_{fi,p} = \frac{Q_r}{\sum_{j=1}^{M} A_{p,j,L} + \sum_{j=1}^{N} A_{w,j,L} + A_{fl}} \tag{4.30}$$

4.3.4.2 One-zone model

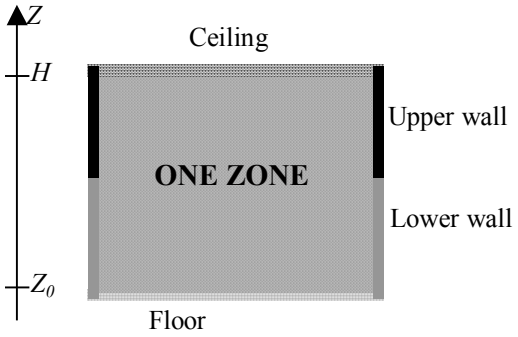

Figure 4.7 1ZM & partition model

When considering a one-zone model during an entire simulation, a vertical partition is consisted of two parts connected to the single zone. The finite element discretisation of the two parts and the boundary conditions are identical. Therefore the temperature distribution in the partitions and the flux densities on the boundaries are the same in the two parts. In a one-zone model a vertical wall would normally not be divided into two. The results obtained with two partitions for a single wall are identical to those with one single partition model. Having two partitions will increase the number of equations to be solved and therefore the computing time. This division in two parts is done in order to allow eventual combination of the 2ZM and 1ZM as explained in section 4.3.6.

The partitions lead to $N_{eq,p}$ differential equations, also given by Eq. (4.25).

The boundary conditions of all type of partitions of 1ZM are given by Eqs. (4.31) & (4.32).

$$\dot{q}_{p,out} = h\left(T_{out} - T_{w,N+1}\right) + \varepsilon_r\sigma\left({T_{out}}^4 - {T_{w,N+1}}^4\right) \tag{4.31}$$

$$\dot{q}_{pj,in} = h\left(T_g - T_{w,1}\right) + \varepsilon_r\sigma\left({T_g}^4 - {T_{w,1}}^4\right)$$
$$\dot{q}_{g,p} = \sum_j A_{p,j}\dot{q}_{pj,in} \tag{4.32}$$

4.3.5 Time integration

In a 2ZM, Eqs. (4.8) to (4.11) and Eqs. (4.24) form a set of $N_{eq,part}$+4 differential equations which can be passed on to the numerical solver. This solver will integrate the equations taking into account the coupling between the compartment and the partition and solving the $N_{eq,part}$+4 variables, which are the pressure variation, the temperature in the upper zone, the temperature in the lower zone, the height of the zone interface and the temperatures at each node of the partitions.

The same procedure holds for a 1ZM with Eqs. (4.15), (4.16) and Eqs. (4.24) built $N_{eq\ part}$ times.

The system of ODE describing the situation is stiff. A physical, although not rigorous from a mathematical point of view, interpretation of stiffness is that the time constant relative to the pressure variation is much shorter than the time constant of the temperature variation. It is therefore usual to rely on a specialised library solver specifically written for this kind of problem. In the code OZone, the solver DEBDF (Shampine and Watts, 1979) is used.

4.3.6 Switch from two-zone to one-zone model

If some criteria are encountered during a two-zone simulation, the code will automatically switch to a one-zone simulation, which better describes the situation inside the compartment at that moment. The simulation will continue until the end of the fire under the hypothesis of a one-zone model. The aim of this section is to show how the code deals with the basic variables of the zone models, how it sets the initial conditions of the one-zone model and how it deals with partition models. The criteria for switching are also listed. A complete description of the criteria and of their effect on the simulation process is given in (Cadorin 2003b).

4.3.6.1 Zone models formulation

t_s is the time at which the switch from the 2ZM to the 1ZM occurs. The values of the eleven basic variables describing the gas in the two zones are known at t_s. To continue the simulation with a one-zone model, it is possible to start solving Eqs. (4.15) and (4.16). The point is to set the 1ZM initial values.

In one-zone model there are six variables describing the gas in the compartment as a whole, linked by four constraints. Two new constraints are thus needed to fix the new initial conditions.

These two additional conditions are obtained by setting that during the transition from 2 zones to 1 zone, the total mass and the total energy of gas in the compartment are conserved.

$$m_g(t_s) = m_U(t_s) + m_L(t_s) \tag{4.33}$$

$$E_g(t_s) = E_U(t_s) + E_L(t_s) \tag{4.34}$$

The initial one-zone temperature $T_g(t_s)$ and one-zone pressure $p(t_s)$ can be deduced from Eqs. (4.33), (4.34) and (4.12).

A consequence of this procedure is that $T_g(t_s)$ is lower then $T_U(t_s)$ and higher then $T_L(t_s)$ and thus the temperature curves are discontinuous at the time of switch.

4.3.6.2 Wall model formulation

The partition temperatures, the height of the lower and upper walls (vertical partitions) $Z_S(t_s)$ and $H\text{-}Z_S(t_s)$ are known at time t_s. From t_s to the end of the calculation, the one-zone model is linked to the lower and upper walls which keep the dimension they had at time t_s, i.e. $Z_S(t_s)$ and $H\text{-}Z_S(t_s)$. During the transition no modification of partition temperatures or wall dimension is made; only the boundary conditions at the interface with the compartment are modified. This way to proceed enables to fully respect the conservation of energy during the transition from the two-zone to the one-zone model.

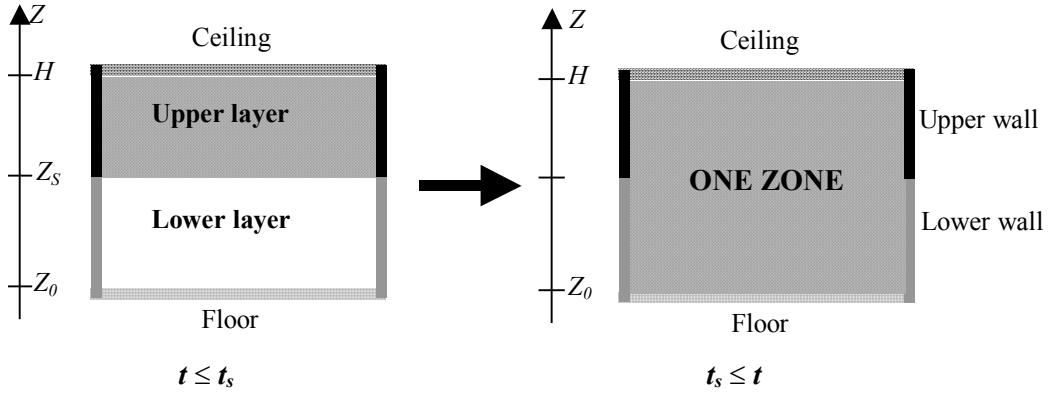

Figure 4.8

With a two-zone model, upper walls (and ceiling) exchange energy by radiation and convection with the upper layer that is considered opaque while lower walls (and floor) are heated directly by radiation from the fire, and they give back energy to the lower layer by convection. After the switch is encountered, all partitions (upper and lower walls, ceiling and floor) exchange energy by radiation and convection with the single zone that is considered opaque.

4.3.6.3 Ignition and switch criteria

The switch from 2ZM to 1ZM can be activated by four criteria. Two criteria are linked to the ignition of the fuel and two others are related to the loss of validity of the two zone assumption. While the first two criteria are related to physical phenomenon which may occur during compartment fires, the last two are related to the limits of applicability of the two-zone model assumptions.

It is important to note that users have the possibility to activate or not any of these criteria and to decide on the value of the relevant parameters at which criteria are met. The default value proposed here are only informative and not necessarily applicable to any situation.

4.3.6.3.1 Flashover Criterion

A high temperature of the upper layer leads to a flashover. All the fuel in the compartment is ignited by radiative flux from the upper layer;

In a recent overview of flashover studies (Peacock et al., 1999, see chapter 2), the upper layer temperature and the heat flux received by the fuel leading to flashover obtained in different experimental studies have been collected. The temperature values are between 450 and 800°C with most values between 600 and 700°C. The heat flux values are between 15 and 33kW/m². This shows the high level of pure uncertainty on the flashover phenomenon. Anyway, if the definition has to be unique, the most common value admitted to characterise flashover is 600°C which correspond to a heat flux of about 20kW.

In OZone, the default value of the upper layer temperature leading to flashover is 500°C. The temperatures between 600 and 700°C given in the literature correspond to temperatures near the ceiling, while the upper layer temperature of a two-zone model is an average temperature in the upper layer volume and is therefore lower than the local temperature near the ceiling.

4.3.6.3.2 Ignition Criterion

If the gases in contact with the fuel have a higher temperature than the ignition temperature of

fuel, the propagation of fire to all the combustible of the compartment may occur by convective ignition;

Babrauskas (2001) reports that ignition temperature of wood exposed to the minimum heat flux possible for ignition is around 250°C. The surface temperature of fuel is usually used as an empirical parameter to describe the ignition of fuel. Nevertheless it is particularly convenient to use the temperature of the environment to characterise ignition in compartment fire modelling because the environment temperature is the main result of zone models. Even in test built-up for ignition temperature evaluation, the environment temperature is often used as criterion. (see chapter 2)

Taking into account a difference between the surface and the surrounding environment temperatures, the default value of the zone temperature at which ignition occurs has been set in the code to 300°C.

4.3.6.3.3 Interface Height Criterion

The interface height may go down and lead to a very small lower layer thickness, which is not representative of two-zone phenomenon.

It is not correct to have an upper layer thickness nearly equal to the compartment height and still to consider the two-zone model assumptions. For example, the heat transfer by radiation from the fire to the lower partitions is overestimated if the lower layer is too thin, the radiant part of the flame being in reality mainly included in the upper layer. Moreover numerical problems will be encountered for very thin lower layer.

In the code, the default value of the interface height criterion is 20% of the compartment height.

4.3.6.3.4 Fire Area Criterion

The fire area may be too large compared to the floor surface of the compartment to consider a localised fire. In this situation the volume of the plume itself may be quite big and the 2 zone assumption ignores this fact.

For example, in a 8 x 8 m^2 compartment, 25% of the area is covered by the fire if a square fire of 4 x 4 m^2 is in the centre of the room, which means that only a 2 m wide "corridor" of non burning floor surface is left between the fire and the walls. Models based on a localised fire, for example air entrainment models, should not be applied in this case. The hypothesis of a uniform temperature is then a better representation.

In OZone, the default value of the fire area criterion is 25% of the floor compartment area.

4.4 Exchanges through the vents

Three types of vent models have been introduced in OZone: vertical vents; horizontal vents and forced vents.

Although the pressure is uniform in the compartment when solving the basic equations of the problem, the pressure is not uniform in the compartment when calculating the mass flow through the openings. In this case, the variation is exponential with the height.

4.4.1 Vertical vents

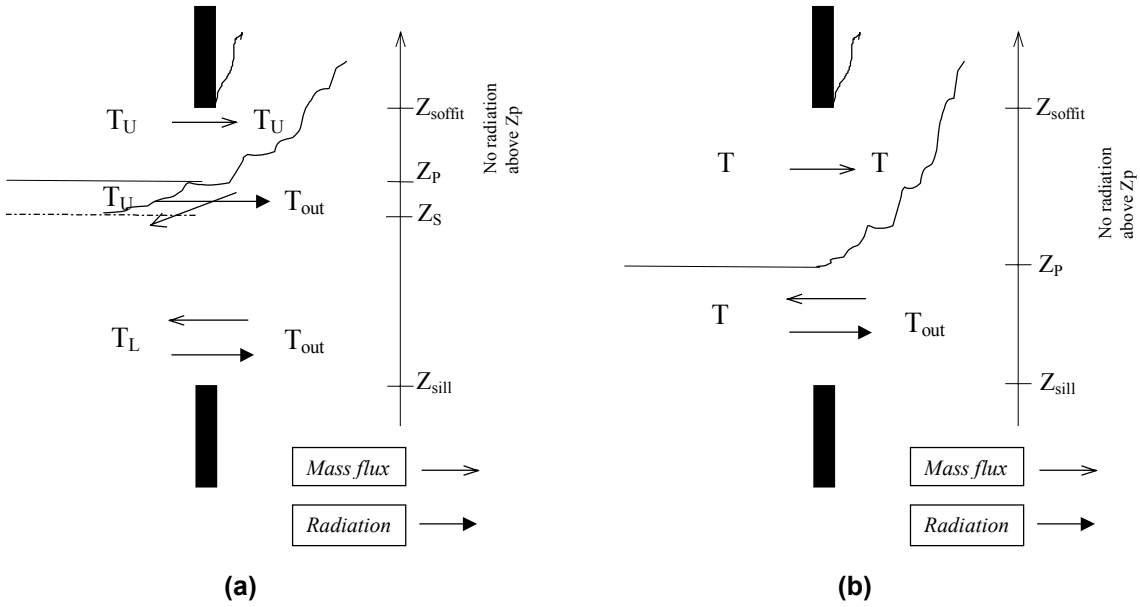

Figure 4.9 Exchanges through vertical vents in (a) 2ZM and (b) 1ZM

4.4.1.1 Convective exchanges

The mass flow through vents is calculated by integrating the Bernoulli law on each opening, Eq. (4.35) (Forney 1990).

$$\dot{m}_{i,VV,\beta} = sign\ K\ b_w(T\ or\ t)\int_{Z'}^{Z''}\frac{p_A(z)}{R\,T_A}\sqrt{2\,R\,T_A\left(1-\frac{p_B(z)}{p_A(z)}\right)}\,dz \qquad (4.35)$$

With A : variable at origin of the flux
B : variable at destination of the flux
Z' & Z'': bounds of integration on height Z
ι : U if the integration is made in the upper layer, L if the integration is made in the lower layer and g in case of one-zone model.
β : *in* if gas goes in the compartment, *out* if gas goes out of the compartment
sign : (+1) if gas goes in the compartment, (-1) if gas goes out of the compartment

If the height where the pressure inside the compartment is equal to the pressure outside of the compartment is in a vertical vent, the vertical vents is divided in two parts, one where the mass flow goes inside the compartment and another one where the mass flow goes outside. This height is called the neutral plane height. Moreover in two-zone model, if the height of separation between the zone is in the opening, another subdivision is encountered. In 1ZM, three possibilities exist depending on the neutral level position. In 2ZM, 10 possibilities exist depending on the neutral level and the zone separation height positions. For each vertical vent, Eq. (4.35) is evaluated 1 to 3 times with the appropriate bounds of integration on the height (Z' & Z'' can be the sill of the vent, the soffit of the vent, the neutral plane height or the separation between the zone height). Figure 4.9 shows in case of 2ZM and 1ZM one possible situation of relative position of Z_{sill}, Z_P, Z_S and Z_{soffit}.

The energies contained in these mass fluxes are calculated by Eqs. (4.36).

$$\dot{q}_{i,VV,\beta} = c_p(T_i)\dot{m}_{i,VV,\beta}T_i \qquad i = U,\ L,\ g\ ;\ \beta = in, out \tag{4.36}$$

In the two-zone model, all the mass coming in the compartment through vertical vent is added to the lower layer. This hypothesis has been made considering the fact that the gas coming in has a higher density then the gas inside and thus, due to buoyancy, goes downward when coming in (Figure 4.9a).

4.4.1.2 Radiative exchanges

The radiation through vertical vents is taken into account by the Stefan-Boltzman law. It is considered that the radiation exists only below the neutral axis. Above this level, the gases go out of the compartment and the temperature outside (in the plume) is assumed to be equal to the temperature in the compartment and it is considered that the net radiation flux is equal to zero (Figure 4.9). This latter hypothesis may be too conservative when the outflow is very thin and not completely opaque. Nevertheless this effect should only be significant for very large opening sizes.

$$\dot{q}_{i,VV,r} = \varepsilon_g \sigma \left(T_i^4 - T_{out}^4\right) b_w \left(Z_p - Z_{sill}\right) \qquad i = U, L \text{ or } g \tag{4.37}$$

If the opening is closed no mass exchange exists through it. The opening can either be assumed to be adiabatic and thus no radiation through it is considered or be assumed to be non adiabatic and the radiation flux is evaluated by Eq. (4.38).

$$\dot{q}_{i,gl,r} = \varepsilon_{gl} \sigma \left(T_i^4 - T_{out}^4\right) A_{i,VV,cl} \qquad i = U, L \text{ or } g \tag{4.38}$$

$A_{i,VVcl}$ is the area of the closed opening. ε_{gl} is a parameter which includes the relative emissivities of the gases and the part of energy which is reflected on the interfaces between gas and glass and absorbed by the glazing material.

4.4.2 Horizontal vents

Gas flow through a horizontal ceiling vent is not always driven by the single pressure difference, buoyancy can also have a significant effect. These forces may lead to bi-directional exchange flow through the vent. Therefore it is not appropriate to unconditionally use Bernoulli's equation to model flow through horizontal vent.

Cooper has proposed a model and the associated FORTRAN subroutine for calculating flows through circular, shallow (i.e. small depth to diameter ratio), horizontal vents (Cooper, 1995, 1996 and 1997). This model gives the flow considering the pressure driven forces and, when appropriate, the combined pressure and buoyancy effects. This subroutine has been included in the code.

4.4.3 Forced vents

Forced vent model is built to represent the effect of mechanical ventilation. The forced vents are defined by the volume rate flow that they induced, $\dot{V}_{FV}$, their height Z_{FV} and their diameter D_{FV}.

When the zone interface is above the forced vent elevation + 1.5 D_{FV}, the exhausted gas is from the lower layer only. When the zone interface is below the forced vent elevation - 1.5 D_{FV}, the exhausted gas is upper layer air only. When the zone interface is between Z_S + 1.5 D_{FV} and Z_S - 1.5 D_{FV}, the mass of extracted air from each layer is given by a linear interpolation (Figure 4.10).

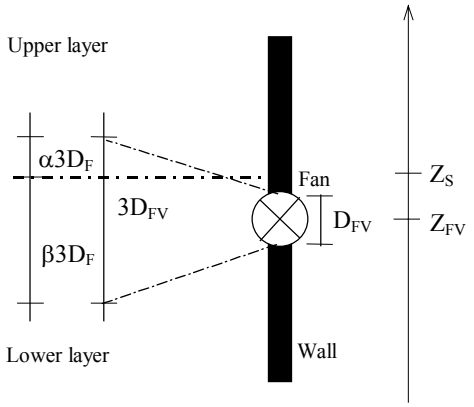

Figure 4.10 Schematic view of forced vent model in a vertical partition

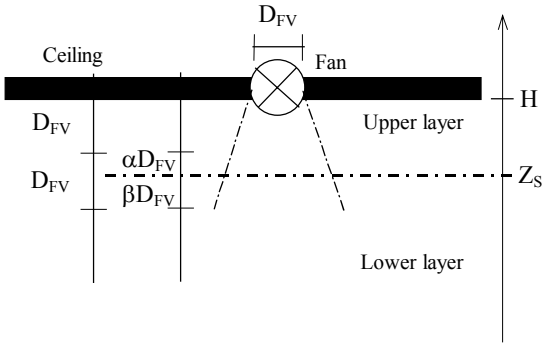

Figure 4.11 Schematic view of forced vent model in the ceiling

If the forced vent is in the ceiling the interpolation is made as shown in Figure 4.11. When the zone interface is above the forced vent elevation - D_{FV}, the exhausted gas is lower layer air only. When the zone interface is below the forced vent elevation - 2 D_{FV}, the exhausted gas is upper layer air only. When the zone interface is between Z_S-D_{FV} and Z_S-2D_{FV}, the mass of extracted air from each layer is by a linear interpolation (Figure 4.11).

$$\begin{aligned} &\dot{m}_{i,FV,\beta} = \rho_A \dot{V}_{FV} \\ &\dot{q}_{i,FV,\beta} = c_p(T_A)\dot{m}_{i,FV,\beta} T_A \end{aligned} \qquad i = U,\ L,\ g\ ;\ \beta = in, out;\ A \triangleq origin\ of\ the\ flow \tag{4.39}$$

The latter procedure to decide whether the flow is exchanged with the upper or with the lower layer is based on the fact that the volume on which forced vent flow has an influence should depend, among other things, on the fan diameter. The bounds of the influence zone (3D_{FV} and 2D_{FV}) have been fixed arbitrarily. The parameter D_{FV} is only used in this definition of these bounds, thus, if a more precise knowledge of this phenomenon is know, it can be fixed to any value, not necessarily linked to the real dimension of the vent.

Moreover, in case of 2ZM, if the mass was extracted at a single height from the corresponding zone and if the mass extracted was bigger then the entrained mass in the plume, some numerical problems would be encountered. The proposed procedure enables to avoid these numerical problems.

4.4.4 Opening size variation (glazing breakage)

During the course of a fire the number of vents that are open can vary. Their size can also be modified. This can be the result of glazing breakage, automatic opening or firefighter action… In this code, the opened vent size can be defined to be a function of the temperature of the zone in contact with the glass or to be a function of time.

The size variation of a vertical vent is modelled by a variation of its width. The size variation of a horizontal vent is modelled by a variation of its area.

4.5 Fire source - Input of heat and of combustion products in the compartment

To represent the fire, the basic inputs are the heat release rate *RHR(t)* [W], the pyrolysis rate $\dot{m}_{fi}$ *(t)* [kg/s] and the fire area $A_{fi}(t)$ as a function of time. The pyrolysis rate is taken into account in

mass balances and the heat release rate in energy balances. The fire area is used in some air entrainment models. This section explains the physical parameters used to define the fire source, how they are related and how OZone deals with them in function of the oxygen available in the compartment. The strategy of calculation may also influence these input as explained in chapter 5. A more complete description of these terms can be found in chapter 2.

4.5.1 Basic parameters

The basic parameters have been defined in chapter 2 and are the:

- Heat release rate - *RHR*
- Heat release rate density - RHR_{fi}
- Pyrolysis Rate - $\dot{m}_{fi}$
- Combustion Heat of Fuel - H_c
- Fire Area - $A_f(t)$: The fire area is the floor area of burning fuel. In real fires, it is usually varying with time. In some cases (ex. pool fire tests), the fire area can be constant. The maximum fire area in a compartment is the floor area on which combustible is present. The pyrolysis rate and the heat release rate are of course linked to the fire area (see next paragraphs). Moreover, some air entrainment models depend on the fire diameter and therefore on the fire area.

The fire source is defined by three parameters, the pyrolysis rate, the heat release rate and the fire area. They can be linked by Eqs. (4.40)and (4.41) (for instance the heat release rate and the pyrolysis rate can be linked as shown on Figure 4.12 and Figure 4.13) or defined independently ones from the others.

$$RHR(t) = H_{c,eff}\ \dot{m}_{fi}(t) \tag{4.40}$$

$$RHR(t) = A_{fi}(t)\ RHR_{fi} \tag{4.41}$$

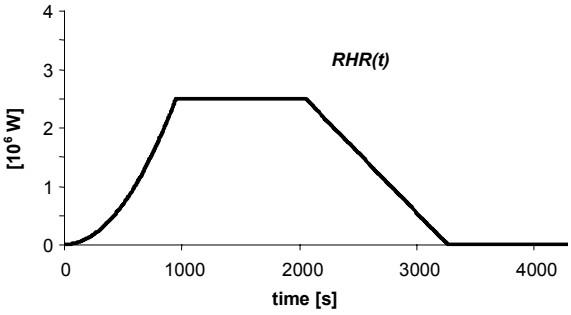

Figure 4.12 Input Heat release rate Curve

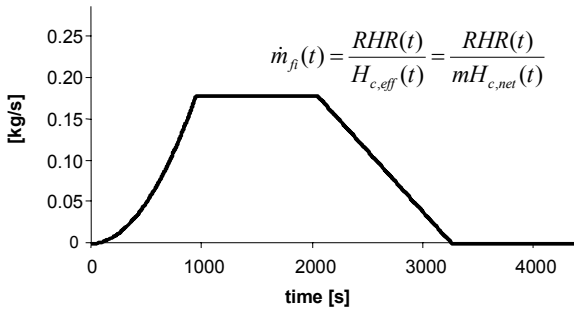

Figure 4.13 Input Pyrolysis Rate Curve

4.5.2 Combustion chemistry

The following chemical reaction is considered (see Chapter 2, Section 2.4.1 for the background of this assumption):

$$1\ \ kg\ of\ \ fuel + 1.27\ \ \ \ kg\ of\ \ 0_2 = 2.27\ kg\ of\ \ combustion\ products + H_{f,eff}\ \ \ \ MJ \tag{4.42}$$

This equation is representative of stoichiometric combustion of wood that is represented by $\boldsymbol{CH_{1.5}O_{0.7}}$ (Drysdale 1999).

4.5.3 Oxygen balance

The mass of oxygen in the compartment is calculated at each time by integrating the oxygen balance:

$$\dot{m}_{ox} = \dot{m}_{ox,in} + \dot{m}_{ox,out} - 1.27\dot{m}_{fi} \tag{4.43}$$

The initial mass of oxygen in the compartment is considered to be 23% of the initial mass of gas, supposed to be fresh air. The mass of oxygen coming in the compartment is considered to be 23% of the mass of gas coming in the compartment through vents. The mass of oxygen going out of the compartment is considered to be ξ_{ox} % of the mass of gas going out of the compartment. ξ_{ox} is the concentration of oxygen in the gas inside the compartment and is calculated by Eqs. (4.44).

$$\begin{aligned} \xi_{ox} &= \frac{m_{ox}}{m_U + m_L} && (2ZM) \\ \xi_{ox} &= \frac{m_{ox}}{m_g} && (1ZM) \end{aligned} \tag{4.44}$$

The concentration of oxygen is supposed to be uniform in the compartment.

4.5.4 Combustion models

The users has to choose between three different combustion models. Each of them has been designed to represent a different situation of utilisation of the code.

a) With the "predetermined" combustion model, the oxygen content in the compartment does not influence the heat release rate and the pyrolysis.

b) The "external flaming" combustion model limits the amount of energy released inside the compartment when the concentration of oxygen in the compartment falls to zero, i.e. when all of the oxygen initially present in the compartment has be consumed and when all of the oxygen entering the compartment is directly consumed by combustion within the compartment.

c) In the same case, the "extended fire duration" combustion model limits the amount of energy release rate inside the compartment and all the fire load is burned in the compartment by extending the initial fire duration.

4.5.4.1 Predetermined combustion model

With this model, the pyrolysis rate and the heat release rate set in the data are used in the mass and energy balances without any modification regarding to the oxygen concentration in the compartment. At each time, Eqs. (4.45) will be satisfied.

$$\begin{aligned} \dot{m}_{fi}(t) &= \dot{m}_{fi,data}(t) \\ RHR(t) &= RHR_{data}(t) \end{aligned} \tag{4.45}$$

This model is used for the simulation of experimental tests where the mass loss and the heat release rate have been measured independently. It is also suitable for situations where the pyrolysis rate is known and where the fire is assumed to be fuel controlled.

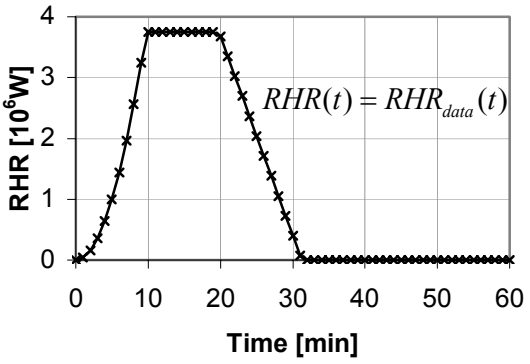

Figure 4.14 Predetermined combustion model Heat release rate Curve

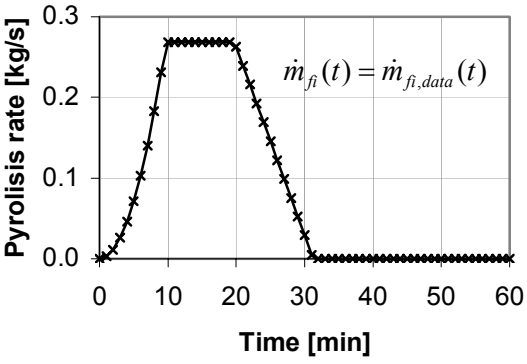

Figure 4.15 Predetermined combustion model Pyrolysis Rate Curve

4.5.4.2 External flaming Combustion model

In this model external combustion is assumed, all the fire load is transformed into gases in the compartment but only a part of it delivers energy in the compartment. The heat release rate may be limited by the quantity of oxygen available in the compartment but the pyrolysis rate remains unchanged.

When oxygen is still present in the compartment, the fire is fuel controlled and all the mass loss of fuel delivers energy inside the compartment.

$$\begin{aligned} &\dot{m}_{fi}(t) = \dot{m}_{fi,data}(t) \\ &RHR(t) = RHR_{data}(t) = \dot{m}_{fi}(t) H_{f,eff} \end{aligned} \tag{4.46}$$

When all of the oxygen initially present in the compartment has be consumed and when all of the oxygen entering the compartment is directly consumed by combustion within the compartment, the fire is ventilation controlled and the combustion is not complete. The energy released is governed by the rate of oxygen coming in the compartment through vents:

$$\begin{aligned} &\dot{m}_{fi}(t) = \dot{m}_{fi,data}(t) \\ &RHR(t) = \frac{\dot{m}_{ox,in}(t)}{1.27} H_{f,eff} \end{aligned} \tag{4.47}$$

When oxygen is again available in the compartment, for example during the decreasing phase of the fire, see Figure 4.16, the fire is coming back to fuel controlled regime and Eqs. (4.46) governs the pyrolysis and the heat release rates.

This model is used for the simulation of experimental tests where the mass loss or the heat release rate has been measured. It can also be used in design situation when the mass loss rate is known and when the user wishes to consider that some part of energy is released outside the compartment by external flaming.

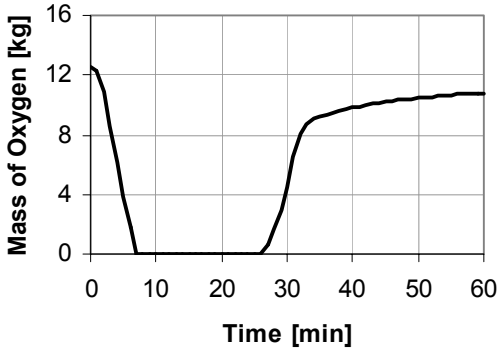

Figure 4.16 External flaming combustion model Oxygen mass curve

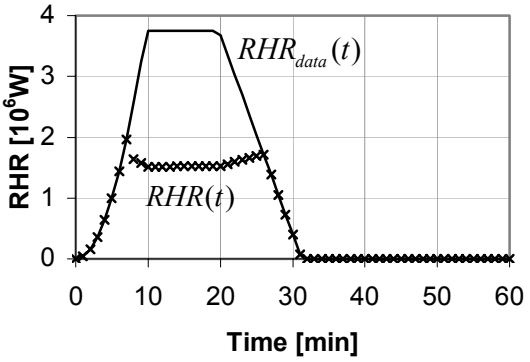

Figure 4.17 External flaming combustion model Heat release rate Curve. *RHR$_{data}$* is the RHR defined by the user and *RHR* is calulcated.

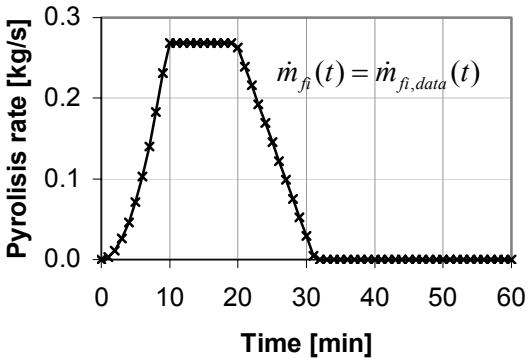

Figure 4.18 External flaming combustion model Pyrolysis Rate Curve

4.5.4.3 Extended fire duration combustion model

When all of the oxygen initially present in the compartment has been consumed and when all of the oxygen entering the compartment is directly consumed by combustion within the compartment, the pyrolysis rate is proportional to the quantity of oxygen coming in the compartment through openings. The total mass of fuel is burnt inside the compartment and the fire duration is increased compared to the input one.

When oxygen is available in the compartment, the fire is fuel controlled and the input pyrolysis and heat release rates are not modified.

$$\begin{aligned} &\dot{m}_{fi}(t) = \dot{m}_{fi,data}(t) \\ &RHR(t) = RHR_{data}(t) = \dot{m}_{fi}(t) H_{f,eff} \end{aligned} \tag{4.48}$$

If the fire is ventilation controlled, the mass lost by the fire is governed by the mass of oxygen coming in the compartment and all the pyrolysed gas are involved in the combustion process inside the compartment.

$$\begin{aligned} &\dot{m}_{fi}(t) = \frac{\dot{m}_{ox,in}(t)}{1.27} \\ &RHR(t) = \dot{m}_{fi}(t) H_{f,eff} = \frac{\dot{m}_{ox,in}(t)}{1.27} H_{f,eff} \end{aligned} \tag{4.49}$$

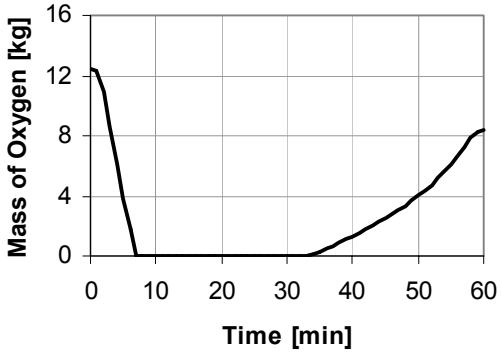

Figure 4.19 Extended fire duration combustion model Oxygen mass curve

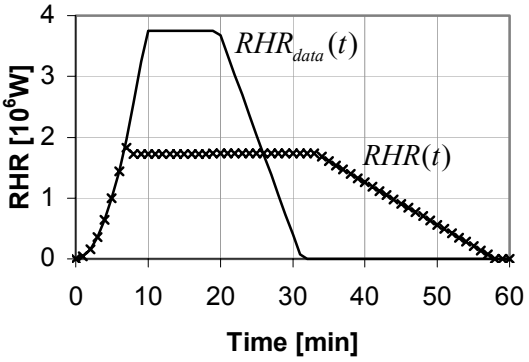

Figure 4.20 Extended fire duration combustion model Heat release rate Curve. RHR_{data} is the RHR defined by the user and *RHR* is calulcated.

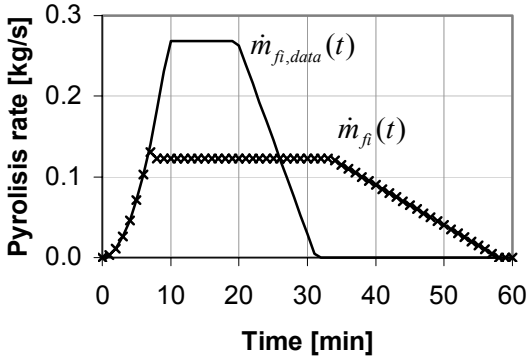

Figure 4.21 Extended fire duration combustion model Pyrolysis Rate Curve $m_{fi,data}$ is the pyrolysis rate defined by the user and m_{fi} is calulcated.

The linear decreasing phase has been assumed to start when 70% of the total fire load is consumed.

In this model no external combustion is assumed, all the fire load delivers its energy into the compartment. If the fire is ventilation controlled, the pyrolysis rate is proportional to the oxygen coming in the compartment.

This model has been established for design purposes, in order to avoid uncertainties in the maximum pyrolysis rate and therefore to be on the safe side for the design of structural elements.

4.6 Air entrainment

Air entrainment models are of primarily importance in two-zone models. Different analytical expressions of the behaviour of fire plume have been proposed by several authors. Four of them (that are describe in chapter 2 or in: Heskestad 1995, Karlsson, 2000, Drysdale, 1999) have been implemented, allowing users to use the more appropriated plume model for their simulations. These models are usually referred as Heskestad, Zukoski, McCaffrey and Thomas models. They have been implemented in the code with the formulations reported by Karlsson and Quintiere (2000) (see chapter 2, section 2.6).

The fire area is used in Heskestad and Thomas air entrainment models. The hypothesis of a

circular fire is made in this work, so the fire diameter is obtained by Eq. (4.50).

$$D = \sqrt{4\frac{A_{fi}}{\pi}} \tag{4.50}$$

The rate of entrained air mass is $\dot{m}_e$. The rate of energy transferred from the lower to the upper layer by the plume $\dot{q}_e$ is given by Eq. (4.51).

$$\dot{q}_e = c_p(T_L)\dot{m}_e T_L \tag{4.51}$$

4.7 Default values

In this section, a summary of the default values set in the code is given. Most of these values can be modified by the user, nevertheless others are can not be modified and if so are noted "(fixed)".

- Convective part of the RHR: $RHR_c = 0.7\ RHR$ (fixed)
- Radiative part of the RHR: $RHR_r = 0.3\ RHR$ (fixed)
- Oxygen/Fuel stoechiometric ratio: 1.3 (fixed)
- Discharge coefficient for vertical openings: $C_f = 0.7$
- Emissivity of gas: $\varepsilon_g = 1$
- Emissivity of partition: $\varepsilon_w = 0.8$
- Relative emissivity of partition-gas interface: $\varepsilon_p = \varepsilon_g\ \varepsilon_w = 0.8$
- convective heat transfer coefficient of partition-gas interface: $h = 25$ on the inner face of partitions and $h = 9$ on the outer face of partitions
- "Heskestad" plume model

4.8 Conclusions

The discretisation of the partitions by a traditional finite element approach allows formulating the differential equations that govern the heat transfer by conduction within the partition material. These equations can be added to the usual set of differential equations describing the evolution of the situation within the compartment. These two sets of equations can be solved simultaneously by the numerical solver. Because the two sets of equations are coupled by the temperature of the inside surface of the wall, the energy balance between the compartment and the wall is strictly respected in case of one-zone model simulation.

This proposed procedure provides an elegant and robust way to account for the heat transfer to the walls that does not require the introduction of hypotheses on the time evolution of the interface temperature.

Three different combustion models have been introduced to allow the user to run the code for different purposes. With the predetermined combustion model or with the external flaming combustion model it is possible to model full scale fire tests. These two combustion models can also be used in a design procedure if the fire source is well known or imposed by the user. The extended fire duration combustion model should be used in fire safety design procedures.

A combination of a two and a one-zone model is included. The criteria of transition offer to the user an automatic procedure to check whether a two-zone model is still appropriated to the fire stage which is modelled.

The compartment fire model described here is included in a tool which enables to design steel

elements submitted to compartment fires. The general methodology implemented in this tool and an example of design are presented in the next chapter. Comparisons of this new compartment fire model with a set of about 100 full scale fire tests are provided in chapter 6.

5

Methodology for designing steel elements submitted to compartment fires

5.1 Introduction

Prescriptive codes for structural fire resistance tend to be replaced by performance based codes. Yet, particularly in Europe, structural engineers are not used to model fires and their effect on structures. The software presented here has thus been elaborated to help them to design structural steel elements submitted to compartments fires.

Basic knowledge and understanding has been gained over the last decades by specialists in fire modelling. Other specialists in the structural behaviour of buildings submitted to the fire have also made progress in their field. Too often yet, very little communication has taken part between these two fields of fire safety engineering; whereas the former used to think of the structural problem only in terms of a critical temperature of, say, 540°C, the latter used to represent the fire by a single nominal time-temperature curve, either the ISO 834 or the ASTM E119 curve.

Most of the knowledge is thus present to allow a real engineering analysis of the structural aspects related to fire safety in buildings. This analysis requires the determination of the fire development in the compartment, then of the temperatures in the structural elements and, finally, of their mechanical behaviour. This knowledge was yet disseminated and it was not straightforward for a single individual to integrate all these notions for use in a practical, although simple application.

OZone has been developed as a practical design tool to realise a performance based analysis of the behaviour of simple steel elements in a compartment fire situation. Some particular new features have been introduced, the most significant being that the user has not to make a predetermined choice as to the description of the situation of the fire in the compartment: one-zone or two-zone model? The model is able to consider the initial phase of the fire as a localized fire with a two-zone development and, under certain circumstances, to switch later automatically to a one-zone description if required.

The aim of this chapter is to present the general methodology used in this tool, i.e., how are defined the compartment and the fire source; when the 2ZM or the 1ZM are considered, and how, in function of the fire phase, steel profile are heated... An example of application is then given and, from this example, a sensitivity study is performed to assess the influence of various parameters (fire load, boundary thermal properties, ventilation conditions, etc.) on the results given by the model.

The formulation of the compartment fire model has been given in chapter 4.

5.2 Overview of the methodology

The methodology of the design can be divided in 6 main steps. The steps are:

1. description of the compartment;
2. definition of a design fire;
3. calculation of the temperatures in the compartment;
4. a. definition of the thermal and mechanical properties of the section, of the thermal properties of the insulation material if the section is protected and of the thermal boundary conditions of the section;
   b. calculation of the temperature of steel elements, taking into account if necessary, the localised effect of the fire.
5. a. definition of the dimensions, the effects of actions, and static boundary conditions of the member;
   b. calculation of the fire resistance of the steel element.
6. acceptance or not of the fire resistance obtained in step 5. If the fire resistance is not accepted, the section or the thermal resistance of the insulation has to be increased and the process must be restarted from step 4.

These steps are described in the subsequent sections of this chapter.

5.3 Compartment

The compartment is described by:

- Its plan and elevation dimensions.
- The partition characteristics: layers thickness and thermal properties of materials.
- The size and position of openings: vertical and horizontal openings and forced vents can be modelled.

5.4 Design fires

The basic input to define the fire (see chapter 4) are the rate of heat release *RHR(t)* [W], the pyrolysis rate $\dot{m}_{fi}(t)$ [kg/s] and the fire area $A_{fi}(t)$ as functions of time. This section presents the definition of design fire proposed as standard options in the model. In this context, the expression '*Design fire*' refers to the definition of the fire source development (*RHR(t)* mainly) and not to temperature time curves. The procedure is based on the "Natural Fire Safety Concept" method which is first briefly presented.

5.4.1 Probabilistic basis of the method "Natural Fire Safety Concept"

The procedure to define the design fires is a semi probabilistic approach developed in the research project "Competitive Steel Structures through Natural Fire Safety Concept" (NFSC1, 1999 & Schleich, 2001). From pure probabilistic calculations, some partial safety factors γ on the fire load have been evaluated. The design fire load density is obtained by multiplying the characteristic fire load by the partial safety factors. The probability of structural failure due to a fire during the whole life of a structure, p_f, can be obtained from the theorem of conditional probabilities given in Eq. (5.1). The probability p_f is acceptable if it is lower than a target value, p_t.

$$\begin{aligned} p_f(\text{failure from a fire}) &= p_{fi}(\text{getting a fully developed fire}) \\ &\quad \times p_{f,fi}(\text{failure in case of a fully developped fire}) \\ &\leq p_t(\text{target probability}) \end{aligned} \qquad (5.1)$$

The methodology used to establish the partial safety factors was to:

a) collect statistics;

b) from these statistics, deduce probabilities that:
   - a fire starts,
   - the occupants fail in stopping the fire,
   - the automatic active measures to extinguish the fire fail in stopping the fire;
   - the fire brigade does not succeed in stopping the fire;

c) from these probabilities, calculate partial safety factor with the method of Annex A of ENV 1991-1 (1994).

The design fire load density is given by Eq. (5.2) of section 5.4.2.

5.4.2 Construction of the design fire

The construction of the design fire requires the development of the rate of heat release curve (Figure 5.1), the mass loss rate curve (Figure 5.2) and the fire area curve. The procedure described here is made according to the Annex E of the Eurocode 1 (EN1991-1-2, 2002) that proposes value of the different parameters and partial safety factors defined below.

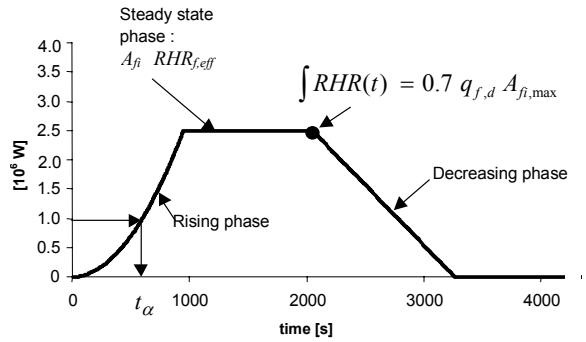

Figure 5.1 Rate of Heat Release Design Curve

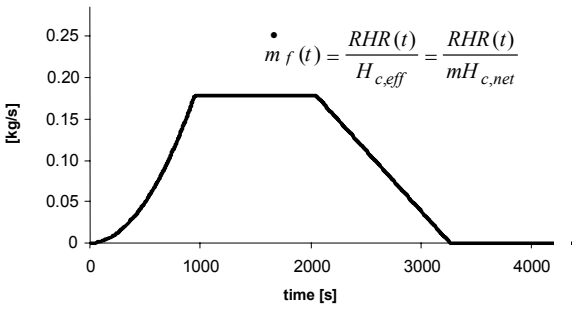

Figure 5.2 Rate of Pyrolyssis Design Curve

Design Fire Load Density - q_f

The design fire load density $q_{f,d}$ is given by Eq. (5.2).

$$q_{f,d} = \left(\gamma_{q1} \gamma_{q2} \prod_i \gamma_{n,i} \right) m\ q_{f,k,net} \tag{5.2}$$

The influence of the compartment area on the probability of starting of a fire is taken into account by γ_{q1} factor. The influence of the danger of fire activation on the probability of fire start is taken into account by γ_{q2} factor. The danger of fire activation is related to the type of occupancy of the building. The influence of active measures are taken into account by $\gamma_{n,i}$ factors. The active measures are: Automatic Water Extinguishing System; Automatic Fire Detection by Heat; Automatic Fire Detection by Smoke; Automatic Alarm Transmission to Fire Brigade; Work Fire Brigade; Off Site Fire Brigade.

Fire Growth Rate - t_α

The growing phase of fire is assumed to follow the t-square evolution, characterised by the fire growth rate t_α, which is the time at which the fire area A_{fi} has grown to a value leading to an effective rate of heat release of 1MW. The rate of heat release during the growth phase is given by Eq. (5.3).

$$RHR(t) = 10^6 \left(\frac{t}{t_\alpha} \right)^2 \tag{5.3}$$

The t-square fire is a very usual design assumption (Karlsson, 2000) for the growing phase of a fire. It assumes in fact that the fire is circular with a constant radial flame speed.

Rate of Heat Release per Unit Area of Fire - $RHR_{fi,eff}$

The effective rate of heat release per unit area of fire $RHR_{fi,eff}$ is the maximum quantity of energy which can be released by unit area of fire in steady state situation on the assumption that the available ventilation does not limit the rate of heat release. The values of $RHR_{fi,eff}$ are for real fires and assumed to take into account the incomplete combustion. This quantity is also assumed to be constant during the fire.

Maximum Fire Area - $A_{fi,max}$

The maximum fire area is the area of floor on which combustible is present.

Steady state phase of the fire development

The steady state phase is reached when the maximum fuel area is involved. It is the maximum rate of heat release that can be encountered for a given design fire. This phase may stand during a certain amount of time or may not exist if the decreasing phase begins during the growth phase.

$$RHR(t) = A_{fi,max} RHR_{fi,eff} \tag{5.4}$$

Decreasing phase

The decreasing phase of the fire starts when 70% of the design fire load is consumed. This phase is considered to be linear.

Pyrolysis rate

From the rate of heat release curves built with the parameters above, the pyrolysis rate is given at any time by Eq. (5.5)

$$\dot{m}_{fi}(t) = \frac{RHR(t)}{H_{c,eff}} = \frac{RHR(t)}{mH_{c,net}} \tag{5.5}$$

Fire area

The fire area is calculated at any time by Eq. (5.6)

$$A_{fi}(t) = \frac{RHR(t)}{RHR_{fi,eff}} \tag{5.6}$$

5.4.3 Comments

A) With the proposed procedure, the rate of heat release curve is first built; the pyrolysis rate curve and the fire area curve are then deduced from the rate of heat release curve. This procedure is the result of the fact that in the literature fire sources are found in terms of energy, and thus data are expressed in terms of energy.

Because the parameters used to define the fire are either effective parameters (t_α and RHR_{fi}) or net parameters (q_f), modifying the combustion efficiency in the design procedure will not change the rate of heat release curve during the growth and the steady state phases but will modify the design fire load and thus modify the fire duration. It will also modify the rate of mass loss curve. For example, when decreasing the *m* factor for a constant energy release rate, the fire duration will be decreased and the rate of mass loss will be increased. The physical meaning of this is the following: to release the same quantity of energy, more fuel is needed if the combustion efficiency is lower.

B) This design fire curve is based on the hypothesis that the heat release rate density is constant during the whole fire duration and therefore any modification of the heat release rate is due to a variation of fire area. This assumption may be quite crude, particularly in the early fire stages, but should have a small influence on the overall design process.

C) If some parameters taken from literature are used, the users must check whether the values are either effective or net values.

D) The "extended fire duration" combustion model, see chapter 4, is recommended for a design procedure; when all of the oxygen initially present in the compartment has be consumed and when all of the oxygen entering the compartment is directly consumed by combustion within the compartment, the rate of heat release will be controlled by the ventilation and the fire duration will be extended so that all the energy of the fuel will finally be released inside the compartment. The strategy of calculation may also influence the rate of mass and the rate of heat release as explained in section 5.5.3.

5.5 Gas temperature

The evaluation of the gas temperature in the compartment is made by the zone model described in chapter 4. Inputs are described in the two previous sections. The purpose of this section is to explain the strategy of the calculation, i.e. when the 2ZM and when the 1ZM are to be used, what are the criteria to be adopted to decide which model has to be applied, when and how the input rate of heat release has to be modified. Eventually the different scenarios that may be encountered are presented.

5.5.1 Field of application of two- and one-zone models

Two-zone and one-zone models are based on different hypotheses and one can not say that one is a better model than the other. Indeed they correspond to different types of fires or different stages of the same fire. They simply have different application domains and in fact are complementing each other. When modelling a fire in a given compartment, it is important to know whether a two-zone or a one-zone model is most appropriate.

A first important remark has to be made on the fire load distribution. The fire load can be considered to be uniformly distributed if the real combustible material is present more or less on the whole floor surface of the fire compartment and when the real fire load density (quantity of fuel per floor area) is more or less uniform. In contrast, the fire load is localised if the combustible material is concentrated on a quite small surface compared to the floor area, the rest of the floor area being free of fuel.

A. Uniformly distributed fire load

Fire ignitions are in most cases localised and therefore a fire remains localised during a certain amount of time. If temperatures are sufficiently high to induce spontaneous ignition of all the combustible present in the compartment, a fully engulfed fire occurs. Generally two-zone models are valid in case of localised fires or pre-flashover fires and one-zone models are valid in case of fully engulfed fires or post-flashover fires.

If the thickness of the lower layer is small compared to the height of the compartment, the two-zone assumption is no longer applicable and a one-zone model is more appropriate.

Finally, if the fire area is a large proportion of the floor area, the one-zone model assumption is better then the two-zone one.

These considerations imply that to model fires in a compartment with uniformly distributed fire load, a two-zone model is well adapted for the first stages of the fire and then a one-zone model will be a better assumption if some conditions on temperatures, fire area and smoke layer thickness are encountered.

B. Localised fire load

In case of localised fire load, when the temperature of the upper layer is sufficiently high to ignite the fuel by radiation, all the fuel starts to burn and the rate of heat release is modified. If the fire remains localised and two different zones remain, a two-zone model is thus still appropriate. In this case a one-zone model can be more appropriate only if the thickness of the upper layer is large compared to the height of the compartment.

5.5.2 Choice of the model

In many cases, it is difficult to know a priori whether a fire will remain localised during its entire course or whether flashover will happen, and, in general, to know whether a two or a one-zone model is more appropriated.

An automatic strategy has been implemented that determines which model has to be used at any time within the course of the fire. With this strategy, the simulation always begins with the two-zone model assumption and if one of the above described conditions is encountered, the simulation will switch from the two-zone model to the one-zone model and/or will modify the mass and energy released by the fire.

The modifications of the main variables and of the basic equations when the switch to the one-zone model occurs are presented in chapter 4. The consequences of flashover on the fire source model and the criteria of transition from two to one-zone are discussed in sections 5.5.3 and 5.5.4 hereafter.

5.5.3 Fully developed fire

If a fire is modelled in the data by the plain curve of Figure 5.3, the growing phase, represented here by a t² curve, is reaching a maximum at the time at which all the fire area has been ignited. If the fuel ignition happens only by flame spread, the maximum is reached without modification of the initial t² curve. If the temperature of hot gases of the upper layer reaches a sufficiently high level (in the range 500°C to 700°C), flashover will occur. This modification is reflected by modifying the initial rate of heat release curve as indicated by the dotted line in Figure 5.3. At the flashover time, the input *RHR* curve is abandoned and *RHR* goes to its maximum value equal to the maximum fire area multiplied by the rate of heat release density $RHR_{fi,eff}$.

If there is ignition of the fuel in a hot layer by conveciton (see criterion C2 below) than the rate of heat release is also increased to its maximum value.

Again, the decreasing phase is assumed to be linear and to start when 70% of the design fire load is consumed.

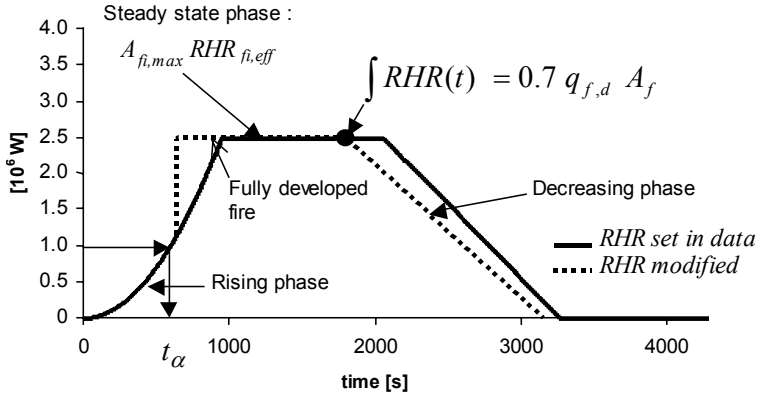

Figure 5.3 Modification of *RHR(t)* in case of flashover.

5.5.4 Criteria of transition from two to one-zone model and/or of modification of the input of energy

The criteria of transition from two to one-zone and/or of modification of the fire source are:

Criterion 1 (C1): $T_U > T_{fl}$

High temperature of the upper layer gases, composed of combustion products and entrained air, leads to a flashover. All the fuel in the compartment is ignited by radiative flux from the upper layer.

Criterion 2 (C2): $Z_s < H_q$ *and* $T_Z > T_{ign}$

If the gases in contact with the fuel have a higher temperature than the ignition temperature of fuel (T_{ign}), the propagation of fire to all the combustible of the compartment will occur by convective ignition. The gases in contact (at temperature T_Z) can belong either to the lower layer of a two-zone model, to the upper layer if the decrease of the interface height Z_S leads to put combustible in the smoke layer (H_q is the maximum height of the combustible material) or to the unique zone of one-zone model.

Criterion 3 (C3): $Z_S < a_1 H$

The interface height goes down and leads to a very small lower layer thickness, which is not representative of two-zone phenomenon.

Criterion 4 (C4): $A_{fi} > a_2 A_f$

The fire area is too high compared to the floor surface of the compartment to consider a localised fire.

Criteria 1 and 2 lead necessarily to a modification of the rate of heat release as specified in §5.5.3. If the fire load is localised the simulation will continue using a 2ZM and if the fire load is uniformly distributed, a 1ZM will be considered. If one of the criteria C3 or C4 is fulfilled, the code will switch to a one-zone model but the RHR will not be modified, except if criterion C1 or C2 happens simultaneously.

Table 5.2 and Figure 5.4 summarise the four criteria.

The default values of T_{fl}, T_{ign}, a_1 and a_2 proposed in the code are given in Table 5.1 but users can modify any of them.

A discussion on these default values is given in Chapter 4, Section 4.3.6.

Table 5.1 Parameter value of transition criteria

Criteria	Parameter value
C1	$T_{fl} = 500°C$
C2	$T_{ign} = 300°C$
C3	$a_1 = 0.2$
C4	$a_2 = 0.25$

Table 5.2 Summary of transition criteria

Criteria	Effect	
	Localised q_f	**Distributed q_f**
C1 : $T_U > T_{fl}$	$A_{fi} = A_{fi,max}$	1ZM *and* $A_{fi} = A_{fi,max}$
C2 : $Z_s < H_q$ and $T_U > T_{ign}$ (2ZM) or $Z_s > H_q$ and $T_L > T_{ign}$ (2ZM) or $T > T_{ign}$ (1ZM)	$A_{fi} = A_{fi,max}$	1ZM *and* $A_{fi} = A_{fi,max}$
C3 : $Z_s < a_1 H$	1ZM	1ZM
C4 : $A_{fi} > a_2 A_f$	-	1ZM

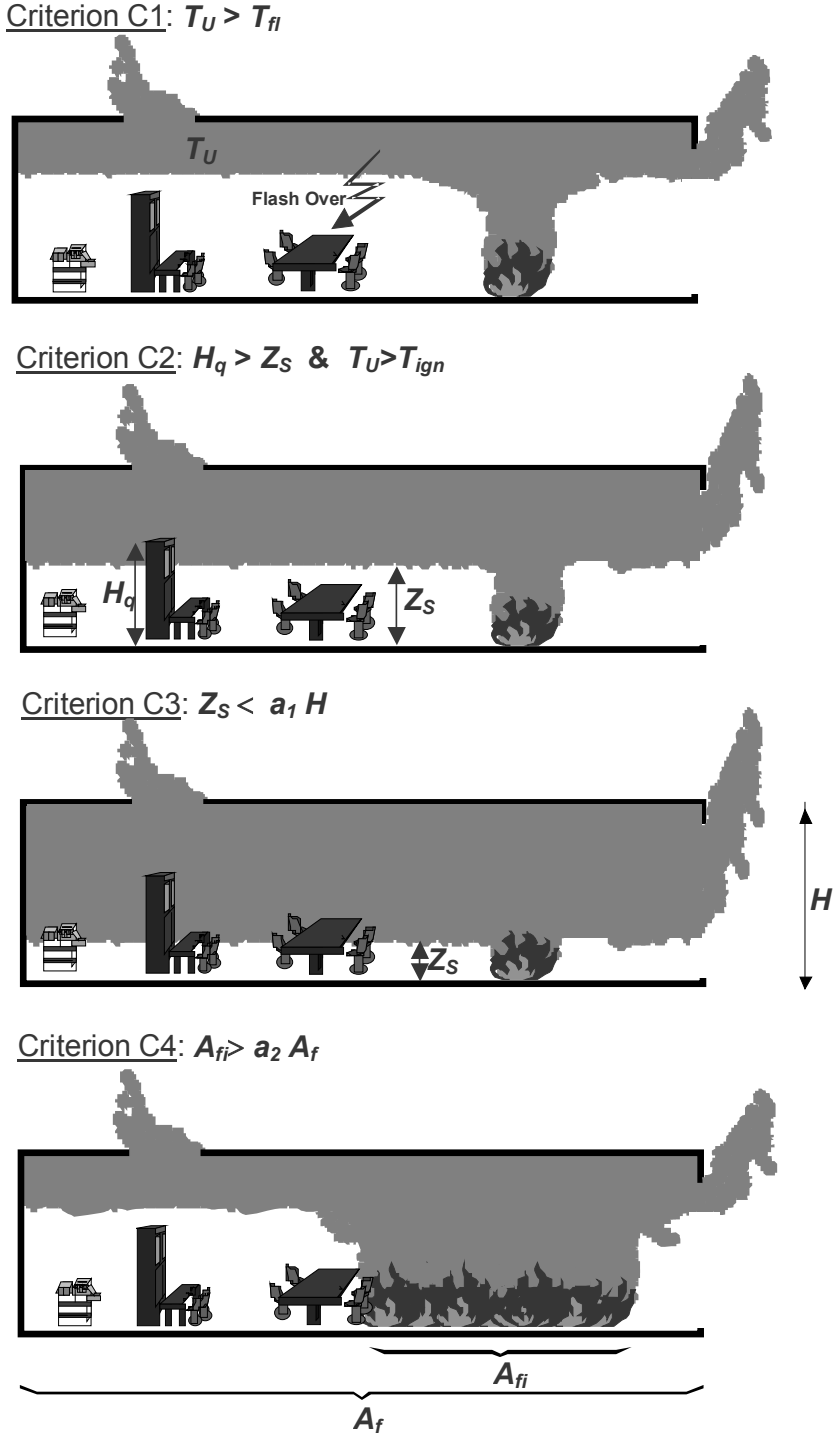

Figure 5.4 Four criteria to switch from two-zone to one-zone model and/or modify the rate of heat release

5.5.5 Fire scenarios

During the course of a simulation, the different criteria may or may not be encountered. Eight different possibilities exist: five if the fire load is localised; three if the fire load is uniformly distributed.

Localised fire load :

SCENARIO 1 - No criterion is encountered, the model will remain with two zones and the RHR curve will not be modified until the end of the fire.

SCENARIO 2 - Criterion C1 or C2 is first encountered, leading to a RHR modification. Criterion C3 is not encountered, the model remains a two-zone one.

SCENARIO 3 - Criterion C1 or C2 is first encountered, leading to a RHR modification. Criterion C3 is then encountered and the model switches from a two-zone to a one-zone.

SCENARIO 4 - Criterion C3 is first encountered, the model switches from a two-zone to a one-zone. The criteria C1 and C2 are not encountered, leading to no RHR modification.

SCENARIO 5 - Criterion C3 is first encountered, the model switches from a two-zone to a one-zone. Criterion C1 or C2 is then encountered, leading to a RHR modification.

Uniformly distributed fire load :

SCENARIO 6 - Criterion C1 or C2 is encountered, leading to a RHR modification and a simultaneous switch from a two-zone to a one-zone model.

SCENARIO 7 - Criterion C3 or C4 is first encountered, the model switches from a two-zone to a one-zone. The criterion C1 and C2 are not encountered, leading to no RHR modification.

SCENARIO 8 - Criterion C3 or C4 is first encountered, the model switches from a two-zone to a one-zone. Criterion C1 or C2 is then encountered, leading to a RHR modification.

Figure 5.5 shows the organisation chart of the different scenarios a simulation can follow.

As the definition of the limit between uniformly and localised fire load is based on the criterion C4, it is obvious that criterion C4 is never encountered in case of localised fire load. For the same reason, in case of uniformly distributed fire load, criteria C4 will undoubtedly be fulfilled and therefore a simulation with uniformly distributed fire load will always switch to one-zone model.

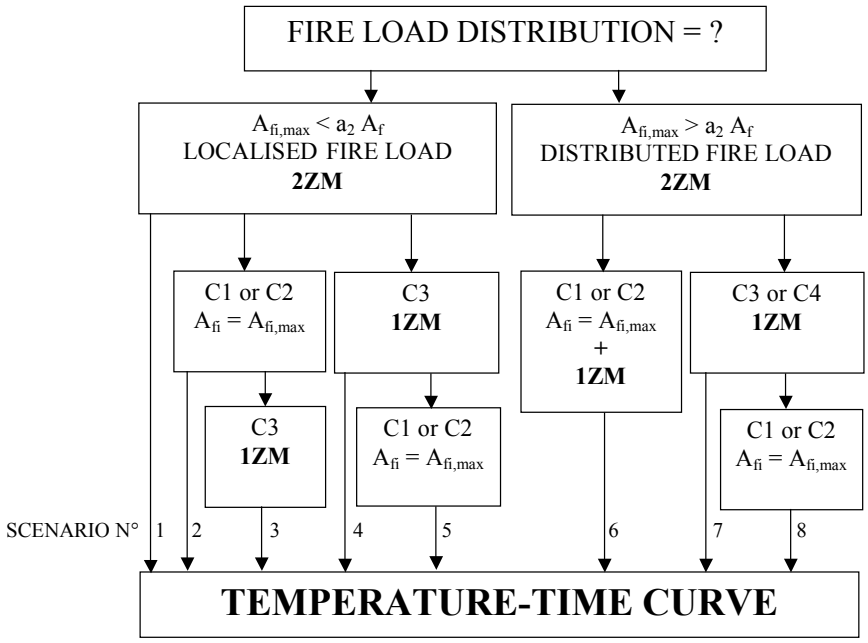

Figure 5.5 Organisation chart of the 2ZM/1ZM combination strategy

5.6 Heating of steel profile.

The upper zone temperature which is calculated in a two-zone fire situation can be considered as the average value of the temperature field in the gas of the upper layer. In fact, the thermal impact of a localised fire can be much more severe on structural elements located in the vicinity of the flames than the impact coming from the fire gases at the average temperature. As a consequence, if the failure of the structural elements located close to a fire may be critical for the stability of the whole structure, then the localised effect of the fire must be taken into account.

The correlation formula proposed by Alpert (1972) allows to calculate the maximum gas temperature in the ceiling jet flow which forms when a vertical buoyant fire plume impinges on a horizontal ceiling and the gases spread laterally. Yet, as indicated by the title of Alpert's publication, his work was done with the objective of predicting response times of detectors and not the structural behaviour of the structure. Whereas the local gas temperature is a good indication for the response time of a detector, temperature of a structure, which is here of interest, is not only influenced by the temperature of the gases flowing on its surface but also, via radiation, by the fire itself. If the temperature of a structure has to be calculated, it is therefore preferable to use a model giving directly the heat flux received by the surface

Hasemi has proposed such an empirical model based on tests in which the flux were directly measured (Hasemi et al., 1984 & 1995; Ptchelintsev et al., 1995 & Wakamatsu et al., 1996). Franssen et al. (1997 & 1998 and CCP 1997) have modified somewhat the original model in order to have a better fit with the original tests. Franssen et al. (1998)also compared the modified model to four full scale tests and found reasonable agreement.

Myllymäki & Kokkala (2000) made 10 additional tests, compared the results to calculations with the improved model and found that the improved model gives safe estimation of the tests results.

The combination of the local (Hasemi) and the global (2ZM) effect of a fire on a steel element is shown on Figure 5.6. The heat transfer to the steel profile located near the fire source is estimated with the Hasemi model, while in the far field it is estimated as the thermal response due to the upper layer temperature. It has to be noted that this model does not take into account longitudinal heat fluxes in the steel elements.

The heat flux to the element q'' is given by the Hasemi's model in function of the heat released by the fire, *RHR*, the diameter of the fire, *D* and of the relative position of the steel element and the fire, *r*. The formulation of the Hasemi model is given in the next section.

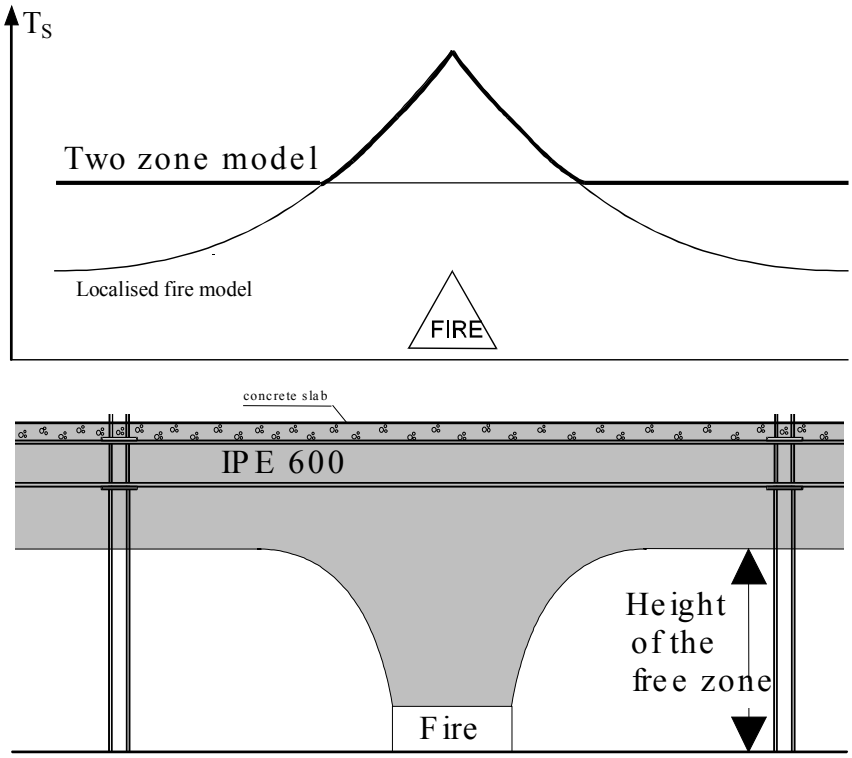

Figure 5.6 combination of localised fire model and zone model for thermal impact on steel beam

5.6.1 Non dimensional model of Hasemi for localised fires

The model is based on non dimensional coefficients. Hasemi uses the Froude number, given by Eq. (5.7).

$$Q^* = \frac{RHR}{\rho_\infty \, c_p \, T_\infty \, g^{1/2} \, D^{5/2}} \tag{5.7}$$

Introducing in Eq. (5.7) the appropriate values for the specific mass, specific heat and room temperature of air as well as the acceleration of the gravity leads to the more convenient form of Eq. (5.8).

$$Q^* = \frac{RHR}{1.11\,x\,10^6 \, D^{5/2}} \tag{5.8}$$

This variable is used to estimate the vertical position of the virtual source with respect to the surface of the fire. This position is the one where a virtual point source would produce the same effects as the real fire. The position of the virtual source z' is calculated according to Eq. (5.9).

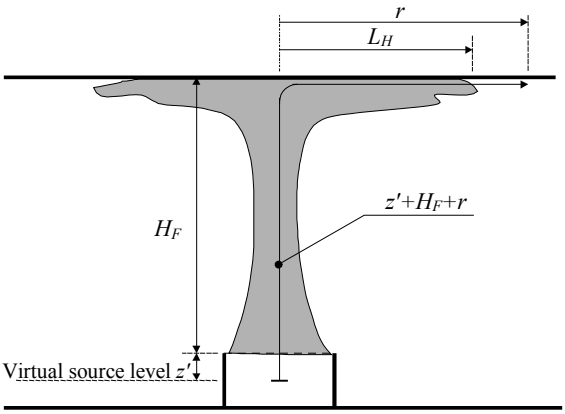

Figure 5.7 Horizontal flame length

$$\begin{aligned} \frac{z'}{D} &= 2.4\ \left(Q^{*2/5} - Q^{*2/3}\right) \qquad for \quad Q^* \le 1 \\ \frac{z'}{D} &= 2.4\ \left(1 - Q^{*2/5}\right) \qquad for \quad Q^* > 1 \end{aligned} \tag{5.9}$$

When the flame impinges on the ceiling, it is deflected and develops horizontally on a distance L_H, see Figure 5.7. Whereas the position of the heat virtual source is influenced by the dimension of the burner, D in Eq. (5.8), the relative length of the flame with respect to the compartment is linked to the vertical distance between the burner and the ceiling, H_F on Figure 5.7. The Froude number that gives indications on the length of the flame is therefore calculated according to Eq. (5.10), very similar to Eq. (5.8).

$$Q^*_H = \frac{RHR}{1.11\ x\ 10^6\ H_F{}^{5/2}} \tag{5.10}$$

It is observed during the tests that the ratio of the length of the flame from the burner, $H_F + L_H$, and the burner to ceiling distance H_F is proportional to the Froude number with the exponent 1/3. This fact is reflected in Eq. (5.11).

$$\frac{L_H + H_F}{H_F} = 2.90 \quad Q^{*1/3}_H \tag{5.11}$$

y is the non dimensional ratio between the distance from the virtual source and the total length of the flame, Eq. (5.12).

$$y = \frac{z' + H_F + r}{z' + H_F + L_H} \tag{5.12}$$

The heat flux to the element q'' (Franssen, 1998) is given by Eq. (5.13).

$$\begin{aligned} q'' &= 100000 && \text{for} \quad y \le 0.30 \\ q'' &= 136300 - 121000y && \text{for} \quad 0.30 < y \le 1.00 \\ q'' &= 15000\ y^{-3.7} && \text{for} \quad 1.00 < y \end{aligned} \tag{5.13}$$

The net heat flux at the boundaries of a steel profile q_{net}, taking into account the flux lost due to the temperature of the section, is given by Eq. (5.14).

$$q_{net} = q'' - h\left(T_s - 293\right) - \sigma\ \varepsilon^*\left(T_s^4 - 293^4\right) \tag{5.14}$$

5.6.2 Heating

The temperature, supposed to be uniform on the section, of unprotected or protected steel profile is calculated with the ENV1993-1-2 (1993) methods. The temperature of the gas which heats the steel profile is the maximum between the upper zone temperature and the fictitious gas temperature obtained by Hasemi's method.

5.7 Fire Resistance

The fire resistance of members is determined based on the assumptions stated in ENV 1993-1-2, § 2.4.4 - Member analysis (ENV1993-1-2 ,1995) using Eq. (5.15):

$$E_{\mathrm{fi,d}} \leq R_{\mathrm{fi,d,t}} \tag{5.15}$$

where:

$E_{\mathrm{fi,d}}$ is the design effect of actions for the fire situation, determined in accordance with ENV 1991-2-2;

$R_{\mathrm{fi,d,t}}$ is the corresponding design resistance at elevated temperatures, depending on the temperature of the steel profile.

The calculation of fire resistance is implemented in the software for:

- Tension members (ENV 1993-1-2, § 4.2.3.1)
- Compression members with Class 1, Class 2 or Class 3 cross-section (ENV 1993-1-2, § 4.2.3.2)
- Beams with Class 1, Class 2 or Class 3 cross-section (ENV 1993-1-2, § 4.2.3.3 and 4.2.3.4)

The fire resistance is the time at which Eq. (5.15) becomes unsatisfied.

5.8 Application

An academic example of application of this model is presented in this section.

The fire resistance of a steel beam which supports a concrete slab (without composite action) in a compartment is estimated in case of an unprotected and a protected steel section.

The data are:

- The compartment is used as a library.
- The square floor is 5m on 5m wide. The height is 3m. (inner dimension)
- All partitions are made of normal weight concrete (unit mass: 2300 kg/m³; Conductivity: 2 W/mK; specific heat: 900 J/kgK) and are 10 cm thick.
- There are two openings, one door (width : 1 m; height: 2 m) in first wall and one window (sill at 1m; soffit at 2 m; width: 4 m) in the third wall. Both openings are supposed to be opened from the beginning of the fire.
- The beam is an IPE400. Steel S355.
- The beam is simply supported from the middle of wall one to the middle of wall three and the load is uniformly distributed.
- The design bending moment at mid span in the fire situation is 100 kNm.
- The protection material is sprayed vermiculite (unit mass: 350 kg/m³; conductivity: 0.12 W/mK; specific heat: 1200 J/kgK)

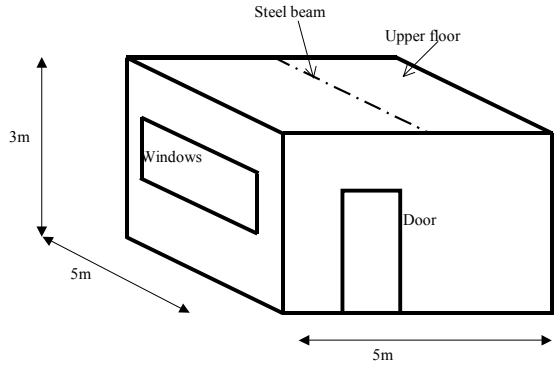

Figure 5.8 Schematic view of the compartment

Step 1: Define the compartment

The compartment is defined: internal dimensions, openings positions and sizes and partitions characteristics.

Step 2: Define the design fire

The suggested value of the NFSC method (Scheilch and Cajot, 2001, Eurocode 1, 2002) for a library are :

- Fire load uniformly distributed with a characteristic value $q_{f,k}$ = 1824 MJ/m²
- $H_{c,net}$ = 17.5 MJ/kg; m = 0.8
- The fire growth rate t_α is 150 s.
- The maximum rate of heat release density is 500 kW/m^2.
- The partial safety factor which consider the benefits of the automatic fire detection by heat is $\gamma_{n,3}$ = 0.87
- The partial safety factor which consider the benefits of off site fire brigade is $\gamma_{n,7}$ = 0. 78
- The fire risk area is equal to 25m^2 thus $\gamma_{q,1}$ = 1.12
- The danger of fire activation is medium thus $\gamma_{q,2}$ = 1
- The design fire load density is then calculated with Eq. (5.2), giving: $q_{f,d}$ = 1109 MJ/m^2.

The rate of heat release data curve is built automatically as shown on Figure 5.9 (RHR data curve).

Step 3: Run the compartment fire model

The main output are the rate of heat release curve calculated (Figure 5.9), the hot zone temperature and the cold zone temperature (Figure 5.10).

The transition to the one-zone model happens at 4.5min, time at which criteria C4 is encountered. The flashover occurs at 5.6min. At this time, the rate of heat release increases to its steady state value of 12.5MW. The oxygen inside the compartment is then quickly consumed. Thus a ventilation regime occurs, leading to a rate of heat release of 8.6MW. The fire duration is increased. The areas below the two curves of Figure 5.9 are equal, all the energy available is released inside the compartment.

Step 4: Calculate the steel temperature

The steel temperature is evaluated for the unprotected and protected section. (Figure 5.11)

In this case, the design temperature time curve is the equivalent local temperature just above the fire source (Figure 5.10), obtained with the Hasemi's model, until the switch to the one-zone model at 4.5min. From 4.5 min to the end of the calculation, it is the one-zone model temperature.

The drop in the design temperature time curve which occurs at 4.5 min is due to the fact that, until this time, Hasemi's model is used and, afterwards, a one-zone model is used. This brief drop is of course not physical but the results of the design hypotheses which changes during a simulation. Moreover, just after flashover (at 5.6min) the temperature is reaching approximately the same value as the one given by Hasemi model at 4.6min. This is only fortuitous, in fact a bigger difference is possible.

Step 5: Calculate the member resistance

The fire resistance of the unprotected steel section IPE400 is 10.2min.

With a protection thickness of 20mm of spray vermiculite, the maximum steel temperature (472°C) is lower than the critical steel temperature (507°C) of the member. In other words, the member resists during the whole fire duration; no failure of the member will occur.

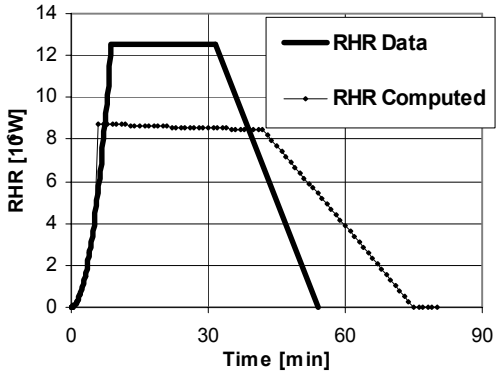

Figure 5.9 Input and calculated rate of heat release

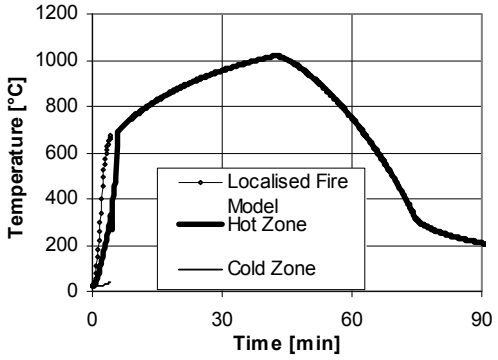

Figure 5.10 Calculated compartment temperatures

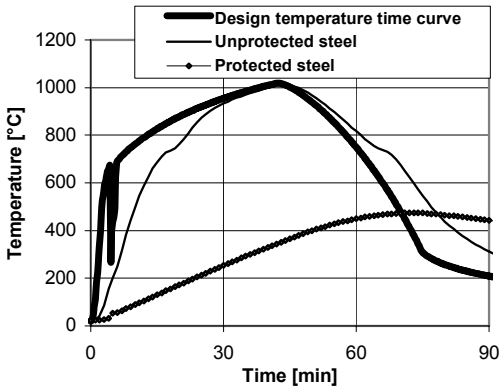

Figure 5.11 Design temperature-time curve and steel element temperatures

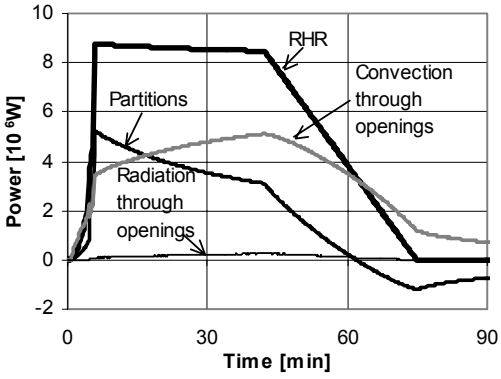

Figure 5.12 Energy balance

Energy balance

The energy balance for this example is presented on Figure 5.12. The contribution of the vent and of the partition are on the same order of magnitude while the radiation through openings is quite small compared to the other terms. During the quasi steady state phase, which is driven by the ventilation, the rate of heat release is nearly constant (only a small decrease), the partition losses decreases faster and the convective heat losses through openings increase.

5.9 Sensitivity study

The aim of this section is to assess the influence, on OZone calculation, of a modification of the value of the parameters listed in section 5.9.1. This influence is shown on the gas temperatures (temperature time curves and maximum temperature in the compartment) and on the value of the fire resistance of a member submitted to that fire.

5.9.1 Description of the study

From a reference case, a single parameter is modified at once, all other parameters remaining constant.

The compartment and the design fire of the reference case are fully identical to the one of section 5.8. The values of the parameters of the reference case are the bold values given below into brackets.

The parameters and the range of variation are:

- The design fire load density, between 100 and 2000 MJ/m^2 (**1109 MJ/m^2**);
- The size of the openings, width between 0 and 15m (**4 m**);
- The floor area, between 10 and 80 m^2 (**25 m^2**);
- The specific heat and density between 90 10^3 and 3600 10^3 J/m^{3}K (**10^3 J/m^{3}K**);
- The conductivity of the materials, between 0.01 and 20 W/mK (**2 W/mK**);
- The thickness of the partitions, between 2 and 20cm (**10 cm**);
- The relative emissivity at partition/compartment interface, between 0.1 and 1 (**0.8**).

The steel profile is an IPE 450. The steel grade is S235. The beam is 5m long and is simply supported. The static load is uniformly distributed and is applied to the shear centre of the element. The design bending moment in the fire situation is 100 kNm.

The protection material is sprayed vermiculite with the following characteristics:

- Unit mass: 350 kg/m3;
- Specific heat: 1200 J/kgK;
- Conductivity: 0.12 W/mK;
- Thickness: 10 mm.

The maximum temperature in the compartment of the reference case calculated by OZone is 1018°C after 42min. The fire resistance of the beam is 43.6min. The temperature time curve of the reference case is presented on the graphs of Figure 8.13 as bold lines.

5.9.2 Results of the study

The results of the study are presented on Figure 8.13 to Figure 8.15.

5.9.2.1 Design fire load density

All the fires are ventilation controlled, thus the rate of heat release is constant and therefore if the fire load density is increased, the fire duration increases and the maximum temperature reached by the gas is higher, see Figure 8.13a. The temperature-time curves are identical up to the beginning of the decreasing phase and the maximum temperature in function of the fire load, see Figure 8.14a, is in fact the temperature time curve obtained with a very high fire load for which the abscises is changed from time to fire load.

The fire resistance in function of the fire load density is presented on Figure 8.15a. If the design fire load density is lower than 830MJ/m^2, no failure of the member occurs and the fire resistance can be consider being infinite. For higher fire load density, the fire resistance tends to a constant value, independent of the fire load. The reason is that if the failure of the member occurs, the temperature in the compartment after the failure has no influence on the fire resistance (defined to be the time at which the failure occurs).

5.9.2.2 Size of the openings

For windows width up to 8m, the fire is ventilation controlled. The bigger is the width, and thus the area, of the window, the higher is the gas temperature and the shorter is the duration of the fire. In this situation, if the ventilation is increased, the fire load is burnt at a higher rate and thus in a shorter time, see Figure 8.13b and Figure 8.14b.

For windows width bigger than 8m, the fire is fuel controlled. The rate of heat release and thus the fire duration are independent of the ventilation conditions. If the window area is increased, the mass exchange through it is increased and the temperatures are lower, see Figure 8.13b and Figure 8.14b.

In case of ventilation controlled fire, even if the maximum temperature is increasing with decreasing opening area, the fire resistance of the beam increases because the fire duration and therefore the time during which the beam is heated is decreased, see Figure 8.15b. For opening width bigger than 8.5m, the fire resistance becomes infinite because the steel section never reaches its critical temperature.

5.9.2.3 Floor area and fire area variation

The parameter which vary is the floor area. The fire are is kept equal to the floor area and thus vary in the way than the floor area.

For floor area lower than 20 m^2, the fire is fuel controlled and for bigger floor area, it is ventilation controlled, Figure 8.13c. This is due to the fact that the maximum rate of heat release for fuel controlled conditions is proportional to the fire area and, for this situation, it is equal the rate of heat release in ventilation controlled conditions when the fire area is about 20 m^2 (actually 18 m^2).

For fuel controlled fires, for bigger floor area, the overall temperature time curves are higher. Thus the maximum temperature in the compartment is higher for a bigger floor area.

For ventilation controlled fires the rate of heat release is mainly driven by the size of the opening. So if the fire area is increasing: the total fire load and thus the fire duration are increasing; the post-flashover temperatures are lower but during more time. The maximum temperature in the compartment , Figure 8.14c, is lower for bigger floor area.

The fire resistance is infinite for floor area lower than 20m, Figure 8.15c. As the temperature are lower for these fire area, the critical temperature of the steel is not reached.

The minimum fire resistance time is encountered for a floor area of 20m2. For bigger floor area, the fire resistance is increased, due to the slower heating of the steel.

5.9.2.4 Floor area with constant fire area

If the fire area is constant, the total fire load is constant and thus the fire duration is also constant. This is due to the fact that as the fire is ventilation controlled, the maximum rate of heat release dependent mainly of the size of the openings and is thus here constant.

As the heat loss to partitions increases with the partition area, the gas temperatures are lower for bigger compartment (Figure 8.13d, Figure 8.14d).

The fire resistance is thus increasing with the compartment size, see Figure 8.15d.

5.9.2.5 Conductivity of the materials

If the conductivity is increased, the maximum temperature in the compartment, Figure 8.14e, and the rate of temperature, Figure 8.13e, decrease. For higher conductivity, on one hand, the heat transfer by conduction into the wall is higher, and on the other hand, the thermal penetration is higher, so the heat can be accumulated in a bigger volume of partition material and thus the heat transfer from the compartment to the partitions is higher.

As the fire duration remains the same, the fire resistance is directly related to the maximum gas temperature. The fire resistance increases if the maximum gas temperature decreases, Figure 8.15e.

5.9.2.6 Specific heat and density

It is first important to note that, in the equations of the partition model of OZone (Chapter 4 section 4.3.3) the density and the specific heat of partition material are always multiplied ($c\rho$). It is thus obvious that it is the product of these two parameters which influence the results of a simulation. For example, the multiplication of the specific heat by two combined to the division of the density by two will not influence simulation.

For all $c\rho$ values, the temperatures in the compartment tend to a value of about 1230°C, see Figure 8.13f. In this study, this value is reached before the decreasing phase (at 44min) for $c\rho$ below 500 kJ/m³K, but would be reached for every values of $c\rho$ after an infinite time. The temperature rise in the compartment increase faster for lower $c\rho$ values.

The maximum temperature in the compartment is thus decreasing for increasing $c\rho$, Figure 8.14f, and is independent of $c\rho$ for very long fire duration or very low $c\rho$ values.

Because on one hand, $c\rho$ does not influence the fire duration and, on the other hand, the temperatures are lower with higher $c\rho$ values, the fire resistance is increasing with $c\rho$, see Figure 8.15f.

5.9.2.7 Thickness of the partitions

In this case; the thickness of partitions has a very low influence on the gas temperatures evolution, Figure 8.13g, Figure 8.14g, and therefore on the fire resistance of an element in that compartment, Figure 8.15g.

Nevertheless a higher influence of the thickness of partition on the gas temperature might be encountered in certain circumstances. For example, if the partitions are protected with an insulating material, the thickness of the protection should have a big influence if it is lower than a minimum value linked to the thermal penetration of the heat in the wall.

5.9.2.8 Relative emissivity of the inside surface of the partitions

If the relative emissivity at partition/compartment interface increases, the temperatures of the gas in the compartment and therefore the fire resistance decrease (Figure 8.13h, Figure 8.14h). For relative emissivities at partition/compartment interface upper than 0.5 (which is the case in most situations), the influence on the temperature time curves (Figure 8.14h) and on the fire resistance (Figure 8.15h) is very small.

5.9.2.9 Summary of the study

The results of this parametrical study are summarized in Table 5.3.

Table 5.3 Summary of the results of the sensitivity study

Parameter		Maximum temperature	Fire duration	Fire resistance
Design fire load density	↑	↑	↑	∞ then ↓ then →
Windows area	↑	↑ then ↓	↓ then =	↓ then ↑ then ∞
Floor area & fire area	↑	↓ then ↑	↑	∞ then ↓ then ↑
Floor area only	↑	↓	=	↑ then ∞
Conductivity of partition material	↑	↓	=	↑ then ∞
$c\rho$ of partition material	↑	↓	=	↑
Partition thickness	↑	≈	=	≈
Relative emissivity at partition/compartment interface	↑	≈	=	≈

Legend: ↑ increase; ↓ decrease; ∞ infinity; ≈ approximately equal; = equal

5.9.3 Conclusions of the study

The parameters that most influence the temperatures in the compartment are: the fire load, the compartment dimension, the ventilation conditions, the fire size and the thermal properties of the partitions.

For fuel controlled fire, the rate of heat release density, not investigated in this study; is an important parameter as it defines, with the fire area, the maximum rate of heat release.

The fire resistance is also mainly influenced by the same parameters of the compartment fire.

The fire resistance is a non continuous function of the compartment fire parameters.

The effect of the section dimensions and of the insulation properties are not investigated.

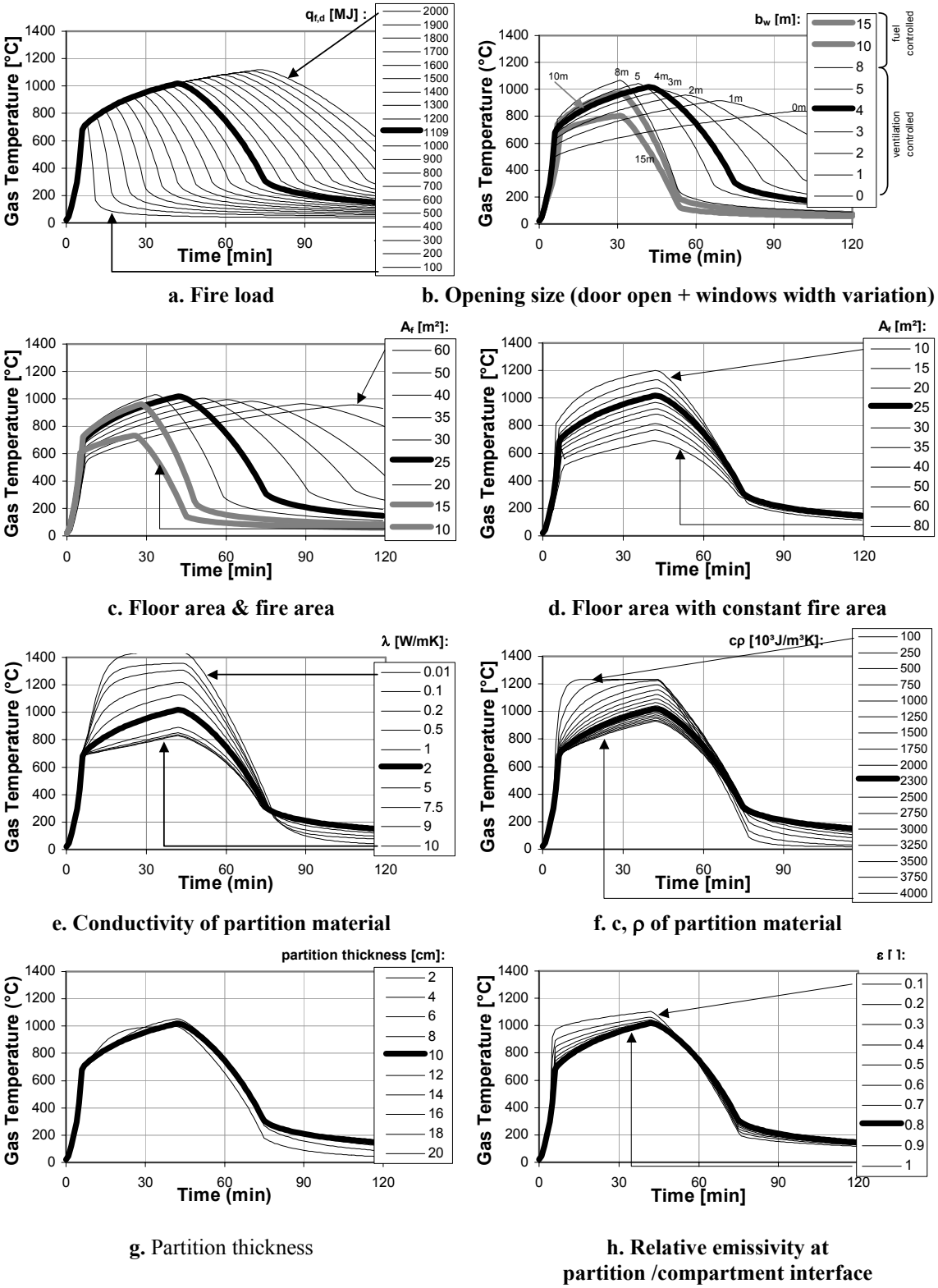

a. Fire load

b. Opening size (door open + windows width variation)

c. Floor area & fire area

d. Floor area with constant fire area

e. Conductivity of partition material

f. c, ρ of partition material

g. Partition thickness

h. Relative emissivity at partition /compartment interface

Note: the bold line is the reference case and is thus identical on each graphs

Figure 8.13 Temperature time curves of the sensitivity study

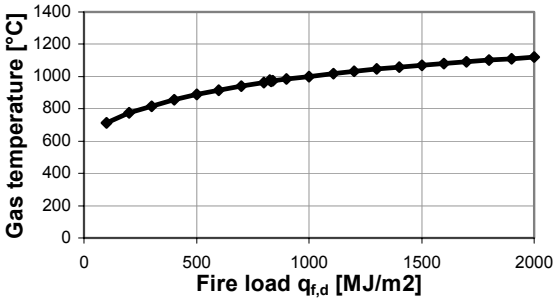

a. Fire load

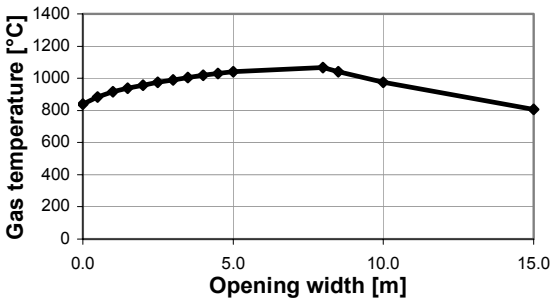

b. Opening size (width variation)

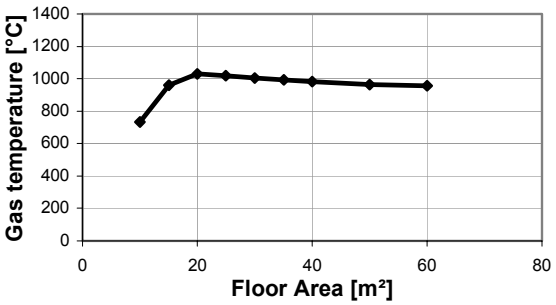

c. Floor area & fire area

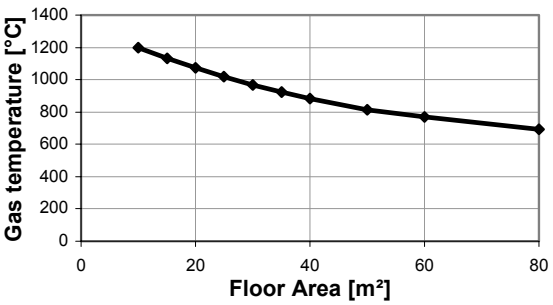

d. Floor area with constant fire area

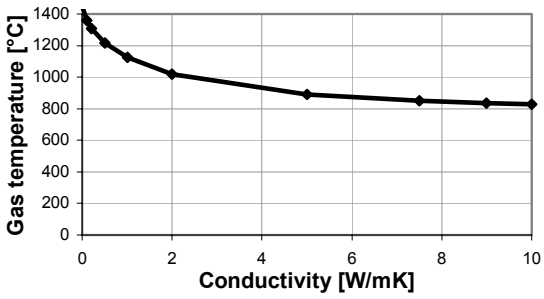

e. Conductivity of partition material

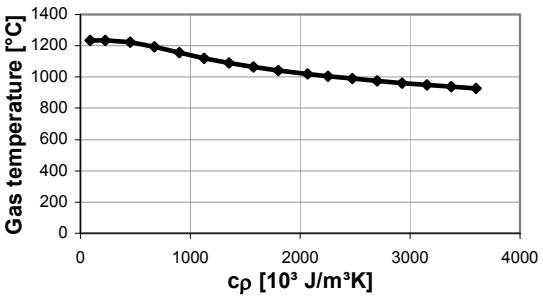

f. c, ρ of partition material

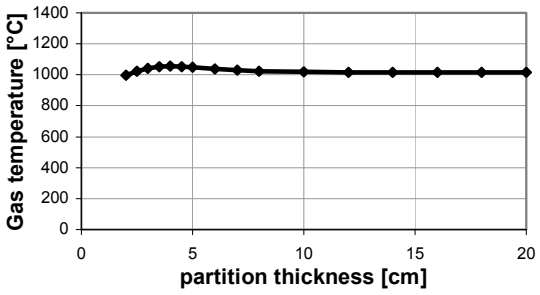

g. Partition thickness

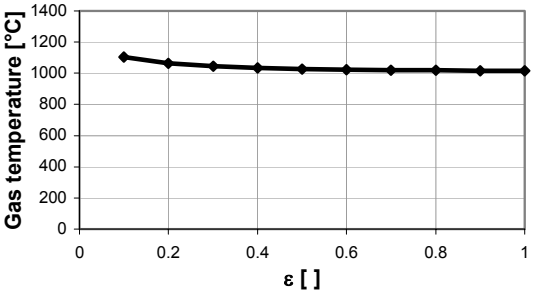

h. Relative emissivity at partition /compartment interface

Figure 8.14 Maximum temperature obtained in the sensitivity study

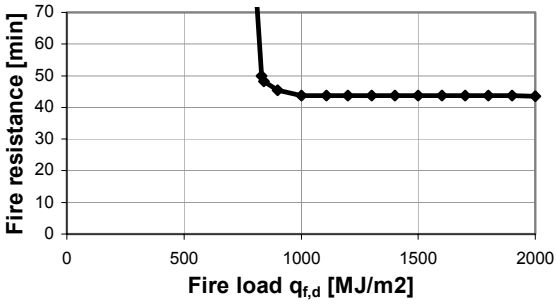

a. Fire load

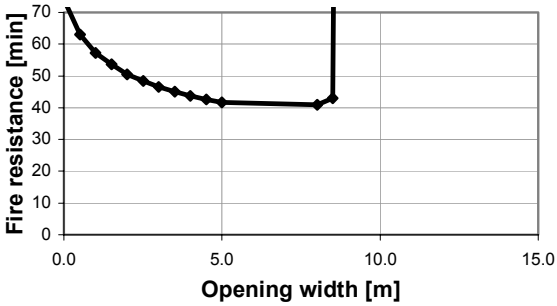

b. Opening size (width variation)

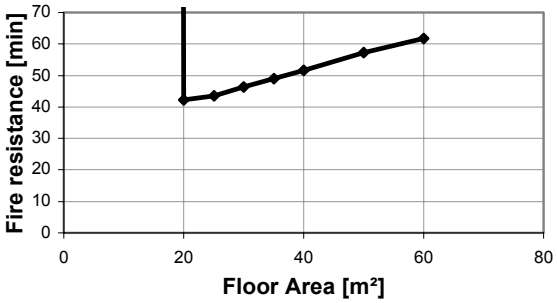

c. Floor area & fire area

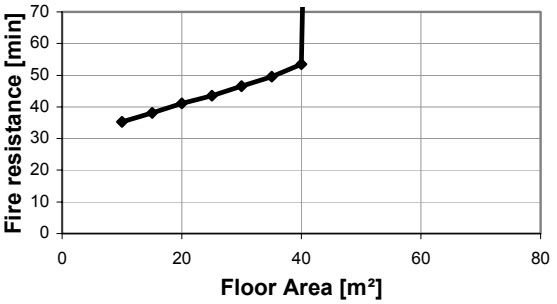

d. Floor area with fixed fire area

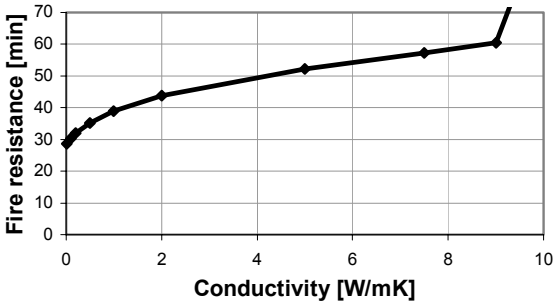

e. Conductivity of partition material

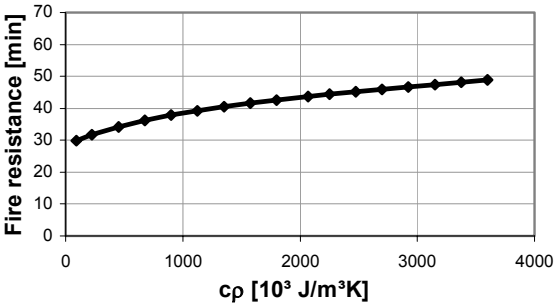

f. c, ρ of partition material

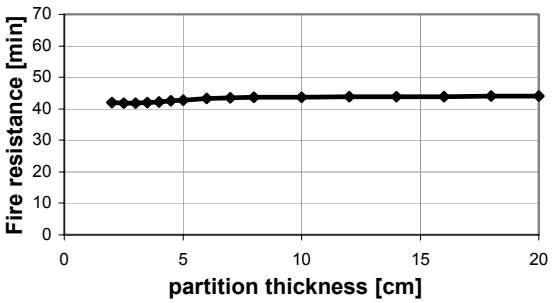

g. Partition thickness

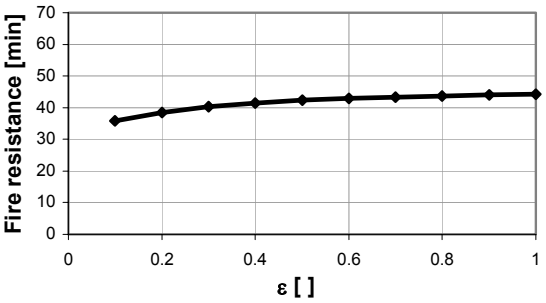

h. Relative emissivity at partition /compartment interface

Figure 8.15 Fire resistance obtained in the sensitivity study

5.10 Conclusions

A model has been developed, and built as a computer based tool, to design steel elements submitted to compartment fires. This software calculates successively:

- The design fire source (rate of heat release and rate of mass loss);
- The gas temperature in the compartment;
- The temperature of a steel element in that fire compartment;
- The structural fire resistance of this element.

The definition of the design fire source is made according to a semi probabilistic method developed recently in a European research. This method enables to take into account active fire fighting measures.

The gas temperature calculation is made by a zone model. Different scenarios may occur depending on the results of the simulation. A two-zone model is first applied, a switch to a one-zone can occur if this model is more appropriate to the conditions inside the compartment. A modification of the rate of heat release may also occur if flashover conditions are encountered.

The temperature of steel section is calculated with the ENV1993-1-2 methods. The thermal solicitation is either the zone temperature or the equivalent localised temperature that includes the gas temperature and the direct radiant flux from a localised fire. The Hasemi's method has been implemented to evaluate this local effect.

The structural fire resistance is evaluated according to ENV1993-1-2.

An example of application and a sensitivity study on the model are presented in order to better understand the background of the model, its use and the impact of the different parameters on the fire resistance.

This software has a quite large field of application; it is suitable for pre- and post-flashover conditions; localised or fully engulfed fires. Nevertheless, it is limited to :

- A single compartment with quite a simple shape suitable for zone modelling;
- A single fire source;
- In case of localised fire, fire resistance of beams at ceiling level.

Even if the software is primarily built to use the proposed design methodology, it remains open to other utilisations. Among other things, it enables to define new parameter values of the design fire curve, to modify the parameter values of the transition criteria or to build, point by point, other fire source (for example to simulate fire tests or more sophisticated design fires). It is also possible to force a two-zone or a one-zone model for the entire duration of a fire.

6

Comparison between the numerical compartment fire model and full scale fire tests

6.1 Introduction

The aim of this chapter is to compare the numerical compartment fire model developed in this thesis and presented in chapter 4 to full scale fire tests. This exercise is of primary importance because it shows the capability of the model to predict real fires, or at least under which conditions a prediction is reliable.

The code has been compared to 98 full scale fire tests: 39 localised fires with typical two-layers phenomena coming from 3 different test series and 59 fully developed fires coming from 5 different test series.

The work described in this chapter is also important because it enables to better understand the compartment fire model, its hypothesis and its field of application. The comparison of OZone has also enabled to better understand the dynamic of compartment fires, see for example the deep compartment fire tests (Kirby 1994), section 6.5.5.

6.2 Objectives of comparisons of the model with fire tests.

The comparisons with full scale fire test have two main objectives.

The first one is to investigate whether the main model formulations (zone equations and partition model) and the sub-models formulation are able to represent the course of a fire. This first objective includes the assessment of the empirical parameter values that have been set by default in the code (see Chapter 4 Section 4.7). It should also be noted that the Heskestad plume correlation has been used for all simulation (localised fire and pre-flashover period of fully developed fires).

The second objective is to see whether the design fire curve (defined in chapter 5) is able to represent a real fire source.

In this chapter, the main questions that will be tackled are:

1. Is OZone able to give a good prediction of the gas temperatures encountered during the fire tests?
2. Is the NFSC design fire curves able to represent real fires?
3. Is OZone able to give a good prediction of the upper layer thickness in a two zone fire situation?

Other questions, related to the sub-models are also raised:

4. Does the vent models give a good estimation of mass and heat transfer?
5. Does the partition model give a good estimation of heat transfer?
6. Is the combustion models/fire chemistry implemented in the code appropriated?
7. Is the flashover (transition) model appropriated?

6.2.1 A priori, Blind and Open comparisons

In publications on comparisons of fire models with experiments, it is often difficult to know which procedure has been used exactly in the comparison. It is particularly important to know whether data measured during the experiment have been used. To clarify the descriptions of comparisons with tests, Beard (2000) has proposed to subdivide comparisons into three categories : a priori, blind and open comparisons.

The conditions, adapted from Beard, that a comparison has to fulfil to be classified in a category are listed hereafter for the three categories from the most to the least demanding one.

6.2.1.1 'A priori'

An a priori comparison between theory and experiment may be characterized by the three conditions:

- The test results of the variable being used for the comparison have not been used in the modelling.
  As temperature is the variable being used for this comparison, the temperatures resulting from the tests have not been used.
- No data from the experiment have been used.
  In this case, the NFSC design fire has been used to define the fire source.
- No adjustment of input parameter values has taken place.
  All the default values of parameters have been used.

6.2.1.2 "Blind".

A blind comparison between theory and experiment may be characterized by the three conditions:

- The test results of the variable being used for the comparison have not been used in the modelling.
  As temperature is the variable being used for this comparison, the temperatures resulting from the tests have not been used.
- Data from the experiment have been used;
  In this work, the mass loss rate or the heat release rate obtained from oxygen depletion measurements is used.
- No adjustment of input parameter values has taken place.
  All the default values of parameters have been used.

6.2.1.3 "Open"

An open comparison between theory and experiment may be characterized by the following conditions :

- The test results of the variable being used for the comparison are used in the modelling. The temperatures resulting from the tests can be used in the comparison.
- Some data from the experiment can be used.
- Adjustments of input parameter values can taken place. Any modification in the input parameters can be done to improve the agreement between the calculations and the experiment results.

6.2.2 Objectives versus types of comparison

The choice between the type of comparison depend on the pursued objectives. The main characteristic of the comparison types and their objectives are listed hereafter:

- A priori:
  Characteristic: No result of the test is used. The comparison is done in the conditions of design, i.e. as if the test has not been performed. No adjustment of the results is done.
  Objective: This comparison enables to investigate whether the design procedure proposed in the code gives safe results or not. In particular, the NFSC design fire is assessed.
- Blind:
  Characteristic: The fire source is defined thanks to measurements made during the test. No adjustment of the results is done.
  Objective: This comparison can assess the basic model, the sub-models, except the fire source, and the choice of the empirical parameters that are set in the code.
- Open:
  Characteristic: Any adjustments of the data can be done to obtain a better fit of the calculations on the measurements.
  Objective: This comparison is used when there is disagreement between the model and experiments in an a priori or a blind comparison. By adapting input data or parameters of the code, it can be shown that default parameters did not suit to the situation or that a physical phenomenon is not taken into account by the model. Limits of use of the code might be deduced or some design rules or some improvements of the model might be proposed.

6.3 Measurements during tests

Some parameters used in the comparisons are obtained from measurements made during the test. In particular, the effectiveness of the modelling is evaluated by comparison of measured and calculated temperatures. It is thus essential to know which temperature measurements are used and how they are treated for the comparisons.

Moreover blind and open comparisons are made using some measurement of the fire source as data for the modelling. It is also very important to know how they are obtained from test measurements.

The measurements made during the tests presented in this work have been either treated by the performers of the tests or, for few of them, in the frame of this work.

6.3.1 Fire source

The rate of heat release and/or the rate of mass loss may or may not have been measured during the tests. These terms are described in chapter 2 and the ways they are estimated is presented in section 2.4.4.1.

6.3.2 Compartment temperatures

As this work is focused on the effect of fire on structures, the comparison of fire tests and simulations is made using the gas temperature as variable. Steel temperature could also be used as it is closely related to the failure of structural steel element. Nevertheless the gas temperatures have been preferred because the influence of the steel section and insulation properties can be important. Two main parameters are important: the maximum gas temperature and the fire duration. The first parameter is important for all structures; the second is particularly important for protected steel or concrete structures and less important for unprotected steel as any gas temperature variation is closely followed by the temperature in the steel element. Gas temperature histories will thus be used for comparison.

During full scale fire tests, gas temperatures are usually measured by several thermocouples, placed in different location in the fire compartment. It is obvious that the temperatures measured by the different thermocouples are different. The procedure used to reduce the number of parameters to a limited amount of representative parameters is explained in the two next paragraphs for pre- and post-flashover fires.

6.3.2.1 Localised fires / Pre-flashover fires

The obvious variables for the comparison of the pre-flashover test and calculation results is the upper and lower layer temperatures in association with the height of the layer interface. Hostikka et al. (2001) have reviewed the methods for their experimental determination.

- A traditional method of Cooper et al. (1982) is the so-called N-percent rule. In this method the interface height z_i at time t is defined to be the elevation at which the temperature satisfies the following Eq. (6.1).

$$\frac{T(z_{i1},t)-T_{amb}}{T(z_{top},t)-T_{amb}}=\frac{N}{100} \tag{6.1}$$

In the literature the values suggested for N range from 10 to 20. The average temperatures in the upper and lower layers (T_{up1} and T_{low1}) are then calculated as mean values of the measurements in the upper and lower sides of z_{i1} , respectively.

- Mathematically more consistent method for the comparison of experimental and zone model data is to calculate the volumetric temperature and density integrals of the room space and find the three unknowns, z_{i2} , T_{up2} and T_{low2}, that produce the same values for the integrals

$$\left(H - z_{i2}\right)T_{up2} + z_{i2}T_{low2} = \int_0^H T(z,t)dz = I_1 \tag{6.2}$$

$$\left(H - z_{i2}\right)\frac{1}{T_{up2}} + z_{i2}\frac{1}{T_{low2}} = \int_0^H \frac{1}{T(z,t)}dz = I_2 \tag{6.3}$$

Eq. (6.3) results from the definition of the zone model concept, and Eq. (6.4) from the conservation of mass in the zone model approximation. Assuming that T_{low2} can be taken from the lowest measurement points, the interface height can be solved from the above equations

$$z_{i2} = \frac{T_{low2}\left(I_1 \cdot I_2 - H^2\right)}{I_1 + I_2 T_{low2}^2 - 2T_{low2}H} \tag{6.4}$$

T_{up2} is then calculated as a mean value of $T(z,t),\ z \geq z_i$.

- Another method is presented by He et al. (1998) where the three unknowns z_i , T_{up} and T_{low} are calculated by minimizing the quadratic error of assumed zone shape temperature profile and the measured profile. A square root of the quadratic error was used in a form

$$E(z_i, T_{up}, T_{low}, t) = \left\{ \int_0^{z_i} \left[T(z,t) - T_{low}\right]^2 dz + \int_{z_i}^H \left[T(z,t) - T_{up}\right]^2 dz \right\}^{1/2} \tag{6.5}$$

and the resulting interface height and layer temperatures were chosen such that

$$E(z_{i3}, T_{up3}, T_{low3}, t) = \min_{\Omega^-}\{E\},\ \ (z_i, T_{up}, T_{low}) \in \Omega^- \tag{6.6}$$

where Ω^- is a local neighbourhood of the values z_{i3} , T_{up3} and T_{low3} at time t-Δt, where Δt is the measurement time step. Here, for numerical stability of the minimization process a little bit smoothed version of the step function can be used by defining arbitrarily the temperature profile. However, the calculation of the minimum with this function can be relatively slow.

$$T_3(z) = T_{low3} + \frac{T_{up3} - T_{low3}}{2}\left\{1 + erf\left[10 \cdot \left(z - z_{i3}\right)\right]\right\} \tag{6.7}$$

For the localised fire tests presented in this work, the integral method, ie. Eq. (6.4), was used. These calculations have been done by the tests performers. The reliability of the interface height results was checked by applying the other two methods as well. It was observed that all the methods gave very similar results, which is natural as the fire scenarios were very typical two layer situations (Hostikka et al. 2001).

6.3.2.2 Fully developed fires / Post-flashover fires

In case of post-flashover fires, it is usual to consider that the temperature is uniform within the whole compartment. It is the main hypothesis made in numerical one-zone model. Figure 6.1a presents the temperatures measured in different places by thermocouples in a compartment during a fully developed fire in a full scale test. This test has been made at BRE in the NFSC2 research project (NFSC2 2000). It can be observed that during the steady state phase (approximately between 18min and 40min) there are differences of about 300°C between the maximum and the minimum measured temperature. Thus it has been decided to present for each post-flashover fire test the mean, the maximum and the minimum temperatures measured at each time, Figure 6.1b, Eq. (6.8).

$$
\begin{aligned}
T_{g,mean}(t) &= \frac{\sum_i T_{TCi}}{N_{TC}} \\
T_{g,max}(t) &= maximum\ \ of\ \ T_{TCi}(t) \\
T_{g,min}(t) &= minimum\ \ of\ \ T_{TCi}(t)
\end{aligned}
\tag{6.8}
$$

The maximum and minimum temperatures are the envelope of the temperatures measured by the thermocouples and thus do not necessarily happen at the same position in the compartment during the fire course.

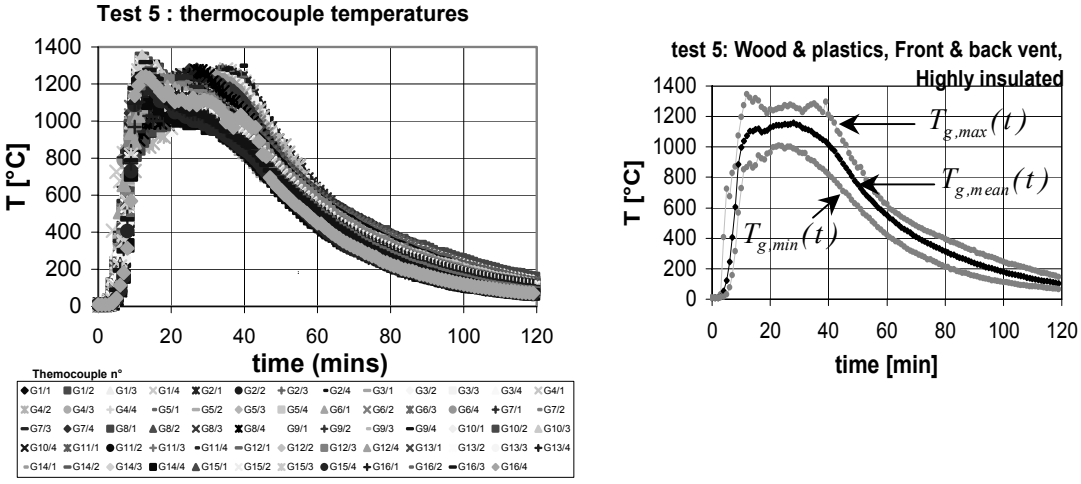

a. Thermocouples temperature measured during test b. Mean temperature & envelopes

Figure 6.1 Post-Flashover Test temperature

6.4 Comparisons with full scale localised fire tests

6.4.1 DSTV tests, Germany, 1999

This tests series has been performed in the NFSC2 research at the technical university of Braunschweig, Germany for DSTV. A detailed description of the tests (configuration, data and results) is given in NFSC2, 2000. Data and measurement results are taken from this report with permission of the authors. Some information, not reported in the tests report, have been obtained from personal communications with Mr Dobbernack (TU Braunschweig).

6.4.1.1 Test data

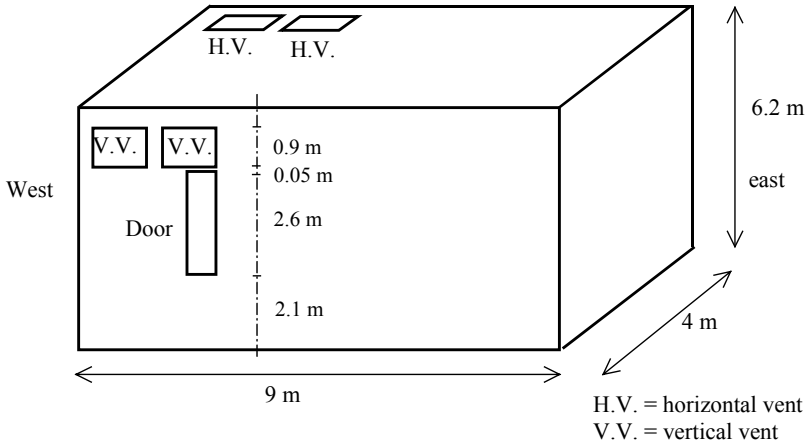

Figure 6.2 Schematic view of the fire compartment - perspective view

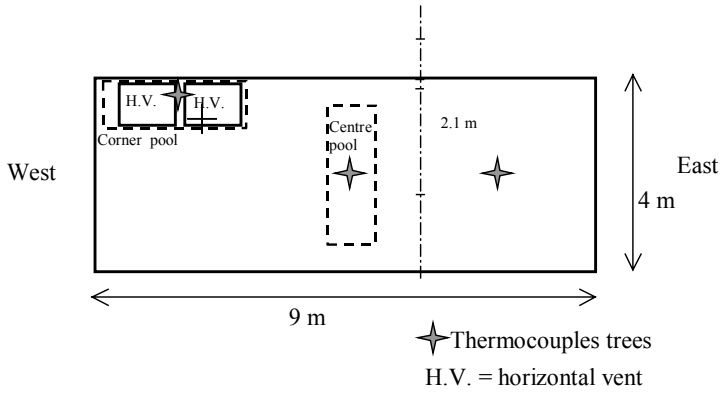

Figure 6.3 Schematic views of the fire compartment - plan view

The series comprises ten fire tests in a compartment.

The compartment has the following dimensions: length, 9.00 m; width, 4.00 m; and height 6.20 m -Figure 6.2 and Figure 6.3. The upper part of partitions and the ceiling are made of 20cm thick aerated concrete with thermal properties given in Table 6.1. The lower part of partitions (up to 1.7m) is made of firebricks. The floor is made of normal concrete. A door (width 0.625m, height 2.60m, sill height 2.10m) is open during all tests. Two horizontal vents of 1m² are open in tests 1 to 6, closed by concrete blocks in tests 7 and 8 and closed by glass in tests 9 and 10. Two vertical vents of 1m² are closed by concrete blocks in tests 1 to 6, 9 and 10, and closed by glass in tests 7 and 8. The glass did not break in tests 7 and 10 but melted after 12 – 15 min in tests 8 and 9. The fire load is wood cribs for the first three tests and spirits for the other tests. The net combustion heat of spirits is quoted to be 25.28 MJ/kg. Table 6.2 gives a summary of the test configurations.

Three thermocouples trees have been used to measure the temperatures at different elevation. For each thermocouple tree, the upper and lower layer temperature and the interface height have been deduced by the method given in section 6.3.2.1. During the ten tests, the heat release rate has been measured by oxygen depletion. The mass of fuel has also been measured during all tests but measurements failed during tests 4 and 6. The mass loss rate has been deduced from the mass measurements.

Table 6.1 Thermal properties of partition material

material type	Density ρ [kg/m²]	Specific heat c [J/kg K]	Thermal conductivity λ [W/m K]	$b = \sqrt{c\rho\lambda}$
Aerated concrete	700	900	0.21	364

Table 6.2 Summary of test configurations

Test n° - date	Fuel	Fire load	location	size	Horizontal vent	vertical vent
01-07/05/99	wood	247 kg	centre	2 cribs	2 x 1 m²	no
02-10/05/99	wood	247 kg	corner	2 cribs	2 x 1 m²	no
03-17/05/99	wood	51 kg	centre	1 crib	2 x 1 m²	no
04-18/05/99	spirits	120 l	corner	1.5 m²	2 x 1 m²	no
05-19/05/99	spirits	120 l	centre	1.5 m²	2 x 1 m²	no
06-24/05/99	spirits	200 l	centre	3 m²	2 x 1 m²	no
07-28/05/99	spirits	200 l	centre	3 m²	no	glas[1]
08-28/05/99	spirits	200 l	centre	3 m²	no	glas[2]
09-01/06/99	spirits	200 l	centre	3 m²	glas[2]	no
10-03/06/99	spirits	200 l	centre	3 m²	glas[3]	no

[1] ESG glas (Single Pane Safety Glass) –no failure during test
[2] polyacryl double glas – melt after 12 - 15 min in both tests
[3] VSG glas (Sandwich Safety Glass) – no failure during test

6.4.1.2 Heat and mass release rates.

As heat release and mass loss rates have been measured, it is of great interest to compare them. The effective combustion heat of fuel can be calculated for the eight tests during which both measurements of heat and mass succeeded by dividing the total heat release by the total mass burnt.

Assuming that the net combustion heats are 17.5 MJ/kg for wood and 25.28MJ/kg for spirits, the average value of the combustion efficiency factor during the test can be calculated by dividing the effective combustion heat by the net combustion heat. The net value considered here have not been measured, they are taken from literature. The value obtained for the eight tests (during which both measurements of heat and mass succeeded), are shown on Figure 6.4. The values obtained for wood are between 0.61 and 0.82 with a mean value of 0.71. The values for spirits are between 0.74 and 0.88 with a mean value of 0.80. These values are in the range of those found in the literature, for example Karlsson and Quientiere (2000) report that the combustion efficiency is typically around 60 to 70% in case of fuels that produce sooty flames (which is the case for wood) and higher values for fuels like alcohols which burn with a hardly visible flame, indicating that little soot is produced.

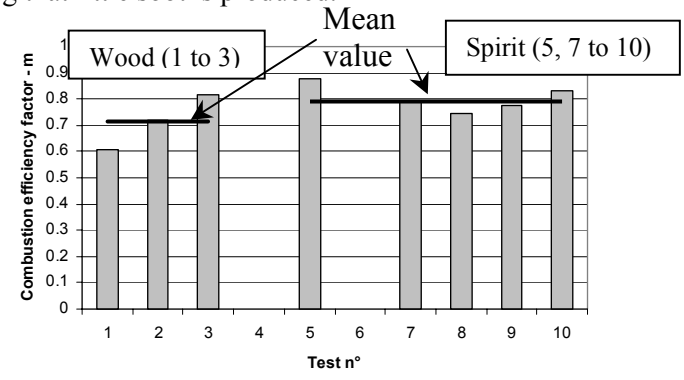

Figure 6.4 Combustion efficiency factor for DSTV tests

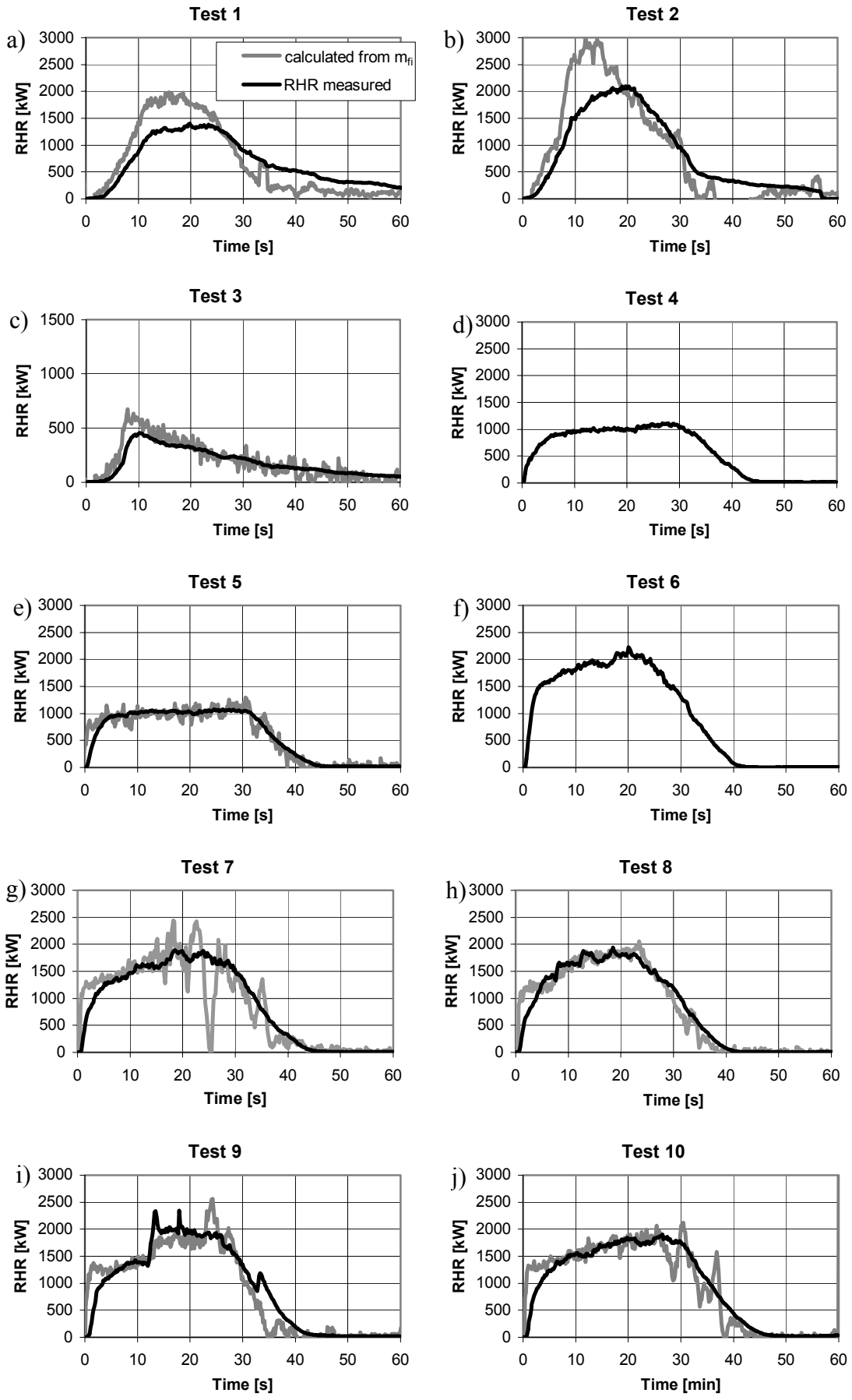

Figure 6.5 RHR measured and calculated for mass loss rate measurements (except for tests 4 and 6)

Using the mean effective combustion heat of each test, it is possible to compare the mass loss rate and the heat release rate on a single graph. The effective combustion heat calculated for the test multiplies the mass loss rate curve of this test, giving the heat release rate calculated from mass loss rate (see Figure 6.5).

The two ways of evaluating the heat release rate for the tests give similar results for tests where spirits is used as fuel load (tests 4 to 10). The maximum heat release is approximately the same with the two methods. Anyway, a time shift encounters, the heat release rate derived from mass loss measurements increases and decreases a little faster and earlier than the heat release rate curve measured by oxygen depletion. The time shift corresponds to the time that gases particles take to reach the heat release rate measurements device. This phenomenon is clearly visible in this test series. A delay of 2 to 4 minutes is present in all tests.

For the tests where the fire load is made of wood (tests 1 to 3), the time shift is still present but moreover the maximum heat release rate is quite different. The ratio between mass loss and heat release rates is not constant with time.

The combustion efficiency factor *m* calculated with the procedure described at the beginning of this section is a global one; it is actually varying with time. This phenomenon is quite weak in case of spirits but is very important in case of wood for which differences of about 50% can be found on the combustion efficiency during the course of a fire (see test n°2). As the mass loss rate is obtained by derivation of the mass measurement, it is more unstable than the heat release rate.

6.4.1.3 Blind comparison

A blind comparison is made. The tests have been simulated twice, once using the mass loss rate measurement and once using the heat release rate measurements. The net heat of combustion are 17.5MJ/kg for wood and 25.28MJ/kg for spirits; the combustion efficiency factor is set to 0.8.

The upper layer temperatures are shown on Figure 6.8. The lower layer temperatures are shown on Figure 6.9. The layer interface elevations are shown on Figure 6.10.

Two comments have to be made on the tests results. On one hand, as the fire is localised, it is obvious that the temperature which are in the vicinity of the fire are higher than the more distant ones. The upper layer temperatures presented on Figure 6.8 (a to j) are in three locations, the highest upper layer temperature is the one obtained from the thermocouple tree which is closest to the fire location. So the comparison here are made ignoring the measurements made in the fire source vicinity. On the other hand, on Figure 6.10, it can be observed that the horizontal vent (tests 1 to 6 and 9) lead to obtain in the tests an upper layer thickness which is not uniform. These two phenomena can not be represented by a zone model based on the assumption of an upper layer with a uniform thickness and with a uniform temperature.

The results of the calculations with on one hand the mass loss rate and on the other hand the rate of heat release obtained by oxygen depletion are very similar for the tests where spirits is used as fire load. For the tests with wood, the simulations with the mass loss rate give higher temperatures. This is a direct consequence of the fact that the maximum heat release rate obtained by multiplying the mass loss rate by the effective combustion heat is higher than the one obtained by oxygen depletion, see previous section.

For tests 1 to 6: The upper layer temperatures are rather well estimated, Figure 6.8 a to f; The calculated temperatures of the lower layer are lower than the measured ones, Figure 6.9 a to f; The calculated layer interfaces are lower than the measured one for, Figure 6.10.

Test 07 & 10 (Figure 6.8, Figure 6.9 & Figure 6.10-g & j): in these two tests, the door is the single opening, nor the windows, nor the horizontal vents are open. A good correlation is obtained on the three parameters; used in this comparison. The lower layer temperature is a little underestimated but the correlation remains good. It seems also that the thermal inertia of the model is a little higher then the real one, this is deduced from the fact that the predicted upper layer temperature increases slower than the measured one.

Test 08 & 09 (Figure 6.8, Figure 6.9 & Figure 6.10-h & i): test 08 is nearly identical to test 07 and test 09 is nearly identical to test 10 until time at which the glass material melts. At about 12 minutes, the windows (test 8) and the horizontal openings are activated. The effect on the measured interface height is to make it unstable, no significant increase of Z_S is observed in the tests while OZone predicts an increase of about 1m for the clear layer thickness.

In test 9 the upper layer temperature is kept to a maximum value of about 400°C. This is the combined effect of the increase of heat release rate on one hand and to the increase of energy loss through the opening on the other hand. The calculation gives a good estimation of these combined effects. Of course the increase of RHR is not predicted but set in the input. In the calculation, these effects are combined to the reduction of the upper layer thickness. Thus, it seems that the horizontal vent model over-predicts the exchange of mass and energy leading to a reasonable estimation of the upper layer temperature due to the opposite effects of, on one side, the reduction of upper layer thickness. The calculated lower layer temperature is too low.

Qualitatively, in test 08 the effect of the vertical vent breakage is very similar to the one of the horizontal vent breakage in test 09. Quantitatively the effect is weaker in test 08, the temperature of the upper layer are still increasing slightly after the windows breakage. Once again OZone slightly over predicts this phenomenon.

Figure 6.6 and Figure 6.7 shows a comparison of the maximum temperature obtained from test measurements and from OZone calculation. A fairly good agreement is found, with the use of either the mass loss rate measurements or the RHR obtained by oxygen consumption.

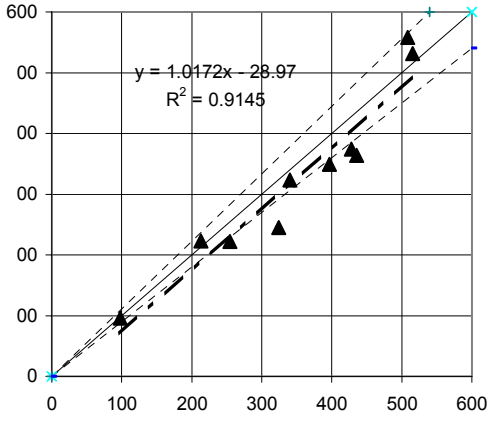

Figure 6.6 maximum temperature; using RHR measurements

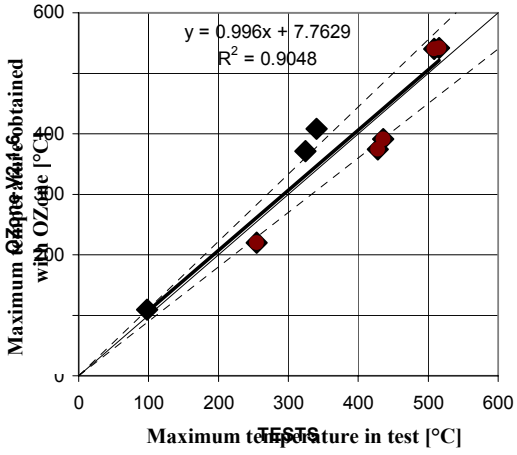

Figure 6.7 maximum temperature; using mass loss measurements

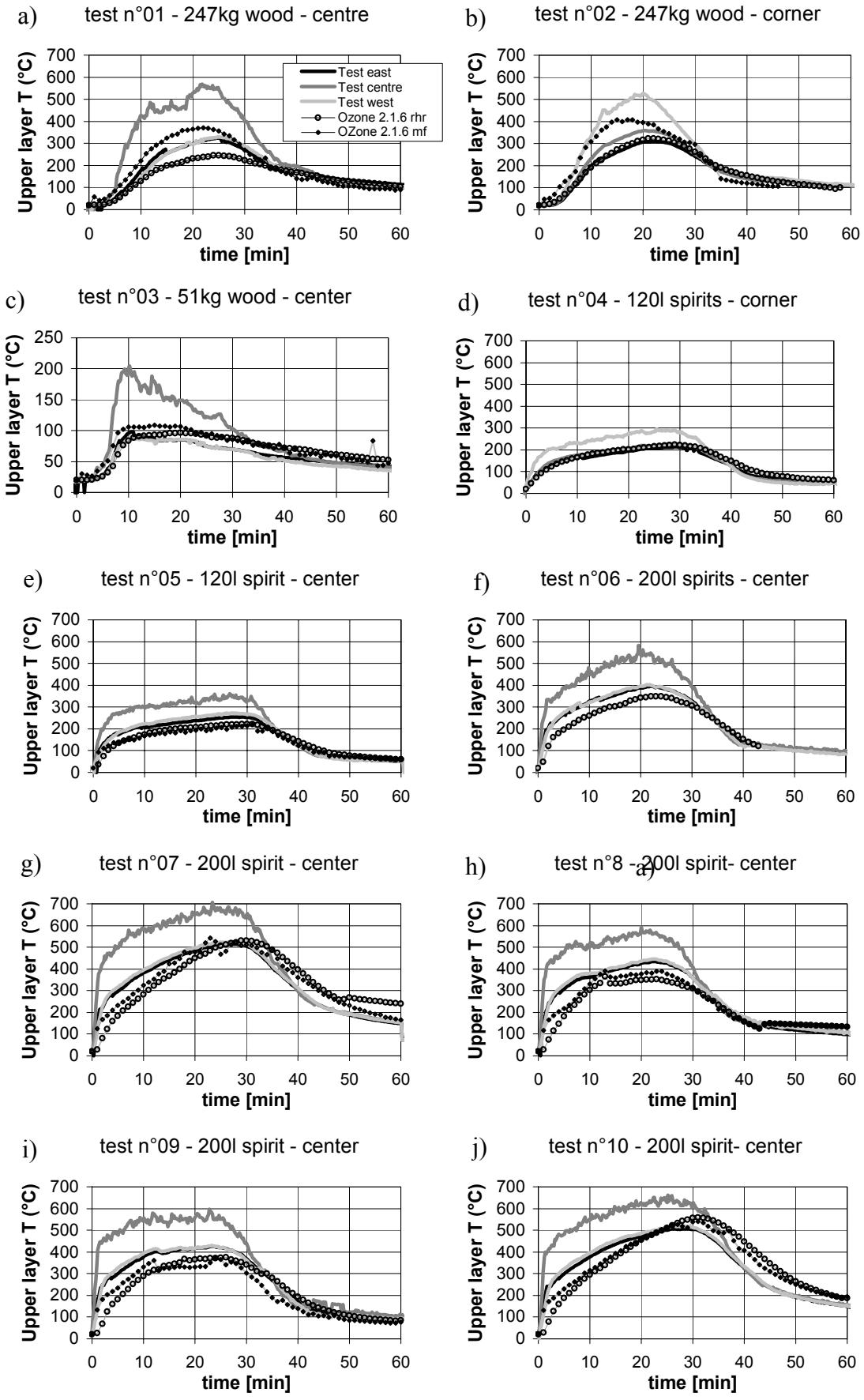

Figure 6.8 Upper layer temperature – comparison between tests (three thermocouple trees location) and OZone calculation based on rhr and mass loss measurements

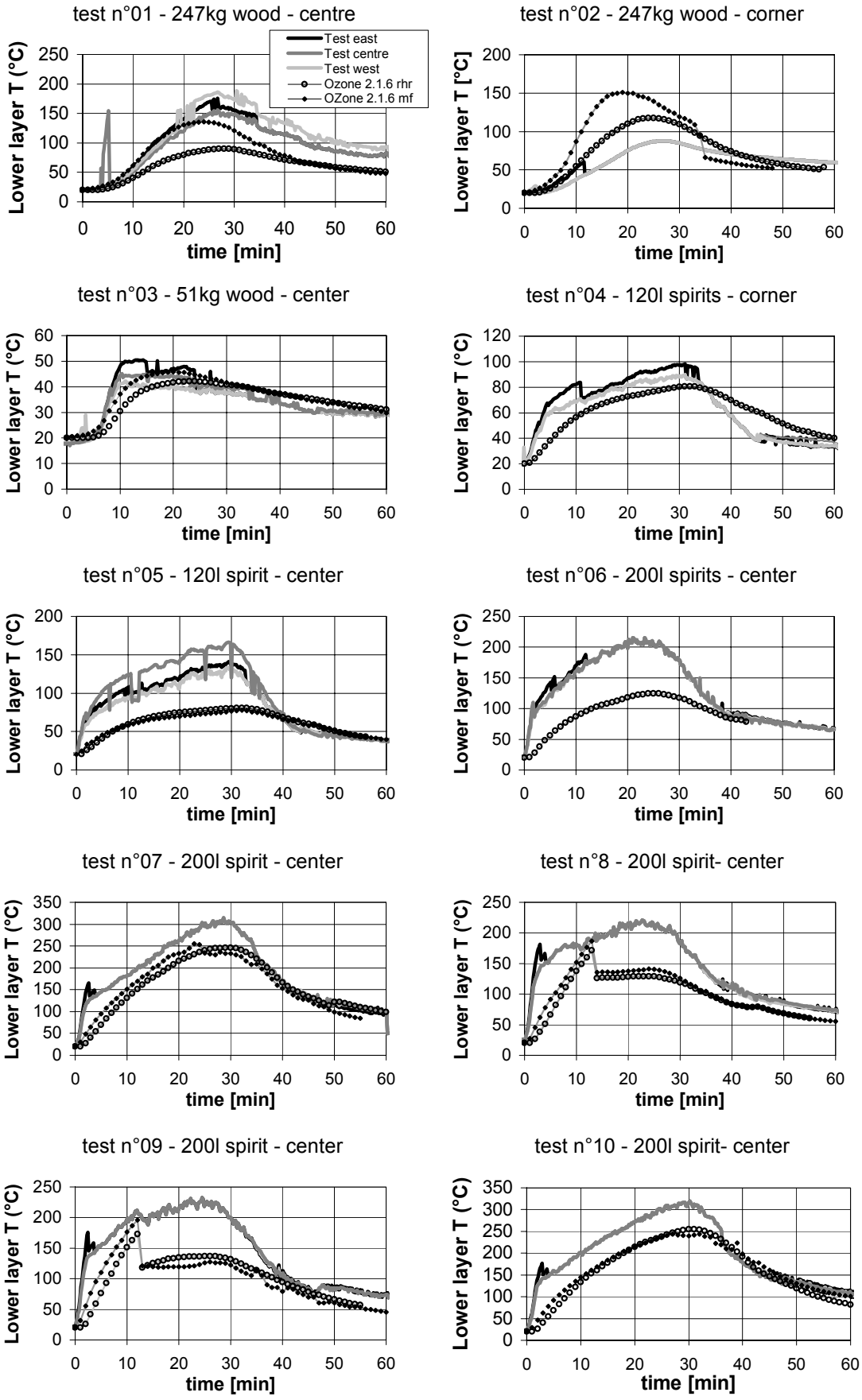

Figure 6.9 Lower layer temperature – comparison between tests (three thermocouple trees location) and OZone calculation based on rhr and mass loss measurements

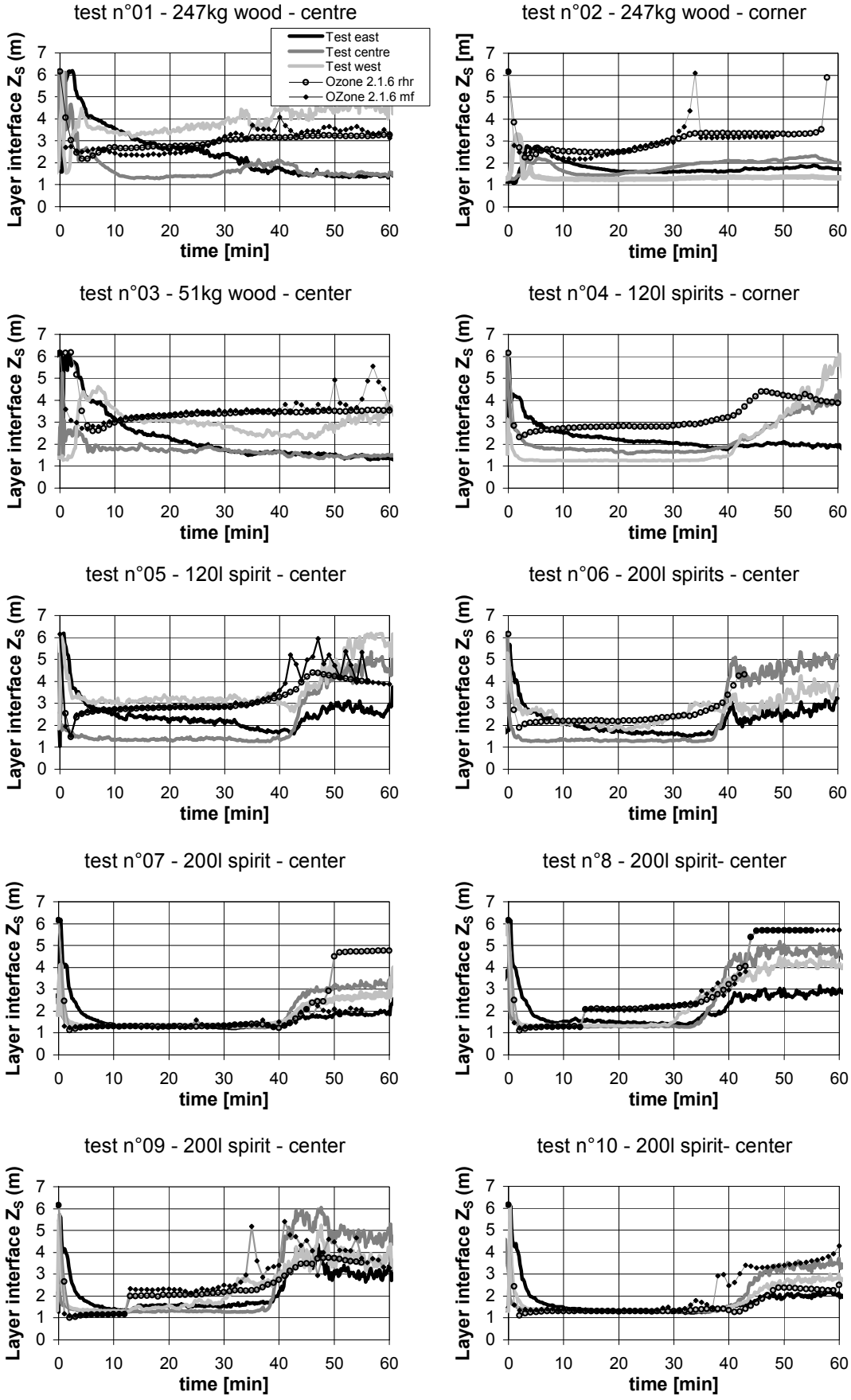

Figure 6.10 Layer interface elevation – comparison between tests (three thermocouple trees location) and OZone calculation based on rhr and mass loss measurements

6.4.1.4 Conclusions

The following conclusions can be raised:

- The two methods (mass loss measurements and oxygen depletion) used to estimate the RHR give similar results if spirits is used as fire load. For wood, the results are quite different.
- The upper layer temperature is well estimated with OZone.
- The predicted lower layer temperature is too low in this test series.
- The smoke layer interface is very well estimated if the horizontal vents are closed;
- If horizontal vents are open, the upper layer thickness is not uniform during the tests and the code tend to predict a thickness which is close to the lowest measured one.

The general conclusion of the comparison between OZone and this test series is that the simulation of a fire in a compartment with horizontal opening in a corner of the roof give a reasonable estimation of the upper layer temperature but that the layer thickness and the lower layer temperature estimation have to be cautiously considered. In this kind of situation, a more sophisticated tool might be necessary for the estimation of the latter parameters.

6.4.2 VTT Hall tests, Finland, 1999

A detailed description of the test series (tests configuration, data and results) is given in NFSC2, 2001. All data, figures and measurement results are taken from this report with permission of the authors.

6.4.2.1 Test data

The experiments were conducted in the large fire testing hall at VTT. The hall has the following dimensions: length 27 m, width 14 m and height 19 m. Schematic views of the hall are shown on Figure 6.11. The walls and ceiling of the hall are made of metal sheets insulated by mineral wool. The concrete floor was partially covered by steel plates.

In both ends of the hall there are 4.0 m high doors. During the first five tests (Fire types 1 and 2) the doors were closed, but during the last three tests (type 3) they were 0.80 m open to allow the flow of the air needed to replace the 11 m^3/s mechanically extracted from the compartment. Mechanical exhaust was taken from the exhaust duct placed in approximately middle of the hall.

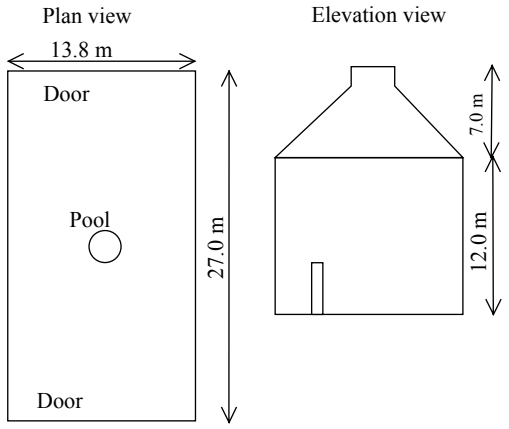

Figure 6.11 Schematic view of the hall

Table 6.3 Fire tests in the NFSC 2 Hall Test series in VTT.

Test No. &Date	Fire Type	Pool size	Duration (min:s)	Fuel mass (kg)	RHR approx. (kW)	Ventilation
Test 1 2.6.99	1	1.07m^2 D=1.17 m	7:03	18.2	2000	NO
Test 2 3.6.99	1	1.07m^2 D=1.17 m	4:10	18.7	2000	NO
Test 3 3.6.99	2	2m^2 D=1.60 m	6:34	30	3700	NO
Test 4 3.6.99	2	2m^2 D=1.60 m	6:26	29.2	3700	NO
Test 5 3.6.99	2	2m^2 D=1.60 m	6:24	29.1	3700	NO
Test 6 7.6.99	3	2m^2 D=1.60 m	5:47	29.3	4000	Exhaust 11 m³/s Doors 2 × 0.8×4.0 m²
Test 7 7.6.99	3	2m^2 D=1.60 m	5:42	29.1	4000	Exhaust 11 m³/s Doors 2 × 0.8×4.0 m²
Test 8 7.6.99	3	2m^2 D=1.60 m	8:37	43.5	4000	Exhaust 11 m³/s Doors 2 × 0.8×4.0 m²

The fuel was heptane burned in circular steel pools placed on load cells for the mass loss measurement. The mass loss rate was then calculated by numerical derivation of the mass curve. Pool size varied from 1.07 m^2 to 2.0 m^2.

Test series consisted of three different fires and eight experiments. The test series is summarised in Table 6.3 showing the approximate duration of the fire, total mass of the burnt fuel, approximate rate of heat release and the ventilation conditions.

6.4.2.2 Blind

A blind comparison is done using the rate of mass loss measured during tests.

For tests 1 to 5, no opening is present in the compartment. A vertical opening with an area equal to 0.5 % of the area of the vertical partitions is included in the model. This vertical opening represents the porosity of the compartment, i.e. the leakage which are present at partitions connections, around the closed openings, etc. The value of 0.5 % has been fixed arbitrarily. A sensitivity study on this has shown that a modification of the porosity from 0.1 % to 1% does not modify significantly the upper layer temperature. Without any opening, the pressure in the compartment rises quickly to very high values, which is unrealistic in this situation because leakages exist really. If we consider the upper layer thickness, the influence of the area of this vertical opening is more significant. If the percentage is increased from 0.5 to 0.6%, a reduction of 35cm of the upper layer thickness is obtained. This latter remark should be considered when analysing the results of the simulations shown below.

Two tests results are presented: test n°3 on Figure 6.12 and test n°8 on Figure 6.13. For both tests, the upper layer temperatures calculated with OZone fit nearly perfectly to the one obtained from measurements. The temperature is in fact well estimated for the 8 tests. Figure 6.14 shows the comparison between the maximum temperature obtained from measurements and from calculations.

The prediction of the upper layer thickness is very good for the test 3, and similarly for test 1, 2, 4 and 5 which have no openings, and is slightly too low for test 8 and similarly for tests 6 and 7 which have the same vents as test 8. The difference between the measured and calculated layer thickness is of about 1.3 m. In the last three tests the additional vertical vent which represents leakages is also considered. Nevertheless its influence on the layer thickness is reduced. For

example, if the percentage is 0.6 % instead of 0.5 %, the upper layer thickness is reduced by 15 cm.

The lower layer temperatures (not represented in graphs) is also well predicted for this test series. The results are comparable to those obtained for the upper layer. As example, for the test 8, the maximum lower layer temperature obtained from measurements and from calculations are respectively, 42°C and 40°C.

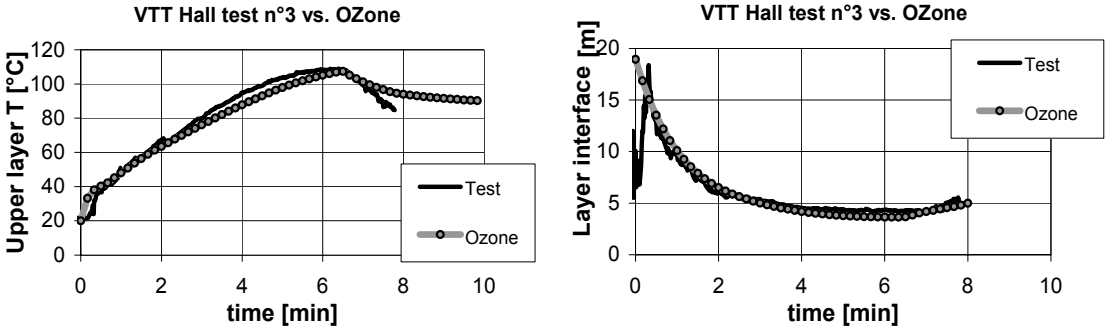

a. Upper layer temperature **b. Layer interface**

Figure 6.12 VTT hall test n°3 – comparison with OZone

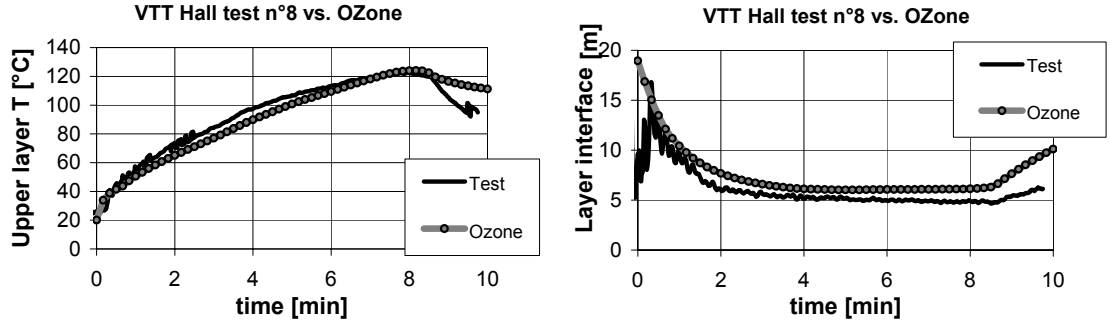

a. Upper layer temperature **b. Layer interface**

Figure 6.13 VTT hall test n°8 – comparison with OZone

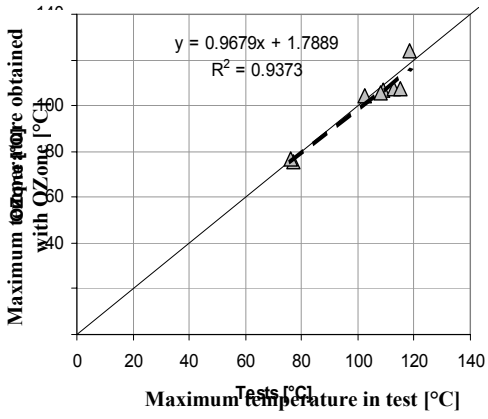

Figure 6.14 maximum temperature -VTT hall series - Blind comparison

6.4.2.3 Conclusions

A very good correspondence exists between calculation and measurements of the upper and lower layer temperatures for all tests of this series. The upper layer thickness is very well

estimated when there is no ventilation but a vertical opening which represents the porosity of the compartment must be considered. The mass flow through the mechanical extraction seems to be slightly overestimated by the model. Nevertheless this affect only slightly the layer thickness and does not affect the temperatures.

6.4.3 VTT Room tests, Finland, 1998

A detailed description of the test series (tests configuration, data and results) is given in Hostikka et al. 2001. All data, figures and measurement results are taken from this report with permission of the authors.

6.4.3.1 Test data

The experiments were conducted in a rectangular room having one door to the large fire testing hall at VTT. The whole room was located inside the hall that has the following dimensions: length 27 m, width 14 m and height 19 m. The test room was approximately in the centre of the hall. Smoke flowing out of the door was collected to the upper part of the hall as the mechanical ventilation of the hall was not used during the experiments.

An overview of the test set-up is illustrated in Figure 6.15 showing a fire plume inside a room and some of the measurement devices. The length of the experiment room was 10 m, width was 7.0 m and height 5.0 m (internal dimensions). The walls and ceiling of the room were made of lightweight concrete (ρ = 475 kg/m3, λ = 0.12 W/Km, c = 900 J/kg.K) and the floor material was normal concrete. The thickness of the walls was 0.30 m and the ceiling 0.25 m. In the beginning of the test series the moisture content of the walls and ceiling material was quite high, but an actual moisture measurement was not made. Approximately 10 % of the floor area was covered by steel plates blocking the air channels inlet under the floor.

The width and height of the door were 2.4 m and 3.0 m, respectively. However, the door width was changed to 1.2 m during some tests to find out the effect of the opening size.

The burning fuel was heptane, except in two tests where a wood crib was burned. Heptane was burned in circular steel pools placed on load cells for the mass loss measurement. Pool size varied from 0.40 m^2 to 2.0 m^2 and four different locations were used for the pools. The locations are shown in Table 4.

A list of the 10 different fire types is given in Table 7.4. The bold values in the table are the value that are changed from the previous fire type. For each fire types, one to three tests were performed with either identical or different fuel quantity.

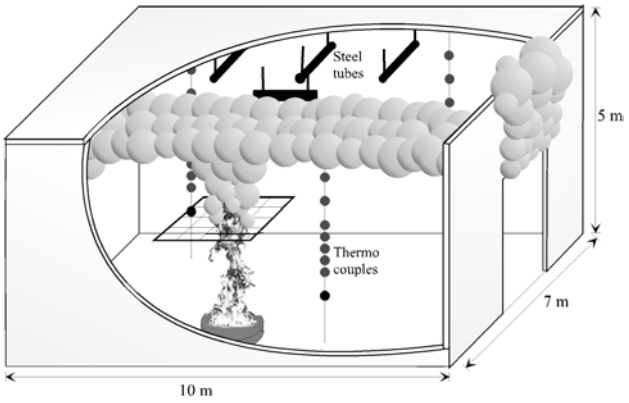

Figure 6.15. Overview of the experimental setup.

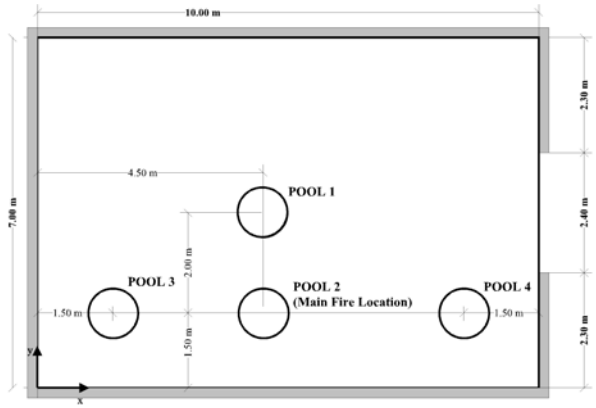

Figure 6.16. Heptane pool locations in test room. The wooden fire load was placed in location 2.

Table 7.4 Fire types in the NFSC 2 Room Test series in VTT.

Fire Type / number of tests	Pool location	Pool area	Pool Diameter	Fuel surface height from the floor	Door width
1 / 3	#2 side wall	0.40 m^2	0.71 m	0.2 m	2.4 m
2 / 3	#2 side wall	**0.61 m^2**	**0.88 m**	**0.21 m**	2.4 m
3 / 1	**#3 rear corner**	0.61 m^2	0.88 m	0.21 m	2.4 m
4 / 2	**#1 center**	0.61 m^2	0.88 m	0.21 m	2.4 m
5 / 1	**#4 front corner**	0.61 m^2	0.88 m	0.21 m	2.4 m
6 / 3	**#2 side wall**	**1.07 m^2**	**1.17 m**	**0.44 m**	2.4 m
7 / 1	**#1 center**	1.07 m^2	1.17 m	0.44 m	2.4 m
7B / 1	#1 center	1.07 m^2	1.17 m	0.44 m	**1.2 m**
8 / 2	**#2 side wall**	1.07 m^2	1.17 m	0.44 m	1.2 m
9 / 2	#2 side wall	**2.00 m^2**	**1.60 m**	**0.25 m**	**2.4 m**
10 / 2	#2 side wall	**Wood cribs**			2.4 m

Mass loss measurements were used to estimate the rate of heat release. The suggested value of the net combustion heat of heptane is 44.6 MJ/kg with a combustion efficiency factor of 0.8, ±0.1. The values of the rate of heat release were thus between 0.7 and 4.8 MW.

The investigated parameters are thus: the fire load, the fire size, the pool location and the door width.

6.4.3.2 Blind and open

The 21 tests performed in the room at VTT were simulated with OZone using the mass loss measurement as data and using an effective combustion heat of heptane of 40.1 MJ/kg (m=0.9).

A blind comparison is first made using all the data defined in the test report. In particular the properties of lightweight concrete are assumed to be: ρ = 475 kg/m3, λ = 0.12 W/Km, c = 900 J/kgK.

The results of the blind comparison are presented on Figure 6.17 for the test n°3. It can be observed that the maximum calculated temperature of the upper layer is about 20% lower than the measured one, i.e. 160°C compared to 200°C. Moreover, except in the early minutes, the calculated temperature is always underestimated by about 20 %. The upper layer thickness calculated with OZone considering the Heskestad model constitute a nearly perfect estimation of the measured one.

A comparison of the measured and calculated maximum temperatures for the 21 tests is shown on Figure 6.18. In fact the comments made on the simulation of test 3 are valid for all the 21 tests. The calculated temperature of the upper layer is underestimated by 20 to 25 %. The upper layer thickness is estimated correctly.

Nevertheless all the variations of the different parameters are quite well represented with OZone.

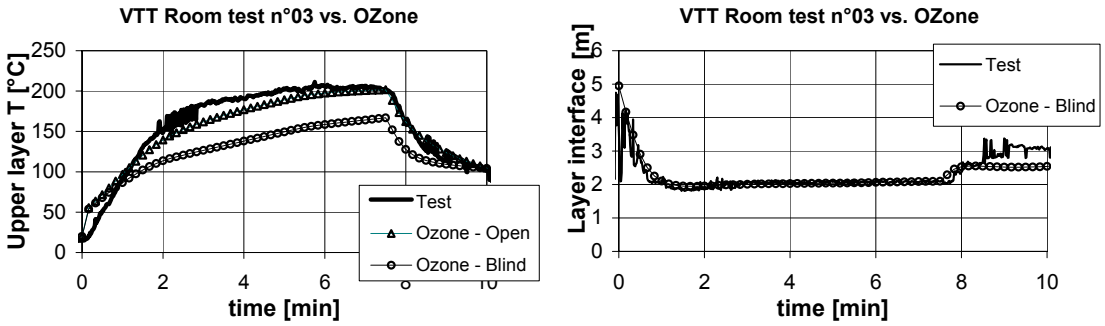

a. Upper layer temperature **b. Layer interface**

Figure 6.17 Comparison VTT room test n°03, measurements vs. OZone

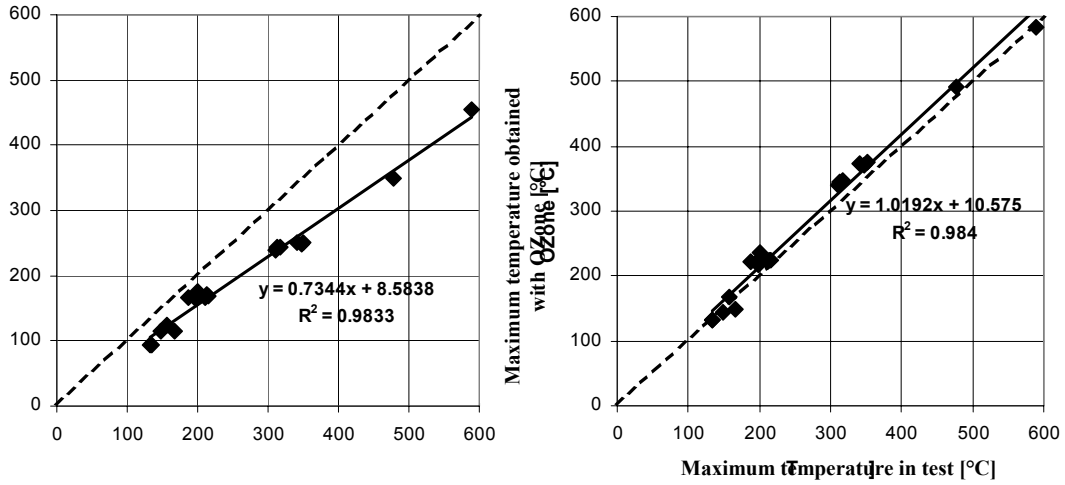

a. Blind comparison **b. Open comparison**

Figure 6.18 VTT room test - Maximum temperature – tests measurements vs. OZone calculations

It has to be noticed that a variation of the pool size or of the fire load has a direct impact on the rate of mass loss which is used in the calculation. Thus we can not consider that the effect of a variation of the pool size or the fire load is well represented in the OZone calculations but we can conclude that the effect of a variation of the rate of mass loss is well represented by the code.

Another important remark has to be made on the pool location. This parameter is not taken into account in OZone but the test series shows that it has a small influence on the zone temperatures and on the layer thickness. Its effect is essentially localised above the fire location.

An open comparison is then made. The first step is to modify the thermal properties of lightweight concrete in the simulation of one test (test 3 is taken here) in order to improve the maximum temperature estimation. A good estimation of the whole temperature history (see Figure 6.17a. and Figure 6.17b.) is found when using the following thermal properties: $\rho = 238$ kg/m^3, $\lambda = 0.06$ W/Km, $c = 450$ J/kgK. These thermal properties are then used in the simulation of the other tests leading to a very good comparison with the measurements, see Figure 6.18. The upper layer thickness calculated with this new partitions properties are nearly identical to the one in the blind comparison.

In fact this open comparison does not prove that the thermal properties used here are the real one. It only shows that for this test series the heat transfer to the partition might be over estimated.

Other causes have also been investigated, for example: The emissivity of the wall surface and of the gas may be lower than the one considered; The combustion heat of fuel may also be higher than the one consider. But even if a lot of measurements have been made in this test series and even if the tests are well documented, it has not been possible to identify with certainty the origin of the bias. The overestimation of the thermal properties of the partition seems however to be the more likely as it enables to better predict the overall temperature histories than with other parameter modifications.

Nevertheless, this OZone prediction of this test series can be considered to be satisfactory as the correlation between calculations and experiments is very good and as some important parameters (thermal properties of boundary materials, combustion heat of fuel) are tabulated data and have not been measured, leading to a high uncertainty on them.

6.5 Comparisons with full scale post-flashover fire tests

6.5.1 Small room - Wood - CTICM, France 1973

6.5.1.1 Test data

The comparison of OZone simulations with 36 compartment fire tests is presented here. These tests have been performed in 1972 at CTICM (Arnault 1973). The compartment is 3.13m high, with a rectangular floor of 3.38m by 3.68m. Three of the walls are made of hard brick. The floor is made of refractory concrete. The ceiling and the wall with the opening are made of lightweight concrete. For 25 tests, the walls and the ceiling are insulated by 2.5cm of vermiculite mortar. The fire load is wood cribs and the fire load density is between 15 and 60 kg per m² of floor area. The opening area varies between 1.062 and 6.366m²; the ventilation factor ($V_f = A_v*(h)^{0.5}$) varies between 1 and 10.8 $m^{5/2}$ and the opening factor ($O = A_v*(h)^{0.5}/A_t$) varies between 0.015 and 0.157 $m^{0.5}$. Six tests are made in the insulated compartment with the same opening dimensions (O = 0.057 $m^{1/2}$; V_f = 3.8 $m^{5/2}$) and the same fire load (30kg/m^2). For these 6 tests, the geometry of the wood cribs is the varying parameter; the wooden lath were by group of 2, 3, 4. The net combustion heat of wood is supposed to be equal to 17.5MJ/kg and the combustion efficiency factor equal to 0.8.

The test series was thus aimed at investigating:

- the difference between fire behaviour in non-insulated and insulated compartments;
- the effect of the vertical vent size and therefore of ventilation and opening factors;
- the effect of the fire load density;
- the effect of the fire load geometry.

The mass of fuel has been measured every 5 minutes during these tests and the mass loss rate has been obtained by derivation of the mass-time curve.

6.5.1.2 Comparisons

Due to the large amount of tests in this series, not all the tests are presented separately. A summary of the blind comparison with the whole test series is first presented. A more detailed presentation is given for some tests which are representative of the parameters investigated in the test series. For the latter tests, an a priori comparison is presented.

Blind comparisons are made using mass loss rate obtained from measurements and choosing the external flaming combustion model. A priori comparisons are made using the NFSC design fire curves and choosing the extended fire duration combustion model. To define the NFSC design fire curve, the following parameter are taken:

- the real fire load;
- a fast fire growth rate (1MW after 150s);
- and the rate of heat release density is equal to 1250 kW/m², which is the value proposed in NFSC for stacked wood pallets of height 0.5m.

6.5.1.3 Blind comparison

For this comparison, the mass loss rate was thus introduced in the simulation. Observation of the results showed that some tests remained in the fuel bed control regime whereas others were clearly ventilation controlled. The "external flaming" combustion model was activated; lack of oxygen leads to a reduction of the RHR but the duration of the fire is not increased, which amounts to assume external flaming.

Figure 6.19 gives a comparison of the maximum mean gas temperature obtained in the tests and the temperature computed by the model. The mean gas temperature is the mean value of the temperature measured by 10 thermocouples placed in the fire compartment.

The correlation between calculated and measured maximum gas temperatures is quite satisfactory. Nevertheless OZone seems to under predict tests with the lowest measured temperatures.

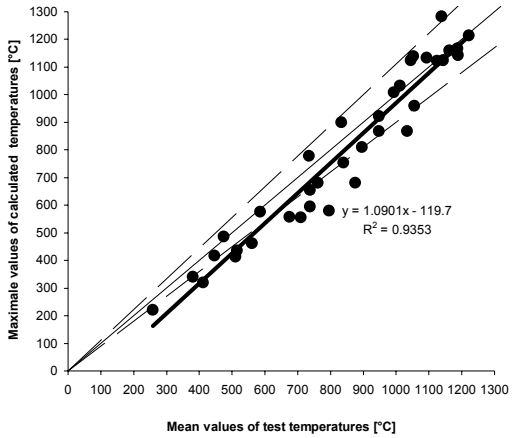

Figure 6.19 maximum mean temperature in the compartment

6.5.1.4 Thermal properties of partitions

The results presented in Figure 6.20a and b are the same than those in Figure 6.19. They are separated between tests in the non-insulated compartment, Figure 6.20a, and tests in the insulated compartment, Figure 6.20b. In the non-insulated compartment, the calculated temperatures are slightly lower than the measured ones while in the insulated compartment the higher temperatures are a little better predicted than the lower ones. Nevertheless, in both situations, the correlation is quite good.

Two tests performed in the non-insulated and the insulated room are shown on Figure 6.21a and b respectively. They are identical, excepted for the thermal properties of partitions. The fire load is 30 kg/m^2 and the ventilation factor is 3.8 m$^{5/2}$.

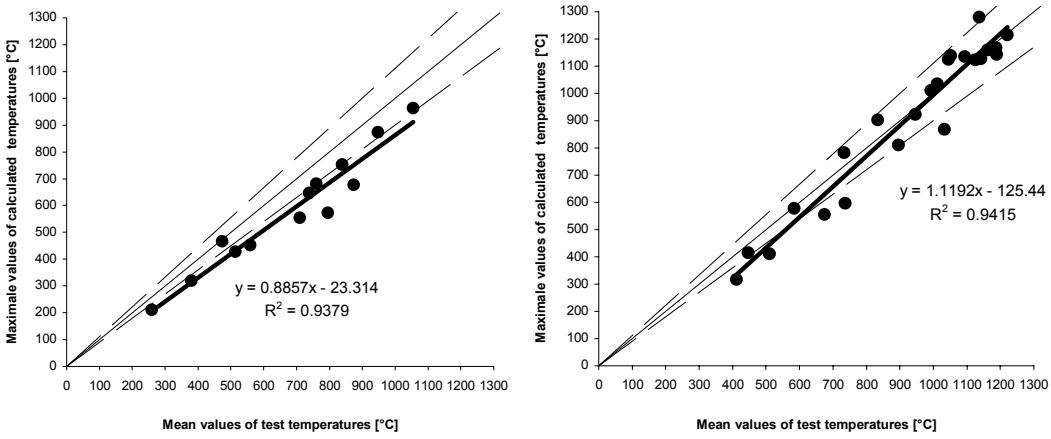

a. Non-insulated compartment b. Insulated compartment

Figure 6.20 maximum mean temperature in the compartment – blind comparison

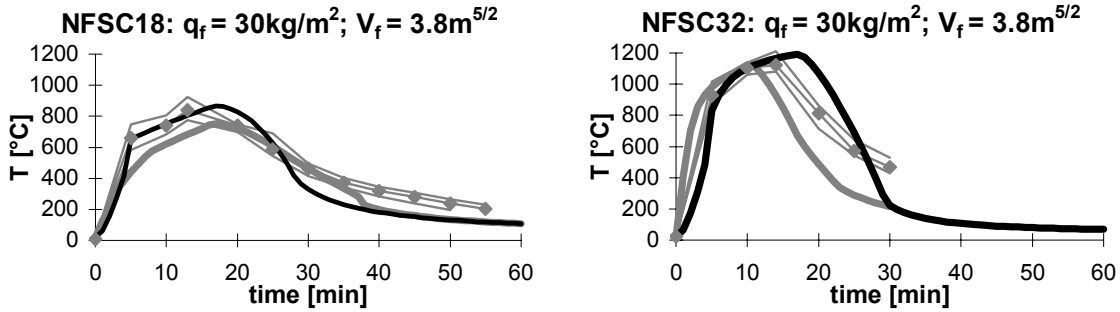

a. Non-insulated compartment b. Insulated compartment

Figure 6.21 Influence of the thermal properties of the compartment[1]

Both comparisons, using the measured mass loss rate or the NFSC design fire, give a good estimation of the temperature evolution in the compartment for the different thermal properties of partitions.

6.5.1.5 Influence of the fire load density

Three tests are presented, the single difference between these tests is the fire load density which is 15, 30 and 60 kg/m^2 for tests NFSC17, 18 and 19 respectively. These tests have been performed in the non insulated room with a ventilation factor of 3.8 m$^{5/2}$.

The blind comparisons give a good estimation of the temperature evolution in the compartment for all the different fire load densities. The a priori comparison give a good estimation of the temperature evolution in the compartment for fire load densities from 30 kg/m² and beyond. According to the calculations, the test with a fire load of 15 kg/m² is fuel controlled. The value of the rate of heat release density of 1250 kW/m² is too high leading to a too short fire duration and too high temperatures.

[1] The legend of Figure 6.22 is valid for Figure 6.21 (and for all figures of section 6.5, excepted if noted).

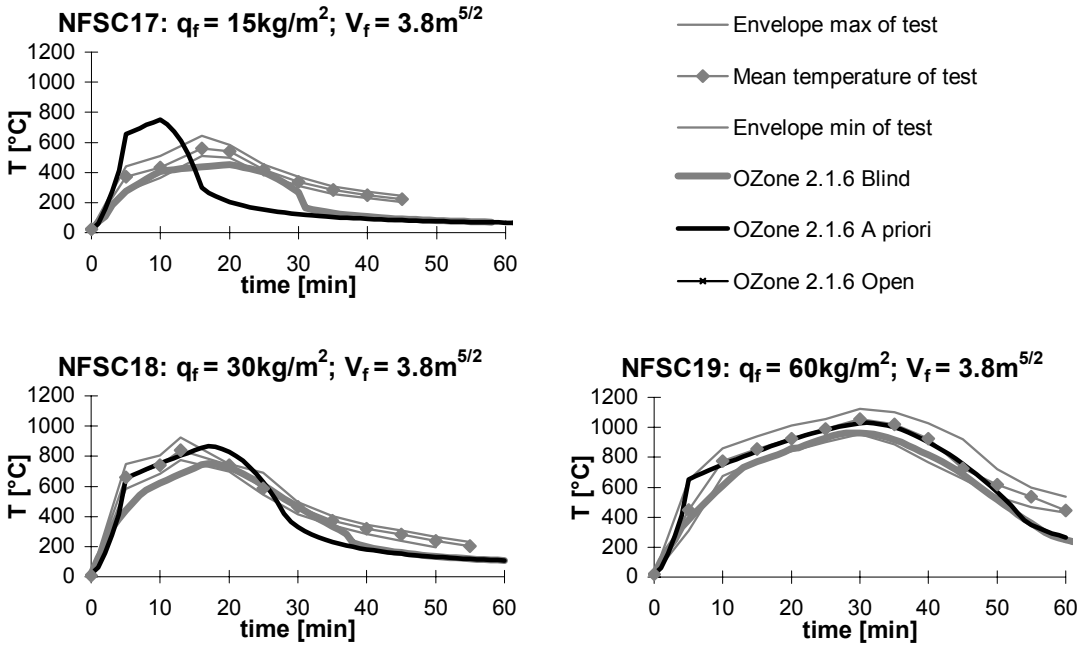

Figure 6.22 Influence of the fire load density

6.5.1.6 Influence of the ventilation

Four tests are presented, the single difference between these tests is ventilation factor which is of 1, 3.8, 6.3 and 10.9 $m^{5/2}$. These tests have been performed in the non insulated room with a fire load density of 30 kg/m^2.

The comparisons give a very good estimation of the temperature evolution in the compartment for the ventilation factor of 3.8 $m^{5/2}$.

For a ventilation factor of 1$m^{5/2}$ (test NFSC16) the predicted temperatures are too low for both blind and a priori comparisons. An open comparison is made in which the mass loss rate measured during the test is set in the data and the predetermined combustion model is activated, i.e. no limitation of the rate of heat release by the ventilation is permitted leading thus to a rate of heat release equal to the mass loss rate multiplied by the effective combustion heat.

For this open simulation of test 16, the temperature prediction becomes very good, showing that the vent flow is probably well estimated but that the limitation of the rate of heat release by the incoming oxygen mass is not appropriated to this situation.

According to the calculations, the tests with a ventilation factor of 6.3 and 10.9 $m^{5/2}$ are fuel controlled. The blind comparisons give good results for both ventilation factors but, while the a priori prediction can be considered to be reasonable for the tests with ventilation factor of 6.3 $m^{5/2}$, it is clearly not good for V_f of 10.9 $m^{5/2}$. The value of the rate of heat release density of 1250 kW/m² that is set in the data is thus too high and the predicted fire is too short with too high temperatures.

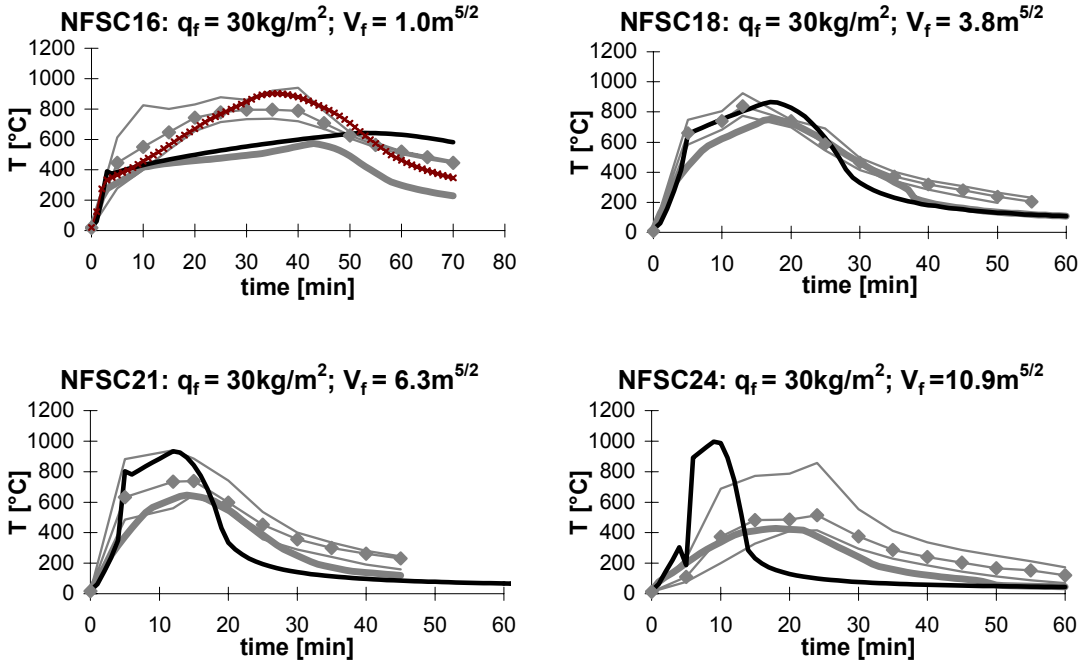

Figure 6.23 Influence of the ventilation[see footnote 1 page 131]

6.5.1.7 Fire source

The results of the "a priori" comparisons above show that the value of the rate of heat release density set in the data and thus of the plateau of the rate of heat release were not appropriate. The mass loss rate measured during the tests have thus been further analysed.

Figure 6.24a shows the maximum measured mass loss rate in function of the ventilation factor. No correlation is found between the mass loss rate and the ventilation factor and Kawagoe correlation does not apply to this test series. Thomas (1967) already showed that for large opening size the Kawagoe correlation does not apply anymore. On Figure 6.24b, the mass loss rate obtained by Thomas for various fire load are shown in regard to the one obtained in this test series, Figure 6.24a, the scale of these two graphs being the same. For an identical fire load, the mass loss rates of this test series are approximately twice the one obtained by Thomas.

Figure 6.25 shows the maximum measured mass loss rate in function of the fire load density. The mass loss rate obtained in the insulated and in the non insulated compartments are separated. For both compartments, the fire load density is the parameter that most influences the mass loss rate and the relation between these quantities is fairly linear.

The thermal properties of the partitions has also a quite big influence, the mass loss rate being higher in the insulated compartment of an average value of about 21%. This can be explained by the fact that the mass loss rate is increased by radiative heat feedback from the surrounding (Drysdale 1999) that is higher in the insulated room than in the non insulated room. No model for burning wood cribs that takes this effect into account has been found in the literature.

It is important to note that, in the blind comparison made with the external flaming combustion model of OZone, all the tests with a ventilation factor of 3.8m$^{5/2}$ and a fire load density equal or greater to 30 kg/m² were found to be ventilation controlled, leading to a rate of heat release proportional to the incoming oxygen but to an unmodified mass loss rate.

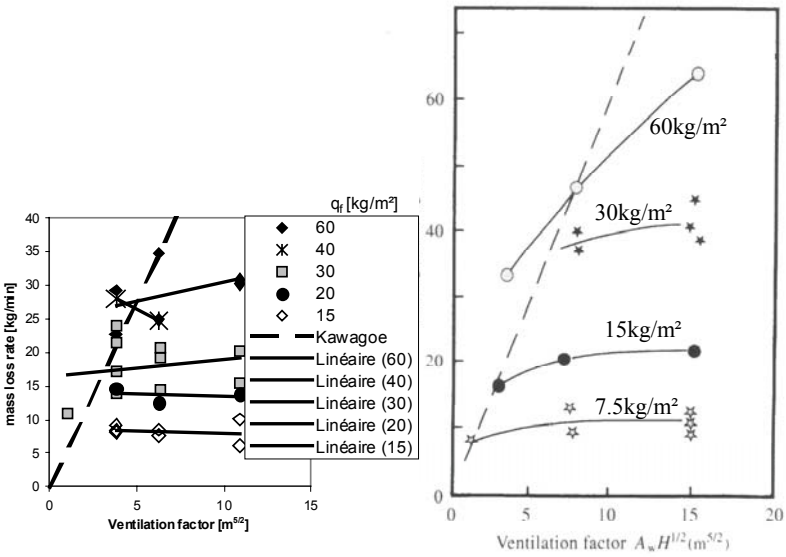

a. CTICM 1973 **b. Thomas 1967 (see chapter 2.4)**

Figure 6.24 Mass loss rate in function ventilation factor and Kawagoe correlation (dotted line)

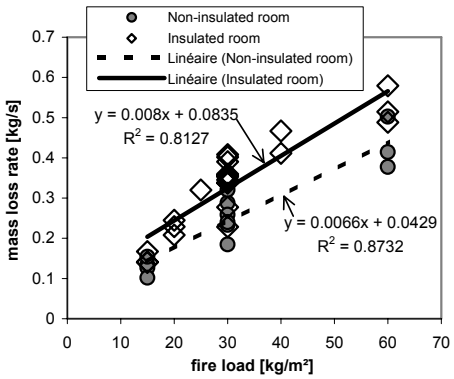

Figure 6.25 Mass loss rate in the insulated and non-insulated compartments in function of the fire load density

6.5.2 Small room - Furniture and paper fires- CTICM, France, 1974

The comparison of 10 compartment fire tests is now presented. These tests have been performed in 1974 at CTICM (Arnault 1974). Figure 6.26 gives an overview of the temperatures measured during the tests of this series.

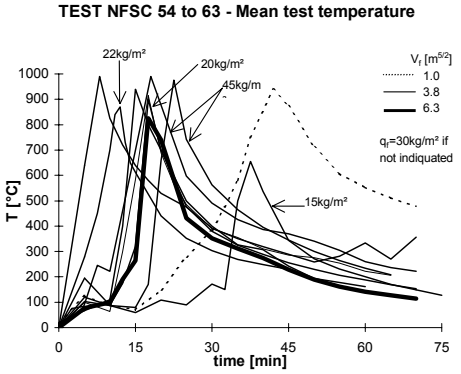

Figure 6.26 Overview of the mean temperatures measured in the 10 tests

6.5.2.1 Test data

The compartment was 3.13m high, with a rectangular floor of 3.38m by 3.68m. It is in fact the same room as the one used for the tests presented in section 6.5.1.

Three walls are made of bricks, covered by vermiculite mortar. The ceiling and the fourth wall are made of cellular concrete. The opening is made in the cellular concrete wall. The thermal properties of partition materials are given in the test series reports and a summarized in Table 6.5.

The opening area is 0.954m² for the first test, 4.251m² for the last test and 2.572m² for all other tests. The opening factors ($A_v*(h)^{0.5}/A_{t,net}$) is thus 0.015 $m^{0.5}$ for the first test, 0.099 $m^{0.5}$ for the last test and 0.058 $m^{0.5}$ for other tests.

Table 6.5 Thermal properties of partition material

material type	Density ρ [kg/m²]	Specific heat c [J/kg K]	Thermal conductivity λ [W/m K]	$b=\sqrt{c\rho\lambda}$
Normal brick	1600	840	0.69	963
Vermiculite	200	1850	0.2	272
Cellular concrete	450	1000	0.3	367
Refractory concrete	2300	1000	1.6	1918

The fire load was made of different percentage of wood, furniture and paper. The fire load density was between 15 and 45 kg per m² of floor area. The mass of fuel has been measured during these tests.

An overview of the geometry of the compartment and of the fire load is given for each test in Table 6.6.

Table 6.6 CTICM tests (1974) data

Test	D	L	H	W_w	h_w	A_f	$A_{t,net}$	V	A_w	$A_{t,eff}$	O_f	%wall	V_f	$q_{f,m}$	$q_{f,net}$	$q_{f,eff}$
NFSC	m	m	m	m	m	m²	m²	m³	m²	m²	$m^{1/2}$		$m^{5/2}$	kg/m²	MJ/m²	MJ/m²
54	3.36	3.6	3.13	0.90	1.06	12.10	67.76	37.86	0.954	66.81	0.015	10	0.98	30	525	420
55	3.36	3.6	3.13	1.18	2.18	12.10	67.76	37.86	2.572	65.19	0.058	25	3.80	15	262.5	210
56	3.36	3.6	3.13	1.18	2.18	12.10	67.76	37.86	2.572	65.19	0.058	25	3.80	20	350	280
57	3.36	3.6	3.13	1.18	2.18	12.10	67.76	37.86	2.572	65.19	0.058	25	3.80	22	385	308
58	3.36	3.6	3.13	1.18	2.18	12.10	67.76	37.86	2.572	65.19	0.058	25	3.80	30	525	420
59	3.36	3.6	3.13	1.18	2.18	12.10	67.76	37.86	2.572	65.19	0.058	25	3.80	30	525	420
60	3.36	3.6	3.13	1.18	2.18	12.10	67.76	37.86	2.572	65.19	0.058	25	3.80	30	525	420
61	3.36	3.6	3.13	1.18	2.18	12.10	67.76	37.86	2.572	65.19	0.058	25	3.80	45	787.5	630
62	3.36	3.6	3.13	1.18	2.18	12.10	67.76	37.86	2.572	65.19	0.058	25	3.80	45	787.5	630
63	3.36	3.6	3.13	1.95	2.18	12.10	67.76	37.86	4.251	63.51	0.099	40	6.28	30	525	420

6.5.2.2 Blind

The mass loss rate is calculated by deriving the mass measurements and is introduced in the simulation. The "external flaming" combustion model is activated. The net combustion heat of fuel and the combustion efficiency factor are supposed to be equal to 17.5MJ/kg and 0.8.

A good agreement is generally found on the maximum temperature and on the shape of the temperature-time curve, see Figure 6.28.

In test 54, a poor correspondence of maximum temperature is obtained while a good estimation of the rising phase and decreasing phase is found. The maximum temperature is limited to 732°C in the calculation although the measured one reaches 940°C. The calculation lead to a ventilation controlled fire. The poor correlation of the maximum temperature is the result of a poor estimation of the maximum rate of heat release by the combustion model. Unfortunately, test 54 is the only one of the series with a ventilation factor of $1m^{5/2}$ but this results is similar to the one obtained in the simulation of the test NFSC16 of the CTICM 1973 series described in section 6.5.1.

Tests 55 to 58 and 60 to 62 are also ventilation controlled. In these tests a very good agreement between measurements and calculations is obtained.

In test 59, the peak in the temperature curve is not well predicted. This is due to the absence of peak in the measured mass loss rate. In this case, the calculation leads to a fuel controlled fire. As this test is very similar to tests 58 and 60, it seems that the mass loss measurements are not fully reliable in this case.

In test 63, the ventilation factor is $6.3m^{5/2}$. The calculation leads to a fuel controlled fire, which is physically consistent as the opening is large. A very good agreement is found between the experiment and the calculation.

6.5.2.3 A priori

Ignoring the mass loss measurement, an 'a priori' comparison is made, see Figure 6.29. The objective is now to investigate whether the NFSC design fire is able to represent the behaviour of the fire source.

As the fire load is made of furniture and papers, the design fire that is considered is the Office NFSC design fire. It is defined by a medium fire growth rate (t_α = 300 s) and a rate of heat release density of 250 kW/m². The design fire load is the fire load set in the compartment during the tests (given in the test report and summarized in Table 6.6).

The results are presented on Figure 6.29.

For test 54, the calculation leads to a ventilation controlled fire. The maximum temperature of the gas is quite well estimated but the temperatures are too high during the rising and the decreasing phases. The calculated fire is much more severe than the experimental one. This is due to the fact that in the 'extended fire duration' combustion model all the fire load is forced to burn in the compartment. The hypothesis that no external flaming exists is very safe in this case.

All other calculations lead to fuel controlled fire. It is thus not consistent with the results obtained in the blind comparison. It is due to the fact that the plateau of the design fire curve does not exist in the experiment (as example; RHR in tests 57 and 63 are shown on Figure 6.27). Nevertheless the calculated curves are relatively close to the experimental ones and on the safe side in all case.

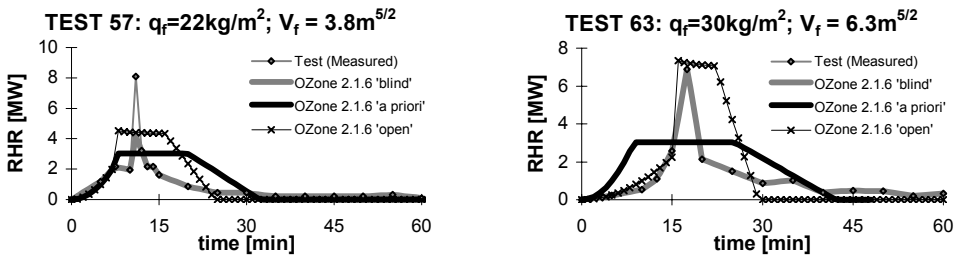

Figure 6.27 Measured and Calculated Rate of heat release in test 57 and 63.

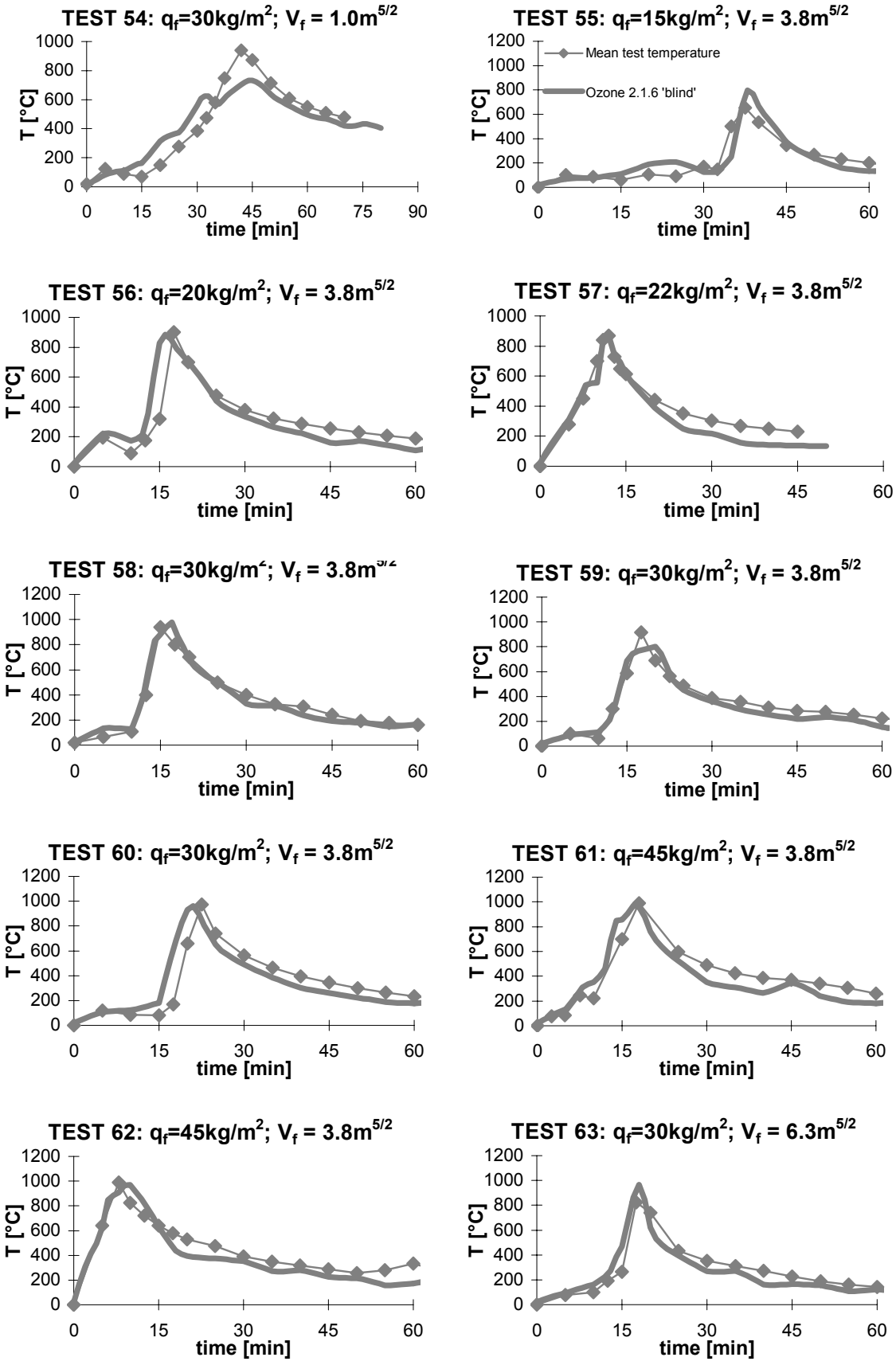

Figure 6.28 Blind comparison between OZone and CTICM tests

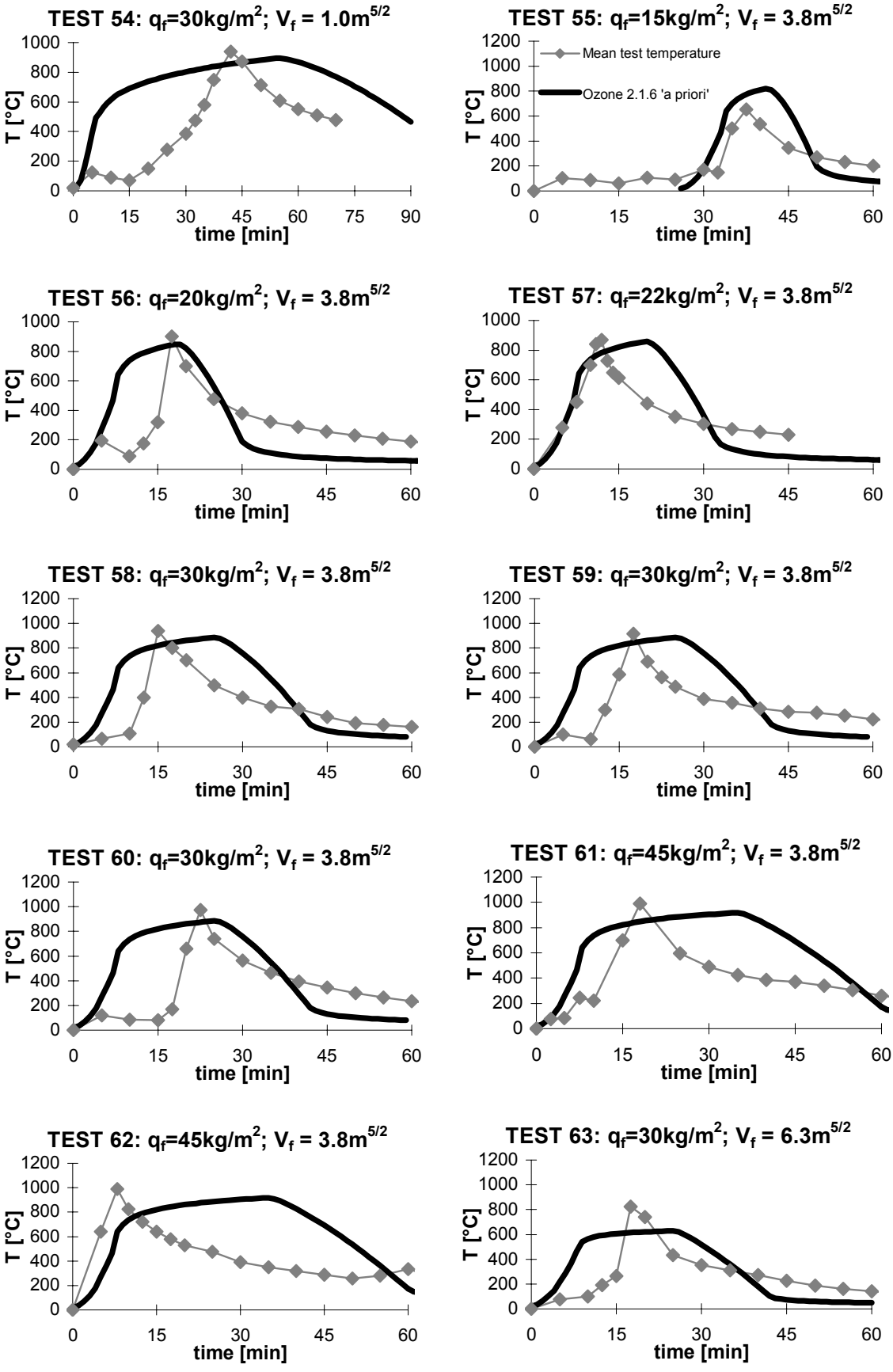

Figure 6.29 A priori comparison between OZone and CTICM tests

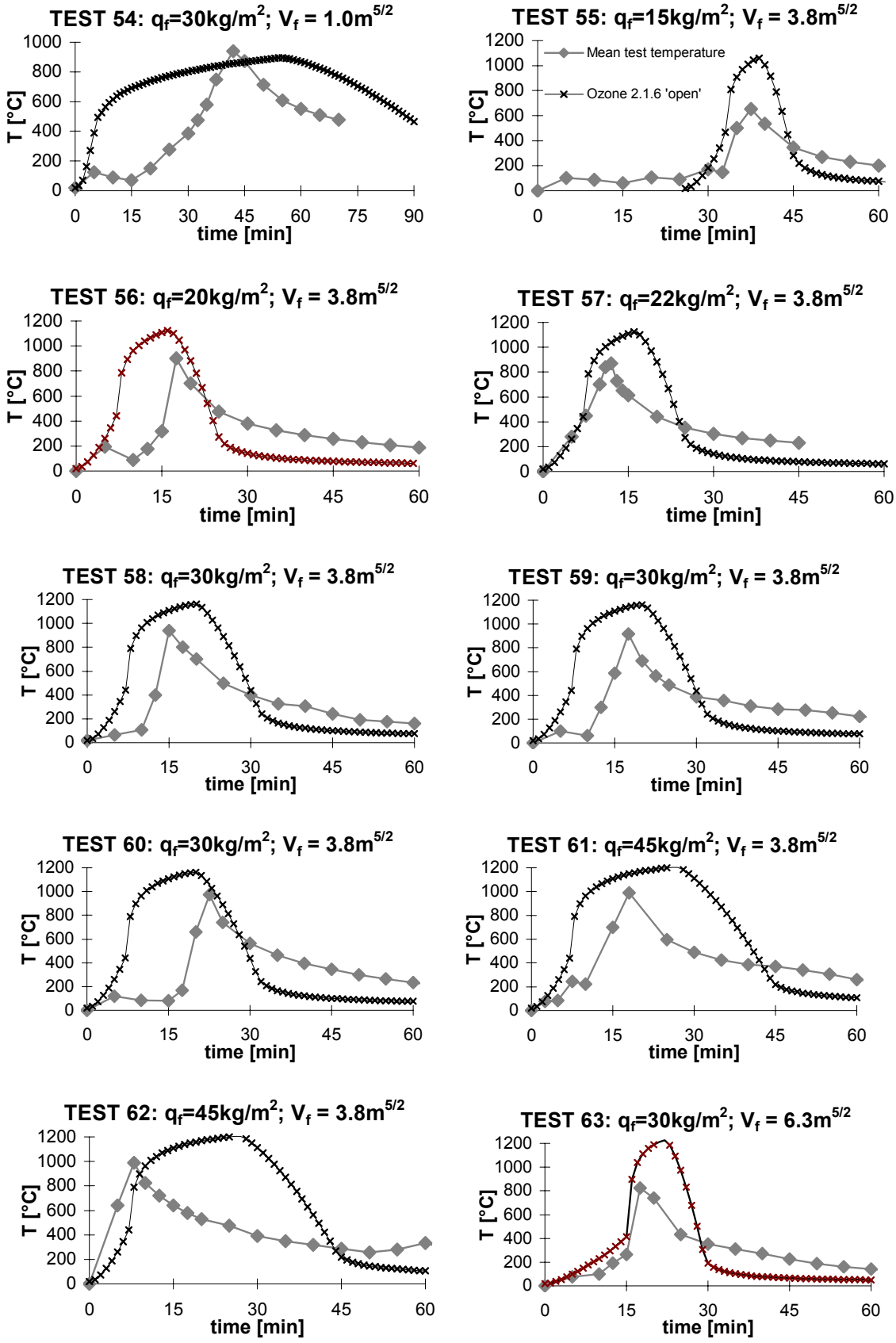

Figure 6.30 Open comparison between OZone and CTICM tests

The a priori comparison generally gives safe results for nearly all tests; except in test 63 where the maximum temperature obtained in the simulation of test 63 is slightly too low.

This study shows that the calculated fire source behaviour is quite different from the experimental one but that the design procedure is safe in all but one case. The value of the rate of heat release density is questionable. Thus an open comparison is made to better understand the influence of this parameter.

6.5.2.4 Open

In case of fuel controlled fire, the plateau of the design fire curve is of primary importance to predict the temperature in a fire compartment. In the a priori comparison, the fires were fuel controlled in all tests but one, while in the blind simulation these tests were ventilation controlled.

In this comparison the rate of heat release density is increased to a high value so that OZone will limit the rate of heat release to the ventilation controlled one (see Figure 6.27 for tests 57 and 63), in other word, the fire is forced to be calculated as a ventilation-controlled fire. The results are presented on Figure 6.30.

In this case, all the calculations give safe results.

6.5.2.5 Conclusion

A summary of the different comparisons between OZone and the test series is given on Figure 6.31.

The blind comparison has shown that, in a small fire room with ventilation factor up to 6.3$m^{5/2}$, OZone give a very good estimation of the fire course if the mass loss rate is known.

The a priori comparison has shown that the NFSC design fire give a safe prediction of the fire course in all but one tests. Nevertheless some restriction are made on the rate of heat release density defined in NFSC for office buildings.

The open comparison has shown that the simulations can be safe in all cases by increasing the rate of heat release density so that the fire becomes ventilation controlled.

Table 6.7

Test	$q_{f,m}$	V_f	Ventilation controlled ?			T_{max} Test	T_{max} Blind	T_{max} A priori
NFSC	kg/m^2	$m^{5/2}$	*blind*	*a priori*	*open*	*[°C]*	*[°C]*	*[°C]*
54	30	0.98	yes	yes	yes	940	733	895
55	15	3.80	no	no	yes	655	798	821
56	20	3.80	yes	no	yes	900	886	848
57	22	3.80	yes	no	yes	870	870	860
58	30	3.80	yes	no	yes	940	977	886
59	30	3.80	no	no	yes	915	803	886
60	30	3.80	yes	no	yes	975	962	886
61	45	3.80	yes	no	yes	990	972	917
62	45	3.80	yes	no	yes	990	971	917
63	30	6.28	no	no	yes	825	965	629

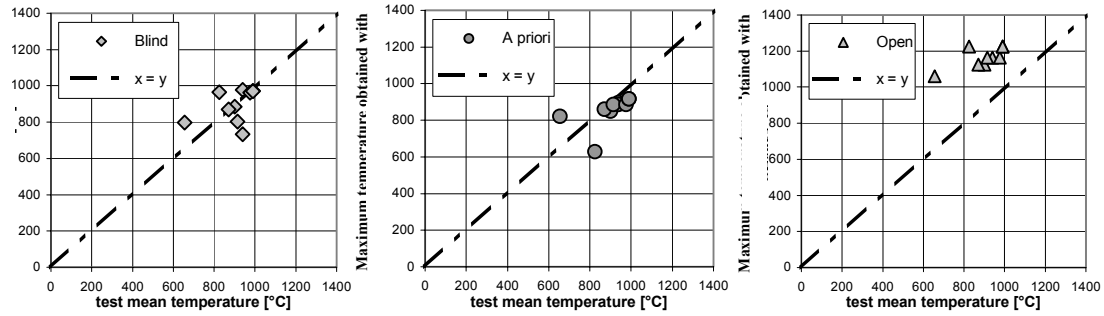

Figure 6.31 Comparison of the maximum calculated and measured mean temperatures for the three types of comparison

6.5.2.6 Design proposal

It is advised that, in a real design situation, if the uncertainty on the rate of heat release density is high and if a fire is found to be fuel controlled in a simulation, an other simulation, leading to a ventilation controlled fire, has to be done. This is obtained by increasing the input rate of heat release density. The design of structural elements has to be done twice, once with the fuel controlled fire (lower temperatures, longer fire duration) and once with the ventilation controlled fire (higher temperatures, shorter fire duration).

6.5.3 Fires in Hotel, France, 1996 & 1997

6.5.3.1 Test Data

Three tests have been performed by CTICM to investigate characteristic hotel fires.

Two tests have been done in rooms with fire load representative of contemporary hotel rooms (bed, desk etc.).

The first test was done in a compartment with a floor area of 31.8 m^2 and a single opening of 2.7 m^2.

In the second test the room has been divided in two by a plasterboard partition with a door. Some important leakage occurred through the upper part of the door during the tests but the door did not completely collapse.

The last test was performed in a linen room connected to an office room, both rooms contained fire load type representative of their use.

Table 6.8 Data of hotel fire tests

Test	D	L	H	W	h_w	A_f	A_t	V	A_w	$A_{t,net}$	Vf	O	q_f	$q_{f,net}$	$q_{f,eff}$
NFSC	*m*	*m*	*m*	*m*	*m*	m^2	m^2	m^3	m^2	m^2	$m^{5/2}$	$m^{1/2}$	kg/m^2	MJ/m^2	MJ/m^2
69	5.76	5.5	2.6	1.4	1.9	31.74	122.08	82.52	2.660	119.42	3.667	0.031	14.2	248.5	198.8
70	2.72	5.8	2.6	0.93	2	15.67	75.43	40.73	1.860	73.57	2.630	0.036	9.6	168	134.4
71	2.72	5.8	2.6	1.86	2	15.67	75.43	40.73	3.720	71.71	5.261	0.073	18.3	320.25	256.2

6.5.3.2 Blind and a priori

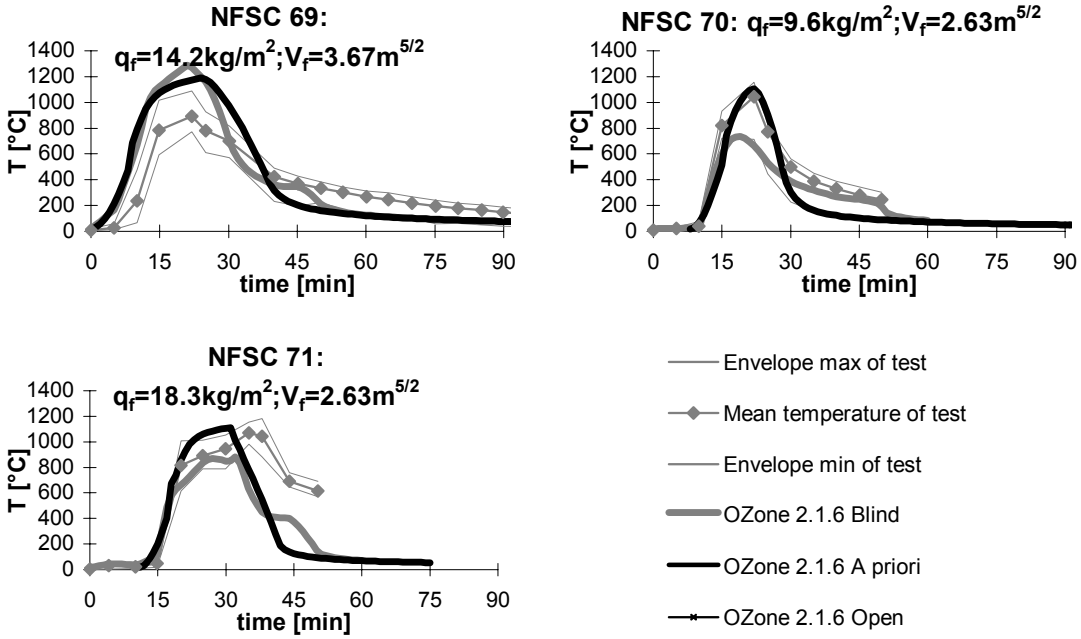

Figure 6.32 Hotel rooms, blind and a pri

An 'blind' comparison is first done. The mass loss rate is calculated by deriving the mass measurements and is introduced in the simulation. The “external flaming” combustion model is activated. The net combustion heat of fuel and the combustion efficiency factor are supposed to be equal to 17.5MJ/kg and 0.8.

An 'a priori' comparison is also made. The design fire that is considered is the Hotel NFSC design fire. It is defined by a medium fire growth rate (t_α = 300 s) and a rate of heat release density of 250 kW/m². The design fire load is the fire load set in the compartment during the tests. Both blind and a priori comparisons give a rather good estimation of the fire course. With this type of fire load, the NFSC design fire curve gives a good estimation of the test temperature history, even with very low fire load.

6.5.4 Fires in school, France, 1996 & 1997

6.5.4.1 Test Data

One test has been performed by CTICM to investigate a fire in a real school building. The fire load is made of wood.

The room has 4 identical windows with a height of 1.41 m and a width of 1.7m and thus having a ventilation factor of 2.85 m$^{5/2}$ each.

Table 6.9 Data summary of the test

Test	D	L	H	W	h_w	A_f	A_t	V	A_w	$A_{t,net}$	Vf	O	q_f	$q_{f,net}$	$q_{f,eff}$
NFSC	*m*	*m*	*m*	*m*	*m*	*m²*	*m²*	*m³*	*m²*	*m²*	*m$^{5/2}$*	*m$^{1/2}$*	*kg/m²*	*MJ/m²*	*MJ/m²*
67	8.95	7	2.5	6.8	1.41	62.20	203.91	155.51	9.588	194.32	11.385	0.059	31.7	554.75	443.8

6.5.4.2 A priori

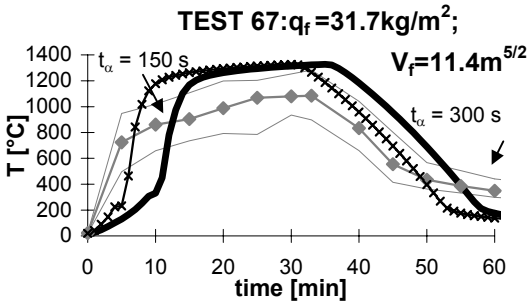

Figure 6.33 Fire in school – A priori comparison with OZone

As no measurement of the fire source is done, an 'a priori' comparison is performed. The design fire that is considered is the School NFSC design fire. It is defined by a medium fire growth rate (t_α = 300 s) and a rate of heat release density of 250 kW/m². The design fire load is the fire load set in the compartment during the tests.

The calculation with OZone gives a too slow growing phase and little too high temperatures of the steady state phase, see Figure 6.33. Modifying the fire growth rate from t_α = 300 s to t_α = 150 s enables to better represent the growing phase. Nevertheless, no conclusion can be raised on the validity of the NFSC design fire on this situation as the fire load is not representative of the real occupation of a school.

The OZone prediction is on the safe side on both temperatures and fire duration.

6.5.5 Natural Fire Tests in Large Compartment BRE, UK, 1994

The comparison of OZone with 9 tests performed at Cardington, UK, by the British Steel Technical in collaboration with BRE is presented. The tests were performed in 1993 and described in (Kirby 1994). These tests are in the database of the NFSC1 research (NFSC1 1999) with numbers NFSC7 to NFSC15.

The tests were originally aimed at investigating whether the relationship for time equivalent of fire severity presented in Eurocode 1 can be safely applied to buildings with large compartments.

6.5.5.1 Tests Data

The compartment has a length L_1 of 22.86 m, a width of 5.6m and a height of 2.75m for 7 tests (tests 1 to 6 and 9) and slightly different dimensions for one test (test 8 : some centimetres of difference due to additional lining on partitions). One test (test 7) was performed in a small compartment with a length L_2 of 5.6 m, a width of 5.6m and a height of 2.75m. (Figure 6.34).

For all tests but test 8, the walls and ceiling are made of concrete blocks insulated, on the inside surface, by ceramic fibre blanket. In test 8, an additional layer of fireline plasterboard has been set on the inside surface of partitions. The floor is a concrete slab covered by loose sand.

The thermal properties of partition materials are given in the test report and reported in Table 6.10. The fire load, made of uniformly distributed wood cribs, is either 20 kg of wood/m^2 or 40 kg of wood/m^2. The net combustion heat of wood is reported to be 19MJ/kg.

Vertical openings are made in only one of the short wall. Four tests are made with the wall completely open; Two tests with an opening of half of the front wall surface; two test with one fourth and one test with one eighth.

Thus the compartment is large (about 128m^2 of floor area) and has the particularity to be much longer than larger and to have opening(s) in a single short wall.

In tests 1 to 8, the rear line of wood cribs has been ignited. In test 9, all the wood cribs have been ignited simultaneously. During the tests with the rear line ignition, a flame front with higher temperature than in the rest of the compartment started on the rear of the compartment, went quite quickly to the front and went back slowly to the rear and finally burned out (see Figure 6.35).

This phenomenon is impossible to model with a zone model due to the assumption of uniform temperatures in zones. Nevertheless numerical results should give an estimation of the mean temperature in the overall compartment.

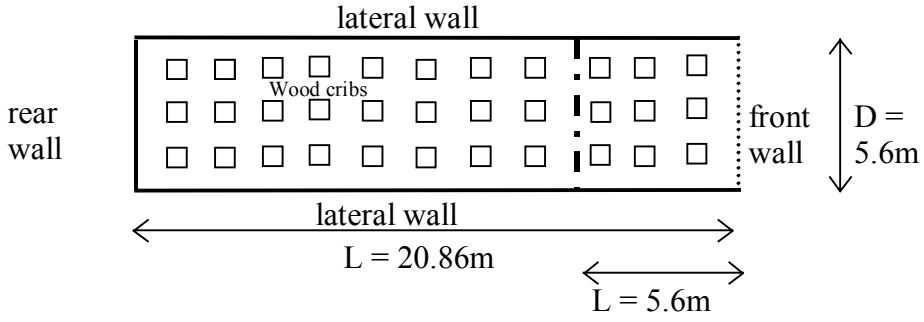

Figure 6.34 Schematic plan view of the compartment

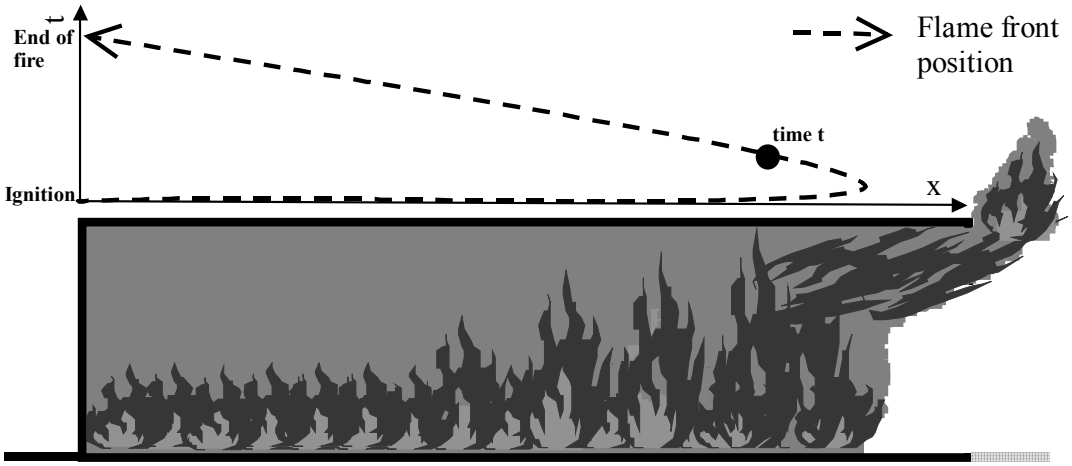

Figure 6.35 Schematic view of the front flame progression in the compartment

Table 6.10 Thermal properties of partition material

material type	**Density** ρ **[kg/m³]**	**Specific heat** c **[J/kg K]**	**Thermal conductivity** λ **[W/m K]**	$b = \sqrt{c \rho \lambda}$
concrete	1375	753	0.42	659
ceramic fibre	128	1130	0.02	54
fireline plasterboard	900	1250	0.24	520
Fluid sand	1750	900	1.0	1255

Table 6.11 Summary of the main data of the tests

Test	D	L	H	A_f	A_t	V	W	h	A_w	$A_{t,net}$	V_f	$V_f/A_{t,net}$	q_f	q_f
n°	m	m	m	m²	m²	m³	m	m	m²	m²	$m^{5/2}$	$m^{1/2}$	kg/m²	MJ/m²
1	5.59	22.855	2.75	127.87	412.22	351.65	5.6	2.75	15.38	396.8	25.515	0.064	40	700
2	5.59	22.855	2.75	127.87	412.22	351.65	5.6	2.75	15.38	396.8	25.515	0.064	20	350
3	5.59	22.855	2.75	127.87	412.22	351.65	5.6	1.47	7.63	404.5	9.261	0.023	20	350
4	5.59	22.855	2.75	127.87	412.22	351.65	5.2	1.47	7.63	404.5	9.261	0.023	40	700
5	5.59	22.855	2.75	127.87	412.22	351.65	2.1	1.73	3.70	408.5	4.869	0.012	20	350
6	5.59	22.855	2.75	127.87	412.22	351.65	5.2	0.375	1.94	410.2	1.193	0.003	20	350
7	5.59	5.595	2.75	31.30	124.15	86.09	1.4	2.75	3.76	120.3	6.248	0.052	20	350
8	5.46	22.78	2.68	124.49	400.38	333.64	5.6	2.68	14.99	385.3	24.547	0.064	20	360.5
9	5.59	22.855	2.75	127.87	412.22	351.65	5.6	2.75	15.38	396.8	25.515	0.064	20	350

6.5.5.2 A priori

The geometry (compartment size and opening dimensions) and the partitions characteristics are defined as described in the tests report. The net combustion heat of wood is set to 17.5MJ/kg with a combustion efficiency factor of 0.8, both values are the default values in the code. The extended fire duration combustion model is used. The discharge coefficient C_f is 0.7 (this value has in fact been used in all other tests). The flashover temperature T_{fl} is 500°C. These values are the default ones in OZone.

To define the NFSC design fire curve, the following parameter are taken:

- the real fire load;
- a fast fire growth rate (1MW after 150s);
- the rate of heat release density is equal to 1250 kW/m², which is the value proposed in NFSC for stacked wood pallets of height 0.5m.

Observing the "a priory" comparison results, Figure 6.36, it can be noticed that :

- During the rising phase, a fast fire gives a good correlation for 5 of the 9 tests (n°1, 4, 5, 6 and 7); a reasonable correlation for 2 tests (n°2 and 9) and a poor correlation for 2 tests (n°3 and 8).
- The calculated temperatures and fire durations are really close to the measured ones, in case of opening area equal to one fourths and one eights of the front wall area. This comparison is very good as well in terms of maximum temperature as in term of fire duration.
- The calculated temperature are too high for test with a large opening. The prediction is nevertheless acceptable for opening area equal to the half of the front wall area but is unacceptable with the front wall completely open.
- When the temperatures are too high, the fire duration is too short.

In summary, the calculations give very good estimation of the mean temperature histories for opening areas up to the half of the front wall area (i.e. a ventilation factor of 9.3 $m^{5/2}$). For higher opening area, the code is not able to predict the fire course.

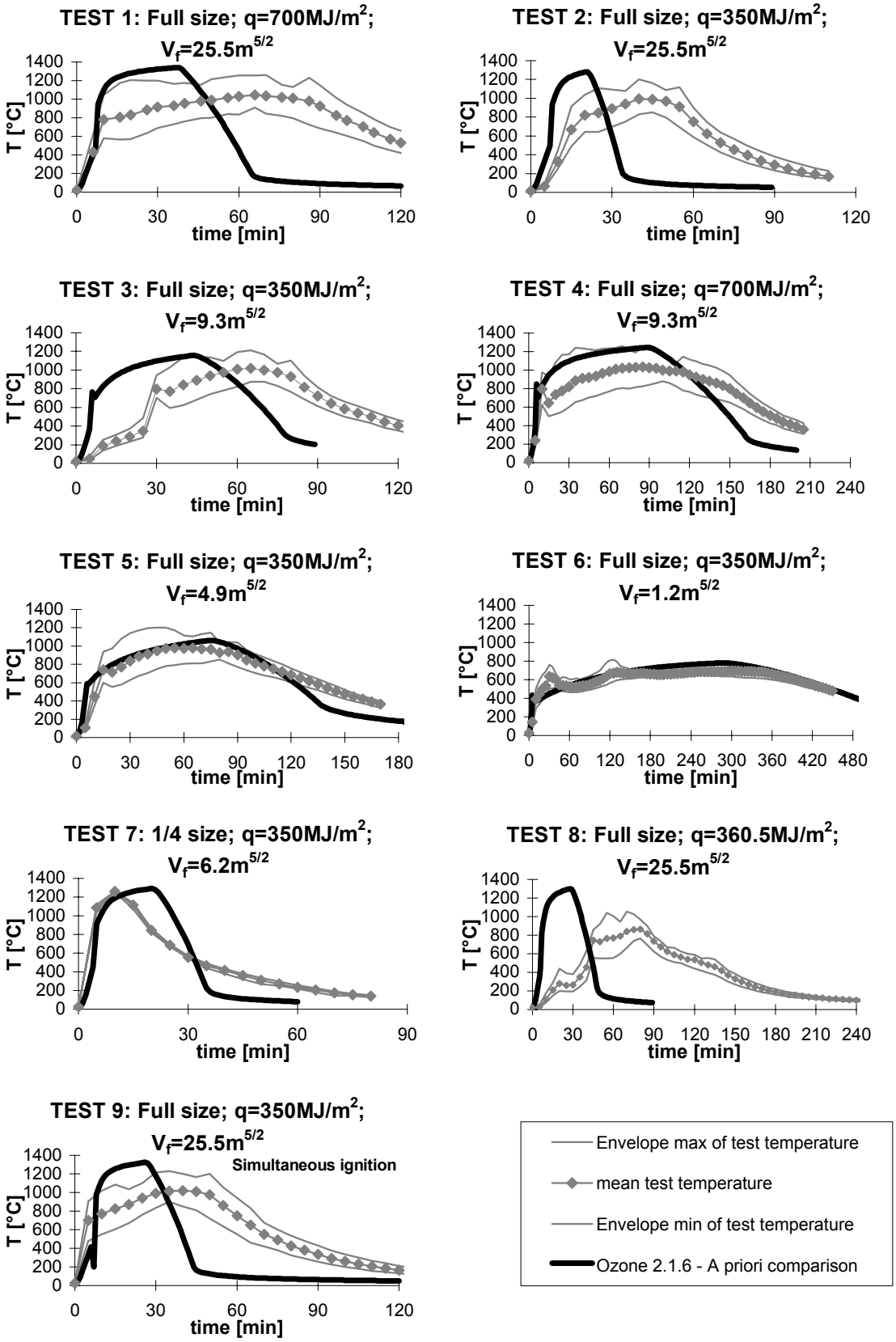

Figure 6.36 "A priori" comparison of temperatures histories

6.5.5.3 Open

In test 3, although the rising phase is not well modelled, the post-flashover phase modelling is quite good. Thus the calculation is improved by setting t_α to 900s (ultra slow), all other parameters being unchanged.

In test 1, the fire duration is too short, thus the heat release rate is set in the data so that the fire duration is the one obtained during the test. The end of the plateau is defined to be at 76min. That leads to a maximum heat release of 14.5MW. In other words, the fire load was burned in the "a priori" procedure in 65min, in this procedure it is imposed to burn the fire load slower, i.e. in 136min, see Figure 6.38.

The calculated temperatures obtained with this RHR are too low. That means that the cooling of the gas in the compartment by the gas flow through the vent is overestimated. The discharge coefficient C_f is thus reduced from 0.7 to 0.45. Leading to a very good estimation of the fire course.

The other open simulations (tests 2, 8 and 9) are made with the modified parameters obtained in test 1, i.e. a maximum RHR of 14.5MW and a reduced value of C_f of 0.45. In these 3 tests, the rising phase is also modified: t_α is set to 300s for tests 2, to 900s for test 8 and to 75s for tests 9. The results (Figure 6.37) are quite good for the five tests.

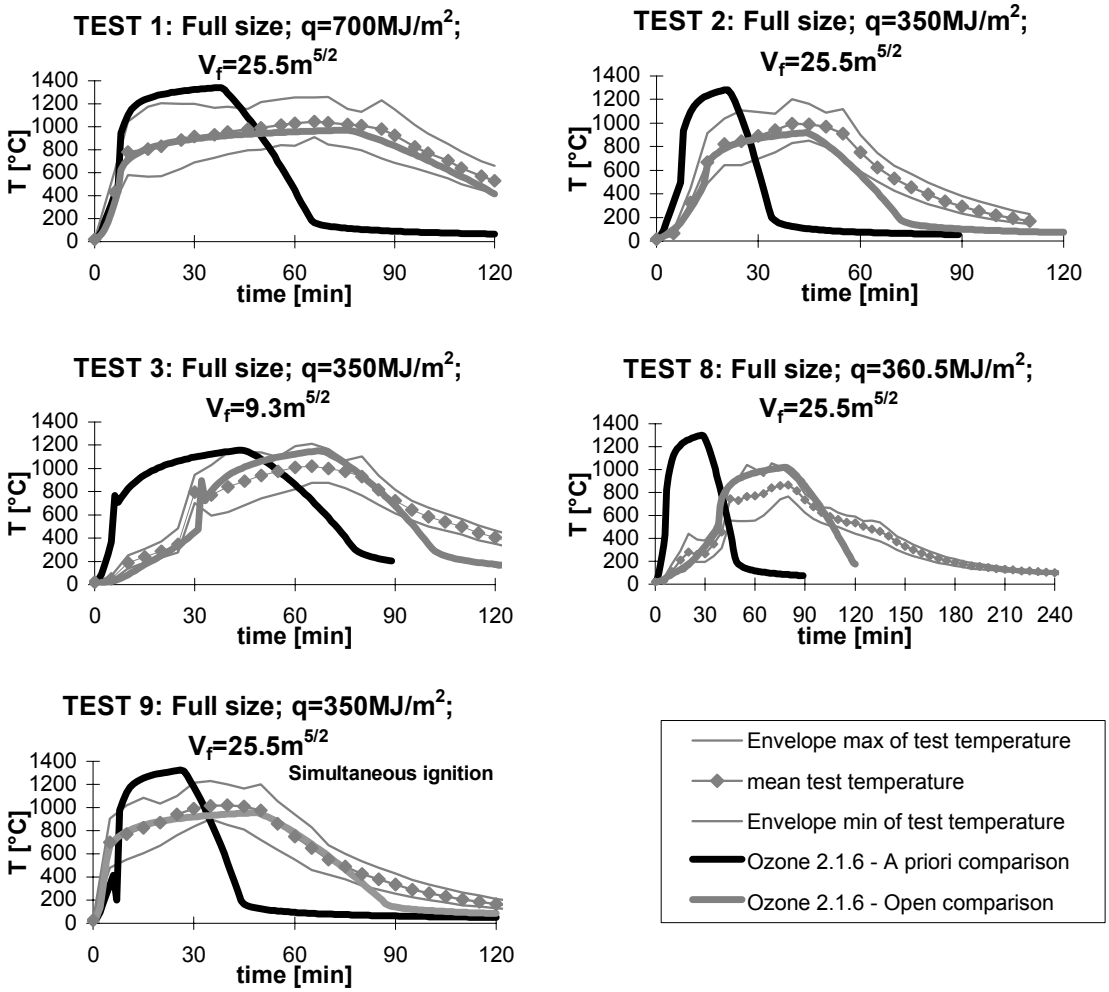

Figure 6.37 "Open" comparison of temperatures histories

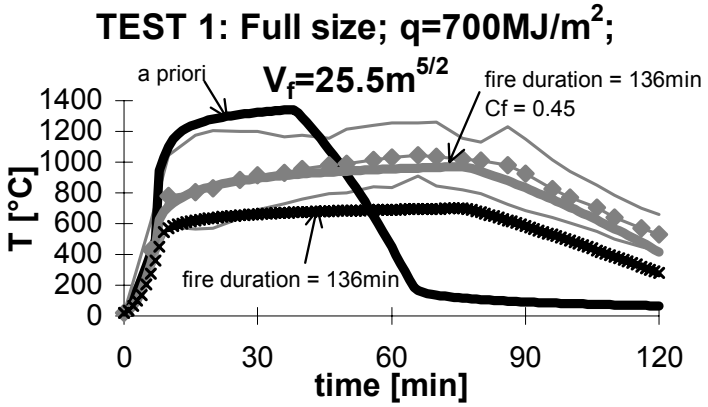

Figure 6.38 Modification of the fire duration and of the discharge coefficient to improve the modelisation of test 1

6.5.5.4 Rate of Heat Release

The rates of heat release set in the data and computed by the code for the 'a priori' simulation of test n°5 are shown on Figure 6.39. As the rate of heat release density is set to 1250 kW/m² and the maximum fire area is equal to 80 m^2, the maximum RHR set in the data is about 62 MW (the plateau of the NFSC design fire curve is in fact not reached) while the maximum RHR computed is about 6 MW. It is here evident that the external flaming combustion model would have been unrealistic and unsafe, giving a too short fire and overestimating the external flaming. With this model the fire would have finished after 22 min. This comparison shows that the extended fire duration combustion model must be used in design procedure. This combustion model is based on the hypothesis that the incoming air flow limits the rate of mass loss (cf. chapter 4).

Table 6.12 is a summary of the rate of heat release calculated in the 'a priori' comparison and set in the 'open' one for the 9 tests. Figure 6.42 (giving the same information that Table 6.12 on a graphical form) is a plot of the heat release rates function of the ventilation factors of the different tests.

A linear regression, Eq. (6.9) on the 'a priori' RHR value function of the ventilation factor shows a very good correlation of these two parameters.

$$RHR \approx 1.1\, A_w \sqrt{h_w} \qquad [MW] \tag{6.9}$$

Considering an effective combustion heat of 14MJ/kg, Eq. (6.9) can be transformed into Eq. (6.10).

$$\dot{m}_f = \frac{RHR}{H_{c,eff}} = \frac{1.1 A_w \sqrt{h_w}}{14} = 0.08 A_w \sqrt{h_w} \qquad [kg/s] \tag{6.10}$$

The Kawagoe law, Eq.(6.11), obtained from tests measurements, links the mass loss rate and the ventilation factor:

$$\dot{m}_{fi} \approx 0.09\, A_w \sqrt{h_w} \qquad [kg/s] \tag{6.11}$$

A remarkable agreement is found between OZone's results and Kawagoe's correlation.

Drysdale (1999) reports that a similar agreement can be found by using a simple analytical model to determine the air inflow in a compartment and using an overall chemical reaction similar to the one considered in OZone. The fact that the rate of burning is directly coupled to the air inflow is surprising. This agreement (Drysdale 1999) is thought to be fortuitous and only be valid in case of wood cribs fires, in which the burning surfaces are largely shielded from radiative heat feed back from surroundings which is known to have an important influence on burning rate.

In the particular condition of this test series, it is probable that another phenomenon is also present: The quantity of combustible gases produced by pyrolysis can be higher than the one predicted by Eq.(6.11). This correlation gives only the part of it involved in the combustion process, the compartment atmosphere is thus rich in fuel vapour. Moreover only a low quantity of combustible gases is going out through the opening, leading to few external flaming.

Table 6.12 Heat release rate obtained from the a priori comparison and set in the open comparison

Test n°	V_f	O	q_f	*RHR 'a priori'*	*RHR 'open'*
	$m^{5/2}$	$m^{1/2}$	MJ/m^2	*[MW]*	*[MW]*
1	25.515	0.064	700	28.5	14.5*
2	25.515	0.064	350	29	14.5*
3	9.261	0.023	350	10.5	10.5
4	9.261	0.023	700	11	11
5	4.869	0.012	350	6	6
6	1.193	0.003	350	1.5	1.5
7	6.248	0.052	350	7	7
8	24.547	0.064	360.5	25	14.5*
9	25.515	0.064	350	28.5	14.5*

* values set in the data

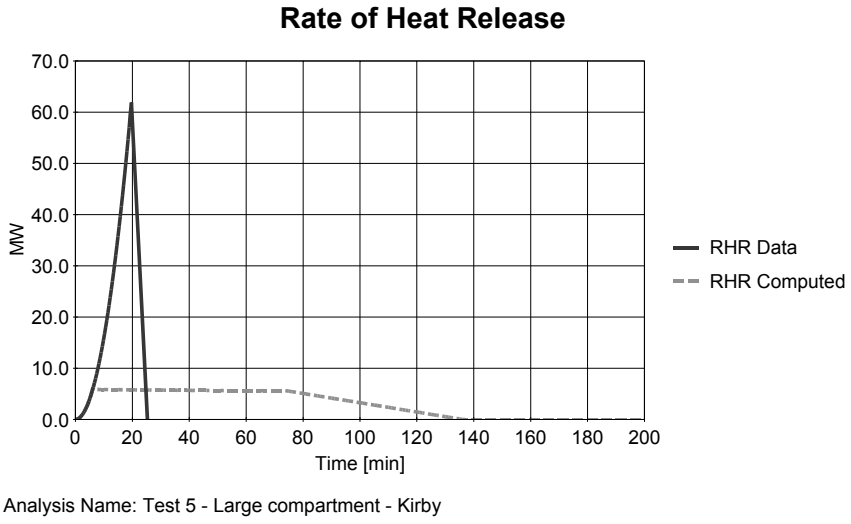

Figure 6.39 Heat release rate set in the data and calculated

Figure 6.40 Natural Fire Tests in Large Compartment BRE, UK, 1994 - Test 6
V_f =1.2m$^{5/2}$ – q_f = 350 MJ/m^2

Figure 6.41 Natural Fire Tests in Large Compartment BRE, UK, 1994 - Test 2
V_f =25.5m$^{5/2}$ – q_f = 350 MJ/m^2

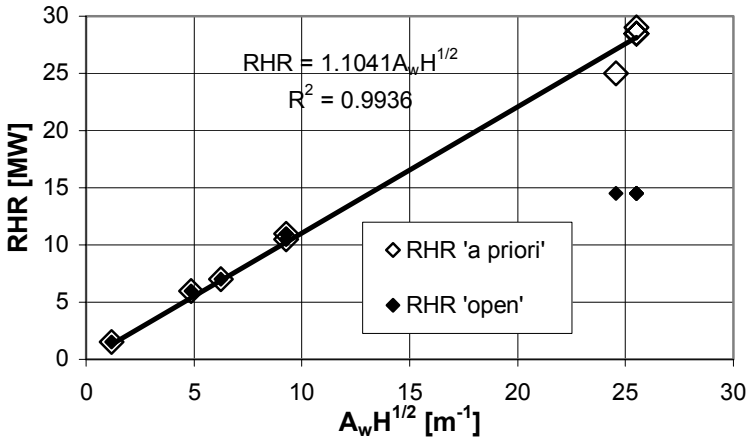

Figure 6.42 Heat release rate function of ventilation factor

6.5.5.5 Conclusion

The results obtained with the open simulation are quite good but show that the rising phase and the mass exchange through a large vertical vent may be difficult to model.

No reason are stated in the test report for having different rising phase during the different tests, except test 9 during which a simultaneous ignition of the wood cribs has been made. There is thus a big variability of the growing phase from one test to another and it is very difficult to be predict it as the parameters that affect it are not well identified.

The procedure used to improve the simulation results shows that the vertical vent model implemented in OZone is not applicable to very large opening. With this model it can be observed that the neutral level is nearly systematically at about the third of the total height of the opening. Looking on the picture taken during the tests 2 (Figure 6.41) coming from the test report, it is clear that the neutral level is much higher than 1/3 of the opening height (while it is the case on test 6, Figure 6.40). It is probable that some cold air is going out of the compartment as shown on Figure 6.43. A part of the cold gases coming in the compartment goes directly out without any mixing with the inside gases.

The tests with opening area up to the half of the front wall area were clearly ventilation controlled. The other tests are probably also ventilation controlled but the influence of the geometry is high.

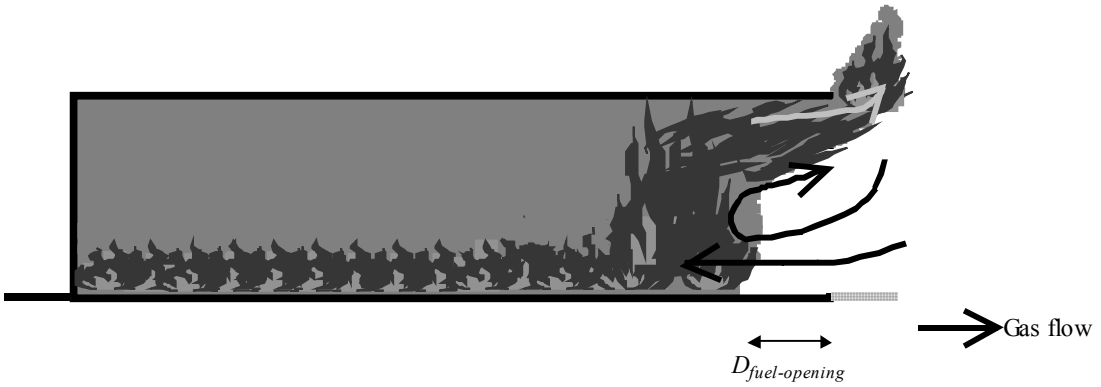

Figure 6.43 Schematic view of the gas flow through the opening

6.5.5.6 Design proposal

In this test configuration, the application of the simple rule of Eq. (6.12) give satisfactory results for the four tests with an opening area equal to the front wall area. The rule limit the height of large opening to the half of the height of the compartment. This fully empirical formula has to be confirmed/improved with other tests. Among other things, the distance between the fuel and the opening ($D_{fuel\text{-}opening}$ on Figure 6.43) should influence this phenomenon.

$$If \;\; V_f \geq 9.3m^{5/2} \;\; then \;\; h_{w,model} = min(h_w, \frac{1}{2}H) \tag{6.12}$$

Figure 6.44 present the simulation of test 1 with the application of the rule of Eq. (6.12). The results the application of this rule on tests 2, 8 and 9 are not presented here but are comparable to the one of test 1.

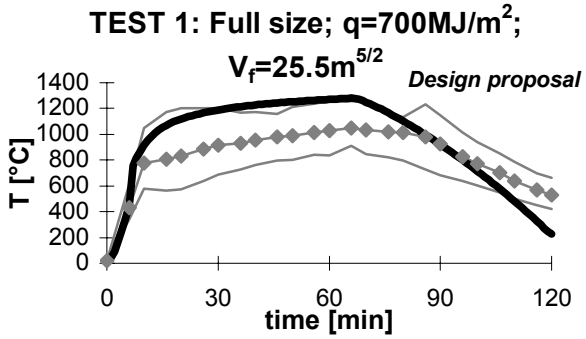

Figure 6.44 Application of the design proposal to test 1.

6.6 Conclusions

Localised fires

The comparison of OZone with the three localised fire tests series (DSTV, VTT Hall and VTT Room) shows that:

- The upper layer temperatures are well estimated with OZone for DSTV and VTT Hall test series. They are underestimated of about 20% in VTT room test series but the correlation between measured and calculated temperatures is very good; a possible reason of it is that the real thermal properties of partitions are probably lower than the one given in the test report.
- The lower layer temperatures are somewhat under-estimated in DSTV tests. This particular point has no consequence on structural safety but might be more important for the safety of people during the evacuation.
- The layer thickness is very well estimated if no horizontal and no forced vents are present.
- If horizontal vents are present in one corner of a room and if they are open, the upper layer thickness is not uniform during the tests and the code tend to under-estimate it (DSTV). More comparisons with tests with horizontal openings in other configurations are needed to verify the horizontal vent model and its implementation in OZone.
- The forced vent model seems to overestimate slightly the extracted mass.

For structural safety, the two zone model of OZone gives in general a relatively good estimation of the environment conditions in a compartment with a localised fire .

If the goal of the design is the estimation of the safe egress time, OZone gives a very good estimation of the layer thickness if no horizontal and no forced vents are present. If there are horizontal or forced vents, a more advanced calculation should be recommended if the safety margin is quite small, for example if a clear smoke-free height of 2 m is needed, a design leading to a calculated free layer of 4 m could be accepted while 2.1 m should lead the designer to make further studies.

Fully developed fires

Comparisons with tests in small to large compartments have shown that the partition model gives a very good estimation of the heat exchange to partitions. The vertical vent model predicts the vent flows with a good agreement for openings with a ventilation factor up to 9 $m^{5/2}$.

If the pyrolysis rate has been measured, the "external flaming" combustion model enables a good prediction of the fire course to be made. For a ventilation factor of 1$m^{5/2}$, this combustion model is not appropriate but if the rate of heat release is defined to be equal to the mass loss rate multiplied by the effective combustion heat (predetermined combustion model) the prediction becomes quite good.

When the pyrolysis rate is not known or ignored (a priori comparison), the NFSC design fire give safe results if the fire is ventilation controlled for wood and typical fire load of hotel rooms. For large opening, leading to the fuel controlled fires, the uncertainty on the fire source definition is quite high. In particular, the rate of heat release density has a strong influence on the temperatures and very few information on it can be found in the literature.

For furniture and papers fires in a small compartment, a double t^2 design fire (see chapter 2 section 2.4.4.4) should be better than the NFSC design fire shape. Nevertheless the NFSC design fire gives safe results in all but one test.

The comparison with the large compartment series shows that the design procedure, i.e. the NFSC design fire combined to the transition criteria (see chapter 5), implemented in OZone is very good for ventilation factor up to 9.3$m^{5/2}$. For higher ventilation factor, OZone is not able to give a good prediction of the fire course because the vent model is deficient in this domain. A design rule is proposed. This rule must be confirmed/improved.

The comparisons between the numerical compartment fire model and full scale fire tests presented in this chapter show that the model has the potential to predict the course of compartment fires. More research is nevertheless needed to better understand the flow behaviour in large openings. Such study would be of primary importance as there is the strong tendency at present time to make buildings with very large openings.

The NFSC design fire, considered in this work, is appropriate for modelling ventilation controlled fires. For fuel controlled fires, the definition of the design fire is quite difficult as data for fully-developed fire that are fuel controlled are scarce. The improvement of the knowledge of such fires, that would include experimental research work, would be valuable for the safety in case of building fires.

It should also be of primary interest to perform experimental research in large deep compartment with large openings such as the one presented in section 6.5.5 but using more realistic fire load such as real office fire load instead of wood cribs.

7

Proposal for a new parametric fire model

7.1 Introduction

Although the new parametric fire curves proposed in the last edition of the Eurocode 1 EN1991-1-2 (2002) show a fairly good ability to predict the fire course obtained in a large series of full scale fire tests, additional research work, presented in this chapter, has been done to build a new parametric fire model. The main reason is that it appears that the formulation chosen in the EC1 method is not appropriate to all situations.

Other comments on the parametric fire curves of Eurocode 1 presented in the conclusions of chapter 3 also lead to propose a new method:

- The Eurocode method has been build by fitting equations on numerical simulations made by a zone model and by additional improvements, some being based on theoretical developments but others being fully empirical. As a consequence, the formulation of the method is questionable.
- There is no pre-flashover phase.
- The method gives temperatures which always tend to 1350°C when t tends to infinity. This value should depend on the heat release rate and on the compartment characteristics.
- There is only an indirect link to the heat release rate. As a consequence, the method should only be applied for cellulosic fire load. Moreover, the decreasing phase duration is not equal to the heating phase duration which is inconsistent with other hypotheses.
- In general, the hypotheses on which the method is based are not explained.

It is thus proposed to:

- combine a pre- and post-flashover model;
- establish a new parametric fire model on the basis of the design fire (in terms of rate of heat release) developed in the NFSC1 research. This design fire has been presented in chapter 5.
- base the temperature-time curves on solutions of the energy balance derived from the different phases of a compartment fire;
- point out the parameters needed to define the temperature-time curve;
- use the numerical fire model OZone V2 developed in this thesis (see chapters 4 and 5) and extensively compared to full scale fire tests in order to calibrate these parameters of the temperature-time curve;
- define clearly each assumption of the method.

The main difference in the process used to define this new parametric fire model and one used to obtain the Eurocode method is thus that the new one is derived directly from the energy balance of a compartment fire and then calibrated by comparisons with zone model results. On the contrary, the Eurocode method has been obtained on the basis of numerical results obtained from a zone model.

7.2 Principle, basic parameters and shapes of functions

The basic ideas of the method are explained using a simulation made with OZone. The fire source is represented by the NFSC design fire curve. Two typical fire scenarios are modelled, the first one in a compartment with a medium fire load density and the second one in the same compartment with a very high fire load density. The data of the simulation are:

- The compartment is a parallelepiped.
- The floor is 5 m x 4 m. The height is 2.5 m. (inner dimension)
- All partitions are made of lightweight concrete (unit mass: 1500 kg/m³; conductivity: 1 W/mK; specific heat: 840 J/kgK) and are 10 cm thick.
- There is one opening, width : 2 m; height: 2 m
- The fire is defined the NFSC design fire (Figure 1) with the following parameters: $A_{fi,max}$ = 20 m²; t_α = 1000 s; RHR_f = 250 kW/m²; $q_{f,d}$ = 760 MJ/m² or a very high fire load density.

The results of the two OZone simulations with a fire load density of 760MJ/m² and with a very high fire load are presented on Figure 7.1

For the fire load of 760 MJ/m², the *RHR* curve set in the data is reaching a plateau of 5 MW after 37.3 min. The *RHR* plateau ends at 60.7min and the fire at 91.4 min. At 29 min (t_{fl}, see Figure 7.2) the temperature of the gas is 500°C (T_{fl}), the flashover occur and the RHR calculated is thus set to 5 MW, the plateau of the data (RHR_{max}), showing that the fire is not controlled by the ventilation. The maximum temperature (T_{max}) of 944°C occurs at the time of the end of the plateau of the RHR (t_{Tmax} = 58.3 min). The decreasing phase begins at 58.3 min ($t_{dec} = t_{Tmax}$) and the fire ends at 89 min (t_{end}). At the end of the fire, the temperature is 239°C.

If a very high fire load is present, the plateau of the *RHR* is very long and the temperature tends to a steady state temperature (T_{∞}). The steady state temperature is in fact the temperature which occurs in the compartment submitted to a constant rate of heat release during a long time.

The method consists in first calculating the terms defined above, and then drawing the temperature time curve of the three fire phases: the pre-flashover fire curve; the post-flashover fire phase and the decreasing phase, see Figure 7.2. During the pre-flashover fire phase, the gas temperature is assumed to vary with a power function of the time. In the post-flashover phase the gas temperature is assumed to vary according to a negative exponential function of the time. In the decreasing phase, the gas temperature is assumed to be a linear function of the time.

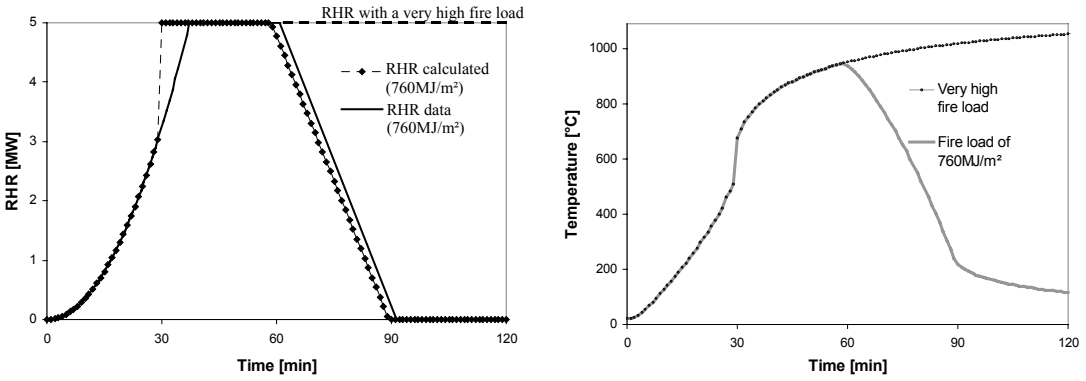

a. Rate of heat release **b. Gas temperature**

Figure 7.1 OZone results

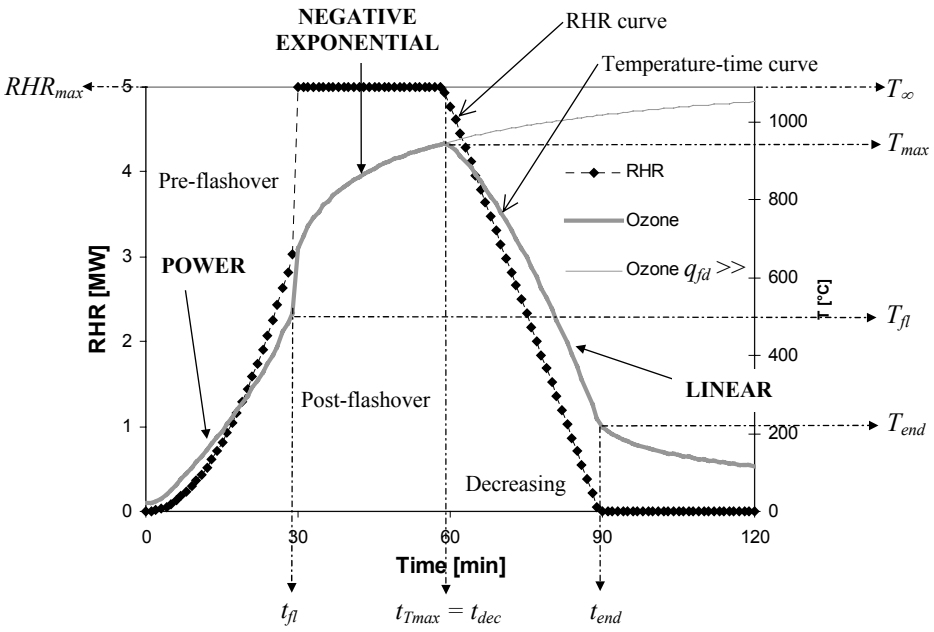

Figure 7.2 OZone results, parameters and shape of functions chosen to represent the fire phases

7.3 Methodology

The methodology used to establish the formula giving the evolution of the temperature in the compartment is the following:

(1) Replace the different terms of the heat balance of the compartment fire by simplified or empirical expressions;
(2) Find the analytical solution of the gas temperature from the simplified energy balance;
(3) Calibrate the formula on numerical results obtained with OZone.

The calibration with OZone is done for two main reasons: the first is that the number of assumptions in OZone is much lower than in the proposed method and the second one is that the numerical code has been validated on a large number of fire tests. This calibration is done through empirical coefficients that have no theoretical justification and which aim is improving the estimation of the fire course.

In the following subsections 7.3.1 to 7.3.4, the energy balance of a compartment fire will first be established, then, simplified analytical solutions for the different terms will be proposed.

7.3.1 Energy balance

The energy balance of a compartment fire can be written as stated in Eq. (7.1). This equation express the fact that, at each instant, the energy released by the fire (*RHR*) is equal to the energy transmitted to the partitions by conduction ($\dot{q}_p$), plus the energy transmitted by convection ($\dot{q}_{v,c}$) and radiation ($\dot{q}_{v,r}$) through the openings, plus the energy used to heat the gas in the compartment ($\dot{q}_g$). The control volume is the upper layer for the pre-flashover phase and the whole compartment for the post-flashover phase.

$$RHR - \left(\dot{q}_p + \dot{q}_{v,c} + \dot{q}_{v,r} + \dot{q}_g \right) = 0 \tag{7.1}$$

The energy used to heat the gas is very small and may thus be neglected. The quantity of energy transmitted by radiation through the openings should be low for small openings size, it may be higher for larger openings but should stay lower than the other losses (convection through vent and conduction through walls) and is therefore neglected. Neglecting these two terms, the simplified energy balance can be written as stated in Eq. (7.2).

$$RHR - \left(\dot{q}_p + \dot{q}_{v,c} \right) = 0 \tag{7.2}$$

The method is based on the solution of the simplified energy balance of Eq. (7.2). For the different fire phases, this equation can be solved analytically under some assumptions related to the assessment of the different terms.

7.3.2 Heat loss to partition

The general heat conduction equation in a solid with internal heat sources is given by Eq. (7.3) (Hogge 1993, Lienhard and Lienhard, 2003).

$$\lambda_p \nabla^2 T = \rho_p c \frac{\partial T}{\partial t} + \dot{q}_{gen} \tag{7.3}$$

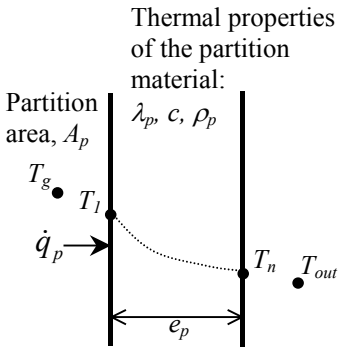

Figure 7.3 A partitions with its boundary conditions and a possible temperature profile

A partition, represented on Figure 7.3, can be considered as a one dimensional system (through the thickness) and thus the general heat conduction equation when no internal heat source ($\dot{q}_{gen} = 0$) is present is

$$\lambda_p \frac{\partial^2 T}{\partial x^2} = \rho_p c \frac{\partial T}{\partial t} \tag{7.4}$$

With some additional assumptions, it is possible to find a first analytical solution of this equation which is adapted to the pre-flashover fire phase and another one which correspond to the post-flashover fire phase.

7.3.2.1 Pre-flashover phase

In the early stage of a fire, the thickness of the partition e_p can be considered as infinite because the heat has not penetrated to the rear face of the partition and the heat loss from the compartment environment by the inner surface to the material is not affected by the heat loss to the rear face, see Figure 7.4.

In this case, it is possible to give an analytical solution of Eq. (7.4) (MacCaffrey et al. 1981, Karlsson and Quintiere 2000, Lienhard and Lienhard 2003) when T_1 and T_n are known. As the partition is considered semi-infinite $T_n = T_{out}$. In the development of the fire T_1 is not known and in order to use the following solution, it is assumed to equal to T_g. If furthermore no internal heat source is present in the partitions, the solution of the general heat conduction equation for this particular situation is the one described by Figure 7.4 and given by Eq. (7.5).

$$\dot{q}_p = \sqrt{\frac{c\rho_p\lambda_p}{\pi t}} A_p \left(T_g - T_{out}\right) = \frac{b}{\sqrt{\pi t}} A_p \left(T_g - T_{out}\right) \tag{7.5}$$

Eq. (7.5) will be considered valid for the early stage of a fire, i.e. the pre-flashover phase.

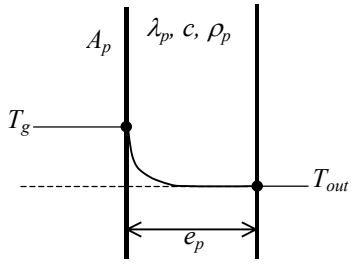

Figure 7.4 Assumed temperature distribution in the partition for the pre-flashover phase

In a first step, even if in the pre-flashover phase the control volume is the upper layer the total area of the partitions (ceiling, walls and floor, excluding openings) A_p is considered. This assumption will be discussed when comparing the formula to OZone simulations.

7.3.2.2 Post-flashover phase

For the post-flashover fire phase, the hypothesis on the field of temperature in the partitions is different than in the pre-flashover phase. In this situation, the temperature are assumed to vary linearly between the two surfaces of the partitions, see Figure 7.5. Here also, the temperature of the partition surface will be assumed to be equal to the surrounding gas temperature.

For a one dimensional partition of thickness e_p and of area A_p with no internal heat source, with constant thermal properties, with a linear temperature field, and with surface temperature equal to the surrounding gas temperature, the solution of heat conduction equation is given by Eq. (7.6).

$$\dot{q}_p = \frac{1}{2} e_p c \rho_p A_p \frac{\partial \left(T_g - T_{out} \right)}{\partial t} + \frac{\lambda_p}{e_p} A_p \left(T_g - T_{out} \right) \tag{7.6}$$

Eq. (7.6) is in fact the heat balance of the partition. This equation states that at each time the heat which comes into the partition through the inner surface is on one hand stored in the partition (first term of the right hand of Eq. (7.6) represented by the grey triangle on Figure 7.5b) and on the other hand transferred through the partition by conduction (second term of the right hand of Eq. (7.6)).

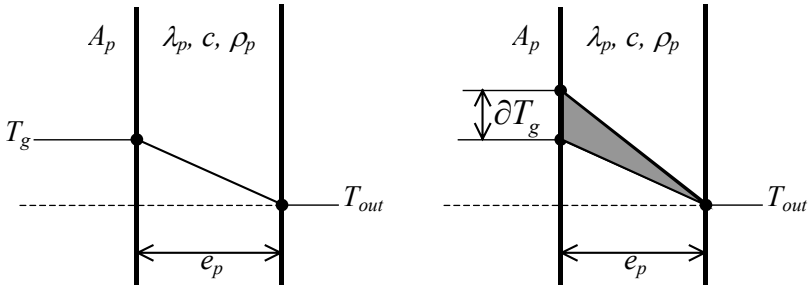

a. at time *t* **b. at time *t*+δt**

Figure 7.5 Assumed temperature distribution in the partition for post-flashover phase.

7.3.3 Heat loss through openings

The mass flow through openings can be estimated by the simple relationship given by Eq. (7.7). This relation is a well-known empirical relationship the validity of which can been shown on theoretical bases (Karlsson and Quintiere 2000, chapter 2).

$$\dot{m}_{VV} = 0.5\, V_f \tag{7.7}$$

The heat transfer by convection through the opening is then given by Eq. (7.8).

$$\dot{q}_{v,c} = \dot{m}_{VV}\, c_p\, T_g - \dot{m}_{VV}\, c_p T_{out} = \dot{m}_{VV} c_p \left(T_g - T_{out} \right) = 0.5\, V_f c_p \left(T_g - T_{out} \right) \tag{7.8}$$

It should be noted that even if this equation is related to post-flashover fires, it will be applied here to both pre- and post-flashover fire phases.

7.3.4 Rate of heat release

The NFSC design fire is considered. The initial design rate of heat release curve is defined by t_α , RHR_{max}, $A_{fi,max}$ and $q_{f,d}$ as shown on Figure 7.6. The reader is invited to refer to Chapter 5, section 5.4.2 to examine the complete methodology of building NFSC design fires.

The rising phase is defined by Eq. (7.9).

$$RHR = 10^6 \left(\frac{t}{t_\alpha} \right)^2 \tag{7.9}$$

The plateau in fuel controlled conditions is defined by Eq. (7.10).

$$RHR_{max} = RHR_{fi} \, A_{fi,max} \tag{7.10}$$

The decreasing phase is linear and begins when 70% of the total fire load is consumed in fuel controlled conditions.

If flashover occurs, the initial rate of heat release curve is modified. At flashover time, the curve goes to a plateau. This plateau is either the initial plateau, defined by Eq. (7.10), or a new plateau, defined by the ventilation condition, Eq. (7.11).

$$RHR_{max} = 0.09 H_{c,eff} A_w \sqrt{h_w} = 0.09 H_{c,eff} V_f \tag{7.11}$$

The linear decreasing phase begins also when 70% of the total fire load is consumed.

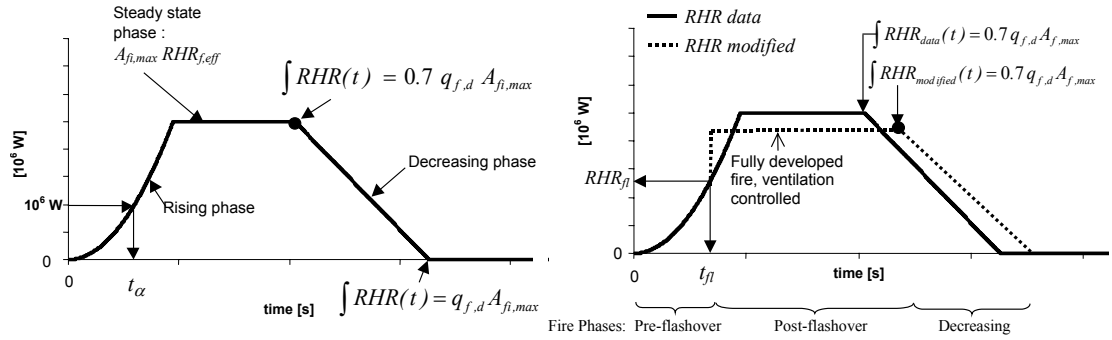

a. Input **b. modified if flashover and ventilation controlled**

Figure 7.6 RHR considered in the model

7.4 Flashover time and pre flashover phase

7.4.1 Estimation of the time of flashover occurrence

Considering the simplified energy balance of Eq. (7.2), and the estimation of energy transmitted to partitions for the early stages of a fire given by Eq. (7.5) and through openings Eq. (7.8), and considering that the RHR is varying with the time squared, Eq. (7.12) can be written:

$$10^6 \left(\frac{t}{t_\alpha} \right)^2 = \frac{b}{\sqrt{\pi t}} A_p \left(T_g - T_{out} \right) + 0.5 c_p V_f \left(T_g - T_{out} \right) \tag{7.12}$$

This equation is assumed to be valid during the entire duration of the pre flashover phase i.e. from ignition until flashover.

If flashover is assumed to occur when T_g is equal to 500°C and if the ambient temperature is equal to 20°C, at flashover time Eq. (7.12) becomes Eq. (7.13).

$$\left(\frac{t}{t_\alpha}\right)^2 = (500-20)\,10^{-6}\left(\frac{b}{\sqrt{\pi t}}A_p + 0.5 c_p V_f\right) \tag{7.13}$$

The time of flashover occurrence t_{fl} is thus given by Eq. (7.14)

$$t_{fl} = 22\,10^{-3}\left(\frac{b}{\sqrt{\pi t_{fl}}}A_p + 0.5 c_p V_f\right)^{\frac{1}{2}} t_\alpha \tag{7.14}$$

This equation has to be solved iteratively. Beginning with t_{fl} equal to t_α, 3 or 4 iterations are generally sufficient to get the convergence.

7.4.2 Calibration of t_{fl} formula on OZone results

The time at which flashover occurs has been calculated by OZone for 200 compartment fires, varying the geometry of the compartment, the thermal properties of the boundaries and t_α within the discrete value given below.

The geometries of the compartments, Table 7.1, are defined by: H : 2.5 m; B : from 2.5 to 10 m; L : from 4 to 8 m; h_w : from 1 to 2.5 m; W : from 1 to 4 m.

And thus these compartments have: A_f : 10 to 80 m^2; V: 25 to 200 m^3; A_t: 52.5 to 250 m^2; A_p: 51 to 248 m^2; V_f: 1 to 15.8 m$^{5/2}$; O: 0.007 to 0.186 m$^{1/2}$; F_c: 0.007 to 0.211 m$^{1/2}$.

And for each compartment: t_α : 75, 150, 300, 600s and
b: 127, 254, 509, 1017 and 2035 J/m^{2}s$^{1/2}$K

A comparison between the results of OZone simulations and the values given by formula of Eq. (7.14) applied to each of the 200 compartment fires is presented on Figure 7.7a. The relative error calculated with Eq. (7.15) is given on Figure 7.8a in function of OZone results. A good correlation is found but the formula predicts shorter flashover times than those obtained with OZone. The relative error decreases for increasing OZone computed values.

$$relative\ error = \frac{t_{fl}(OZone) - t_{fl}(formula)}{t_{fl}(OZone)} \tag{7.15}$$

As the formula of Eq. (7.14) contains some crude assumptions, the different terms have been multiplied by correction coefficients c_1, c_2, c_3 as stated in Eq. (7.16).

$$t_{fl} = 22\,10^{-3} c_1\left(c_2\frac{b}{\sqrt{\pi t_{fl}}}A_p + c_3 0.5 c_p V_f\right)^{\frac{1}{2}} t_\alpha \tag{7.16}$$

The coefficients have been tuned by trials and errors to improve the correlation between simulation and formula results.

The best correlation is found when the coefficients are set to c_1=1.2; c_2 = 1 and c_3 = 1. The correlation is not improved but the slope of the trend line obtained by linear regression is closer to 1 (Figure 7.7b).

Table 7.1 Geometry of the compartments

7.4.2	H [m]	B [m]	L [m]	A_f [m^2]	W [m]	h_w [m]	V [m^3]	A_t [m^2]	A_w [m^2]	A_p [m^2]	V_f [$m^{5/2}$]	O [$m^{3/2}$]	F_c [$m^{3/2}$]
1	2.5	5	8	40	1	1	100	145	1	144	1.0	0.007	0.007
2	2.5	10	8	80	2	1	200	250	2	248	2.0	0.008	0.008
3	2.5	5	8	40	2	1	100	145	2	143	2.0	0.014	0.014
4	2.5	5	4	20	2	1	50	85	2	83	2.0	0.024	0.024
5	2.5	5	8	40	4	1	100	145	4	141	4.0	0.028	0.028
6	2.5	2.5	4	10	2	1	25	52.5	2	51	2.0	0.038	0.040
7	2.5	5	6	30	4	1.5	75	115	6	109	7.3	0.064	0.067
8	2.5	5	6	30	4	2	75	115	8	107	11.3	0.098	0.106
9	2.5	5	4	20	4	2	50	85	8	77	11.3	0.133	0.147
10	2.5	5	4	20	4	2.5	50	85	10	75	15.8	0.186	0.211

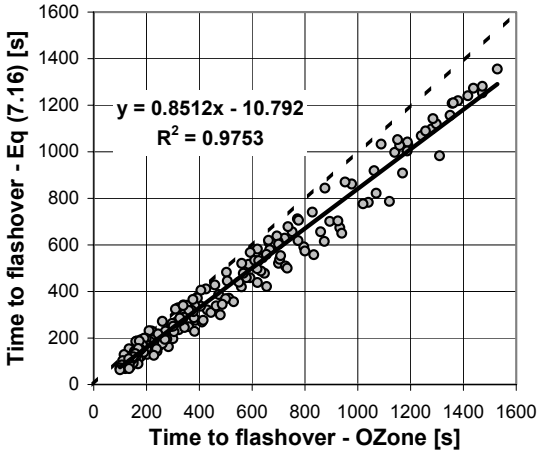

a. uncalibrated formula (c_1= c_2 = c_3 = 1)

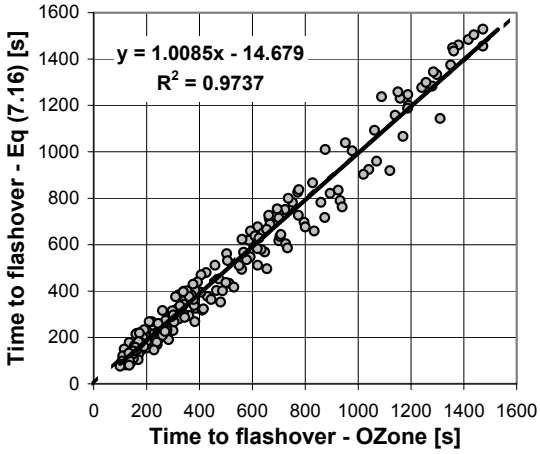

b. calibrated formula (c_1=1.2; c_2 = 1, c_3 = 1)

Figure 7.7 Comparison of t_{fl} obtained with OZone and formula

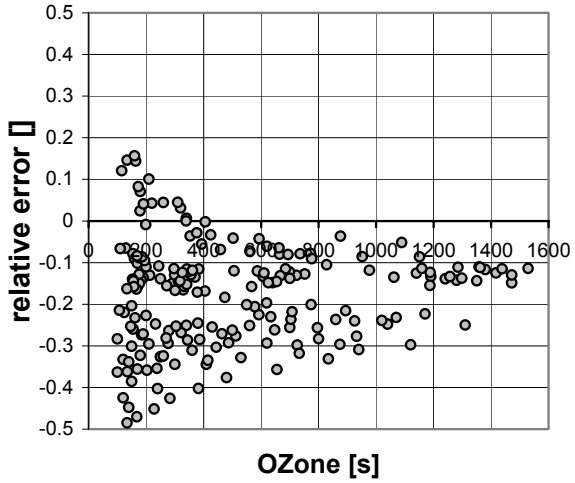

a. uncalibrated formula (c_1= c_2 = c_3 = 1)

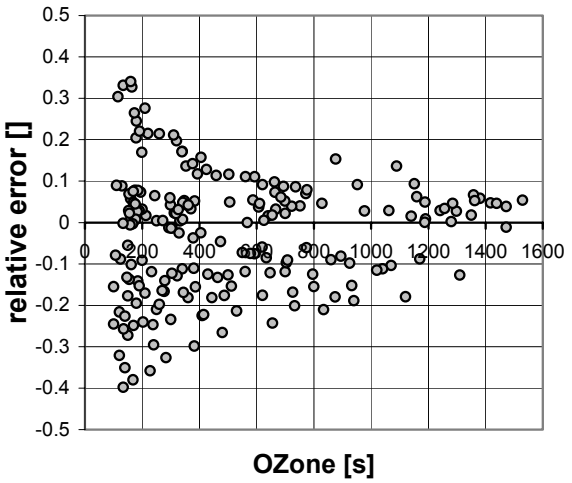

b. calibrated formula (c_1=1.2; c_2 = 1, c_3 = 1)

Figure 7.8 Relative errors on t_{fl}

7.4.3 Additional consideration on partition heat transfer

As written previously, in the heat balance of the pre-flashover phase considered above, the total partition area A_p that includes floor area and the lower part of the wall (but excluding openings) is considered to be involved in the heat transfer process. Nevertheless, during this phase a two

layer phenomena is considered and thus the area of partitions that enclose the upper layer does not include the floor and a lower varying part of the walls. The heat balance can be thus written considering that the floor is excluded from the heat transfer and the time to flashover, Eq. (7.17) , can be obtained as shown previously. The height of the walls that is in the lower layer is unknown and thus the total height is included in the heat balance.

$$t_{fl} = 22\,10^{-3}\left(\frac{b}{\sqrt{\pi t_{fl}}}A_{pu} + 0.5 c_p V_f\right)^{\frac{1}{2}} t_\alpha \tag{7.17}$$

Where A_{pu} is the area of the ceiling and of the walls but excluding the floor and the openings.

Eq. (7.17) is then compared to OZone on the 200 simulations described in section 7.4.2, Figure 7.9. The agreement between the numerical results and the one given by Eq. (7.17) is good but is a little lower than the one obtained with the formula that include the floor area, Eq. (7.14). It is thus proposed to use the total partition area (including floor area) for the evaluation of the pre-flashover fire phase.

It should be noted that, each simulation used in this study has been made with the same material for each partitions. If the floor material is very different than other partitions material, the conclusion raised above might be different. For this situation it is probable that ignoring the floor material in the model and replacing it by the material of other partitions would give better results but this particular point should be further study.

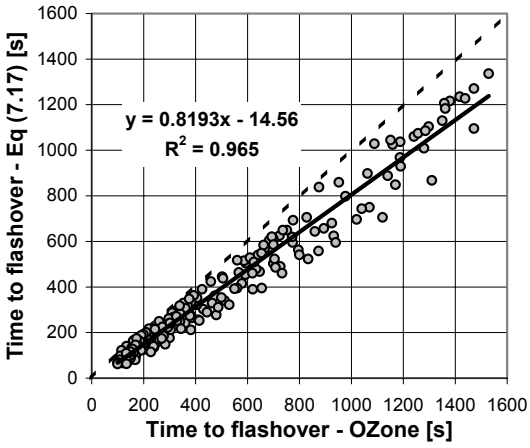

Figure 7.9 Comparison of t_{fl} obtained with OZone and Eq. (7.17) (without floor)

7.4.4 Comparison with McCaffrey & al. (1981) method

The method of McCaffrey et al. (see chapter 4) and the proposed one are very similar. They are both based on the simplified energy balance of a pre-flashover compartment fire. Nevertheless two main differences exist. McCaffrey & al. have chosen to represent the solution by the product of two dimensionless factors and to determine the coefficients of this solution by correlation on fire tests. In the proposed method, the solution is directly obtained from the energy balance equation, without modification of the formulation, and is calibrated on OZone results.

Assuming a t-square fire growth and introducing Eq. (7.9) into the McCaffrey method, it is easy to get the flashover time.

The McCaffrey method has been applied to the 200 compartment fires described above. The comparison between the results obtained by OZone and given by McCaffrey method are shown on Figure 7.10. There is a good agreement between both methods, but the results predicted by McCaffrey method underestimate those obtained by OZone with a mean value of about 22%. These results are comparable with the one obtained by the uncalibrated proposed formula of Eq. (7.14). Nevertheless the relative error is not decreasing with increasing OZone value of t_{fl}, see Figure 7.11. The proposed formula is thus better to predict the bigger value of t_{fl} given by OZone.

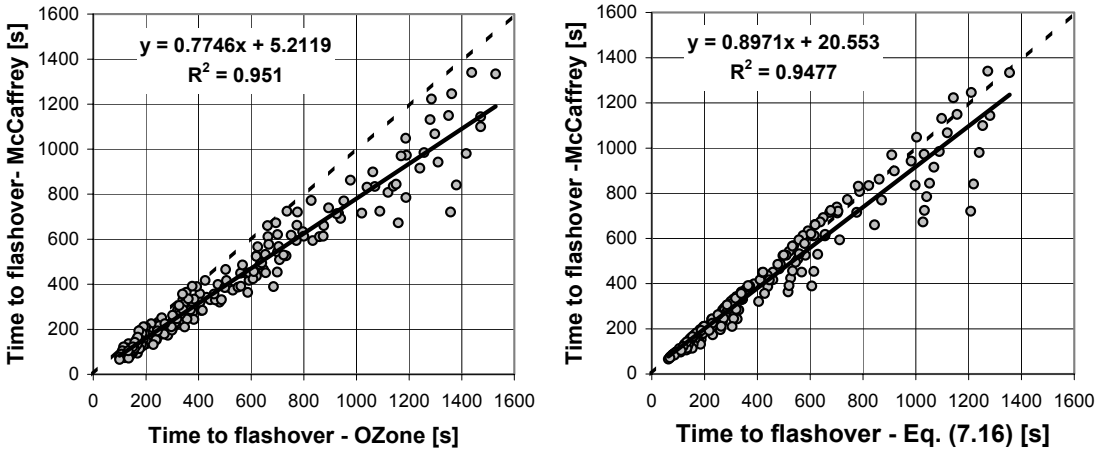

(a) McCaffrey & al. vs. OZone **(b)McCaffrey vs. Uncalibrated formula**

Figure 7.10 Comparison of t_{fl} obtained by two methods

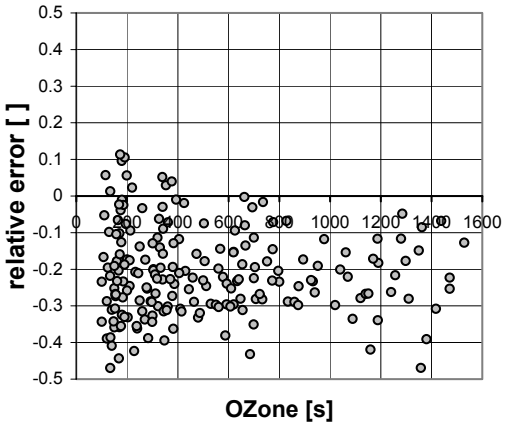

Figure 7.11 Relative errors of McCaffrey & al. formula

7.4.5 Time to flashover

The following relationship is thus proposed for the method, Eq. (7.18).

$$t_{fl} = 22\,10^{-3}\left(\frac{b}{\sqrt{\pi t_{fl}}}A_p + 0.5\,c_p V_f\right)^{\frac{1}{2}} t_\alpha \tag{7.18}$$

It is preferred to use the uncalibrated formula instead of the one calibrated on OZone as the correlation between McCaffrey method, that has been calibrated on full scale fire tests, and this one is good.

7.4.6 Temperature-time curve during the pre-flashover period

The temperature in the pre-flashover phase may be obtained by solving Eq. (7.12) at each time. Few transformations of Eq. (7.12) enable to obtain the gas temperature function of time during the pre-flashover phase, Eq. (7.19).

$$T_g = T_{out} + \frac{10^6 \left(\frac{t}{t_\alpha}\right)^2 \sqrt{\pi t}}{b\, A_p + 0.5\, c_p V_f \sqrt{\pi t}} \tag{7.19}$$

A simpler formulation, Eq. (7.20), is nevertheless preferred because a high precision of the temperature history in the pre-flashover phase is usually not required. As the rate of heat release in the pre-flashover phase is supposed to be proportional to the squared time, a power function has been chosen to represent the temperature time history during this phase. The best agreement with a limited number of numerical results is found with η equal to 1.5, Eq. (7.20).

$$T_{pre}(t) = \left(T_{fl} - T_{ini}\right)\left(\frac{t}{t_{fl}}\right)^{\eta} + T_{ini} = 480\left(\frac{t}{t_{fl}}\right)^{1.5} + 20 \tag{7.20}$$

It is obvious that the value 1.5 for the η factor has to be taken as a first proposal, since it has been obtained by comparison on a limited number of OZone simulation.

7.4.7 Rate of heat release at flashover time

The heat release rate at flashover time, Eq. (7.21), is obtained by replacing t_{fl}, obtained from Eq. (7.18), in Eq. (7.9).

$$RHR_{fl} = 10^6 \left(\frac{t_{fl}}{t_\alpha}\right)^2 = 484 \left(\frac{b}{\sqrt{\pi t_{fl}}} A_p + 0.5\, c_p V_f\right) \tag{7.21}$$

If the design rate of heat release (used as input to the method) does not reach the rate of heat release at flashover time, flashover is not likely to occur.

7.5 Post-flashover fire

The main assumption in the post-flashover phase is that the rate of heat release is constant. Two situations will be considered: a ventilation controlled fire, during which the RHR is proportional to the incoming air and a fuel controlled fire, during which the rate of heat release is proportional to fuel area and not dependent on the ventilation conditions.

7.5.1 Formulation

Introducing Eqs (7.6) and (7.8) into Eq. (7.2) of conservation of energy, the following Eq. (7.22) is found.

$$RHR - \left(\frac{1}{2} e_p c \rho_p A_p \frac{\partial\left(T_g - T_{out}\right)}{\partial t} + \frac{\lambda_p}{e_p} A_p \left(T_g - T_{out}\right)\right) - 0.5\, V_f c_p \left(T_g - T_{out}\right) = 0 \tag{7.22}$$

Which can be written into Eq. (7.23).

$$\frac{1}{2} e_p c \rho_p A_p \frac{\partial(\Delta T)}{\partial t} + \left(\frac{\lambda_p}{e_p} A_p + 0.5\, V_f c_p \right) \Delta T = RHR \tag{7.23}$$

As the form of Eq. (7.23) is identical to a well known equation of electricity, an electrical analogy is used to explain the form of the solution adopted for the formulation of the post-flashover phase of a compartment fire.

A post-flashover fire can be seen to be equivalent to the electrical system of Figure 7.12. The partitions are equivalent to a resistance plus a capacity. The vents are equivalent to a resistance proportional to the inverse of the ventilation factor V_f. The rate of heat release is equivalent to a constant source of electrical current. The electrical potentials are equivalent to the temperatures.

The very simple system is described by the ordinary differential equation of Eq. (7.24).

$$C \frac{\partial V(t)}{\partial t} + \frac{1}{R} V(t) = I \tag{7.24}$$

Where I is equivalent to the rate of heat release for the fire (RHR); R, given by Eq. (7.25), is the resistance equivalent to the partition and vent resistances, r_p and r_V, and C, given by Eq. (7.26), is the thermal capacity of the partitions.

$$\frac{1}{R} = \frac{1}{r_p} + \frac{1}{r_v} = \frac{\lambda_p}{e_p} A_p + 0.5 V_f c_p \tag{7.25}$$

$$C = \frac{1}{2} e_p c \rho_p A_p \tag{7.26}$$

If I does not vary with the time, the solution of Eq. (7.24) is well know and has the form of Eq. (7.27).

$$V(t) = K \left(1 - e^{-\frac{t}{t_c}} \right) \tag{7.27}$$

K is the static gain and t_c is the time constant, given by Eq. (7.28).

$$\begin{aligned} K &= IR \\ t_c &= CR \end{aligned} \tag{7.28}$$

This solution is shown on Figure 7.13 in the particular situation K=1 and T=1.

When considering the thermal response of the compartment submitted to a constant rate of heat release the static gain K is the variation of the temperature of the gas in the compartment after an infinite time, ΔT_∞, given by Eq. (7.29).

$$K = \Delta T_\infty = T_\infty - T_{out} = \frac{RHR}{\frac{\lambda_p}{e_p} A_p + 0.5 V_f c_p} \tag{7.29}$$

If the fire is ventilation controlled, Eq. (7.30) applies.

$$RHR = 0.09 H_{c,eff} A_w \sqrt{h_w} = 0.09 H_{c,eff} V_f \tag{7.30}$$

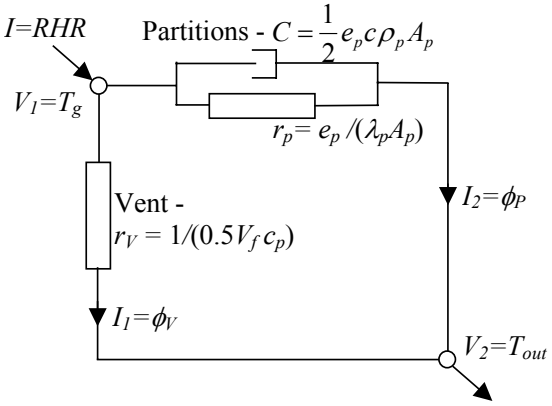

Figure 7.12 Electrical analogy of the post-flashover phase of a compartment fire

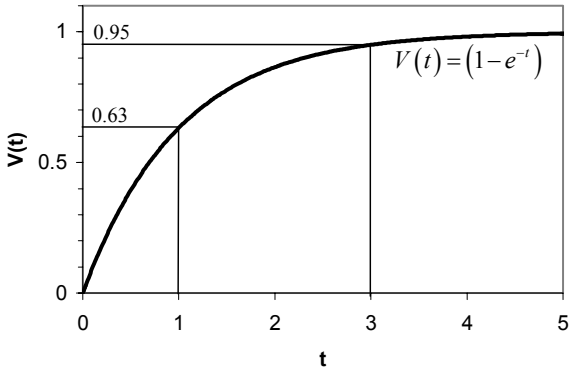

Figure 7.13 Solution of the system for *K*=1 and *T*=1

And then Eq. (7.29) can be transformed into Eq. (7.31).

$$\Delta T_\infty = \frac{0.09 H_{c,eff} V_f}{\frac{\lambda_p}{e_p} A_p + 0.5 V_f c_p} = \frac{0.09 H_{c,eff} F_c}{\frac{\lambda_p}{e_p} + 0.5 c_p F_c} \tag{7.31}$$

In case of cellulosic fire, $H_{c,eff}$ is equal to 14MJ/kg giving Eq. (7.32).

$$\Delta T_\infty = \frac{1.26\,10^6 F_c}{\frac{\lambda_p}{e_p} + 0.5 c_p F_c} \tag{7.32}$$

$F_c = V_f/A_p$ will be called the compartment factor as it is related to the geometry of the compartment, i.e. windows dimensions and area of partitions, excluding windows area. It is prefered to the opening factor $O = V_f/A_t$ because the compartment factor is deduced directly from the energy balance.

t_c is the time constant of the compartment fire, given by Eq. (7.33)

$$t_c = \frac{e_p c \rho_p A_p}{2\left(\frac{\lambda_p}{e_p} A_p + 0.5 V_f c_p\right)} \tag{7.33}$$

The solution of the gas temperature in the compartment in the post-flashover period is obtained according to Eq. (7.34).

$$T_g(t) = T_{out} + (T_\infty - T_{out})\left(1 - e^{-\frac{(t-t_{fl})}{t_c}}\right) \tag{7.34}$$

7.5.2 Calibration of steady state temperatures on OZone

There are three main limitations on the use of Eq. (7.34):

1) the radiation through the openings is neglected.
2) the surface temperatures are not equal to the gas temperature, the effect of the radiation and convection heat transfer at the boundary interface is not negligible;
3) the initial temperature in the compartment is T_{fl}, equal to 500°C, and not T_{out}. At time of flashover, the temperatures inside the partitions are also higher than the ambient temperature;

By comparing Eq. (7.34) with OZone results, it is proposed to:

- introduce of a coefficient C_1, giving a instantaneous temperature rise at flashover time;
- calibrate the steady state temperature T_∞ on OZone results, sections 7.5.2.1 and 7.5.2.2.

Eq. (7.35) is thus proposed to describe the post-flashover fire phase.

$$T_{post}(t) = T_{fl} + (T_\infty - T_{fl})\left(1 - C_1 e^{-\frac{(t-t_{fl})}{t_c}}\right) \tag{7.35}$$

with
$$\begin{aligned} C_1 &= \frac{b}{2035} \quad if \quad 0 \le b \le 2035 \\ C_1 &= 1 \quad if \quad b > 2035 \end{aligned} \tag{7.36}$$

7.5.2.1 Ventilation controlled fires

A comparison of steady state temperatures T_∞ obtained with the formula of Eq. (7.32) for under-ventilated fires has been made with OZone calculations (Figure 7.14a). The compartments are the same as those used for the flashover time formula (section 7.4.2). The ratios of the value obtained with the formula and with OZone are presented in function of the compartment factor on Figure 7.15a. A good correlation is obtained but the formula predicts too low temperatures for small opening size and too high temperatures for large opening size.

The discrepancy appears to be very high for low compartment factors and decreases when the compartment factor increases. This means that the formula gives a bad estimation of OZone results when the heat loss to partition takes a higher importance than the ventilation in the energy balance. In this situation, the predicted temperatures are too low. For higher compartment factors the discrepancy on the predicted temperature is small but temperatures are too high. These analyses lead to calibrate the formula by multiplying the different terms by constants. A good correlation is found for the calibrated formula of Eq. (7.37) with c_1=2/3; c_2=4/3. (See Figure 7.14b and Figure 7.15b)

$$\Delta T_\infty = \frac{1.26\,10^6\, F_c}{c_1 \frac{\lambda_p}{e_p} + c_2 0.5 c_p F_c} \tag{7.37}$$

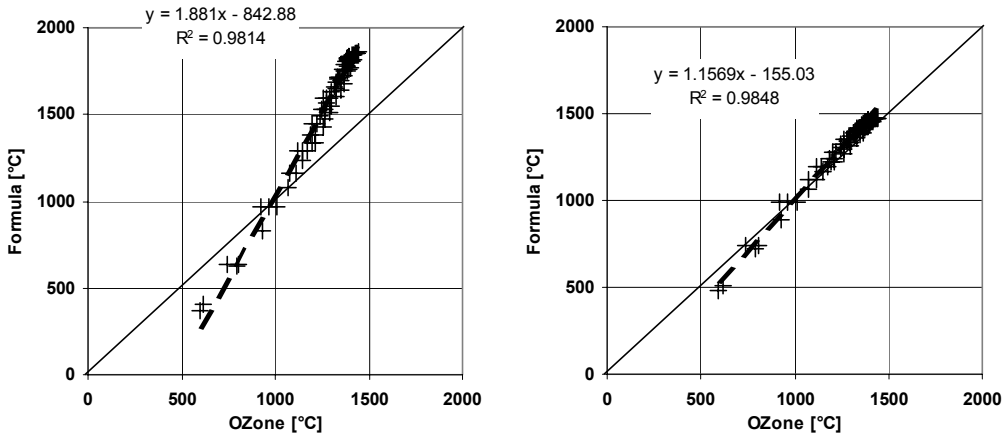

a. Uncalibrated **b. Calibrated (c_1=2/3; c_2=4/3)**

Figure 7.14 Comparison of T_∞ calculated with OZone and with formula of Eq. (7.37)

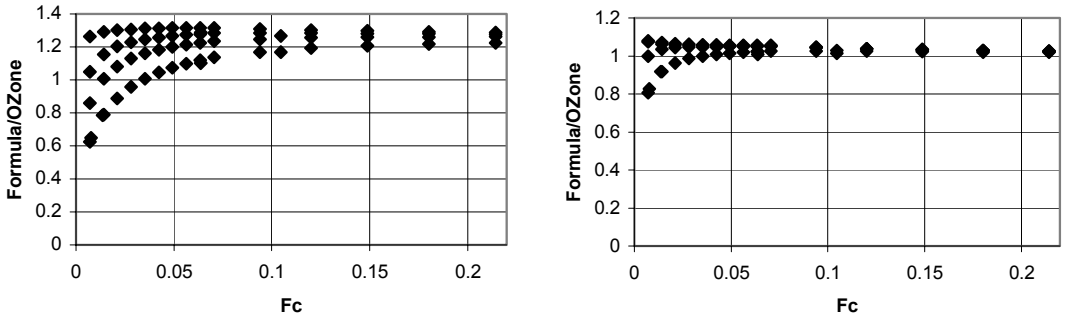

a. Uncalibrated formula of Eq. (7.37) b. Calibrated formula of Eq. (7.37) (c_1=2/3; c_2=4/3)

Figure 7.15 T_∞(Formula)/T_∞(OZone) in function of the compartment factor F_c

7.5.2.2 Fuel controlled fires

In case of fuel bed controlled fires, the steady state temperature is obtained by Eq. (7.38).

$$\Delta T_\infty = \frac{RHR}{\frac{\lambda_p}{e_p} A_p + 0.5 c_p V_f} \tag{7.38}$$

This equation has been compared with OZone results for different compartment and rate of heat release up to 4MW. The compartments are the same (geometry and thermal properties of partitions) as the ones used for the flashover time formula (section 7.4.2). These comparisons are presented on Figure 7.16a.

If the formula is calibrated, Eq. (7.39), by multiplying the different terms by constants, a better correlation (Figure 7.16b) is found with the coefficient c_1=0.8, c_2=0.5 and c_3=1.

$$\Delta T_\infty = \frac{c_1 RHR}{c_2 \frac{\lambda_p}{e_p} A_p + c_3 0.5 c_p V_f} \tag{7.39}$$

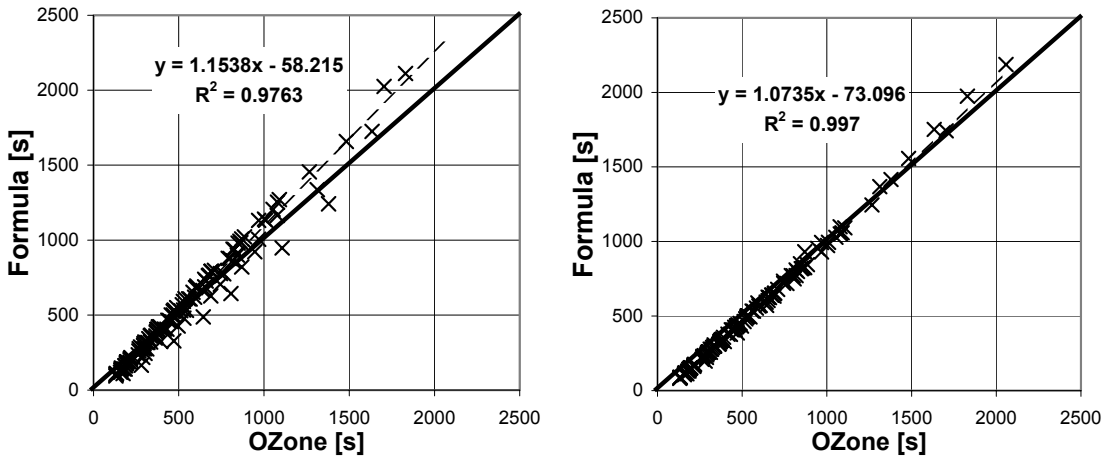

a. Uncalibrated, Eq. (7.38). **b. Calibrated (c_1=0.8; c_2=0.5; c_3=1), Eq. (7.39).**

Figure 7.16 Comparison of T_∞ given by OZone and by the formula in case of fuel controlled fire

7.6 Decreasing phase

In a first approach, Eq. (7.40) is proposed to define the decreasing phase.

$$\Delta T_{end} = T_{end} - T_{out} = \frac{\Delta T_{max}}{\mu} = \frac{\Delta T_{max}}{3} \tag{7.40}$$

As a first proposal, the μ factor has been fixed to 3. It should in fact depend on the characteristics of the compartment.

7.7 Summary of the proposed method

The methodology to build the parametric fire curve proposed here is to

1. Build the NFSC design fire curve for the given situation. - Section 7.3.4.
2. Calculate the time to reach flashover t_{fl} with the proposed formula. - Section 7.4.1.
3. Build the fire curve with the equations for pre flashover phase. - Section 7.4.6.
4. Modify the initial design fire curve as shown on Figure 1. At flashover time, the rate of heat release is leaving the initial t² curve and is going to a plateau. The plateau can be the initial one in case of fuel controlled fire or defined by the ventilation conditions. The decreasing phase is beginning when 70% of the design fire load is burnt. - Sections 7.4.7 and 7.3.4.
5. Calculate the post flashover temperatures until the decreasing phase with formula proposed in section 0.
6. Calculate the temperature at the end of the fire and evaluate the slope of the fire curve during the decreasing phase. - section 7.6.

7.8 Comparison between OZone and the proposed method

The proposed parametric fire method and OZone have been applied to four different compartment fires in order to compare the temperature histories obtained with the two methods.

The first compartment, Figure 8.17, is a parallelepiped with a length of 6 m, a width of 8 m and a height of 5 m. All partitions are made of 10 cm of normal weight concrete (unit mass: 2300kg/m³; conductivity: 1.5 W/mK; specific heat: 900 J/kgK). There is one opening with a

width of 3m and a height of 3m. The fire is defined by the NFSC design fire with the following parameters: $A_{fi,max}$ = 25 m²; t_a = 300 s; RHR_f = 500 kW/m²; $q_{f,d}$ = 608 MJ/m².

The second compartment, Figure 8.18, is identical to the first one, except that the partitions are made of 10cm of gypsum (unit mass: 900 kg/m³; conductivity: 0.25 W/mK; specific heat: 1000 J/kgK).

The third compartment, Figure 8.19, is a parallelepiped with a length of 5 m, a width of 5 m and a height of 2.5 m. All partitions are made of 10 cm of normal weight concrete (unit mass: 2300 kg/m³; conductivity: 1.5 W/mK; specific heat: 900 J/kgK). There is one opening with a width of 2 m and a height of 2 m. The fire is defined by the NFSC design fire with the following parameters: $A_{fi,max}$ = 25m²; t_a = 300 s; RHR_f = 500 kW/m²; $q_{f,d}$ = 1109 MJ/m².

The fourth compartment, Figure 8.20, is identical to the third one, excepted that the partitions are made of 10 cm of gypsum (unit mass: 900 kg/m³; conductivity: 0.25 W/mK; specific heat: 1000 J/kgK).

The results are presented on Figure 8.17 to Figure 8.20. The comparison between the two methods is quite satisfactory. The maximum temperatures are quite well predicted with a maximum difference of 50°C, the time at which the maximum temperature occurs and the duration are comparable (maximum difference of 10%). The temperature histories are similar.

Nevertheless, it should be noted that four examples are not enough to conclude to a good agreement between the two methods and that the formula of the method giving the steady state temperature has been calibrated on OZone simulations. Although other comparisons, not presented here, have been performed by the author, additional cases should be examined.

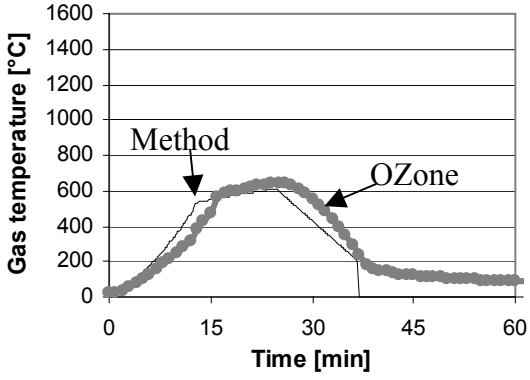

Figure 8.17 Compartment fire n°1

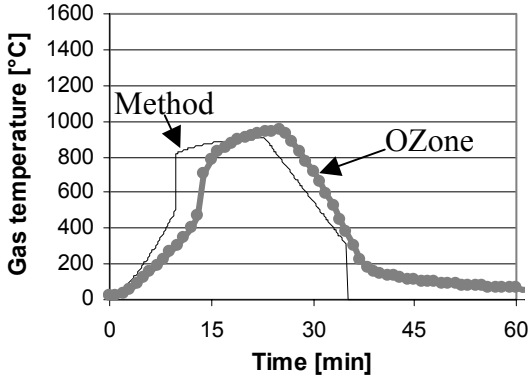

Figure 8.18 Compartment fire n°2

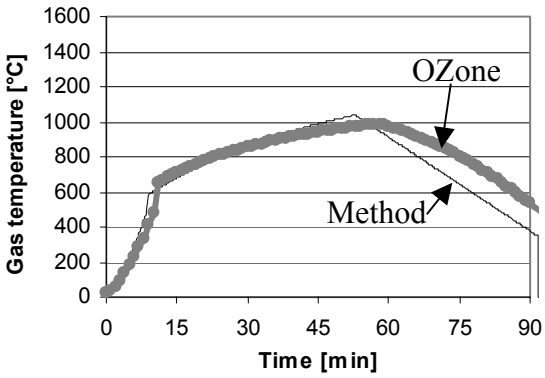

Figure 8.19 Compartment fire n°3

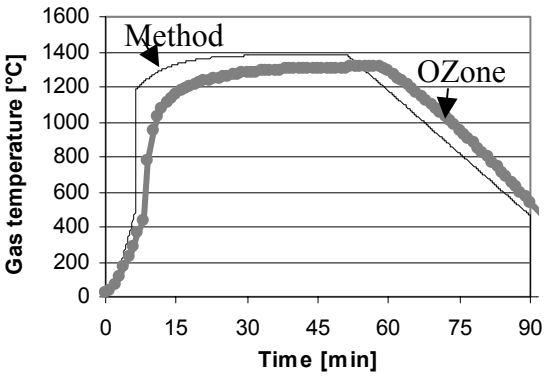

Figure 8.20 Compartment fire n°4

7.9 Advantages of the method

The following benefits of this method compared to existing ones can be quoted:

- The method is closer to physics because:
  - it is based on the direct solution of the energy balance;
  - the RHR curve is first built and then temperatures are calculated.
- It combines the pre- and post-flashover phases.
- It deals with ventilation or fuel controlled fires in an explicit way.
- The ventilation terms are separated for cooling and for effect on RHR.
- The method is not limited to cellulosic fire load (wood), it can easily be extended to other type of fuel.
- The decreasing phase is related to the end of the design fire.

7.10 Limitation of the method

As the different parameters of the solution have been fitted on simulations made with OZone, it is obvious that this method has at least the same limitations as OZone (see chapter 6). In fact the proposed method assumes that a two zone assumption is valid up to flashover time and that a one zone assumption is valid after flashover.

In particular, the method is not appropriate for compartments with openings leading to a ventilation factor greater than $10 m^{5/2}$ (see 6.5.5).

The method is based on the RHR design fire curve developed in the NFSC research and is thus valid for compartment fires during which this design fire curve is valid.

The pre-flashover phase was fuel controlled in each of the OZone simulations. Thus if the fire becomes ventilation controlled in the pre-flashover phase, the method does not apply.

If the design rate of heat release (used as input to the method) does not reach the rate of heat release at flashover time, flashover is not likely to occur. The method is not applicable to this situation.

The method should be limited to the domain in which the simulations have been done (see section 7.4.2), i.e. :

- H : 2.5 m;
- B : from 2.5 to 10 m;
- L : from 4 to 8 m;
- h_w : from 1 to 2.5 m;
- W : from 1 to 4 m.
- A_f : from 10 to 80 m^2;
- V: from 25 to 200 m^3;
- A_t: from 52.5 to 250 m^2;
- A_p: from 51 to 248 m^2;
- V_f: from 1 to 15.8 $m^{5/2}$;
- O: from 0.007 to 0.186 $m^{1/2}$;
- F_c: from 0.007 to 0.211 $m^{1/2}$;
- t_α : from 75 to 600 s;
- b: from 127 to 2035 $J/m^2s^{1/2}K$.

7.11 Conclusions

The bases of a new method to evaluate the time history of the temperature in a compartment fire are proposed. The formulation is based on the analytical solution of the simplified energy balance of a compartment fire.

Different parameters of the solution have been calibrated on simulations made with the compartment fire model of OZone, which has been built by the author and described in this dissertation. This code has been compared to numerous full scale fire tests and some limitations of its use have been pointed out. This calibration enables to compensate the error due to some coarse assumptions on which the method is based. Moreover, the domain on which the OZone simulations have been done should not be overlooked.

The validity of the method relies thus, up to now, on the facts that, on one hand, it compares very well with OZone results and on the other hand, OZone has been compared with a good agreement to a large number of full scale fire tests.

The method has not yet been directly compared to full scale fire tests. It is obvious that this should be done and that some improvements will probably come out.

Some of the proposed parameter solutions are very simple and could probably be improved easily. In particular the temperature T_{end} at the end of the fire should depend on the compartment itself, at least of the thermal properties of the boundaries. The η factor in equation (7.20), giving the pre-flashover temperature-time shape, could also be improved. And finally equation (7.36), empirically proposed to better fit numerical results, needs refinements.

8

Conclusions

The work presented in this dissertation is a contribution to the modelling of fires in compartments. Existing models have been examined and analysed, a computer code has been developed and a new analytical model is proposed. These tools have been elaborated in such a way that they will helps engineers to design structures submitted to compartment fires.

The analyses of existing models have shown that:

- The effect of the section dimensions and of the thermal properties of the insulation on equivalent time has been shown to be non negligible. The equivalent time method does not take these parameters into account. There is an urgent need for further research. The use of equivalent time methods in case of unprotected steel sections is particularly questionable and more generally .
- The parametric fire curves given in EN1991-1-2 have been shown to correlate quite well with full scale fire tests (ARBED 2002). Nevertheless the choice of the formulation and of the basic parameters of the method might still be improved.
- A comparison of 7 zone models on a well-defined example showed a very high dispersion of the results. As the origin(s) of the dispersion of the results was difficult to understand, it was decided to develop a new numerical compartment fire model.

A new numerical compartment fire model that combines a two-zone and a one-zone model has been developed. It enables to model the pre- and post-flashover fire phases. Several original development have moreover been included: three combustion models aimed at different use of the code (design or test simulation); no predetermined choice between one-zone or two-zone model has to be done; the partition model is fully coupled to the zone model...

The computer tool OZone V2 has been developed to design steel elements submitted to compartment fires. This tool calculates successively :

- The design fire source (rate of heat release and rate of mass loss);
- The gas temperature in the compartment thanks to the new numerical compartment fire model;
- The temperature of a steel element in that fire compartment;
- The structural fire resistance of this element.

Comparisons of the compartment fire model of OZone with full scale fire tests have shown that:

- The prediction of the gas temperatures in the compartment is very good in a large field of application:
  - small to large compartments,
  - low and high fire load densities,
  - wide range of thermal properties of walls;
- The simulations of compartment fire with openings with ventilation factors from 3.6 to $9.3 m^{5/2}$ give good predictions. The prediction is poor for smaller ventilation factor and not satisfactory for larger ventilation factor, for which a design rule is proposed.
- The NFSC design fire curves give good results for ventilation controlled fires. In case of fuel controlled, the definition of the design fire is quite difficult as data for fully-engulfed fire that are fuel controlled are scarce;

The bases of a new parametrical fire model, i.e., a method to evaluate analytically the time history of the temperature in a compartment fire, are proposed. The formulation is based on the analytical solution of the simplified energy balance of a compartment fire.

Different parameters of the solution have been calibrated on simulations made with the compartment fire model OZone. This calibration enables to compensate the error due to some coarse assumptions on which the method is based. Of course the assumptions made in OZone lead to other limits. Moreover, the domain on which the OZone simulations have been done should not be over-passed. The method, even if already applicable, needs to be improved on some aspects and must be directly compared to full scale fire tests.

Beyler (2001) has raised the main Fire Protection Challenges for this new century. He pointed out four main axes:

1. Develop methods for higher level performance-based design and technical documents to support fire safety analysis and design.
2. Develop methods for assessing the fire safety performance and costs of prescribed fire safety measures.
3. Rationalize our prescriptive fire safety measures through the use of method for assessing fire safety performance.
4. Reinvigorate basic fire research and focus the research to provide a solid foundation for fire protection engineering.

In relation with these four axes, the research work presented here is a direct contribution to the development of higher level performance-based design. The proposal of the new parametric fire curves is based on the unquestionable energy balance of a compartment fire and is therefore an attempt to consolidate the foundation of fire protection engineering methods.

To conclude, some ideas on the future directions in relation with the research work presented in this dissertation are given hereafter.

In the frame of a new European Community Fifth Framework Program research project called "FIRENET, Under-ventilated compartment fire", the code OZone will be further developed.

Among other things, the glazing behavior will be modeled in a more detailed manner, the potential of prediction of backdraft will be assessed and other full scale fire tests will be collected in order to extend our knowledge on the application field of OZone. The new parametric temperature-time curve will also be further developed and compared to full scale fire tests.

Another undergoing European project with ARBED, Luxembourg and VTT, Finland is dedicated to include OZone in a Probabilistic Fire Simulator developed at VTT. The aim is to build a tool that makes the risk assessment of a structure submitted to fire on the basis of Monte-Carlo simulations.

References

Alpert, R. L., Calculation of Response Time of Ceiling-mounted Detectors, Fire Technology, 8, 181-195, 1972.

ARBED, Background document on Parametric temperature-time curves according to Annex A of prEN1991-1-2 (24-08-2001), Document n° EC1-1-2 / 72, CEN/TC250/SC1/N298A. August 2001.

Arnault, P., Ehm, H., Kruppa, J., Rapport expérimental sur les essais avec des feux naturels exécutés dans la petite installation – Maizières-Les-Metz. Doc. C.E.C.M. – 3/73 – 11 – F. Centre Technique Industriel de la Construction Métallique, Puteaux, France, Juin 1973.

Arnault, P., Ehm, H., Kruppa, J., Incendies naturels avec des meubles et du papier – Doc. n°2.10.20-3 - CTICM, Puteaux, France- Juillet 1974

Babrauskas, V. and Williamson, R.B., Post flashover compartment fires: basis of a theoretical model, Fire and Material, 2, pages 39-53. 1978.

Babrauskas, V., Grayson, S., Eds., Heat Release in Fires,E. & F.N. Spon, London, 1992.

Babrauskas, V.; Ten Years of Heat Release Research With the Cone Calorimeter. CIB W14/93/2 (J); Tsukuba Building Test Laboratory, Center for Better Living. Japan Symposium on Heat Release and Fire Hazard, First (1st) Proceedings. Session 3. Scope for Next-Generation Fire Safety Testing Technology. May 10-11, 1993, Tsukuba, Japan, III/1-8 pp, 1993.

Babrauskas, V., Designing Products for Fire Performance: the State of the Art of Test Methods and Fire Models, Fire Safety Journal, Volume 24, Issue 3, 1995, Pages 299-312.

Babrauskas, V. and Wetterlund, I., Testing of furniture composites in the Cone Calorimeter; A new specimen preparation method and round robin results, Fire Safety Journal, Volume 30, Issue 2, 27 March 1998, Pages 179-194.

Babrauskas, V., Burning Item Sub-Models. NISTIR 6527; 270 p. June 2000. - Measurement Needs for Fire Safety: Proceedings of an International Workshop. National Institute of Standards and Technology. April 4-6, 2000, Gaithersburg, MD, Ohlemiller, T. J.; Johnsson, E. L.; Gann, R. G., Editors, 57-77 pp, 2000.

Babrauskas, V., Ignition of Wood: A Review of the State of the Art, Interflam 2001-Proc. 9th Intl. Conf., Interscience Communications Ltd., London (2001). pp. 71-88.

Barnett, C. R., BFD curve: a new empirical model for fire compartment temperatures, Fire Safety Journal, Volume 37, Issue 5, July 2002, Pages 437-463.

Beard, A. N., Fire model and design, Fire Safety Journal, Volume 28, march 1997, Pages 117-138

Beard, A. N., On a priori, blind and open comparisons between theory and experiment, Short Communication, Fire Safety Journal, Volume 35, July 2000, Pages 63-66

Beyler, C. L., Fire Safety Challenges in the 21st Century. Journal of Fire Protection Engineering. Sage Publications. Volume 11, Number 1/February 2001. Pages 4-15

Bryl, S., Brandbeslastung im Hochbau Schweizerische Bauzeitung, Schweizer Ingenieur und Architekt, Generalsekretariat, Senaustrasse 6, Postfach, CH-8039, Zürich. 243-249. 1975.

Buchanan, A. H., Structural Design for Fire Safety, Chichester, Wiley, 2001

Cadorin, J-F., Franssen, J-M., The One Zone Model OZone - Description and Validation Based On 54 Experimental Fire Tests, Rapport interne SPEC/99_05, Département des Structures, University of Liège, 1999.

Cadorin, J-F., Cajot, L-G., Schleich, J. B., Comparison of Equivalent Times from Eurocode 1 part 2.2 annex E and Experimental Tests, IAFSS Proc. of 6th int. Symp. on Fire Safety Science, Poitiers, IAFSS, Curtat ed., Poitiers, 2000

Cadorin, J-F., Franssen, J-M., A tool to design steel elements submitted to compartment fires - OZone V2 - Part 1 : Pre and post flashover compartment fire model, Fire Safety Journal, accepted for publication, in the editorial process, 2002, a.

Cadorin, J-F., Pintea, D., Dotreppe, J-C, Franssen, J-M., A tool to design steel elements submitted to compartment fires - OZone V2 Part 2: Methodology and application, Fire Safety Journal, accepted for publication, in the editorial process, 2002, b.

Capus, M.. Prise en compte du couplage entre flux diffusifs bidimensionnels dans les parois et modèles d'incendie à deux zones, Travails de fin d'études, Université de Liège, 1998. (In French).

Campbell, J.A. Confinement of Fire in buildings. section 5.9, SFPE Handbook, NFPA, 1981.

CEC Agreements 7210-SA/210/317/517/619/932. "Development of design rules for steel structures subjected to Natural Fire in Large Compartment", draft final report; Mars 97.

CCP: CEC Agreement 7210-SA/211/318/518/620/933. Development of design rules for steel structures subjected to natural fires in Closed Car Parks. Final Report, February 1997.

CFX-5 User Manual, AEA Technology, Harwell, UK, 2000.

Cooper, L.Y., Harkleroad, M., Quintiere, J. & Rinkinen, W. (1982). An Experimental Study of Upper Hot Layer Stratification in Full-Scale Multiroom Fire Scenarios. Journal of Heat Transfer, vol. 104, November 1982, pp. 741-749. 1982a

Cooper, L.Y., "A Mathematical Model for Estimating Available Safe Egress Time in Fires", Fire and Materials, Vol. 6, pp. 135-144, 1982b.

Cooper, L.Y., A Concept for Estimating Safe Available Egress Time in Fires, Fire Safety Journal, Vol. 5, pp. 135-144, 1983.

Cooper, L.Y. and Stroup, D.W., "ASET – A Computer Program for Calculating Available Safe Egress Time," Fire Safety Journal, Vol. 9, pp. 29-45, 1985.

Cooper, L. Y., Combined buoyancy and pressure-driven flow through a shallow, horizontal, circular vent. J Heat Transfer 117 (1995), p. 659.

Cooper, L. Y., Calculating Combined Buoyancy- and Pressure-driven Flow Through a Shallow, Horizontal, Circular Vent: Application to a Problem of Steady Burning in a Ceiling-vented Enclosure, Fire Safety Journal, Volume 27, Issue 1, July 1996, Pages 23-35.

Cooper, L. Y., VENTCF2: an Algorithm and Associated FORTRAN 77 Subroutine for Calculating Flow through a Horizontal Ceiling/Floor Vent in a Zone-type Compartment Fire Model, Fire Safety Journal, Volume 28, Issue 3, April 1997, Pages 253-287.

Cox, G., editor, Combustion fundamentals of fire, Academic press limites, London, 1995.

Cox, G, Fire research in the 21st century, Fire Safety Journal, 32, 1999.

Culver, C.G., Survey Results for fire loads and live loads in office buildings, NBS Building Science Series 85, US Dpt of Comerce/ National Bureau of Standards, May 1976

Curtat, M., Fromy P.; Prévision par le calcul des sollicitations thermiques dans un local en feu, Première partie: le modèle et le logiciel NAT, Cahiers du CSTB, livraison 327, cahier 2565, mars 1992. (In french).

Dotreppe, J.C., Résistance au feu des structures, Commission Nationale Belge de Recherche Incendie, Liège, Gent, 1983.

Drysdale, D., An introduction to fire dynamics. New York: Wiley, 1999.

Eurocode 1 – ENV 1991-1 : Basis of Design and Actions on Structures – Part 1 : Basis of design, CEN, Sept. 1994.

Eurocode 1 – ENV1991-1-2 - Actions on Structures - Part 1-2 : General Actions – Actions on structures exposed to fire, CEN, Brussels, 1993.

Eurocode 1 – Draft prEN1991-1-2 - Actions on Structures - Part 1-2 : General Actions – Actions on structures exposed to fire. FINAL DRAFT (Stage 49). CEN/TC250/SC1/N345, CEN, Brussels, January 2002.

Eurocode 1 –EN1991-1-2 - Actions on Structures - Part 1-2 : General Actions – Actions on structures exposed to fire. CEN, Brussels, November 2002.

Eurocode 3 – Draft ENV 1993-1-2 - Design of steel structures. Part 1.2: General rules Structural fire design, CEN, June 1995.

Eurocode 4 – prENV 1994-1-2. Design of Composite Steel and Concrete Structures. Part 1.2 : Structural Fire Design, CEN , April 1994.

Feasey, R. and Buchanan, A., Post-flashover fires for structural design, Fire Safety Journal, Volume 37, Issue 1, February 2002, Pages 83-105.

Forney, G.P. and Cooper, L.Y., A Plan for the Development of the Generic Framework and Associated Computer Software for a Consolidated Compartment Fire Model Computer Code, NBSIR 86-3500, National Institute of Standards and Technology (formerly National Bureau of Standards), Gaithersburg, MD, 1987.

Forney, G. P., and Cooper, L. Y., The Consolidated Compartment Fire Model (CCFM) Computer Application. VENTS, Parts I, II, III, IV. NISTIR, National Institute of Standards and Technology, 1990.

Forney, G. P. and Moss, W. F., Analysing and exploiting numerical characteristics of zone fire models, Fire Science & Technology, Vol. 14, No.1 & 2, 49-60, 1994.

Franssen, J-M., Cadorin, J-F., Cajot, L-G., Schleich, JB., Schweppe, H., Kindmann R. - Accidental Actions: Fire. Connection between Temperature-time curve and Equivalent time of fire exposure (Annexes B and E of ENV 1991-2-2) - IABSE Colloquium: Basis of Design and Actions on Structures. Background and application of Eurocode 1. Delft, Netherlands - March 1996.

Franssen, J-M., Contributions à la modélisation des incendies dans les bâtiments et de leurs effets sur les structures, Thèse d'agr. de l'ens. sup., F.S.A., Université de Liège, 1997. (In French).

Franssen, J-M., Cajot, L-G., Schleich, J.B., Natural Fire in Large Compartment – Effect caused on the structure by localised fires in large compartment. EUROFIRE, Brussels, pp 19 (CD-ROM). 1998.

Franssen, J.-M., Improvement of the Parametric Fire of Eurocode 1 based on Experimental Tests Results, Proc. 6th int. Symp. on Fire Safety Science, Poitiers, IAFSS, Curtat ed., Poitiers, (2000), 927-938

Franssen, J-M., SAFIR, technical reference, Université de Liège, 2003.

Friedman, R., "An International Survey of Computer Models for Fire and Smoke," SFPE Journal of Fire Protection Engineering, 4 (3), 1992, p. 81-92.

Hasemi, Y. Tokunaga, T., Flame Geometry Effects on the Buoyant Plumes from Turbulent Diffusion Flames, Fire Science and Technology, 4, 15-26, 1984.

Hasemi Y., Yokobayashi S., Wakamatsu T. et Ptchelintsev A., Fire Safety of Building Components Exposed to a Localized Fire - Scope and Experiments on Ceiling/Beam System Exposed to a Localized Fire, First Int. ASIAFLAM Conf. at Kowloon, Interscience Communications Ltd, London, 351-360, 1995.

He, Y., Fernando, A. & Luo, M. Determination of interface height from measured parameter profile in enclosure fire experiment. Fire Safety Journal 21, 1998. pp. 19-38.

Heskestad, G. Fire plumes. The SFPE handbook of fire protection engineering, Quincy, MA: National Fire Protection Association, 1995. pp. 2-9.

Hogge, M. Transferts de chaleur. Notes du cours MECA019-0. Faculté des Sciences Appliquées, Université de Liège, 1993.

Hostikka, S; Kokkala, M; Vaari, J. Experimental Study of the Localized Room Fires. NFSC2 Test Series. Espoo, VTT Building and Transport, 2001. VTT Tiedotteita - Research Notes 2104. 49 p. + app. 46 p. 2001 (available at http://www.vtt.fi)

Hostikka, S; Kokkala, M; Vaari, J. Experimental Study of the Localized Hall Fires. NFSC2 test Series. Espoo, VTT Building and Transport, 1999. (available in NFSC2 research report 2000)

Janssens, M. L., Heat Release Rate (HRR). NISTIR 6527; 270 p. June 2000. Measurement Needs for Fire Safety: Proceedings of an International Workshop. National Institute of Standards and Technology. April 4-6, 2000, Gaithersburg, MD, Ohlemiller, T. J.; Johnsson, E. L.; Gann, R. G., Editors, 186-206 pp, 2000.

Jones, W. W., Modeling Fires - The Next Generation of Tools. Society of Fire Protection Engineers and WPI Center for Firesafety Studies. Computer Applications in Fire Protection Engineering. Technical Symposium. Proceedings. Final Program. June 20-21, 1996, Worcester, MA, 13-18 pp, 1996.

Jones, W. W., Forney, G P., Peacock, R. D., Reneke, P. A., A Technical Reference for CFAST: An Engineering Tools for Estimating Fire Growth and Smoke Transport, NIST Technical Note 1431. 2000.

Jones W. W., State of the Art in Zone Modeling of Fires, International Fire Protection Seminar, 9th. Engineering Methods for Fire Safety. Proceedings. May 25-26, 2001, Munich, Germany, A.4/89-126 pp, 2001. ISBN 3-89288-133-2.

Karlsson, B., Quintiere, J. G., Enclosure Fire Dynamics, CRC Press 2000.

Kawagoe, K., Fire Behavior in Rooms," Report No. 27, Building Research Institute, Toyko,

Japan, 1958.

Kawagoe, K., Sekine, T., Estimation of temperature-time curves in rooms. Occasional Report N°11, Japanese Building Research Institute, Tokyo, 1963.

Kawagoe, K., Sekine, T., Estimation of temperature-time curves in rooms. Occasional Report N°17, Japanese Building Research Institute, Tokyo, 1964.

Kawagoe, K., Sekine, T., Estimation of fire temperature-time curves in rooms. Research paper N°29, Japanese Building Research Institute, Tokyo, 1967.

Kirby, B.R. et al., "Natural Fires in Large Scale Compartments"; BST, FRS. June 1994

Korpela, K. & Keski-Rahkonen, O., Fire Loads In Office Buildings, Proceedings of 3rd International Conference on Performance-Based Codes and Fire Safety Design Methods, Lund, Sweden, June 2000.

Kumar, S., & Kameswara Rao, C.V.S. "Fire Loads in Office Buildings." Journal of Structural Engineering. Vol. 123, No. 3, pp. 365-368,1997

Kumar, S. & Kameswara Rao, C. V. S. Fire Load in Residential Buildings, Building and Environment, Volume 30, Issue 2, Pages 299-305, 1995.

Law, M. A basis for the design of fire protection of building structures. Struct Eng 1983;61A(1).

Law, M., A Review of Formulae for T-Equivalent. Proceedings of the Fifth International Symposium on Fire Safety Science, Australia, 1997.

Lie, T.T., Characteristic Temperature Curves for Various Fire Severities, Fire Technology, 10, 4, 1974.

Lie, T.T., Fire Temperature-Time Relations, SFPE Handbook of Fire Protection Engineering, Society of Fire Protection Engineers, USA, 1995 (Chapter 4-8).

Lienhard, J. H. IV, Lienhard J. H. V, A Heat Transfer Textbook, 3rd edition, University of Houston, Massachusetts Institute of Technology, (c) 2000-2003, John H. Lienhard IV and John H. Lienhard V. pp762 (Available at http://web.mit.edu/lienhard/www/ahtt.html)

Ma, Z. and Mäkeläinen P., Parametric temperature-time curves of medium compartment fires for structural design, Fire Safety Journal, Volume 34, Issue 4, June 2000, Pages 361-375.

Martin and Wiersma (1979) An experimental study of flashover criteria for compartment fires. Final report, Products Research Committee PRC N°. P-77-3-1; Stanford Research Institute.

McCaffey, B. J., Quintiere, J. G., Harkleroad, M. F., "Estimating Room Fire Temperatures and the Likelyhood of Flashover Using Fire Test Data Correlations", Fire Technology, Vol. 17, N°2, pp. 98-119, 1981.

Mitler, H.E., and Rockett, J.A., "Users' Guide to FIRST, a Comprehensive Single-Room Fire Model," National Bureau of Standards, NBSIR 87-3595, 1987.

Klote, J. H., An overview of Atrium Smoke Managment, Fire Protection Engineering, Issue No 7, pp. 24-34, Summer 2000.

Mowrer, F. W., The Right Tool for the Right Job, Fire Protection Engineering Magazine, Issue No 13, pp. 39-44, Winter 2002.

Myllymäki, J.; Kokkala, M. Thermal exposure to a high welded I - beam above a pool fire. Franssen, Jean-Marc (ed.). Structures in fire : proceedings of the first international workshop. Copenhagen, Denmark, 19th and 20th of June, 2000. University of Liege (2000), s.211 - 224.

NBN S 21-208, 1e éd. - Protection incendie dans les bâtiments - Conception et calcul des installations d'évacuation de fumées et de chaleur – Partie 1 : Grands espaces intérieurs non cloisonnés s'étendant sur un niveau. Institut Belge de Normalisation. Bruxelles, 1993.

NFSC1: CEC Agreement 7210-SA/125/126/213/214/323/423/522/623/839/937. “Competitive Steel Buildings through Natural Fire Safety Concept”, Final report, Profil ARBED Research, March 1999. (to be published by the European Commission)

NFSC2: CEC Agreement 7210-PA/PB/PC/PE/PF/PR-060. “Natural Fire Safety Concept- Full Scale Tests, Implementation in the Eurocodes and Development of an User Friendly design tool”, Final report, Profil ARBED Research, December 2000. (to be published by the European Commission)

Olenick, S. M., and Carpenter, D. J., "An Updated International Survey of Computer Models for Fire and Smoke," Journal of Fire Protection Engineering, Volume 13, Issue 02, May 2003, 87-110

Peacock, R. D., Reneke, P. A., Bukowski, R.W. and Babrauskas, V.; Defining flashover for fire hazard calculations, Fire Safety Journal, Volume 32, Issue 4, June 1999, Pages 331-345

Pettersson, O., Magnusson, S.E. and Thor, J., Fire Engineering Design of Structures, Swedish Institute of Steel Construction, Publication 50, Lund, Sweden, 1976.

Ptchelintsev, A., Hasemi, Y. and Nikolaenko, M., Numerical Analysis of Structures Exposed to Localized Fire, First Int. ASIAFLAM Conf. at Kowloon, Interscience Communications Ltd, London, 539-544, 1995.

Robertson, A. F. and Gross, D., Fire load, Fire severity and Fire endurance, Special Technical Publication 464, American Society for Testing and Material, Philadelphia, PA, 1970

Rockett, J.A., Fire induced gas flow in an enclosure, Combustion Science and Technology, 12; 165-175, 1976.

Särdqvist, S., INITIAL FIRES, RHR, Smoke Production and CO Generation from Single Items and Room Fire Tests, Lund University, Institute of Technology Department of Fire Safety Engineering, Lund, Sweden, April 1993

Schleich, J.B, Eurocode 1 / part 2.2, Action on structures exposed to fire - IABSE Colloquium: Basis of Design and Actions on Structures. Background and application of Eurocode 1. Delft, Netherlands –Pages 71-81, March 1996.

Schleich, J.B., Cajot, L-G., Natural Fire Safety for Buildings, INTERFLAM 2001 conference proceedings, Interscience Communications Ltd, London, 359-368, 2001.

SFPE Engineering Guide to Performance-Based Fire Protection Analysis and Design of Buildings, Society of Fire Protection Engineers, Bethesda, MD, 2000.

SFPE Handbook of Fire Protection Engineering, Society of Fire Protection Engineers and National Fire Protection Association, 2nd Edition, Bethesda, MD, 1995.

Shaenman, P, Estimated impact of the Center for Fire Research program on the costs of fire. National Institute of Standards and Technology report NIST GCR 91 591, 1991.

Shampine, L. F. and Watts, H. A., DEPAC - design of a user oriented package of ODE solvers, Report SAND79-2374, Sandia Laboratories, 1979.

Simmons, R. F., Fire Chemistry, Chapter 7 of Combustion fundamentals of fire, Cox, G., editor, Academic press limited, London, 1995.

Sinai, Y., Validation of CFX-5 against a Steckler fire experiment,CFX-VAL15/0103, AEA Technology, 2003.

Sundström, B. editor, CBUF consortium, Fire safety of Upholstered Furniture - the final report, European Commission Measurement and Testing, Report EUR 16477 EN, edited by B. Sundström, Boräs 1995.

Sundström, B., Fire Hazards and Upholstery - Fire Growth., New concepts on describing the burning behaviour of upholstered furniture. Presented at "Fire Hazards, Testing, Materials and Products", A One-Day Conference, organised by RAPRA technology Ltd, UK, 13th March 1997

Thomas, P. H., Effect of fuel geometry in fires, BRE CP 29/74, 1974

Thomas, P. H., Design Guide Structural Fire Safety, Workshop CIB W14, February 1995

Thomas, I. R., Bennetts I.D. Fires in enclosures with single ventilation openings - comparison of long and wide enclosures. Proceedings of the Sixth International Symposium on Fire Safety Science, Poitiers, France, 1999.

Thomas, I. R., Buchanan, A. H., Fleishmann. Structural Fire Design : The Role of Time Equivalence. Proceedings of the Fifth International Symposium on Fire Safety Science, Australia, 1997.

Van Hees, P., Combustion Behaviour of Upholstered Furniture - The CBUF Project - Major findings and applications, Swedish Research and Testing Institute (SP) - Fire Technology, Borås, Sweden (Available on SP website).

Wakamatsu, T., Hasemi, Y., Yokobayashi, Y. and Ptchelintsev, A., Experimental Study on the Heating Mechanism of a Steel Beam under Ceiling Exposed to a Localized Fire, second INTERFLAM 96 conference, Cambridge, 509-518, 1996.

Walton, W. D. and Thomas, P. H., Estimating temperatures in compartment fires. SFPE Handbook of Fire Protection Engineering, Society of Fire Protection Engineers, USA, 1995 (Chapter 3-6).

Wickström, U., Application of the Standard Fire Curve for Expressing Natural Fires for Design Purposes, Fire Safety Science and Engineering. ASTM STP 882, T. Z. Harmathy, Ed., American Society for Testing and Material. Philadelphia, 1985, pp. 145-159.

Glossary[1]

Advanced fire model: design fire based on mass conservation and energy conservation aspects.

Combustion factor: the combustion factor represents the efficiency of combustion, varying between 1 for complete combustion to 0 for combustion fully inhibited.

Compartment factor: factor representing the amount of ventilation depending on the area of openings in the compartment walls, on the height of these openings and on the total area of the partitions (excluding opening area)

Compartment fire: a fire which remain confined within a compartment.

Compartment fire model: a model aimed at estimating the temperature evolution within a compartment during a fire.

Computational fluid dynamic model: a fire model able to solve numerically the partial differential equations giving, in all points of the compartment, the thermo-dynamical and aero-dynamical variables.

Design fire: a specified fire development assumed for design purposes.

Design fire load density: the fire load density considered for determining thermal actions in fire design.

Design fire scenario: a specific fire scenario on which an analysis will be conducted.

Enclosure: used as synonym of *Fire compartment*.

Eurocode: Within an action programme, the Commission of the European Community took the initiative to establish a set of harmonised technical rules for the design of construction works which, in a first stage, would serve as an alternative to the national rules in force in the Member States and, ultimately, would replace them. These harmonised technical rules are gathered in a set of documents called Eurocodes.

The first versions of these Standard have been produced in the eighties and the nineties and numbered ENV1990, ENV1991, ENV1992, etc. These ENV documents were then an alternative to the national rules.

At time of writing (early 2003), the publication of the EN versions of the Eurocodes, replacing the ENV versions and having the status of European Standards, is in progress.

The Eurocodes comprise the following standards generally consisting of a number of Parts: - ENV1990/EN1990, Eurocode: Basis of structural design;

[1] The vocabulary used in this dissertation is, as far as possible, in accordance to the one of the Eurocodes.

- ENV1991/EN1991, Eurocode 1: Actions on structures;
- ENV1992/EN1992, Eurocode 2: Design of concrete structures;
- ENV1993/EN1993, Eurocode 3: Design of steel structures;
- etc.

External fire curve: a nominal temperature-time curve intended for the outside of separating external walls which can be exposed to fire from different parts of the facade, i.e. directly from the inside of the respective fire compartment or from a compartment situated below or adjacent to the respective external wall.

Equivalent time of fire exposure: time of exposure to the standard temperature-time curve supposed to have the same heating effect as a real fire in the compartment.

Fire Compartment: a space within a building, extending over one or several floors, which is enclosed by separating elements such that fire spread beyond the compartment is prevented during the relevant fire exposure.

Fire load: the sum of thermal energies which are released by combustion of all combustible materials in a space (building contents and construction elements).

Fire load density: the fire load per unit area related to the floor area q_f, or related to the surface area of the total enclosure, including openings, q_t.

Fire resistance: the ability of a structure, a part of a structure or a member to fulfil its required functions (load bearing function and/or fire separating function) for a specified load level, for a specified fire exposure and for a specified period of time.

Fire scenario: a qualitative description of the course of a fire with time identifying key events that characterise the fire and differentiate it from other possible fires. It typically defines the ignition and fire growth process, the fully developed stage, decay stage together with the building environment and systems that will impact on the course of the fire.

Fire wall: a separating element that is a wall separating two spaces (e.g. two buildings) that is designed for fire resistance and structural stability, and may include resistance to horizontal loading such that, in case of fire and failure of the structure on one side of the wall, fire spread beyond the wall is avoided.

Flashover: simultaneous ignition of all the fire loads in a compartment.

Fully developed fire: the state of full involvement of all combustible surfaces in a fire within a specified space.

Heat release rate: see rate of heat release

Hydrocarbon fire curve: a nominal temperature-time curve for representing effects of an hydrocarbon type fire.

Localised fire: a fire involving only a limited area of the fire load in the compartment.

Member: a basic part of a structure (such as beam, column, but also assembly such as stud wall, truss,...) considered as isolated with appropriate boundary and support conditions.

Rate of mass loss: the mass of combustible released by a combustible product as a function of time.

Member analysis: the thermal and mechanical analysis of a structural member exposed to fire in which the member is assumed as isolated, with appropriate support and

boundary conditions. Indirect fire actions are not considered, except those resulting from thermal gradients.

Natural Fire Safety Concept: A European research project with the objective of establishing a more realistic approach to analyse the structural safety in case of fire that takes into account of active fire fighting measures and real fire characteristics.

One-zone model: a fire model where homogeneous temperatures of the gas are assumed in the compartment.

Opening factor: factor representing the amount of ventilation depending on the area of openings in the compartment walls, on the height of these openings and on the total area of the enclosure surfaces (including opening area).

Pre-flashover fire phase: fire phase before the simultaneous ignition of all the fire loads in a compartment (flashover).

Pyrolysis: decomposition and/or evaporation of solid fuel to gaseous fuel due to heat transfer from the flame and from the environment back to the fuel.

Post-flashover fire phase: fire phase after the simultaneous ignition of all the fire loads in a compartment (flashover).

Rate of heat release: heat (energy) released by a combustible product as a function of time

Simple fire model: design fire based on a limited application field of specific physical parameters.

Standard fire resistance: the ability of a structure or part of it (usually only members) to fulfil required functions (load-bearing function and/or separating function), for the exposure to heating according to the standard temperature-time curve for a specified load combination and for a stated period of time.

Standard temperature-time curve: a nominal curve defined in a standard for representing a model of a fully developed fire in a compartment. For example the ISO standard fire curve is defined in the prEN13501-2.

Structural members: the load-bearing members of a structure.

Temperature analysis: the procedure of determining the temperature development in members on the basis of the thermal actions (net heat flux) and the thermal material properties of the members and of protective surfaces, where relevant.

Temperature-time curves: gas temperature in the environment of member surfaces as a function of time. They may be:

- nominal: Conventional curves, adopted for classification or verification of fire resistance, e.g. the standard temperature-time curve, external fire curve, hydrocarbon fire curve;
- parametric: Determined on the basis of fire models and the specific physical parameters defining the conditions in the fire compartment.

Thermal actions: actions on the structure described by the net heat flux to the members.

Two-zone model: a fire model where different zones are defined in a compartment: the upper layer, the lower layer, the fire and its plume, the external gas and walls. In the upper layer, uniform temperature of the gas is assumed.

Ventilation factor: factor representing the amount of ventilation depending on the area of openings in the compartment walls and on the height of these openings.